ARTICLE IN PRESS Available online http://jopr.mpob.gov.my/category/article-in-press/

Journal of Oil Palm Research

Vol. 35(3) • September 2023

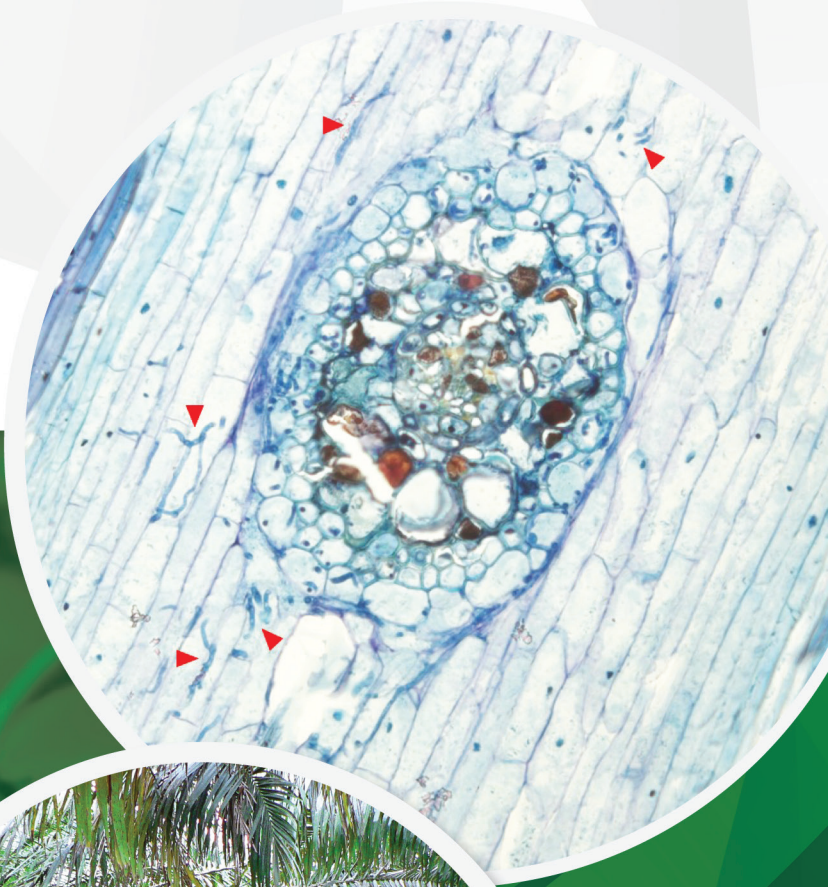

REVIEW ARTICLE

- Fungi in Biological Management of Plant Disease: Current and Future Perspective
- Oil Palm Water Requirement and the Need for Irrigation in Dry Malaysian Areas

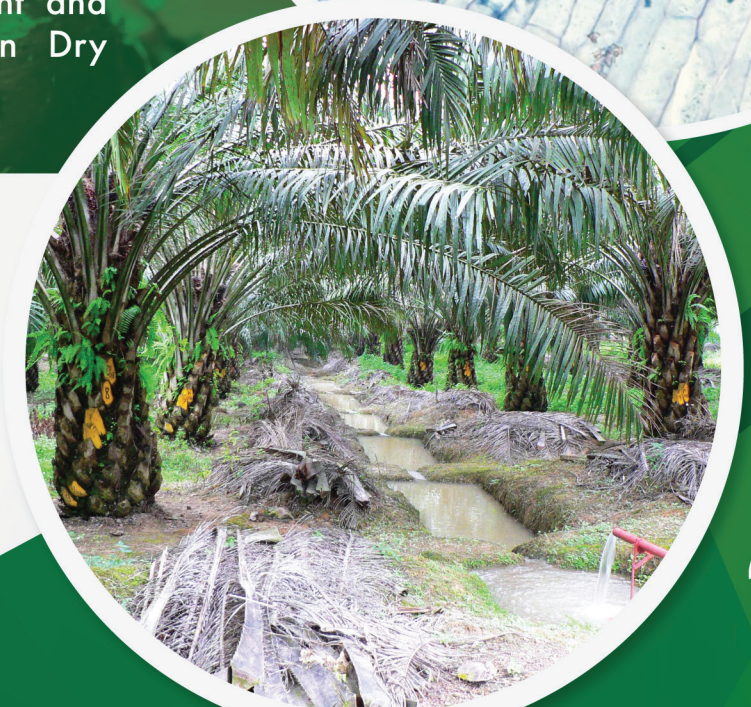

eISSN 2811-4701

MPOB

JOURNAL OF OIL PALM RESEARCH (formerly known as ELAEIS)

JOURNAL OF OIL PALM RESEARCH (JOPR), an international refereed journal, carries full-length original research papers, short communications and scientific review papers on various aspects of oil palm and palm oil and other palms. JOPR is published four times per year, *i.e.* March, June, September and December.

© Malaysian Palm Oil Board (MPOB), 2023

All rights reserved. No part of this publication may be reproduced in any form or by any means without the written permission of MPOB.

Impact Factor:
1.3
data from *2022 Journal Citation Report*® Science Edition
– A Clarivate Analytics product.

For more information on advertisement for the JOPR, please write to:

Editor-in-Chief
Journal of Oil Palm Research
Malaysian Palm Oil Board
6 Persiaran Institusi, Bandar Baru Bangi
43000 Kajang, Selangor, Malaysia

Tel: *603-8769 4400*
E-mail: *jopr.admin@mpob.gov.my*
Website: *jopr.mpob.gov.my*

DISCLAIMER
Views of writers expressed in this publication are not necessarily endorsed by or represent the views of MPOB.

MPOB Press
Malaysian Palm Oil Board
6 Persiaran Institusi, Bandar Baru Bangi
43000 Kajang, Selangor, Malaysia
Tel: +603-8769 4400 | Fax: +603-8925 9446
E-mail: *jopr.admin@mpob.gov.my*

JOURNAL OF OIL PALM RESEARCH

Vol. 35(3) September 2023

CONTENTS

Cover picture:
1. Colonisation of endophytic *Trichoderma virens* (pointed by red arrows) into oil palm root.
2. Irrigation techniques in oil palm plantation as adopted by FASSB in Serting, Negeri Sembilan.

EDITORIAL BOARD

(1 January 2022 – 31 December 2023)

Datuk Dr. Ahmad Parveez Ghulam Kadir
Malaysia (Editor-in-Chief)

Dr. Carl Traeholt
Malaysia

Prof. Dr. Matthias Finkbenier
Germany

Dr. Julie Flood
United Kingdom

Prof. Dr. Dirk Prufer
Germany

Prof. Dr. Douglas G Hayes
USA

Prof. Fredolin Tangang
Malaysia

Prof. Dr. Norzulani Khalid
Malaysia

Prof. Dr. Ir. Azmi Yahya
Malaysia

PUBLICATION COMMITTEE

CHAIRPERSON
Datuk Dr. Ahmad Parveez Ghulam Kadir

SECRETARY
Anita Taib

COMMITTEE MEMBERS
Dr. Zainab Idris
Dr. Ramle Moslim
Dr. Sivaruby Kanagaratnam
Dr. Astimar Abdul Aziz
Dr. Mohamad Arif Abd Manaf
Dr. Meilina Ong Abdullah
Dr. Aki @ Zaki Aman
Dr. Zafarizal Aldrin Azizul Hasan
Ruba'ah Masri
Johari Minal
Mohd Saufi Awang
Iptisam Abdul Wahab

REVIEW ARTICLES

Journal of Oil Palm Research Vol. 35 (3) September 2023 p. 375-390
DOI: https://doi.org/10.21894/jopr.2022.0061

FUNGI IN BIOLOGICAL MANAGEMENT OF PLANT DISEASES: CURRENT AND FUTURE PERSPECTIVE

SHAMALA SUNDRAM[1]*; YUVARANI NAIDU[1]; INTAN NUR AINNI MOHAMED-AZNI[1]; SHARIFFAH-MUZAIMAH SYED ARIPIN[1]; RAMLI, NUR-RASHYEDA[1]; MAIZATUL-SURIZA MOHAMED[1] and MOHD HEFNI RUSLI[1]

ABSTRACT

The fungal genera have a wide range of natural and commercial applications. Apart from the pertinent role in the ecosystem, the antagonistic characteristics of the fungal species have been utilised as biological control agents (BCA) in plant disease management (PDM). PDM is an integral component of agriculture as millions of agricultural produces are lost due to plant diseases annually. With the current emphasis on sustainable developments in the agriculture sector globally, the green approach offers a safe control against plant pathogens. Disease suppression by fungal biological control agents (FBCAs) is also comparable to the synthetic chemical application due to the current advancement in technology. Alas, despite the huge number of candidates screened and identified as potential FBCAs, the commercialisation of these FBCAs does not succeed as anticipated. Therefore, this review comprehensively highlights and discusses fungal genera as BCA, and the necessary changes required in research and development to enhance PDM. The future research on PDM needs to shift from its current focus on traditional screening and targeting modes of action in FBCA to strengthening the formulation, effective delivery modes, microbial population persistence and influence of environmental parameters to achieve a successful control.

Keywords: biological control agents (BCA), fungi, plant disease management, plant pathogen, mode of applications.

Received: 16 March 2022; **Accepted:** 29 July 2022; **Published online:** 23 September 2022.

FUNGI AS BIOLOGICAL CONTROL AGENT

The fungal kingdom has an omnipresent distribution globally with niche roles in the ecosystem. They are typically recognised for their excellent ability in decomposition, nutrient recycling, food source and symbiosis. Fungi emerge as efficient ecosystem engineers, regulators, bioindicators and bio-controllers with no particular reference to the occupied ecosystem (Frąc *et al*., 2018). Soil ecosystem for instance, is most probably one of the ecosystems where fungi elicit a strong influence of three fundamental components: (1) biological controllers, (2) ecosystem regulators, and (3) species participating in organic matter decomposition and compound transformations (Gardi *et al*., 2009; Swift, 2005). Among these niche roles, research on fungi as biological control agents (BCA) has progressed the most in the past 80 years (Tariq *et al*., 2020), with intense acceleration in the last 30 years due to the increased awareness globally for the safe production of food. Evidently, fungi biocontrol agent (FBCA) has been recognised as one of the most potent and powerful alternatives to replace synthetic pesticides and fungicides (Lee *et al*., 2013).

The undesired presence of organism that causes high yield losses in agriculture is termed pests and diseases (P&D). It is reported that approximately 25%-40% of yield losses in agriculture and horticulture systems are due to P&D attacks; this figure constantly changes and sometimes worsens due to biotic and abiotic influence (Lugtenberg,

[1] Malaysian Palm Oil Board,
6 Persiaran Institusi, Bandar Baru Bangi,
43000 Kajang, Selangor, Malaysia.

* *Corresponding author email: shamala@mpob.gov.my*

2015). Pests and diseases affect the plants' physiological processes in several ways: reduced photosynthesis, disruption in water and nutrient translocation, growth retardment and others. If not attended or intervened at an early stage, these physiological damages will cease the potential growth in plants and eventually affect their yield. The yield losses will immediately affect food security, causing some serious disturbance and balance to the food supply. Other consequences of these P&D damages include financial implications at the local, regional and national levels, with the worst implications leading to famine or loss of life (O'Brien, 2017). To date, the potential threats to plant health have been prevented, mitigated, and controlled using chemical applications, resulting in rapid recovery and reduced losses. However, the continuous and excessive use of these chemicals over the years has brought up environmental and sustainable concerns. Plants developing resistance, environmental pollution, aquatic ecosystem disruption, residual effect on human health, reduced soil fertility and biodiversity loss are among the distresses expressed globally with overusing chemicals (Lee *et al*., 2013; Tariq *et al*., 2020). Therefore, the use of FBCAs in integrated pest management (IPM) is highly recommended since the mode of action of these microbial inoculants is species-specific, resulting in harmless contact with the host and other non-specific residential species within the same ecological niche.

Over the years, advancements in research have enabled plants to achieve exceptional yield with the improvements made through breeding, genetics, good agronomic practices (GAP) and fertiliser applications. However, these improvements can substantially be affected by ineffective P&D management. With considerable interest in securing control measures that are cost effective, green and environmentally friendly, the application of FBCA has been welcomed as an integral part of GAP and plant disease management (PDM), and carefully incorporated into the integrated pest/disease management (IPM/IDM). With an expansive exploration over the years, the approach in FBCA is the deliberate application of indigenous or introduced beneficial microbial inoculants to reduce harmful activities of one or more P&D (Tariq *et al*., 2020). The comprehensive control by FBCA prevents and controls P&D incidences through single or combined mechanisms by limiting the growth factors, such as nutrients and space; parasitising through various physical and chemical modes; enhancing immunity; and finally creating an unfavourable abiotic and biotic microenvironment for pests (Köhl *et al*., 2019; O'Brien, 2017). More recently is the use of endophytes in plant protection consisting of different groups of microorganisms since a broad diversity of fungal and non-fungal endophytes is associated with nearly all plants (Wani *et al*., 2015). Endophytic microorganisms can be represented by bacteria, fungi, actinomycetes or viruses (Bao and Roossinck, 2013; Hassan *et al*., 2017; Sundram, 2013; Sundram *et al*., 2015;) while expressing a variety of symbiotic lifestyles ranging from parasitism to mutualism, and inducing resistance according to the genotype of the host plant and/or environmental conditions. A series of fungal endophytes are already in large-scale productions, such as commercial BCA: *Lecanicillium lecanii*, *Paecilomyces lilicinus*, *Beauveria bassiana*, *Fusarium oxysporum*, *Trichoderma harzianum*, *T. virens, Piriformospora indica* and others (Card *et al*., 2016; Mendoza and Sikora, 2009; Sikora *et al*., 2010; Sundram, 2013).

Fungi are one of the most successful BCA candidates that have been screened, characterised, identified, and formulated into fungal or FBCA products, targeting specific pests or pathogens. Even though other organisms such as bacteria and invertebrates (such as parasitoids) have shown potential as BCA, fungi are the most studied, documented and applied as BCA in PDM (Schrank and Vainstein, 2010). Several species of fungi from various genera, such as *Purpureocillium*, *Metarhizium*, *Beauveria*, *Cordyceps*, *Fusarium*, *Trichoderma*, *Clonostachys*, *Phoma* and others have been reported to have the FBCA, commercialisation and application potential in the field (Baron *et al*., 2019; Sun *et al*., 2020). The list in *Table 1* shows the commercially available products with fungi as the active microbe in the last 10 years. The versatile use of fungi has allowed researchers to utilise these multi-trait microbes by optimising specificity, formulation, delivery, application intervals and dosage to dramatically improve IPM holistically. In this review, we focus on the exclusivity of fungi being utilised as effective BCAs against plant diseases by discussing the process flow in the development of FBCA, followed by underlining its modes of delivery while further emphasising the delivery dynamics, success stories, research priorities and challenges in the strategic direction of future IDM.

PROCESS FLOW – SUCCESSFUL DEVELOPMENT OF BIOCONTROL PRODUCT

Successful development of a biocontrol product depends on standard process flow involving four important components highlighted in *Figure 1*: (1) selection/screening, (2) mechanism, (3) formulation and (4) field evaluation. Each of the components requires careful planning and execution to eventually determine the success of the developed FBCA. The following section will briefly highlight the four components of the process flow.

Selection

The preliminary selection of potential FBCA is determined based on the inhibition demonstrated on the target pathogen or pest, and this assessment generally takes place in the laboratory via simple screening bioassays. Generally, the selection and screening of FBCA candidates are from the rhizosphere or the endophyte population. The genus *Trichoderma* is prominent among those species of rhizosphere and the endophytic population that are effective as FBCAs (*Table 1*). However, a successful candidate via the *in vitro* screening does not necessarily warrant the successful selection of effective FBCA (O'Brien, 2017). This is because there are other mechanisms other than pathogen inhibition that can be utilised for selection of successful FBCA such as host growth and defence stimulation apart from occlusion of the pathogen but this will require further exploration. The screening assays are followed by the identification, and the preliminary results on the target species will be explored further at the nursery or field. These few initial steps described for the FBCA selection are interchangeable depending on the suitability and funding strength of the research laboratory. Meanwhile, the selected FBCA candidates are also required to be safe to humans, plants and animals. The effectiveness of FBCA in suppressing target organisms is highly dependent on the myriad modes of action inherently present within the FBCA inoculants. This characteristic will determine the success of the application and the consistency of the FBCA in the given environment.

Mechanism

Most microbial inoculants, including fungi, specialise in suppressing the pathogen of interest with either one or more modes of action. Prominent among the fungal genera as FBCA is the genus *Trichoderma* which is the most researched, leading to the successful production of biofungicides (Abbey *et al*., 2019). The modes of action can be divided according to their nature and the changes taking place: (1) physical, (2) cellular, and (3) environment. For instance, hyperparasitism falls into the physical category because the entire process involves unique physical activity, such as hooking and coiling of the target pathogen as reported by Sundram (2013). Besides that, D'Ambrosio *et al*. (2022) reported the mode of antagonism against soil-borne phytopathogens as deadlock at a distance or with initial contact,

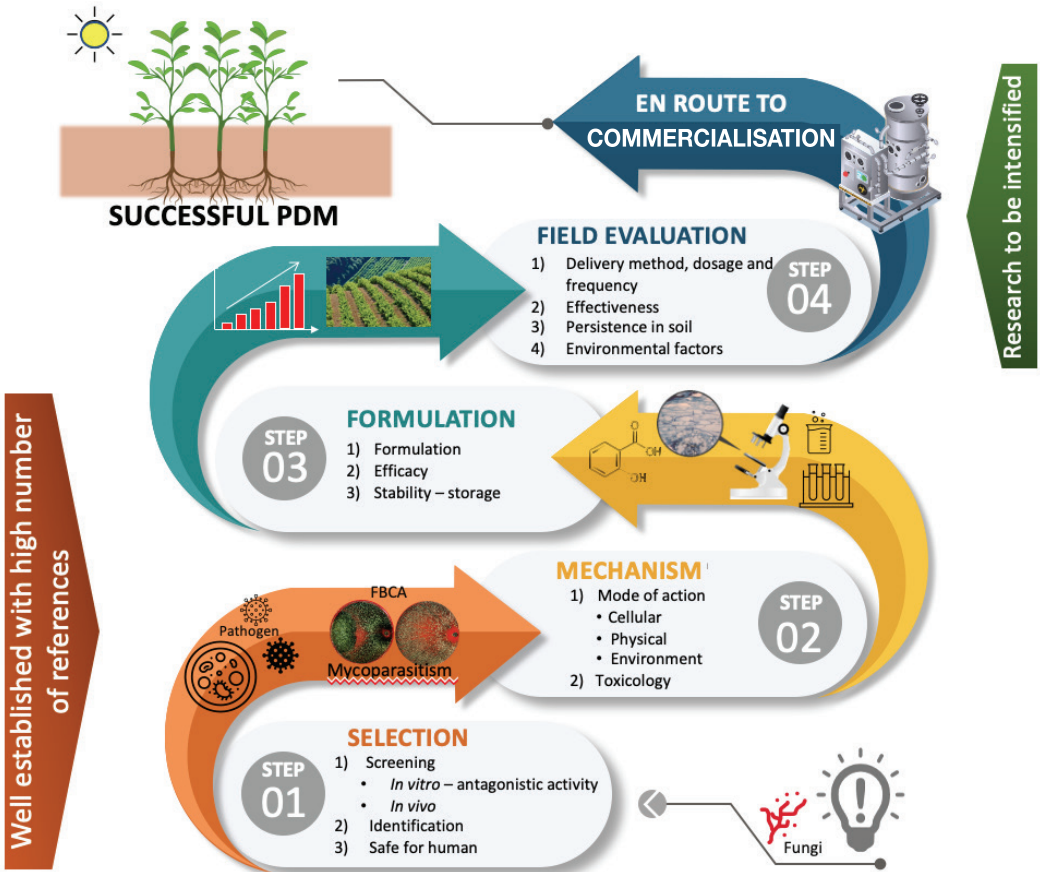

Note: FBCA - Fungal biological control agents.

Figure 1. Flowchart describes four specific processes in developing microbial-based biological control agents and the research needs to be addressed for a successful plant disease management (PDM) in the field.

TABLE 1. EXAMPLES OF COMMERCIALLY AVAILABLE BIOLOGICAL CONTROL PRODUCTS DEVELOPED IN RECENT YEARS USING FUNGI AS ACTIVE INGREDIENT FOR VARIOUS PLANT DISEASES GLOBALLY

Biological control agent (BCA)	Crop/Disease	Causal pathogen	Commercial products/Supplier	References
Coniothyrium minitans	Oilseed rape/ stem rot	*Sclerotinia sclerotiorum*	Contans® WG/ Prophyta Biologischer	Zeng *et al*. (2012)
Fusarium oxysporum non-pathogenic	Wilt	*Fusarium oxysporum*	Fusaclean; Biofox C/ Natural plant protection, France; S.I.A.P.A	Thambugala *et al*. (2020)
Gliocladium catenulatum	Strawberry/ grey mold	*Botrytis cinerea Pers:Fr.*	Prestop-Mix/ Verdera OY, Finland	Karise *et al*. (2016)
Pythium oligandrum	Red clover/ root rot	*Fusarium*	Polyversum/ Bioreparaty spol. s r. o., Czech Republic	Pisarčik *et al*. (2020)
Trichoderma virens G-41	Root disease	*F. oxysporum*	Rootshield® Plus⁺ / BioWorks, Victor, NY, United States	Li *et al*. (2018)
T. harzianum T-22	Root rot	*Sclerotia*	PlantShield® HC/ BioWorks, Victor, NY, United States	Derbyshire and Denton-Giles (2016)
Gliocladium virens GL-21	Root rot	*Pythium, Rhizoctonia,*	SoilGard® / Certis USA LLC	Castañé *et al*. (2020)
T. viride	Citrus/ root rot wilt	*Fusarium solani*	Trieco/ Ecosense Labs Pvt. Ltd., Mumbai, India	Kumar and Ashraf (2017)
T. asperellum T34	Ornamental plants/ root rot	*Fusarium, Rhizoctonia, Pythium, Phytophthora*	Asperello T34/ BIOBEST USA	Preininger *et al*. (2018)
Phlebiopsis gigantea	Root rot diseases	Heterobasidion	Rotstop®/ Kemira Agro Oy, Helsinki, Finland	Bruna *et al*. (2020)
Muscodor albus	Root rot, damping off and wilt	-	Andante™/ AgraQuest, Inc.	Mao *et al*. (2019)
Hendersonia toruloidea	Oil palm/ basal stem rot	*Ganoderma boninense*	GanoEF Biofertilizer/ All Cosmos Industries Sdn. Bhd., Malaysia	Peng *et al*. (2020)
T. virens 159c	Oil palm/ basal stem rot	*G. boninense*	Trichoshield/ True *Trichoderma* Technology Sdn. Bhd., Malaysia	Sundram *et al*. (2016)
Ulocladium oudemansii	Strawberry, grapes/ Fruit rots	*Colletotrichum, Rhizopus, Aspergillus* and *Alternaria*	BOTRY-Zen®/ BOTRYZen Ltd, Dunedin, New Zealand	Thomidis *et al*. (2015)

and partial or complete replacement of the tested phytopathogens in laboratory studies.

The cellular production of potent antibiotics, secondary metabolites and induced immunity are categorised under cellular via pathways affecting either the pathogen or the plant directly or indirectly. *Trichoderma virens* strain 7b has been reported as an active producer of siderophore and antifungal compound such as phenylethyl alcohol (PEA) (Angel *et al*., 2016). Besides that, volatile organic compounds of *Muscodor albus*, *Muscodor roseus* and *Fusarium oxysporum* have been reported in reducing the inoculum density of *Verticillium dahliae* in soil, and suppressing *Verticillium* wilt in eggplant and cotton (Stinson *et al*., 2003; Zhang *et al*., 2015).

Finally, the environment category is attributed to the space and nutrient availability to determine the effectiveness of FBCA by competing for the acquisition of nutrients and survival in the field. These modes of action may also intertwine or provide a combined effect on the target pathogen. *Figure 1* illustrates the combination of modes of action through the application of FBCA and their effects on the plant defence system.

Formulation

The selected biocontrol-potential isolates with strong antagonistic activity towards the pathogen will next be tested under a greenhouse condition using the microbial propagule. The main objective of this assessment is the interaction of the host or host tissues, pathogen and antagonist under controlled conditions that represent the targeted epidemiological perspective and environmental conditions of the crop (Köhl *et al*., 2011). The greenhouse conditions would evaluate the mechanisms related to biocontrol activity without significant interference from the external environmental characteristics and parameters, such as soil type, nutrient availability, and microbial diversity under a semi-natural condition. When the application of FBCA leads to positive results in the PDM, a suitable formulation for a large-scale application is developed because the delivery of the free-cell form is usually impractical. A stable formulation that can withstand extreme environmental conditions is required for a high-quality commercial product. These formulations may be simple mixtures of natural ingredients with

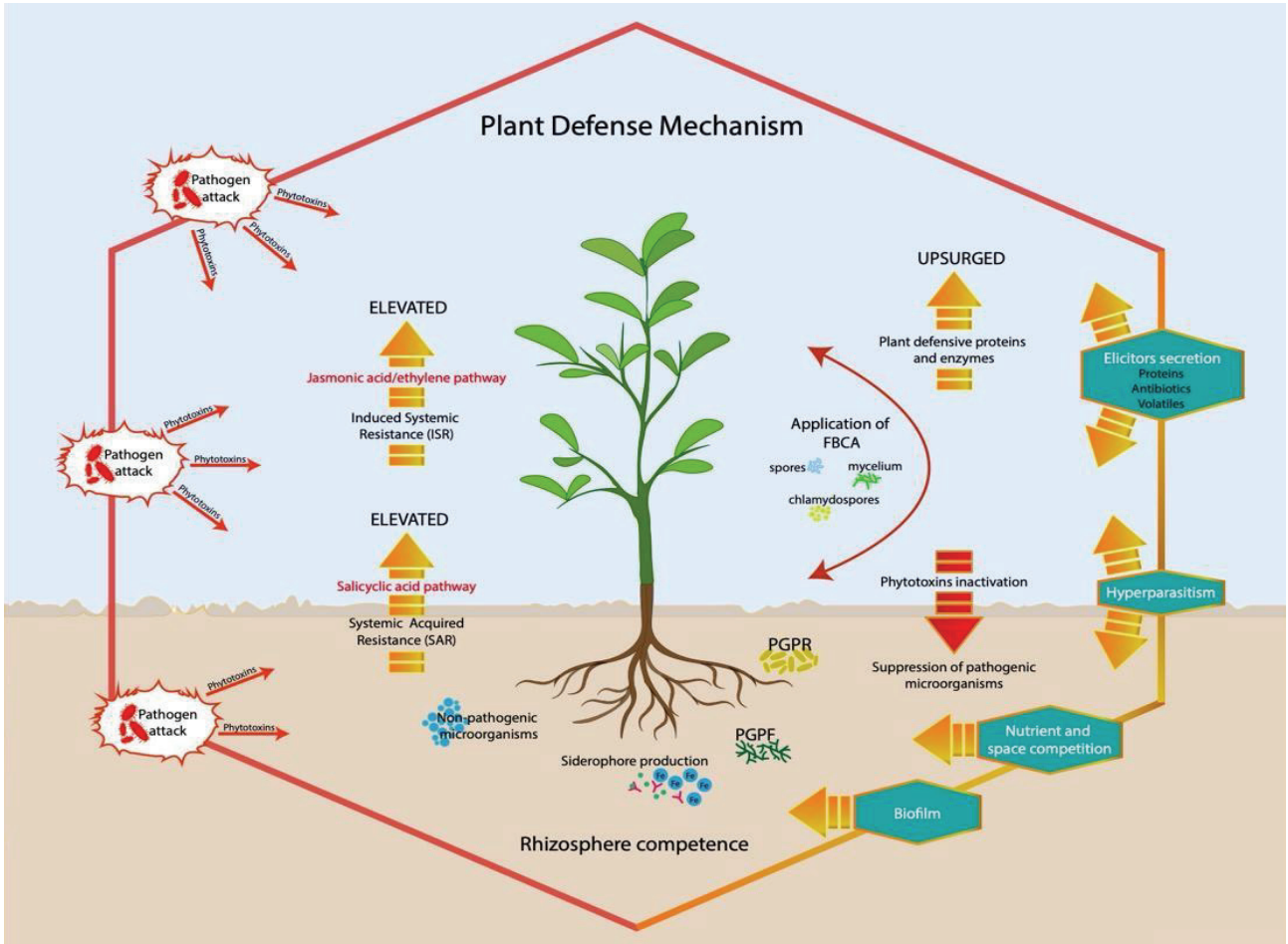

Note: FBCAs - Fungal biological control agents; PGPR - Plant growth promoting rhizobacteria; PGPF - Plant growth promoting fungi.

Figure 2. Plant defence mechanism complemented by the various components of microbial community and the different modes of action.

specific activities or complex combinations with multiple effects on the host or the target pest or pathogen (Nega, 2014). Narayanasamy (2013) has listed several desirable attributes of any BCAs that can be selected for the formulation stage. These attributes are the ability to inhibit target pathogens at low doses; production of antimetabolites or toxins against the target pathogen; increased tolerance to fungicides or other plant protection chemicals and plant activators; and improved adaptability to general crop management practices. It is critical to note that a stable formulation improves the shelf life, stability and field performance of the BCAs (Abdallah *et al*., 2018; Ravensberg, 2011). Besides that, the formulation must sustain the FBCA's viability during storage preferably for 18-24 months at room temperature (21°C), and it is still effective when used. The potential FBCA must also be user-friendly and cost-effective. Xue *et al.* (2014) have reported the successful formulation of *Clonostachys rosea* ACM941, with guaranteed efficacy in controlling *Fusarium* head blight in corn, soybean and wheat under field conditions compared to most field trials that used a conidial or spore suspension of the BCA which yielded inconsistent results.

Field Evaluation

Generally, FBCA inoculant often give promising reproducible results under controlled lab and greenhouse conditions. However, not all successful antagonists in the *in vivo* assessments produce similar effectiveness in natural field environments (Abdallah *et al*., 2018). In order to effectively work under the natural environmental conditions, the FBCAs should be able to survive and maintain their population within the habitat that favours the pathogen that causes severe damage to the host plant (Ghorbanpour *et al*., 2018). Various environmental factors, such as the soil characteristics including temperature, UV, low relative humidity, pH, nutrient availability, presence of chemical pesticides or fungicides, metal/heavy metal ions, and microbial community are often reported as the parameters that influence the growth of the FBCAs and eventually affect the biocontrol activities (Abdallah *et al*., 2018; Ghorbanpour *et al*., 2018). Dagno *et al.* (2011) have demonstrated that the percentage of viable conidia and radial growth rate of three fungal biological control agents of water hyacinth (*Eichhornia crassipes*) decreased with the decreasing water activity. Meanwhile, *Cadophora malorum* was found to be more tolerant to low water activity, and *Fusarium sacchari* was more tolerant to high temperature (35°C) (Daryaei *et al*., 2016; Domingues *et al*., 2016). In another study, an optimum *T. atroviridae* LU132 conidia production was observed at pH 6.5, and an optimum conidium fitness with maximum germination and inhibition of *Rhizoctonia solani* colonies occurred at pH 7.5 (Daryaei *et al*., 2016). A better understanding of the effect of abiotic and biotic interactions with FBCA is necessary to determine the optimal dose and timing of FBCA application. The susceptibility of the host, environmental conditions and agricultural practices are some of the factors that affect the FBCAs application timing. The application technology significantly impacts the efficacy of FBCAs. The application technology should involve standard non-costly agricultural equipment, targeted delivery, deposition, and coverage of the infection for significant disease control. Although the field trials are exhausting and time-consuming, the delivery method, application time, effective dose, and best formula are critical to precisely evaluate the performance of the selected FBCA and to ensure effective control of the phytopathogenic microorganisms. The importance of modes of delivery and the different methods of a delivery system in FBCA system is highlighted in the next section.

MODES OF DELIVERY AND APPLICATION OF FBCA

Apart from establishing a suitable formulation for the FBCA application, the concurrent research on delivery methods enables significant FBCA efficiency. The formulation process is imperative to stabilise effective microorganisms (EM), such as fungal propagules during mass production, distribution, and storage (Leggett *et al*., 2011). In addition, effective formulation of FBCAs is essential in handling and applying the final product; protecting the EM from harmful environmental factors (*e.g*., temperature, moisture, pH); achieving acceptable shelf life; and improving the activity of the FBCAs (Saberi-Riseh *et al*., 2021). Once the formulation is stabilised, it is delivered through several means, relying primarily on the pathogen's survival nature and mode of infection. The introduction of FBCA into the plant ecosystem is the basic principle to enable their multiplication or survival near or within the specific pathogen entry sites in the host plant (Bonaterra *et al*., 2012). The FBCA formulation is applied through inoculative, augmentative, or inundative strategies based on the modes of action of the FBCAs. The inoculative and augmentative strategies involve applying a low initial FBCA population, which then multiplies and reaches an effective population threshold, enabling the control of plant pathogens (Bonaterra *et al*., 2012). On the contrary, the inundative strategy is based on the same principle of microbial pesticides, whereby the FBCAs are applied generally at high concentrations. In order to ensure a wide range of conditions for the

application in practice, an approximate dosage of 10^7 CFU/mL is recommended for FBCAs (Bonaterra *et al*., 2012).

A number of liquid or dried formulations are being used as the FBCA application in the market (Bonaterra *et al*., 2012). Therefore, antagonistic FBCAs must be formulated and applied in an appropriate method to allow successful colonisation and persistence in the desired ecological niche, such as soil rhizosphere. These various application modes include seed treatment, soil/foliar application, stump, microencapsulation, organic amendments and a workable combination of different methods. A summary of each effective mode of a delivery system for the application of FBCA is provided in *Table 2*. Apart from identifying an effective delivery method for FBCA application, equally important is the application frequency at the appropriate intervals. Studies have shown that failure in applying FBCA at a suitable interval to suppress a disease will result in insignificant PDM (Bonaterra *et al*., 2012). Moreover, FBCA is effective as a preventive measure and able to be integrated with other disease management options, such as cultural practices, particularly in situations when the disease has established. Generally, the efficiency of any FBCA is strongly dose-dependent because it is affected by the relative aggregates between the pathogen and FBCA association within the plant defence mechanism (Yan and Khan, 2021).

DISCUSSION

Overview of FBCA in IDM

One of the sustainable development goals (SDG) in agriculture is to ensure safe and optimal food production for the booming global population. In line with this, the conventional approach to manage plant diseases using synthetic chemical applications has been flagged due to the implications for human and the environment. Nonetheless, it may be too ambitious to entirely discontinue chemical applications in disease or pest management because they provide an immediate solution to cease a P&D outbreak that may cause even greater damage. Moreover, stringent regulations govern the safe use of synthetic chemicals in the agriculture sector. Leveraging on the sustainable component development in the agriculture sector, the naturally existing microbial communities can be applied in PDM, and this practice has intensified over the past few decades. The traditional approach of using the already naturally occurring microbes as a component in the IPM is well received due to the negligible impact on humans and the environment. It is considered one of the rising alternate solutions due to its conservative, dependable, and eco-friendly approach in PDM. Apart from being a residential or introduced beneficial microbe, the application of FBCA has also demonstrated increased yield, root mass and plant health in general (O'Brien, 2017). Additionally, FBCA fortification in the relevant environmental niche, including rhizosphere, endosphere or phyllosphere, enriches the resident microbiome component as opposed to the chemical application that causes more harm.

The search for a biological agent is an ongoing continuous effort and the existing impactful publications can guide present and future researchers. With the continuous progress in research, the traditional screening of FBCAs will become a thing of the past as biotechnological tools allow for a rapid selection of candidates to leverage specific genes and proteins (Lee *et al*., 2013). Thus, when identifying a potential microbe becomes simpler, we will witness the improvement in the commercialisation of the FBCAs. This is because, despite a large number of effective FBCAs against plant pathogens being identified, only a few have been commercialised for sustainable management of diseases. This applies to not only FBCAs, but also all BCA products. The following section of the paper will underline the challenges and issues leading to the low rate of FBCA commercialisation, and finally, highlight the specific components for a successful field exploration of FBCA. The limitation of the commercial success of FBCA products can be divided into three main components: the technical aspects of the FBCA development, the customer's financial strength, and the manufacturing and regulatory processes to support the adoption and commercialisation of the FBCAs.

Technical

Apart from identifying the potential candidate of FBCA and understanding disease epidemiology and current disease-control strategies, extensive assessments are required to market FBCA products locally or internationally (Velivelli *et al*., 2014). The technical component is by far the most important as it relates to the final product and its efficacy in the field apart from considering all aspects of the formulation and delivery system. Some of the bottlenecks in marketing a good FBCA are impractical dosage recommendations with limited or variation in control efficacy, and an unrealistic delivery system (Singh *et al*., 2016). Additionally, rushing the process from field trials to commercialisation can severely affect the final product efficacy. Besides that, inconsistent effectiveness of FBCA when evaluated in field trials is one of the major constraints that prevent potential control of diseases. This may have been observed due to various reasons, including extrinsic

TABLE 2. MODES OF DELIVERY AND APPLICATION OF FUNGAL BIOLOGICAL CONTROL AGENTS (FBCA) IN PLANT DISEASE MANAGEMENT (PDM)

Plant disease/ host (Pathogen)	Biological control agents (BCA's)	Mode of delivery and application of FBCA	In combination	Observed efficacy	References
Seed treatment					
Wet root rot/ Mungbean (*Rhizoctonia solani*)	*Trichoderma virens*	Seed dressing	+ Soil applications + fungicides carboxin	Field - increasing seed germination, shoot and root lengths and grain yield and reducing wet root rot incidence in mungbean	Dubey *et al.* (2011)
Web blight/ Urd and Mungbean (*R. solani*)	*T. virens* *Gliocladium virens*	Seed treatment	+ Rhizobium + fungicides vitavax	Highest seed germination, plant vigour, number of root nodules and grain yield with minimum seedling mortality and disease intensity	Dubey (2003)
Chickpea wilt/ Chickpea, *Cicer arietinum* (*Fusarium oxysporum* f. sp. *ciceris*)	*T. viride*, *T. harzianum*, *T. virens*	Seed treatment	+ Fungicide carboxin *T. harzianum* (106 spores/mL/10 g seed) and carboxin (2 g kg^{-1} seed) for seed treatment	Green house - enhancing seed germination, root and shoot length, and decreasing wilt incidence	Dubey *et al.* (2007)
Damping-off/ corn (*Phythium* and *Fusarium* spp.)	*G. virens* isolate Gl-3 and *Burkholderia cepacia*	Seed treatment	10 g samples of seeds (infiltrated and non-infiltrated) mixed with 8 mL sticker, Pelgel and 1.2 g biomass powder	Effectively reducing the disease severity of root rot and increasing the plant growth in terms of seedling stands, plant height, and fresh weight	Mao (1998)
Dry root rot *(R. bataticola)*/ Chickpea, *Cicer arietinum*	*T. harzianum*	Seed treatment (5 g/ kg seed)	+Fungicide mancozeb + carbendazin	Seed treatment with *T. harzianum* @ 5 g/kg seed + *P. fluorescence* @ 5 g/ kg seed followed by soil drenching of mancozeb 50% + carbendazim 25% WS @ 3 g/L water to the infected and surrounding plants showed percent reduction of 71.50% for dry root rot.	Deepa *et al.* (2018)
Cucumber wilt *(F. oxysporum* f. sp. *cucumerinum)*/ Cucumber, *Cucumis sativus* L.	*Penicilium* sp., *Lasiodiplodia theobromae* and *Hypocrea* sp. (endophytic fungi)	Seed treatment (spore suspension 1.6 x 10^6 spores/ mL)	+ Soil drenching	Endophytic fungi suppressed *Fusarium* wilt, and significantly increased the plant height, aerial fresh and dry weight of cucumber plants.	Abro *et al.* (2019)
Cucumber wilt (*Phythium* spp.)/ cucumber	*T. harzianum* strain 1295-22	Seed treatment	+ Binder, Pelgel or Polyox N-10	The coating provided a physical barrier that delayed the pathogen attack and resulted in a conducive environment for *T. harzianum* growth (sown in a *Pythium*-infested soil in a laboratory bioassay).	Taylor *et al.* (1991)
Wet root rot (*R. solani*)/ Mungbean	*T. virens*	Seed dressing	+ Soil applications + fungicides carboxin	Field - increasing seed germination, shoot and root lengths and grain yield and reducing wet root rot incidence in Mungbean	Dubey *et al.* (2011)

TABLE 2. MODES OF DELIVERY AND APPLICATION OF FUNGAL BIOLOGICAL CONTROL AGENTS (FBCA) IN PLANT DISEASE MANAGEMENT (PDM) (continued)

Plant disease/ host (Pathogen)	Biological control agents (BCA's)	Mode of delivery and application of FBCA	In combination	Observed efficacy	References
Foliar treatment					
Powdery mildew (*Uncinula necator*)/ grapes	*T. harzianum* and *T. atroviride*	Foliar suspensions (applied at 10^8 spore/L)	none	Improving crop yield and increasing the total amount of polyphenols and antioxidant activity in grapes	Pascale *et al.* (2017)
Stem rot (*Botrytis cinerea*)/ tomato	*T. harzianum*	Spore suspension in water 0.1 g/100 mL, 10^6 cfu/mL	none	Simultaneous inoculation and pre-inoculation with *T. harzianum* gave good control of *B. cinerea* (50% and 90% disease reduction, 10 days after inoculation)	O'Neill *et al.* (1996)
Powdery mildew and Gray mould (*Sphaerotheca fusca* and *B. cinerea)*/ cucumber	*T. harzianum* T39 (TRICHODEX) and Ampelolyces quisqualis (AQ10)	Foliar spray	none	Reducing powdery mildew severity by up to 97%-98% but its efficacy declined as the epidemic progressed	O'Neill *et al.* (1996)
Grey mould (*B. cinerea*)/ tomato	*Fusarium semitectum* 252 and *T. harzianum* 118	Foliar suspension (applied at 10^7/ mL spore/mL)	none	Foliar spray with both strains significantly reduced disease incidence (65%-95%) and severity (50%-77%) on tomato crop	Dal Bello *et al.* (2011)
Root treatment/Root dipping					
Root-rot nematode (Meloidogyne javanica) and *Fusarium* wilt (*F. oxysporum* f. sp. *lycopersici*/ tomato (*Solanum lycopersicum L.*)	*Purpureocillium lilacinum* (PL) and *Trichoderma harzianum* (TH)	Soil drenching (fungal suspension 1 x 10^7 spores/ g soil)	+ FBCA's + neem + resistant tomato cultivars.	*P. lilacinum* - *T. harzianum*, *P. lilacinum* and *T. harzianum* reduced *Fusarium* propagules and *M. javanica* juveniles in the roots and performed even better when combined with neem in two resistant tomato cultivars	Mwangi *et al.* (2019)
Root treatment/ Root dipping					
Fusarium wilt (*F. oxysporum* . f. sp. *lycopersici*)/ tomato (*S. lycopersicum* L.)	*Funneliformis mosseae* and *Acaulospora laevis* (mycorrhizal fungi, AMF)	Soil inoculation (AMF)	+ *Trichoderma viride* was applied via soil drenching (*T. viride*)	Remarkable increase in the plant phosphorus and nitrogen content. Maximum reduction in disease incidence and severity was recorded in combined inoculation of *F. mosseae*, *A. laevis* and *T. viride*	Tanwar *et al.* (2013)
Fusarium wilt, tomato (*F. oxysporum* f. sp. *Lycopersic*/ tomato (*S. lycopersicum* L.	*T. asperellum* MSST	Talc-based bioformulation	none	Reducing disease incidence by up to 85%, increasing the vegetative parameters and inducing PR proteins	Patel and Saraf (2017)
Fusarium wilt, (*F. oxysporum* f. sp. *lactucae)*/ lettuce	*T harzia*num T22 and *F. oxysporum IF* 23	Talc based formulation	none	Disease control as well as increased growth response were shown by *T. harzianum* T 22	Gilardi *et al.* (2007)
Powdery mildew *(Sphaerotheca fusc*a)/ cucumber	*T. harzianum* T39 (TRICHODEX)	Soil application	none	Application of *T. harzianum* T39 to soil instead of spraying, 75%-90% lower coverage of powdery mildew on the leaves, and induced resistance as the mode of suppression	Elad *et al.* (1998)

environmental factors, reflecting the biological nature of the FBCA (Nega *et al*., 2014). A better understanding of the ecological and epidemiological relationships between the active ingredient (AI) and surrounding residential microorganisms, and the appropriate delivery systems at the correct intervals will allow the fungal strains significantly suppress diseases while reducing the gap between the experimental and commercial results of FBCA use. Therefore, the technicality involving the formulation and the delivery system are the two essential researches to successfully develop FBCA.

Formulation. During the early years of FBCA's research, emphasis was largely placed on the screening of potential candidates, with very little attention to the field implementation success. Subsequently, the research that follows the successful selection of FBCA is critical, requiring careful validation. Evidently, chemical products have a very long shelf life with an easy application methodology. On the contrary, FBCA formulation requires comprehensive studies for large-scale production, including selecting suitable and inexpensive carrier medium either solid or liquid for the proliferation of FBCA, and various additive materials. The addition of carrier and additive materials, such as wetting and dispersal agents, nutrients and UV- and osmotic-protection agents would improve field performance, shelf life and stability (Parnell *et al*., 2016; Ravensberg, 2011). The liquid formulation is typically aqueous, oil-based, or polymer-based, containing FBCA's biomass suspensions. FBCA products with an extended shelf life, good solvability in storage, capability of proliferating under extreme soil conditions, efficient disease control in the field, cost-effective, easy and safe handling have been achieved (Parnell *et al*., 2016; Ravensberg, 2011). For example, Prasad *et al.* (2020) have demonstrated the effectiveness of a chitosan biopolymer-based *Trichoderm*a (Cts-PEG-Th) liquid blend in inhibiting *Aspergillus* collar rot and *Macrophomina* root rot in groundnut and safflower under a greenhouse condition. The viability of *Trichoderma* spores was sustained over a period of six months in two different temperatures of the developed formulation. There is also a high preference for the solid formulation of FBCA, generally in the form of direct application dusts (DP), seed dressing formulations-powders for seed dressing (DS), granules (GR), microgranules (MG), dry formulations for dilution in water-water dispersal granules (WG), and wettable powders (WP). Similarly, liquid formulations have been developed for dilution in water emulsions, suspension concentrates (SC), oil dispersion (OD), suspoemulsion (SE), capsule suspension (CS), and ultra-low volume formulations (Singh *et al*., 2016). The FBCAs can either be applied directly onto the soil, suspended in water or used as seed coatings. Carrier materials such as peat, talc, lignite, kaolinite, zeolite, montmorillonite, alginate, press mud, sawdust, vermiculite and rice husk are among the prominent carriers selected for the preparation of solid formulation. The usage of these carriers increases the survival rate and shelf life of FBCA by protecting them from desiccation and providing a conducive microenvironment for rapid growth after release.

Delivery. The delivery system, bioecology of FBCA, pathogen, and host play an important role in choosing the type of FBCA's formulation. The list of delivery systems available for FBCA has been highlighted in the earlier part of this paper (*Table 2*). For instance, a granular material would be the most suitable for distributing in-furrow or incorporation as a potting mix for a horticultural crop while a wettable powder suspended in water is the most appropriate to be applied as soil drenching and root dips (Lecomte *et al*., 2016). Developing a precise and adequate delivery methodology to introduce the FBCA is one of the crucial steps to ensure the success of biocontrol activity under field conditions. Several factors, such as the type of pathogen, the stage of the crop to be protected, the severity of disease, and the climatic conditions of the region have been reported to influence the selection of an effective delivery method (Desai *et al*., 2002). FBCA products have generally been introduced into the plant ecosystem through direct soil application, seed coating, foliar spray or root dipping (Mahmood *et al*., 2016) to enable multiplication and survival near or at the specific entry sites used by the pathogen to enter the host plant (Bonaterra *et al*., 2012). In addition to an adequate formulation and delivery method, determining the application intervals is critical for effective disease management. For instance, a single application of FBCA may not allow the persistence of the microbe in its environment for effective disease control. In addition to the application intervals, identifying the effective microbial concentration is vital so that the product persists and competes with other microbial species within the niche environment. Meanwhile, various types of propagules persist and interact variably within the environment, contributing to the population dynamics of FBCA in the environment. Failing to deliver the FBCA correctly using the appropriate delivery method and at suitable intervals will result in unsuccessful management of the disease.

Financial Strength

A cost-effective mass production of a stable FBCA formulation would require the use of relatively cheap raw materials. Many chemical-based fungicides, pesticides and herbicides available

in the market are comparatively affordable and more effective than FBCAs. Thus, the potential FBCAs need to be formulated with hassle-free delivery systems, or the products will never reach the market or be used by growers despite the demonstrated effectiveness (Nega *et al*., 2014). An affordable pricing for the end-users of FBCA is crucial to compete with the conventional and effective chemical application (Moosavi and Zare, 2015). Misunderstanding or lack of knowledge on the handling of FBCA products often leads to ineffective disease control, affecting the product sales and customer feedback. Additionally, it is critical to disseminate the updated knowledge and advances in the technology and effectiveness of FBCA in order to educate growers and users on the misconception of FBCA; and the know-how to achieve effective implementation for significant disease management.

It is also essential for a timely analysis of the market size, the return on investment and the potential market for FBCA investors. Surveys on the availability of the potential market and the willingness of growers to invest in biological control will also provide an overview of the potential uptake of FBCA in a particular industry. It must also be taken into consideration that the real market size may be smaller than the potential market size (Ravensberg, 2011), which, in most cases, does not meet the expectation for commercialisation standards by companies. Thus, to be commercially successful, the strategic plan and directions should be aimed to develop products that are consistent in their performance, with a broad spectrum of activities to target different groups of diseases and deliver high investment returns. Therefore, a product that yields reproducible results in several sites with a wide spectrum of activities and target pathogen guarantees a larger market size and greater product sales, making the product development more attractive and economically feasible (Nega *et al*., 2014). There should also be strong support by the local government in providing the necessary funding or subsidies to entice companies to invest in green technologies, such as biofungicides. For instance, in Malaysia, large funding is provided for start-up companies that are interested in biological and sustainable technologies. The funding is managed by the Ministry of Science, Technology and Innovation (MOSTI) with a pre-assessment conducted by the Malaysian Global Innovation and Creative Centre (MAGIC). Pitching sessions for funding allocations are offered for potential companies with good preliminary results even though the companies are not necessarily prepared for a commercial market. Therefore, the strength in technical efficacy while gearing towards developing an end product is an added advantage in acquiring the available funding.

Regulatory

Regulatory frameworks and product registrations are used worldwide to guide the commercial development of microbial fungicides such as the FBCA. The pre-regulatory framework of a new microbial fungicide or pesticide varies depending on the country, the characteristics of the products and their intended usage. These national and international regulations must be taken into consideration at every stage of the product development cycle, starting from its initial stages of the FBCA establishment. The regulatory cycles for developing new bioinoculants and biocontrol products are generally streamlined and well-articulated according to the country's agricultural policies. As a result, microbial products are an appealing and cost-effective option to implement an integrated and system-level approach toward crop productivity and agricultural pests' management. Nevertheless, public health, public safety and protection of the environment must remain important, serving as a basis for judgment on the product's suitability. However, more flexible regulatory requirements could be achieved without compromising this if the regulatory bodies are provided with valid product information, especially on the environmental impact and safety of the microbial agents used in FBCA products.

Trichoderma sp. is one of the successful examples of FBCA genus that has been widely used in agriculture. The genus has long been recognised as a promising FBCA to control diseases and increase plant growth and development. Its biology and uses have been well established and documented. Waghunde *et al.* (2016) described more than 50 formulations of *Trichoderma*-based FBCA products that have been patented and registered worldwide. However, despite the relatively abundant number of patents filed for microbial pesticides, the number of commercial applications is underwhelming. Limitations in registration include multiple levels of following up, adding more cost and slowing down the process to commercialise new technologies. Furthermore, the registration procedure for approving any biopesticide formulation in the market has not been revised to consider the biological aspects of the product, which are far different from those for chemical-based product testing. The regulations involved in registering a microbial product are a very important, complex and dynamic process. Therefore, from developing to registering a biological control system, the cost may be higher compared to other products. For instance, prior to field application on a large scale, the formulation of an FBCA should first be assessed by analysing the risk assessment. According to Chandler *et al.* (2011), these regulations are to protect humans and the safety of the environment and secondly,

to characterise the products to ensure constant and consistent biopesticides quality. According to the Organization for Economic Cooperation and Development (OECD), the guideline for microbial pesticides before commercialisation is as follows: the microorganism and its metabolites do not pose pathogenicity or toxicity to mammals other than the non-target organisms that are likely to be exposed to the microbial product. Besides that, all additives present in microbial formulations are non-toxic, suggesting little risk to human health or environmental hazard. The product includes information on the mode of action, toxicological and ecotoxicological assessments, host range testing and others. These are complex processes that require a considerable amount of time, resources and expertise from the registration authority.

Future Perspective

Therefore, a set of multiple factors should be deciphered so that biofungicides effectively manage the disease. In general, the ecological parameters are the most neglected elements in managing plant diseases. The success of a FBCA may depend entirely on the ecological changes in the environment that may influence the product efficacy. Any changes in the environment may favour the plant, pathogen or microbial product. The ten principles of agricultural practices, include (1) soil, (2) nutrition, (3) water, (4) seed, (5) population density, (6) plant protection, (7) field management, (8) farming machinery technology, (9) light and (10) air, are known to influence the effectiveness of FBCA either independently or in combination (He *et al*., 2016). In order to be economically feasible as an alternative to chemical control, FBCAs must at least comply with the following requirements:

- An effective microbial strain that shows reliable and repeatable effectiveness.
- Understanding of the mechanism underlying biological control activity, ecological requirement, and ecotoxicological safety.
- Development of a cost-effective process for mass production and suitable formulation for long-term storage.
- Ease of application with an effective delivery system in the field.
- Financial support to business investors, *e.g.*, start-up companies.
- Regulatory support for registration, quality assurance and bridging communication barriers.

In the Malaysian palm oil industry, for instance, the government has been advocating the use of green technologies in its supply chain, including the PDM. The industry has been largely scrutinised for its non-sustainable approaches in its early days, but significant changes have been made over the past decades to provide a comprehensive sustainable supply chain. Leveraging on this development, green technologies have been actively explored for a number of P&D problems, namely *Ganoderma* basal stem rot (BSR) disease and bagworm. The BSR disease causes devastating productivity loss since the disease mainly manifests during the prime age of the crop. Two FBCA products, namely GanoEF™ and Trichoshield® have been developed to manage BSR disease and have been well received by the industry. Both formulations went through the registration process and improvements in several ways to cater to the local market. This included switching to cheaper substrates and conducting ongoing awareness programmes on green approaches to the growers. Although growers have been sceptical in the early years, this mindset has changed due to the industry's commitment to sustainable approaches and the long-term effect. Therefore, it is essential to develop a cost-effective formulation of FBCA by exploring the use of low-cost growing media, such as agricultural wastes (rice bran, empty fruit bunch, sawdust, and palm kernel cake or paddy husk) to provide affordable green technologies. Research on FBCA should not only be considered as a scientific and academic achievement but also pursued as a potential precursor study for product development. Thus, to completely realise the benefit and to tap the advantages of FBCA in the management of plant diseases, the research must shift its current focus on conventional screening and identification towards perfecting formulation, delivery, storage stability and suitable application intervals; and understanding population dynamics, persistence and ecological parameters, all of which play a bigger role than anticipated.

ACKNOWLEDGEMENT

The authors would like to thank MPOB management, and everyone involved in the publication of this review article. Conceptualisation and writing were by SS. Co-authors YN, MAINA, SMSA, RNR, MSM, and MHR have co-authored and contributed to the writing of the paper. All authors have read and agreed to the published version of the manuscript.

REFERENCES

Abbey, J A; Percival, D; Abbey, L; Asiedu, S K; Prithiviraj, B and Schilder, A (2019). Biofungicides as alternative to synthetic fungicide control of grey mould (*Botrytis cinerea*) -Prospects and challenges. *Biocontrol Sci. Technol., 29(3)*: 207-228.

Angel, L P L; Yusof, M T; Ismail, I S; Ping, B T Y; Mohamed Azni, I N A; Kamarudin, N H and Sundram, S (2016). An *in vitro* study of the antifungal activity of *Trichoderma virens* 7b and a profile of its non-polar antifungal components released against *Ganoderma boninense*. *J. Microbiol.*, *54(11)*: 732-744.

Abdallah, M F; Ameye, M; De Saeger, S; Audenaert, K and Haesaert, G (2018). Biological control of mycotoxigenic fungi and their toxins: An update for the pre-harvest approach. *Mycotoxins - Impact and Management Strategies* (Njobeh, P B and Stepman, F eds.). IntechOpen, London. p. 59-89.

Abro, M A; Sun, X; Li, X; Jatoi, G H and Guo, L D (2019). Biocontrol potential of fungal endophytes against *Fusarium oxysporum* f. sp. *cucumerinum* causing wilt in cucumber. *Plant Pathol. J.*, *35(6)*: 598-608.

Bao, X and Roossinck, M J (2013). Multiplexed interactions: viruses of endophytic fungi. *Adv. Virus Res.*, *86*: 37-58.

Baron, N C; Rigobelo, E C and Zied, D C (2019). Filamentous fungi in biological control: Current status and future perspectives. *Chil. J. Agric. Res.*, *79(2)*: 307-315.

Bonaterra, A; Badosa, E; Cabrefiga, J; Francés, J and Montesinos, E (2012). Prospects and limitations of microbial pesticides for control of bacterial and fungal pomefruit tree diseases. *Trees*, *26(1)*: 215-226.

Bruna, L; Klavina, D; Zaluma, A; Kenigsvalde, K; Burnevica, N; Nikolajeva, V; Gaitnieks, T and Piri, T (2020). Efficacy of *Phlebiopsis gigantea* against *Heterobasidion conidiospore* and basidiospore infection in spruce wood. *iForest*, *13*: 369-375.

Card, S; Johnson, L; Teasdale, S and Caradus, J (2016). Deciphering endophyte behaviour: The link between endophyte biology and efficacious biological control agents. *FEMS Microbiol. Ecol.*, *92(8)*. DOI: 10.1093/femsec/fiw114.

Castañé, C; van der Blom, J and Nicot, P C (2020). Tomatoes. Integrated pest and disease management in greenhouse crops. *Plant Pathology in the 21st Century, Vol. 9* (Gullino, M; Albajes, R and Nicot, P eds.). Springer, Cham. 691 pp.

Chandler, D; Bailey, A S; Tatchell, G M; Davidson, G; Greaves, J and Grant, W P (2011). The development, regulation and use of biopesticides for integrated pest management. Philosophical Transactions of the Royal Society of London. *Series B, Biological Sciences, 366(1573)*: 1987-1998.

D'Ambrosio, G; Cariddi, C; Mannerucci, F and Bruno, G L (2022). *In vitro* screening of new biological limiters against some of the main soil-borne phytopathogens. *Sustainability*, *14(5)*: 2693.

Dagno, K; Lahlali, R; Diourté, M and Jijakli, M H (2011). Effect of temperature and water activity on spore germination and mycelial growth of three fungal biocontrol agents against water hyacinth (*Eichhornia crassipes*). *J. Appl. Microbiol.*, *110(2)*: 521-528.

Dal Bello, G; Rollán, M; Lampugnani, G; Abramoff, C; Ronco, L; Larran, S; Stocco, M and Mónaco, C (2011). Biological control of leaf grey mould of greenhouse tomatoes caused by *Botrytis cinerea*. *Int. J. Pest Manag.*, *57*: 177-182.

Daryaei, A; Jones, E E; Glare, T R and Falloon, R E (2016). pH and water activity in culture media affect biological control activity of *Trichoderma atroviride* against *Rhizoctonia solani*. *Biol. Control*, *92*: 24-30.

Deepa; Sunkad, G; Sharma, M; Mallesh, S B; Mannur, D M and Sreenivas, A G (2018). Integrated management of dry root rot caused by *Rhizoctonia bataticola* in chickpea. *Int. J. Curr. Microbiol. Appl. Sci.*, *7(4)*: 201-209.

Derbyshire, M C and Denton-Giles, M (2016). The control of sclerotinia stem rot on oilseed rape (*Brassica napus*): Current practices and future opportunities. *Plant Pathol.*, *65(6)*: 859-877.

Desai, S; Reddy, M S and Kloepper, J W (2002). Comprehensive testing of biocontrol agents. *Biological Control of Crop Diseases*. CRC Press, India. p. 401-434.

Domingues, M V P F; Moura, K E D; Salomão, D; Elias, L M and Patricio, F R A (2016). Effect of temperature on mycelial growth of *Trichoderma*, *Sclerotinia minor* and *S. sclerotiorum*, as well as on mycoparasitism. *Summa Phytopathol.*, *3(1)*: 222-227.

Dubey, S (2003). Integrated management of web blight of urd and mungbean. *Indian Phytopathol.*, *56*: 413-417.

Dubey, S C and Ranganaicker Bhavani, B S (2011). Integration of soil application and seed treatment formulations of *Trichoderma* species for management of wet root rot of mungbean caused by *Rhizoctonia solani*. *Pest Manag. Sci.*, *67(9)*: 1163-1168.

Dubey, S C; Suresh, M and Singh, B (2007). Evaluation of *Trichoderma* species against *Fusarium oxysporum* f. sp. *ciceris* for integrated management of chickpea wilt. *Biol. Control*, *40(1)*: 118-127.

Elad, Y; Kirshner, B; Yehuda, N and Sztejnberg, A (1998). Management of powdery mildew and gray mold of cucumber by *Trichoderma harzianum* T39 and *Ampelomyces quisqualis* AQ10. *BioControl*, *43(2)*: 241-251.

Frąc, M; Hannula, S E; Bełka, M and Jędryczka, M (2018). Fungal biodiversity and their role in soil health. *Front. Microbiol.*, *9*: 707.

Gardi, C; Montanarella, L; Arrouays, D; Bispo, A; Lemanceau, P; Jolivet, C; Mulder, C; Ranjard, L; Römbke, J; Rutgers, M and Menta, C (2009). Soil biodiversity monitoring in Europe: Ongoing activities and challenges. *Eur. J. Soil Sci*., *60*: 807-819.

Ghorbanpour, M; Omidvari, M; Abbaszadeh-Dahaji, P; Omidvar, R and Kariman, K (2018). Mechanisms underlying the protective effects of beneficial fungi against plant diseases. *Biol. Control*, *117*: 147-157.

Gilardi, G; Garibaldi, A and Gullino, M (2007). Effect of antagonistic *Fusarium* spp. and of different commercial biofungicide formulations on *Fusarium* wilt of lettuce. *Phytoparasitica*, *25(5)*: 457-465.

Hassan, N; Nakasuji, S; Elsharkawy, M M; Naznin, H A; Kubota, M; Ketta, H and Shimizu, M (2017). Biocontrol potential of an endophytic *Streptomyces* sp. strain MBCN152-1 against *Alternaria brassicicola* on cabbage plug seedlings. *Microbes Environ*., *32(2)*: 133-141.

He, D C; Zhan, J S and Xie, L H (2016). Problems, challenges and future of plant disease management: From an ecological point of view. *J. Integr. Agric*., *15(4)*: 705-715.

Karise, R; Dreyersdorff, G; Jahani, M; Veromann, E; Runno-Paurson, E; Kaart, T; Smagghe, G and Mänd, M (2016). Reliability of the entomovector technology using Prestop-Mix and *Bombus terrestris* L. as a fungal disease biocontrol method in open field. *Sci. Rep*., *6(1)*: 31650.

Köhl, J; Postma, J; Nicot, P; Ruocco, M and Blum, B (2011). Stepwise screening of microorganisms for commercial use in biological control of plant-pathogenic fungi and bacteria. *Biol. Control*, *57(1)*: 1-12.

Köhl, J; Kolnaar, R and Ravensberg, W J (2019). Mode of action of microbial biological control agents against plant diseases: Relevance beyond efficacy. *Front. Plant Sci*., *10*: 845.

Kumar, M and Ashraf, S (2017). Role of *Trichoderma* spp. as a biocontrol agent of fungal plant pathogens. *Probiotics and Plant Health* (Kumar, V; Kumar, M; Sharma, S and Prasad, R eds.). Springer Singapore, Singapore. p. 497-506.

Lecomte, C; Alabouvette, C; Edel-Hermann, V; Robert, F and Steinberg, C (2016). Biological control of ornamental plant diseases caused by *Fusarium oxysporum*: A review. *Biol. Control, 101*: 17-30.

Lee, K; Oh, B T and Seralathan, K K (2013). Advances in plant growth promoting rhizobacteria for biological control of plant diseases. *Bacteria in Agrobiology: Disease Management* (Maheshwari, D ed.). Springer, Berlin, Heidelberg. 495 pp.

Leggett, M; Leland, J; Kellar, K and Epp, B (2011). Formulation of microbial biocontrol agents – An industrial perspective. *Can. J. Plant Pathol*., *33(2)*: 101-107.

Li, N; Alfiky, A; Wang, W; Islam, M; Nourollahi, K; Liu, X and Kang, S (2018). Volatile compound-mediated recognition and inhibition between *Trichoderma* biocontrol agents and *Fusarium oxysporum*. *Front. Microbiol*., *9*: 2614.

Lugtenberg, B (2015). Introduction to plant-microbe interactions. *Principles of Plant-Microbe Interactions* (Lugtenberg, B ed.). Springer, Cham. 447 pp.

Mao, W; Lumsden, R D; Lewis, J A and Hebbar, P K (2018). Seed treatment using pre-infiltration and biocontrol agents to reduce damping-off of corn caused by species of *Pythium* and *Fusarium*. *Plant Dis., 82(3)*: 294-299.

Mahmood, A; Turgay, O C; Farooq, M and Hayat, R (2016). Seed biopriming with plant growth promoting rhizobacteria: A review. *FEMS Microbiol. Ecol. 92*: fiw112.

Mao, L J; Chen, J J; Xia, C Y; Feng, X X; Kong, D D; Qi, Z Y; Liu, F; Chen, D; Lin, F C and Zhang, C L (2019). Identification and characterisation of new *Muscodor* endophytes from gramineous plants in Xishuangbanna, China. *Microbiology Open*, *8(4)*: e00666.

Mendoza, A R and Sikora, R A (2009). Biological control of *Radopholus similis* in banana by combined application of the mutualistic endophyte *Fusarium oxysporum* strain 162, the egg pathogen *Paecilomyces lilacinus* strain 251 and the antagonistic bacteria *Bacillus firmus*. *BioControl*, *54(2)*: 263-272.

Moosavi, M R and Zare, R (2015). Factors affecting commercial success of biocontrol agents of phytonematodes. *Biocontrol Agents of Phytonematodes*. CABI Publishing, Wallingford, UK. p. 423-445.

Mwangi, M W; Muiru, W M; Narla, R D; Kimenju, J W and Kariuki, G M (2019). Management of *Fusarium oxysporum* f. sp. *lycopersici* and root-knot nematode disease complex in tomato by use of antagonistic fungi, plant resistance and neem. *Biocontrol Sci. Technol*., *29(3)*: 229-238.

Narayanasamy, P (2013). *Biological Management of Diseases of Crops, 1 and 2*. Springer Science + Business Media BV., Heidelberg, Germany. 673 pp.

Nega, A (2014). Review on Concepts in Biological Control of Plant Pathogens. *J. Biol. Agric. Healthc*., *4(27)*: 33-55.

O'Brien, P A (2017). Biological control of plant diseases. *Australas. Plant Pathol*., *46(4)*: 293-304.

O'Neill, T M; Niv, A; Elad, Y and Shtienberg, D (1996). Biological control of *Botrytis cinerea* on tomato stem wounds with *Trichoderma harzianum*. *Eur. J. Plant Pathol*., *102(7)*: 635-643.

Parnell, J J; Berka, R; Young, H A; Sturino, J M; Kang, Y; Barnhart, D M and DiLeo, M V (2016). From the lab to the farm: An industrial perspective of plant beneficial microorganisms. *Front Plant Sci., 7:* 1110.

Pascale, A; Vinale, F; Manganiello, G; Nigro, M; Lanzuise, S; Ruocco, M; Marra, R; Lombardi, N; Woo, S L and Lorito, M (2017). *Trichoderma* and its secondary metabolites improve yield and quality of grapes. *Crop Prot*., *92*: 176-181.

Patel, S and Saraf, M (2017). Biocontrol efficacy of *Trichoderma asperellum* MSST against tomato wilting by *Fusarium oxysporum* f. sp. *lycopersici*. *Arch. Phytopathol. Plant Prot*., *50(5-6)*: 228-238.

Peng, S H T; Yap, C K; Arshad, R; Chai, E W; Hamzah, H; Idris, A S and Ramli, N R (2020). Significant of inoculated endophytic fungus, *Hendersonia toruloidea* GanoEF1 within oil palm root at PASFA Bukit Kerisek (Pahang) using GanoEF biofertilizer. *Adv. Agri. Horti. and Ento: AAHE-125, 2020(4)*: 1-3.

Pisarčik, M; Hakl, J and Hrevušová, Z (2020). Effect of *Pythium oligandrum* and poly-beta-hydroxy butyric acid application on root growth, forage yield and root diseases of red clover under field conditions. *Crop Prot*., *127*: 104968.

Prasad, R D; Chandrika, K S V and Godbole, V (2020). A novel chitosan biopolymer based *Trichoderma* delivery system: Storage stability, persistence and bio efficacy against seed and soil borne diseases of oilseed crops. *Microbiol Res., 237*: 126487.

Preininger, C; Sauer, U; Bejarano, A and Berninger, T (2018). Concepts and applications of foliar spray for microbial inoculants. *Appl. Microbiol. Biotechnol*., *102(17)*: 7265-7282.

Ravensberg, W J (2011). *A roadmap to the Successful Development and Commercialization of Microbial Pest Control Products for Control of Arthropods*. Springer, Dordrecht, Netherlands. 386 pp.

Saberi-Riseh, R; Moradi-Pour, M; Mohammadinejad, R and Thakur, V K (2021). Biopolymers for biological control of plant pathogens: Advances in microencapsulation of beneficial microorganisms. *Polymers*, *13(12)*: 1938.

Schrank, A and Vainstein, M H (2010). *Metarhizium anisopliae* enzymes and toxins. *Toxicon*, *56(7)*: 1267-1274.

Sikora, R A; ZumFelde, A; Mendoza, A; Menjivar, R and Pocasangre, L (2010). In planta suppressiveness to nematodes and long-term root health stability through biological enhancement - do we need a cocktail? *Acta Hort*., *879*: 553-560.

Singh, D P; Singh, Singh, H B and Prabha, R (2016). Microbial inoculants in sustainable agricultural productivity. *Vol. 2: Functional Applications*. Springer New Delhi. p. XVI, 308.

Stinson, A M; Zidack, N K; Strobel, G A and Jacobsen, B J (2003). Mycofumigation with *Muscodor albus* and *Muscodor roseus* for control of seedling diseases of sugar beet and *Verticillium* wilt of eggplant. *Plant Dis*., *87(11)*: 1349-1354.

Sun, Z B; Li, S D; Ren, Q; Xu, J L; Lu, X and Sun, M H (2020). Biology and applications of *Clonostachys rosea*. *J. Appl. Microbiol*., *129(3)*: 486-495.

Sundram, S (2013). First report: Isolation of endophytic *Trichoderma* from oil palm (*Elaeis guineensis* Jacq.) and their *in vitro* antagonistic assessment on *Ganoderma boninense*. *J. Oil Palm Res*., *25(3)*: 368-372.

Sundram, S; Meon, S; Seman, I A and Othman, R (2015). Application of arbuscular mycorrhizal fungi with *Pseudomonas aeruginosa* UPMP3 reduces the development of *Ganoderma* basal stem rot disease in oil palm seedlings. *Mycorrhiza*, *25(5)*: 387-397.

Sundram, S; Angel, L P L; Ping, B T Y; Roslan, N D; Mohamed-Azni, I N A and Idris, A S (2016). *Trichoderma virens*, an effective biocontrol agent against *Ganoderma boninense*. TOT 587 p.

Swift, M J (2005). Human impacts on biodiversity and ecosystem services: An overview. *The Fungal Community its Organization and Role in Ecosystems* (Dighton, J; White, J F and Oudemans, P eds.). CRC Press, Boca Raton, FL. p. 627-641.

Tanwar, A; Aggarwal, A and Panwar, V (2013). Arbuscular mycorrhizal fungi and *Trichoderma viride* mediated *Fusarium* wilt control in tomato. *Biocontrol Sci. Technol*., *23(5)*: 485-498.

Tariq, M; Khan, A; Asif, M; Khan, F; Ansari, T; Shariq, M and Siddiqui, M A (2020). Biological control: A sustainable and practical approach for plant disease management. *Acta Agric. Scand. B Soil Plant Sci*., *70(6)*: 507-524.

Taylor, A G; Min, T G; Harman, G E and Jin, X (1991). Liquid coating formulation for the application of biological seed treatments of *Trichoderma harzianum*. *Biol. Control, 1(1)*: 16-22.

Thambugala, K M; Daranagama, D A; Phillips, A J L; Kannangara, S D and Promputtha, I (2020). Fungi *vs*. fungi in biocontrol: An overview of fungal antagonists applied against fungal plant pathogens. *Front. Cell. Infect. Microbiol*., *10*: 718.

Thomidis, T; Pantazis, S; Navrozidis, E and Karagiannidis, N (2015). Biological control of fruit rots on strawberry and grape by BOTRY-Zen. *N. Z. J. Crop Hortic. Sci*., *43(1)*: 68-72.

Velivelli, S L S; De Vos, P; Kromann, P; Declerck, S and Prestwich, B D (2014). Biological control agents: From field to market, problems and challenges. *Trends in Biotechnol*., *32(10)*: 493-496.

Wani, A A; Ashraf, N; Mohiuddin, T and Riyaz-Ul-Hassan, S (2015). Plant-endophyte symbiosis, an ecological perspective. *Appl. Microbiol. Biotechnol*., *99(7)*: 2955-2965.

Waghunde, R; Shelake, R and Sabalpara, A (2016). *Trichoderma*: A significant fungus for agriculture and environment. *African J. Agric. Res., 11:* 1196-1952.

Xue, A G; Chen, Y H; Santanna, S M R *et al.* (2014) Efficacy of CLO-1 biofungicide in suppressing perithecial production by *Gibberella zeae* on crop residues. *Can J. Plant Pathol., 36*: 161-169.

Yan, L and Khan, R A A (2021). Biological control of bacterial wilt in tomato through the metabolites produced by the biocontrol fungus, *Trichoderma harzianum*. *Egypt J. Biol. Pest Control, 31*: 5.

Zhang, Q; Yang, L; Zhang, J; Wu, M; Chen, W; Jiang, D and Li, G (2015). Production of anti-fungal volatiles by non-pathogenic *Fusarium oxysporum* and its efficacy in suppression of *Verticillium* wilt of cotton. *Plant Soil*, *392(1)*: 101-114.

Zeng, W; Wang, D; Kirk, W and Hao, J (2012). Use of *Coniothyrium minitans* and other microorganisms for reducing *Sclerotinia sclerotiorum*. *Biol. Control*, *60(2)*: 225-232.

Journal of Oil Palm Research Vol. 35 (3) September 2023 p. 391-405
DOI: https://doi.org/10.21894/jopr.2022.0052

OIL PALM WATER REQUIREMENT AND THE NEED FOR IRRIGATION IN DRY MALAYSIAN AREAS

AFANDI, A M[1]; ZULKIFLI, H[1]; NUR ZUHAILI, H A Z A[1]; NORLIYANA, Z Z[1]*; HISHAM, H[1]; SAHARUL, A M[1]; DZULHELMI, M N[1]; and VU THANH, T A[2]

ABSTRACT

Water is essential for the growth and productivity of oil palm and hence adequate rainfall contributes to the oil palm water requirement. Sufficient rainfall becomes crucial in attaining good growth and yield. Over the past 23 years, the yield response from irrigated palms in Serting Hilir, Malaysia was reported to be 12 t ha^{-1} yr^{-1} or 56% higher than the non-irrigated palms. The drip irrigation system is selected to irrigate areas with limited water sources but with sufficient nutrient inputs. However, in areas with unlimited water, the furrow irrigation system is favoured. Feasibility analysis on irrigation implementation economics was done for the oil palm plantation. The analysis showed that irrigation is able to increase the yield by 5-6 t ha^{-1} yr^{-1} which is economically acceptable. To irrigate an oil palm plantation, a large source of water is required. Nevertheless, conserving water that penetrates the soil is the most practical approach to resolve issues of limited water supply, unsuitable terrains and logistics. The present paper reviews and discusses various techniques for soil and moisture conservation that are viable to increase oil palm yields.

Keywords: dry area, irrigation, moisture conservation, oil palm, yield response.

Received: 11 October 2021; **Accepted:** 20 July 2022; **Published Online:** 24 August 2022.

INTRODUCTION

Malaysia's climate is similar to that of West Africa, thus it provides a suitable condition for oil palm to grow. Oil palm in Malaysia originates from West Africa and the Tennamaram Estate in Selangor was the first commercial oil palm plantation. *Tenera*, a hybrid of *Dura* and *Pisifera* varieties is an oil palm variety that has been commercially grown in Malaysia (Corley and Tinker, 2003).

Theoretically, the highest oil yield was estimated to be about 18.50 t ha^{-1} yr^{-1} and the average oil yield worldwide stands at around 3.00 t ha^{-1} yr^{-1} (Woittiez *et al*., 2017). Meanwhile, in Malaysia, it was approximately about 3.64 t ha^{-1} yr^{-1} (Malaysian Palm Oil Board Statistics, 2019). Yield prediction through simulation models were applied to determine the oil palm yield. Recent oil palm growth models include PALMSIM (Hoffmann *et al*., 2014), OPRODSIMv1 (Henson, 2009), APSIM-Oil Palm (Huth *et al*., 2014), CLM-Palm (Fan *et al*., 2015), CLIMEX-Oil Palm (Paterson *et al*., 2015) and PySawit (Teh and Cheah, 2018). The most recent PySawit attempts to model oil palm photosynthesis, as well as the microclimate environment within and beneath the canopies and was developed for oil palm planted at a wide range of densities, from about 120-300 palms ha^{-1}, whereas APSIM-Oil Palm, CLM-Palm, and PALMSIM were only validated over a narrow planting density with a range of 127-156 palms ha^{-1}. PySawit predicted the growth and yield parameters of oil palm with good accuracy for total dry matter (TDM), leaf area index (LAI) and trunk height parameters. The yield declines caused by two *El Nino* occurrences (which resulted in dry periods) were

[1] Malaysian Palm Oil Board,
6 Persiaran Institusi, Bandar Baru Bangi,
43000 Kajang, Selangor, Malaysia.

[2] Faculty of Resource Science and Technology,
Universiti Malaysia Sarawak,
94300 Kota Samarahan, Sarawak, Malaysia.

* *Corresponding author e-mail: norliyanazz@mpob.gov.my*

demonstrated in the model simulations. However, discrepancies between yield predictions and observations increased with increasing planting density probably due to very dense canopies which were not well understood and insufficiently characterised by the model. The yields may be limited by factors such as insufficient rainfall, shallow soil depth, inclination and poor drainage. These factors can reduce nutrient availability and productivity of oil palm. Amongst these yield-limiting factors, rainfall plays the most important role because oil palm water requirements depend entirely on rainfall. The suitability of oil palm cultivation areas is also related to rainfall. Vital climatic factors that affect oil palm growth, yield and performance are rainfall amount, and distribution (Paramanathan, 2003). Oil palms require a large amount of rainfall. A monthly rainfall of at least 100 mm that is well distributed throughout the year is preferred (Paramanathan, 2013). Therefore, this signifies those areas with a prolonged dry season are less suitable for growing oil palm as the crop is a rain-fed crop (Kallarackal *et al*., 2004). Even though the average rainfall in Malaysia is high at over 2000 mm yr^{-1}, certain areas receive an uneven rainfall distribution. The rainfall distribution is reported to be more uniformly distributed in the east coast of Peninsular Malaysia as compared to other regions. A higher spatial rainfall variation is observed in the west coast regions of Peninsular Malaysia (Wong *et al*., 2009).

Water-induced stress in oil palm strongly suppresses yields (Carr, 2011; Corley, 1996; Palat *et al*., 2008; Woittiez *et al*., 2017). This is because the oil palm leaves do not wilt even though the opening of new leaves is shown. Besides, deficits in available soil water and air vapour pressure will greatly influence stomatal opening, and thus affect the photosynthesis rate (Caliman, 1992; Henson and Chang, 1989; Smith, 1989). Insufficient water supply has been a short-term problem in certain areas throughout the year, or in years when extreme weather conditions occur (Arifin *et al*., 2002; Chan *et al*., 1985; Corley and Hong, 1982; Henson and Chang, 1989; Kallarackal *et al*., 2004; Turner, 1976). For example, in Kedah water deficits could occur for about three consecutive months each year (Roslan and Haniff, 2004b). The drought conditions may negatively affect oil palm yield and difficult for the oil palm to grow and achieve its optimum potential because oil palm requires sufficient water supply for its growth.

Irrigation was exploited as an option to supplement the rainfall shortages experienced by oil palm fields. Studies on different methods of irrigation for oil palm were compared and the effectiveness of drip irrigation in overcoming water deficit was demonstrated (Rao *et al*., 2018; Tittinutchanon *et al*., 2000). In areas where water is not a limiting factor, a furrow irrigation system is applied. Nevertheless, since oil palm irrigation needs an abundant water supply, the installation of an irrigation system is only economically feasible when the yield is increased (Lee and Izwanizam, 2013). The water shortage for irrigation can be resolved by preserving rainfall water that penetrates the soil through mulching and covering crops.

This review discusses water requirements for oil palm, the effects of rainfall and water shortage in oil palm plantations. The need for irrigation implementation and soil moisture conservation for dry areas in Malaysia is also reviewed. Information about other palm oil-producing countries with similar situations as Malaysia is also included.

Environmental and Climate Conditions for Oil Palm Plantation

Certain climate conditions and soil suitability are required to ensure high yield production for oil palm in Malaysia and they are highlighted as follows: (1) Annual rainfall of at least 2000 mm to 2500 mm evenly distributed throughout the year (Hartley, 1988b); (2) Mean minimum and maximum air temperatures of 22ºC-24ºC and 29ºC-33ºC, respectively (Norman *et al*., 2014); (3) Relative humidity >45% for optimal transpiration (Roslan and Haniff, 2004a); (4) Average 5 hr of daily bright sunlight during the whole year, with up to 16-17 MJm^{-2} d^{-1} of daily solar energy for about 7 hr day^{-1} in some months (Lim *et al*., 2011; Norman *et al*., 2014); (5) Lowland areas (land less than 300 m or 1000 feet above sea level) (Paramanathan, 2015; PORIM, 1993); and (6) Loose soil texture or well-aggregated soils without hard layer will allow roots proliferation (Lim *et al*., 2011). Though the above criteria are best suited for optimum production, oil palm is also successfully grown in less favourable conditions, for example in Thailand and parts of West Africa and South America, whereby the dry seasons occur regularly.

Soil texture plays an important role in oil palm water deficit. Sand-textured soils (less than 10% clay content) have high porosity and are prone to moisture stress and nutritional deficiencies (Paramanathan, 2013). As a result, the oil palm yield potential on these soils is less than 19 t ha^{-1} yr^{-1} FFB, compared to 30-35 t ha^{-1} on clayey soils (Nordiana *et al*., 2008; 2013).

Corley and Tinker (2003) and Hartley (1988a) have summarized the main criteria to grow oil palms are temperature, sunshine and rainfall. Most oil palm planting systems are rain-fed, thus rainfall has become an important determining factor of oil palm yield. However, Corley and Tinker (2003) reviewed the role of water in oil palm productivity

and reported that there was no relation between total rainfall and yield. A good oil palm yield is ensured when the requirement for a total yearly rainfall of at least 1500-3000 mm is achieved. The rainfall should be distributed uniformly throughout the year with a minimum of 100 mm every month and no definite dry season (Nur Nadia and Syuhadatul Fatimah, 2016; Paramananthan, 2003). With sufficient relative humidity (75%-85%), oil palm can tolerate temperatures that are below or equal to 38ºC (Paramananthan, 2003).

At least 20% of rainfall is deflected by the apex, bunches, and frond bases of oil palm, while the remaining rain that penetrates soil is taken up by roots via the transpiration process (Chang and Rao, 1983). Furthermore, the effective rainfall (ER) is determined by the gross rainfall minus [run-off + deep percolation + interception by the vegetation] (Kee *et al*., 2000). The ER is referred to as a percentage of available rainfall to plants and crops. In Malaysia, the monthly ER varies from 11%-84% of gross rainfall. The number of months with soil water deficit varies from 2-12 months with an average of nine months (Claude *et al*., 2013).

In Peninsular and East Malaysia, the production of crude palm oil expresses variations in average oil palm yield. This is partly due to the amount of rainfall (12%-24%) although the seasonality in oil palm yields is possibly slightly independent of the rainfall (Chow, 1992). Oil palm can adapt to a higher amount of rainfall, but prolonged water logging will negatively affect the soil respiration, and flooding will result in the death of palms. Heavy rainfall during pollination can cause poor pollination and consequently reduce bunch fruit set, leading to a decline in the mean fruit bunch weight and bunch oil content (Haniff and Roslan, 2002) while excessive rainfall will increase the moisture in fruitlets, which results in a lower oil extraction rate (Nur Nadia and Syuhadatul Fatimah, 2016). However, continuous low rainfall (<100 mm) for more than two months significantly reduces the palm yield (Haniff *et al*., 2010). In 1998, there were significant reductions of 18.7%, 28.6%, and 14.6% in fresh fruit bunches (FFB) yield as compared to that in 1997 due to the *El Niño* phenomenon in Sabah, Sarawak and Peninsular Malaysia, respectively (Nur Nadia and Syuhadatul Fatimah, 2016).

Paramananthan (2013) estimated and summarised the potential of Malaysian oil palm yields for different rainfall regions. The yields were acquired based on standard agronomic management and the palms were grown on levelled undulating soil terrain (0%-22%). The average FFB yields for wet, moderate, and dry regions were 26, 24, and 18 t ha^{-1} yr^{-1}, respectively. The yields were higher in wet and moderate wet regions as compared to dry regions by about 32% and 27%, respectively.

Water Footprint of Oil Palm

Worldwide, the agricultural sector has the largest water usage, which currently recorded about 85% of freshwater consumption worldwide (Hoekstra and Chapagain, 2007; Shiklomanov, 2000). Crop types and climate influence the water requirement for the crop that can be supplied either by rainfall or irrigation. As in any agriculture-based produce, the general perception that concerns oil palm production is the direct water usage of oil palm.

A technique for communicating and managing water consumption patterns that affect the environment is water footprint (WF) determination. Hoekstra (2003) introduced the WF concept, which was further elaborated by Hoekstra and Chapagain (2008) to quantify the human allocation of freshwater resources. The WF analysis is aimed at achieving a variety of goals from business identification, processes or products based on water consumption level and promotion of sustainable water resources usage (Hoekstra *et al*., 2011). According to Hoekstra and Chapagain (2008), WF is the volume of freshwater used for FFB production. The WF for oil palm plantation is determined by the summation of daily crop evapotranspiration (mm day^{-1}) over the growing period of oil palm.

Based on Hoekstra and Chapagain (2008), the WF includes three components namely green WF, blue WF and grey WF. Green WF is the rainwater that evaporates during crop growth, while blue WF indicates the volume of the surface and groundwater that evaporates during crop growth. Meanwhile, the grey WF is the amount of water required to mitigate pollutants that are released into the natural water system to meet specific water quality standards (Mekonnen and Hoekstra, 2010).

Bluewater usage (m^3 ha^{-1}) is measured by the daily total volume of irrigation-water evapotranspiration. The blue crop water used in oil palm production is often considered zero. The summation of daily evapotranspiration values (mm day^{-1}) over growing period length measures green crop water usage (m^3 ha^{-1}). This is calculated using Hoekstra and Chapagain (2008) method. The green WF and blue WF of oil palm (m^3 t^{-1}) are determined by the total volume of green and blue water usage (m^3 yr^{-1}), which is then divided by the quantity of FFB yield (t ha^{-1} yr^{-1}). In addition, the grey WF of FFB production shows the volume of freshwater pollution, whereby is calculated by measuring the volume of water required to assimilate nutrients that reach the ground or surface water. Nutrients leaching from agricultural fields are the main cause of non-point source pollution of surface and subsurface water bodies. Calculation of the grey WF component (m^3 t^{-1}) involves multiplying the leached fraction of fertiliser / pesticide or runs off

by its application rate (L ha^{-1}). The value obtained is divided by the difference in concentration between maximum acceptable nitrogen concentration (kg ha^{-1}) and natural nitrogen concentration in the receiving water body (kg ha^{-1}) and by the actual crop yield (t ha^{-1} yr^{-1}). Zulkifli *et al*. (2014) reported the first WF of FFB production in Malaysia based on the inventory data obtained from 281 plantations for mineral soils, which covered an area of approximately 440 000 ha. The WF for FFB production were 21 920 m^3 ha^{-1} comprising 4.8 blue, 1054.0 green, and 107.0 grey m^3 t^{-1} FFB, thus, the main source of water used was green water.

As we have insufficient water resources although there is a high demand for water for biofuel feedstock and food production, there is a need for better water management to prevent conflict over water. Furthermore, oil palm's WF is different according to different countries based on the crop yields, climate and agricultural practices amongst countries, which is with or without irrigation. Previously, only WF of oil palm cultivation in Thailand (Piyanon and Shabbir, 2013) and Indonesia (FAOSTAT, 2011) were reported *(Table 1*) as they have implemented irrigation systems due to insufficient rainfall. Generally, in Malaysia, there is an adequate amount of rainfall to support oil palm growth, thus the sustainable use of water resources does not encounter pressing issues.

TABLE 1. THE WATER FOOTPRINT OF OIL PALM CULTIVATION FOR TOP PRODUCERS

Country	FFB yield (t ha^{-1} yr^{-1})	Green +Blue (m^3 t^{-1})
Indonesia	17.9*	802*
Thailand	5.5-16.0**	965–2 353**
Malaysia	20.7***	1 059***

Note: Greywater was excluded in * and **.

Sources: *FAOSTAT (2011); **Piyanon and Shabbir (2013) and ***Zulkifli *et al*. (2014).

Plant and Soil Water Deficit

Water deficit in the soil is defined as soil relative dryness measurement that reflects the water quantity that is removed from the soil within the rooting zone of the crop. It refers to the actual amount of water required to refill the root zone, thus it will balance out the soil moisture level. Different methods can be applied to measure water deficit in soil. One method is by using pan evaporation or Penman's estimate of evaporation. The estimated value is multiplied by the crop factor that is derived directly from crop evapotranspiration measurement. The crop factor is used to estimate how much water a plant can extract. Kumar (1997) indicated that the crop factor of oil palm is 0.7. The product of pan evaporation and crop factor determines the potential evapotranspiration (PE). For example, if the pan evaporation is 5.0 mm day^{-1}, then PE would be 3.5 mm day^{-1} (Roslan and Haniff, 2004b). The percentage of water that remains in the soil for several days and then undergoes saturation determines the field capacity, which is expressed in terms of weight or volume. The palm may encounter water stress whenever there are water deficit events in the soil. Factors that may vary the critical water deficit value and affect yield are soil type, soil depth, rooting density and palm age.

In Malaysia, monthly rainfall of less than 100 mm is considered a dry month (Claude *et al*., 2013). The most crucial moisture stress in oil palms is for 24, 18, and 5 months before fruit bunch maturation (Roslan *et al*., 2013). Ling (1979) reported that the oil palm evapotranspiration value in central Peninsular Malaysia might reach 160 mm $month^{-1}$. Dufrene (1989) found that the maximum evapotranspiration rate was 4-5 mm day^{-1} or 120-150 mm $month^{-1}$. Therefore, moisture loss replacement at 5 mm day^{-1}, or an equivalent of 350 L $palm^{-1}$ of irrigation water should be applied for a planting density of 143 palms ha^{-1}. When relative humidity (RH) reaches 30%-34%, a few oil palm growth limitations may occur. Meanwhile, RH below 30% could induce severe growth limitations (Kumar, 1997). Although palms are sufficiently watered, there are 10% losses in yield as they close their stomata during midday during the peak sun hours (Corley, 1973). Atmospheric stress from low RH and higher temperatures could develop a high vapour pressure deficit (VPD) even with sufficient irrigation. This may affect carbon assimilation. Henson (1991) proved that oil palm stomata are closed during high VPD, even though there is no limit on soil moisture. Kallarackal (1996) reported that oil palm stomatal closure was detected when VPD > 1.0 KPa and stomatal conductance was severely reduced when VPD ≥ 1.9 KPa.

Oil Palm Responses to Water Deficit

Symptoms of water stress in oil palms include unopened leaves accumulation, premature desiccation of pinnae edges, broken green leaves, bunch desiccation which causes abortion, crown collapse, and palm death, especially in newly planted palms (Paramananthan, 2003). Water stress is also associated with high juvenile incidence, fused pinnae and retarded seedlings growth that are thrown away at the end of nursery culling. Water stress reduces photosynthesis and inhibits oil palm growth (Corley, 1976; Ochs and Daniel, 1976; Roslan and Haniff, 2004b). Water deficit in the plant will cause an immediate physiological response such

as stomatal closure and consequent reduction in transpiration and photosynthesis by the canopy. In Malaysia, these oil palm conditions have previously been documented (Corley, 1973; Henson, 1991; Henson and Chang, 1989). The rise in canopy temperature (Henson, 1991; Henson *et al*., 2005) is a direct effect of reduced transpiration rates, which resulted from the stomatal closure.

It is noteworthy that any physiological stress will shift the sex ratio, whereby the number of female inflorescences per total inflorescences is in favour of male flowers, and as consequence productivity is reduced (Rao *et al*., 2018). The flower sex determination occurs 24 months before fruit ripening (Haniff *et al*., 2010). If the palms experience water stress during this peak period, a higher proportion of the inflorescences will turn into male flowers (*i.e.* reduction in sex ratio). Oil palms are regarded to be under severe drought if their soil water potential is less than -1.5 MPa (Méndez *et al*., 2012). This influences the physiological processes involved in growth, development and production. In response to low soil water potential, there is a positive relationship between stomatal conductance and transpiration (Jazayeri *et al*., 2015). In most plants, during water stress the stomata will close and leaves start to wilt. This results in minimal photosynthetic activity at a low carbohydrate status, thus it supports the formation of male inflorescences as less nutrition is required to develop. Since fewer female inflorescences develop, only a small number of fruit bunches are produced. On the other hand, more female inflorescences will be produced when the carbohydrate status is recovered. The time of inflorescence abortion is 18 months before fruit maturity, while the time for pollination is five months before fruit maturity.

The common effects of drought stress as previously described by Darlan *et al.* (2010) are an increase in abortion, failed or rotten bunches, fluctuation and low productivity, and long inflorescences time from eight to nine months. Due to the long developmental period of bunch production during drought periods, the yield will be negatively affected. However, the impact on yield will only become apparent later after more than a year. Water deficit also reduces growth and yield, causing vegetative disorder. Cheng-Xu *et al*. (2011) stated that water stress decreased relative chlorophyll a/b and oil palm yield. The decrease is via inflorescence abortion increment and a decrease in sex ratio (Henson *et al*., 2005; Roslan and Haniff, 2004b; Turner, 1976).

Previous irrigation-based research on water requirement of 4-5 mm day^{-1} showed slight success in ameliorating the yield caused by inadequate water and nutrients (Chan, 1979; Chan *et al*., 1985; Corley and Hong, 1981; Kee and Chew, 1991). Studies on the yield reduction estimation at various annual moisture deficits were conducted (Gawankar *et al*., 2003; Gerritsma and Wessel, 1997; Turner, 1976). The effects of severe droughts on oil palms were also identified where numerous closed spears, broken green leaves, desiccated leaves, toppled spears and the death of palms was observed (Dislich *et al*., 2017). Moreover, water deficit will negatively affect the oil content of fruit bunches because of less oil to the mesocarp ratio. In more severe cases, many fruits tend to be dried up and reduce the extraction rates by 30%-40% for several weeks (Kumar, 1997).

Less availability in soil moisture could also limit nutrient uptake since palms take up nutrients from the soil solution. With a monsoonal climate, the rate of nitrogen application in irrigated oil palm areas may be reduced by half as compared to non-irrigated areas (Kee and Chew, 1991). This is achieved by better nutrient uptake under adequate soil water supply during the year, whereby optimal palm nutritional status is ensured. The palm growth rates may be reduced by either water shortage, drought or poor drainage (Gawankar *et al*., 2003; Roslan *et al*., 2011). However, the effect of drought can be reduced by irrigation. In La Mé, Ivory Coast, irrigation trials revealed that the irrigated plots produced higher yields mainly due to the higher sex ratio and the number of bunches produced per palm (Fairhurst and Härdter, 2003; Hartley, 1988b). On that account, irrigation is required to achieve the maximum response towards the application of mineral fertilisers that tend to improve growth and increase oil palm yield.

Soil Water Management by using Irrigation

The irrigation system. Irrigation is implemented to avoid the restricted growth of plants due to the rainfall shortages, whereby the application rate is dependent on the amount and distribution of water. Moreover, the best method to determine irrigation timing is by measuring the plant water status based on stomatal behaviour and application rate by soil water deficit (Chan, 1979). The Univanich Oil Palm Research Centre (OPRS) in Thailand, successfully conducted irrigation trials since 1993 at Chean Vanich Estate (80º 32″ 06.0′ N, 980º 54″ 27.4′ E) in South Thailand. Based on OPRS trials, a more reliable irrigation system is considered if the four-drip line at every row with dripper rates of 150 L hr^{-1} and 250 L hr^{-1} is adopted for immature and mature palms, respectively. Moreover, to ensure good water distribution the furrow system requires additional maintenance to avoid blockages. In areas where infield mechanisation is practised, bridges over the furrows would increase the capital cost.

The micro sprayer irrigation systems have a high capital cost and need regular maintenance to keep them functioning effectively (Tittinutchanon *et*

al., 2000). The following are some technical issues on oil palm irrigation in Thailand (Afandi *et al*., 2013):

- Root damage may be caused by trenches for the dripper line dug near the palm, which could also cause depression in yields after installation.
- Irrigation near the palm is not necessary since mature palms can find water as far as 36 m.
- Setting up mobile dripper lines from the mainline, can irrigate seedlings at 150 L palm^{-1} day^{-1}.
- The use of dripper lines that are coiled around the palm of a single mobile dripper line would have no significant difference. However, using a dripper line coiled around the palm is more costly.

A drip irrigation system can reduce soil water deficit. Although there are available water sources, optimum benefits could only be achieved by applying a suitable irrigation infrastructure, an appropriate amount of water and frequency of application. The drip system supplies water in small quantities directly to the rooting zone. Therefore, it permits the request for water supply adjustment at any time and concurrently limits the loss through percolation. Most drip systems require water only at a low pressure of 1.0-1.5 kg cm^{-2} as compared to 3.5 kg cm^{-2} in standard irrigations (Kumar, 1997). However, this system has a drawback, whereby it requires frequent maintenance of the drippers, especially when the operation has stopped. By using surface drip irrigation, the upper 150 mm soil layer is much more hydrated as compared to subsurface drip irrigation (Srinivas, 1996).

The success of drip irrigation systems in oil palm depends on the irrigation designs to derive a higher irrigation efficiency (IE) rate, installation, operation, and maintenance. IE is defined as the proportion of consumed water or consumptive use that is beneficially used by a crop (Burt *et al*., 1997). More efficient irrigation systems have increased this proportion [Equation (1)], which allows less water to be applied for a given yield.

$$\text{Irrigation efficiency} = \frac{\text{Effective water}}{\text{Consumptive use of water}} \qquad (1)$$

In the drip system, a small volume of water can achieve an IE of up to 85%-95%, as compared to only 75%-80% IE with a flood and furrow system. The drip irrigation system is selected when water saving is of prime concern, as compared to surface irrigation systems.

In Malaysia, FELDA Agricultural Services Sdn. Bhd. (FASSB) had carried out field irrigation trials by using flatbed and drip systems (FASSB, 2000). The implementation of a drip irrigation system in cotton cultivation increased the yield by 28%-35%, particularly when fertilisation was adopted (Hanna *et al*., 2014). In southern Thailand, irrigation at 4-5 mm day^{-1} shows a positive impact on bunch number per palm (Tittinutchanon *et al*., 2000). Increased production in the total number and weight of FFBs was also recorded by Rao *et al*. (2018), which was due to high female inflorescences when drip irrigation was used as compared to micro-jet irrigation in an 18-year-old oil palm plantation in Andhra Pradesh, India. The drip irrigation systems reduced soil evaporation in narrow rows but did not cause a significant difference with furrow irrigation when soil water was non-limiting (Howell *et al*., 1987). Hodgson *et al*. (1990) had proven higher water efficiency when using drip irrigation systems. Furrow irrigation systems could achieve higher performance if transmission losses are reduced between the pump and irrigated field. This is possible by reducing run-off losses, recirculating run-off water, and reducing waterlogging.

Economics of irrigation. Lee and Izwanizam (2013) reported that the initial capital cost for flatbed irrigation systems was estimated to be about RM4688 ha^{-1}. Combined with the financial cost at an annual interest rate of 6% per year, the total cost was approximated at RM7500 ha^{-1} or RM750 ha^{-1} year^{-1} amortised over a 10 year period. The capital and operating costs of the drip irrigation system at 300 L palm^{-1} in Thailand were about 1300 USD and 70 USD ha^{-1} yr^{-1}, respectively, and it was only over half of the amount for 150 L palm^{-1} (Tittinutchanon *et al*., 2000). The estimated initial cost to set up drip irrigation systems on undulating terrain was about RM18 000 ha^{-1} (Afandi *et al*., 2013). A furrow irrigation system is cheaper than a drip irrigation system. It has to be noted that for any irrigation projects under oil palm to be viable and profitable, the FFB yield should increase by at least 4 t ha^{-1} yr^{-1}, assuming that the FFB price is RM400 t^{-1}. In Malaysia, an increased yield of at least 5-6 t ha^{-1} yr^{-1} would be more economically justifiable for irrigation implementation (Lee and Izwanizam, 2013).

The irrigation rate and water balance. Norizan *et al*. (2021) discovered that the FAO Cropwat model is an excellent method for assessing crop water requirements (CWR) for Malaysian oil palm demands. To calculate the amount of water to be utilised for irrigation, this model requires effective rainfall, soil type, soil water-holding capacity, meteorological and crop data. An accurate estimate of the water amount applied to a field is critical to any irrigation management approach. A minimal amount of water can cause unnecessary water

stress, which will reduce yield. Too much water promotes waterlogging and leaching, which can again result in yield loss. The appropriate water amount can be estimated using information collated from the evaporation pan (E-pan) and meteorological data. E-pan data of 4.0 mm day^{-1} implies that the evapotranspiration is equivalent to 4.0 L m^2 day^{-1}. At a planting density of 148 palms ha^{-1} each palm can occupy an area of 67.6 m^2 (10 000 m^2/148). However, each palm occupies only a fraction of the occupied area. Therefore, with an estimated canopy radius of 3.0 m, it is equivalent to 42% of the estimated occupied area. Each palm requires 113.6 L day^{-1} of water (67.6 m^2 x 0.42 x 4 L m^2 day^{-1}) (Roslan *et al*., 2011), which represents the estimated amount of water needed to be irrigated according to water requirement. Irrigation timing will depend on the water flow rate, which relies on the water pump efficiency.

The use of the water balance concept for irrigation scheduling is based on soil water content estimation. Daily evapotranspiration and transpiration by leaves show the amount of water that is taken out from the field soil profile. This loss could be replaced either by rainfall or irrigation water (Feddes and van Dam, 2005). When the soil water balance is below the minimum level it indicates that irrigation is required. Water balance under oil palm can be determined by examining the total water needed to generate a balance against the total water input by rainfall and irrigation. For a given volume of soil and plant environment, the water balance Equation (2) (Kee *et al*., 2000) is as follows:

$$\Delta S = P + I - ET - R - D \quad (2)$$

where ΔS is the change in soil moisture; P is the precipitation; I is the irrigation; ET is evapotranspiration; R is the surface run-off and D is the drainage.

Yield response. In Malaysia, the variation in FFB yield between dry and wet regions is significant; 10 years after harvesting, the difference in FFB yield between dry and wet regions is between 25.81% and 26.67% (Paramanathan, 2013). Drought reduced palm oil productivity by 10%-30% in Southeast Asia (Paterson and Lima, 2018). Drought raises the temperature as well as affects FFB output; during the drought season, a moisture deficit of 100 mm in a year reduces FFB production by 8%-10% in the year of drought and 3%-4% in succeeding years (Caliman and Southworth, 1998; Fleiss *et al.*, 2017; Suharyanti, *et al*., 2020). It has been reported that an average temperature of more than 27.83°C in the eight months preceding harvesting reduces FFB output (Shanmuganathan *et al*., 2014).

Positive responses to irrigation implementation were reported in Malaysia (Chan, 1979; Chan *et al*., 1985; Kee and Chew, 1991). Nevertheless, there were cases where irrigation was often uneconomical due to limited water supply, high installation and running costs, poor returns, and relatively low response (Goh, 1995). A study by Foong and Lee (2000) involving a lysimeter was conducted at Sungai Tekam, Pahang, Malaysia, and found the daily potential evapotranspiration of a mature palm would be 5.5-6.5 mm day^{-1}. The potential evapotranspiration for an immature oil palm during dry seasons was about 5.5-6.0 mm day^{-1} while 7.0-8.0 mm day^{-1} was recorded for a mature palm. With optimum water and fertilisers, the lysimeter palm produced an FFB yield of 59 t ha^{-1} yr^{-1} and a total oil yield of 15 t ha^{-1} yr^{-1}. It was observed that irrigation did not affect the seasonal yield fluctuation. Enhanced peak yield and increased yield were observed in some cases. However, this could be due to the trial being well fertilised (*Figure 1*). In most previous studies, irrigation had affected the bunch number rather than the bunch weight (Chan, 1979; Foong and Lee, 2000).

In a distinctly dry environment in Serting, Malaysia, Lee and Izwanizam (2013) reported that for over 23 years, there was an average yield increase of 12 t ha^{-1} yr^{-1} (or 56%) in irrigated palms as compared to the non-irrigated palms. The FFB yield of the irrigated and undulating area (23.96 t ha^{-1} yr^{-1}) is significantly higher than the irrigated terrace area (21.93 t ha^{-1} yr^{-1}). Moreover, there was an increase of 8.5% or 2.03 t ha^{-1} yr^{-1} in the former area (*Figure 2; Figure 3*) (Lee *et al*., 2008). The increased yield in both areas was dependent on the increase in the bunch number rather than bunch weight.

Corley and Hong (1981) reported an increase of 5% in yield with irrigation on a 12-year-old palm that was planted in the Ulu Tiram and Harimau soil series in Central Johor, Malaysia. The FFB yield increased from 24.7 to 25.8 t ha^{-1} yr^{-1}. In Thailand, a study was conducted in a dry season between December and April, with an average cumulative annual water deficit of 214 mm for over six years (Titinutchanon *et al*., 2000). In the first trial, two rates of drip irrigation were applied: 150 and 300 L $palm^{-1}$ day^{-1} or 2.1 and 4.3 mm rainfall day^{-1}. As for the second trial, irrigation methods, namely drip, sprinkler, micro-spray and contour furrow were tested at three different rates (120, 240 and 360 L $palm^{-1}$ day^{-1}, or 1.7, 3.4 and 5.1 mm day^{-1}). The irrigation was first applied in the seventh year of field planting, and it was found that at 4-5 mm day^{-1}, the irrigation gave a significant increase in the bunch number per palm but not in the mean of the bunch weight. The dry season had caused higher inflorescence abortion, which resulted in a lower bunch number. However, with irrigation, the bunch number improved.

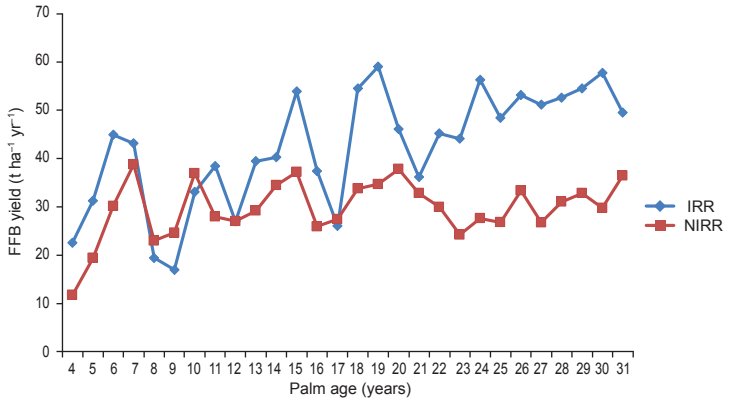

Figure 1. The yearly fluctuation of FFB yields from a single lysimeter study at FELDA's Tun Razak Agricultural Service Centre, Malaysia, where IRR and NIRR denote irrigated and non-irrigated, respectively.

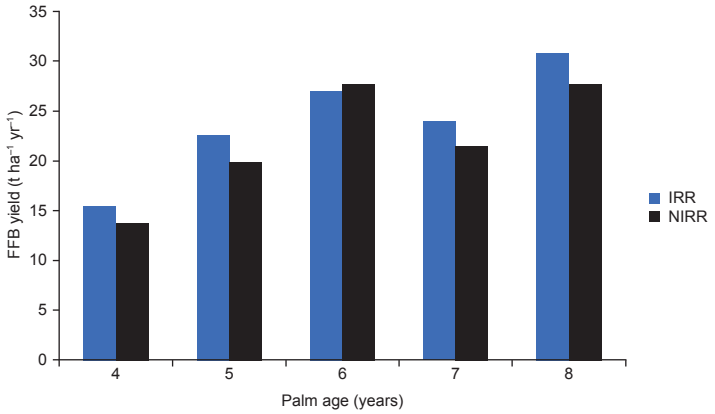

Figure 2. FFB yield from undulating areas with moderate rainfall region in Malaysia with irrigated (IRR) and non-irrigated (NIRR) palms. The mean of extra yield for irrigated palms is about 8%.

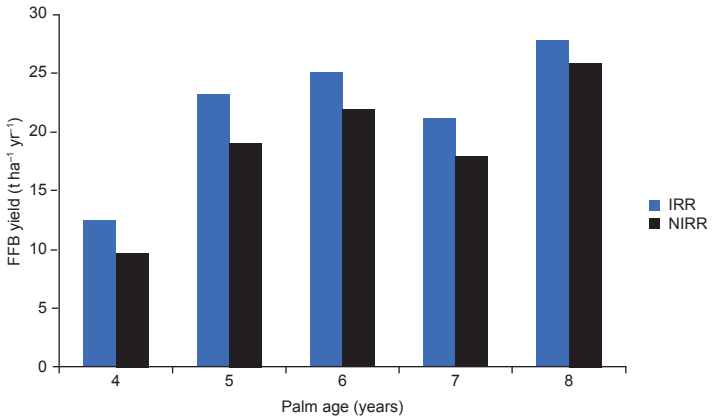

Figure 3. FFB yield from terraced areas with moderate rainfall region in Malaysia with irrigated (IRR) and non-irrigated (NIRR) palms. The mean of extra yield for irrigated palms is about 14%.

Irrigation was only applied when the cumulative water deficit exceeded 30 mm (Roslan and Haniff, 2004b). The FFB yield increase was about 6 t ha^{-1} yr^{-1}. The irrigation showed a significant response, for three out of seven years. Amongst the different irrigation methods, drip and micro-spray irrigation produced higher oil to bunch as compared to those in-furrow and sprinkler irrigation (Roslan and Haniff, 2004b). A review of 15 years of oil palm irrigation implementation in Southern Thailand concluded that the average yield response due to irrigation was about 10 t FFB ha^{-1} yr^{-1} (Tittinutchanon *et al.*, 2000).

Another irrigation trial conducted at La Mé, Ivory Coast revealed that the irrigated plots produced higher yields, which was mainly due to the higher sex ratio and the number of bunches produced per palm (Fairhurst and Härdter,

2003; Hartley, 1988b). In Ouidah, West Africa, a study employed by Chaillard *et al*. (1983) on drip irrigation, used polyethylene tubes which were discharged into irrigation rills dug parallel to the rows of palms. In the first part, the yield was recorded at 20.6 t ha^{-1} yr^{-1} with a residual water deficit of 280 mm in the sex differentiation stage. In the second part, a residual water deficit of 360 mm yielded only 13.9 t ha^{-1} yr^{-1}.

Oil palm is a drought-sensitive crop, especially in areas with a moisture deficit of 400 mm yr^{-1}. It was reported that only half of the yields were obtained in zero deficit areas (Stephen *et al*., 2007). In dry areas with distinctly low rainfall for five to seven months each year, the overall mean FFB yield over nine years of irrigated plots showed a significant increase of 24.4 t ha^{-1} yr^{-1} or 25% higher, as compared to non-irrigated plots at only 18.30 t ha^{-1} yr^{-1} (Lee and Izwanizam, 2013). Irrigation during the seasonal dry period might enhance FFB yield by 56% as compared to no irrigation. However, FFB results in moderately moist areas revealed that irrigated areas provided a minor difference of 9% when compared to those without irrigation (Lee and Izwanizam, 2013; Shahkhirat *et al*., 2012). This implies that selecting suitable areas will have a positive impact on irrigation. Without the right selection of site criteria, this irrigation project will fail to meet its objectives or will take a long time to get a high return on investment (ROI) (Norizan *et al*., 2021).

A study by Darmosarkoro (2010) experienced an increase in spear leaf number and frond fracture. Based on water deficit between 200-500 mm yr^{-1}, the number of spear leaves was between 3-5, while the number of fractured fronds was between 1-16. Cheng-Xu *et al*. (2011) reported on water stress studies, which discovered that fertilisation promoted oil palm growth under well-watered conditions, while the growth was negatively affected in underwater stress conditions.

Soil and Water Conservation Practises in Oil Palm Plantation

Irrigation trials showed that a high volume of water was required for oil palm irrigation. Due to the limitation of water availability, unsuitable terrains and logistics, therefore the most practical approach is to preserve the rainfall water that infiltrates into the soil. The various soil and water conservation practices, following forest clearing and replanting, which could reduce water evapotranspiration are summarised below.

Biomass management during replanting. The growth of palms that were planted in residual piles was greater than those planted without biomass, indicating higher fertility in the piles with residues (Khalid *et al*., 1996; 2000a). The mulched areas showed excellent soil structural properties and were rich in organic matter. Crop residue applications can also improve soil moisture-holding capacity. The mulching showed a more definite effect on soil moisture at the initial treatment but gradually decreased with the decomposition of residues. Khalid *et al*. (2000a) recorded significantly higher soil moisture content in the treatment plots with residues during dry periods, such as chipping and pulverisation, as compared to the control plots. The size to which the residues were chopped affects their decomposition rate and directly affected the mulching method that was used to hold the soil moisture. For example, pulverised materials decompose faster than chopped materials, shortening the effect of the mulching on soil moisture.

Terracing and silt pits. Soil erosion is greatly associated with slope steepness, whereby the rate increases with increasing slope gradient. For example, in the second to the fourth year after oil palm planting, the erosion rates on Munchong series soil, with newly established legume ground covers, were 8.8, 24.0, 35.4 and 50.0 t ha^{-1} yr^{-1} on slopes of 2°, 5°, 9° and 15°, respectively (DID, 1989). This has caused the building of terraces with an adequate back slope and stops bund at regular intervals along the planting and conservation terraces. Soil erosion and run-off can be very severe, even with terraces. Therefore, it is recommended to have silt pits in such areas to reduce the path of water flow, increase water infiltration into the soil, and maximise moisture conservation (Turner and Gillbank, 1974). The construction of silt pits is another typical soil and water conservation strategy in oil palm plantations (Lim, 1989; Soon and Hoong, 2002). The dimensions of silt pits are often 1.2-3.0 m long, 0.6-1.0 m deep and 0.9-1.0 m wide (Lim, 1989; Ramli *et al*., 2016; Soon and Hoong, 2002) built between planting rows and perpendicular to the hill slope direction. Silt pits intend to capture runoff water that contains eroded sediments and nutrients that would otherwise be lost. Following the rainfall event, the collected water and nutrients are redistributed back into the plant root zone around the pits. During land preparation, *Mucuna bracteata* (MB) should be integrated with silt pits or water retention trenches. The length of silt pits varies based on the existing slope and frond placement procedure, but they should be capable of trapping more surface runoff down a slope. When MB and silt pits are used simultaneously, rainwater loss is reduced by 44.83%, illustrating the effectiveness of silt pits in capturing rainwater caused by surface runoff on slopes compared to solely planting legumes. As a result, the combination of MB and silt pits effectively lowers water loss via surface runoff (Afandi *et al*., 2021). Construction of humps and sumps, silt pits in old and new replanting,

conservation terraces, planting platforms and *Ganoderma* pits, all of which can be utilised to collect rainwater and benefit the palms later, are some of the options for harvesting rain in rain-shadow environments (Ramli *et al*., 2016).

Establishment of leguminous cover crops and mulching. Legume cover crops need to be established to fully cover the soil as quickly as possible after land preparation. The cover crops could reduce soil erosion and water evapotranspiration and help to improve soil structure and water holding capacity. Besides this, legume cover will also improve soil fertility, soil physical properties and soil microbiological activities (Chan *et al*., 1977). Furthermore, legume cover crops are useful during dry seasons where they improve water infiltration as well as soil temperature reduction (Giller and Fairhurst, 2003). Studies by Khalid *et al*. (2000b) reported the total dry matter of legumes and weeds in the plantation were approximately 5370 and 1930 kg ha^{-1}, respectively. The nutrient contents in the legumes were quite high, recorded at 113 kg N ha^{-1}, 11 kg P ha^{-1}, 106 kg K ha^{-1}, 28 kg Ca ha^{-1}, and 9 kg Mg ha^{-1}. Therefore, the nutrients in legume cover and weeds will become the transient pool that is recycled in the plantation.

Gurmit *et al*. (1989) did an in-depth study of the empty fruit bunch (EFB) advantages of oil palm growth and productivity, including soil properties improvement. The expected organic mulching benefits with EFB included improved soil structure, increased in water holding capacity, improved soil pH and nutrient status, increased in cation exchange capacity, better root growth, increased microbial activities, and reduction in the surface wash, leaching, and soil surface temperature. All these benefits could improve oil palm growth and productivity. EFB was found to minimise erosion and run-off from bare soil around the palm and reduce soil moisture evaporation, especially during the dry months (Lim and Messchalck, 1979). However, the EFB mulching benefits would taper off over time as it decomposes. It is probably ineffective in conserving soil moisture after about 240 days from the time of application. Therefore, re-mulching is necessary after about 200 days to conserve soil moisture effectively (Arif *et al*., 2003).

CONCLUSION

Oil palm growth and yield depends on adequate water supply and evenly distributed rainfall. Uneven rainfall distribution or rainfall shortage could lead to yield fluctuation and thus, decrease the chance to obtain the potential yield. Cultivation of oil palm in regions with prolonged dry seasons or uneven distribution of rainfall could be successful if an adequate source of water is available for irrigation. However, an irrigation system implementation is only economically viable and feasible if the FFB yield increases, which could be achieved through adequate nutrient management and other crop care practices. Drip irrigation was proven to be the most effective method. Combining this method with a fertigation system can be used to maximise the oil palm yield because it can effectively reduce nutrient losses and increase nutrient uptake. This implementation can also help to reduce field supervision and labour shortage in the plantation. Other practices, such as mulching and cover crops, might also be carried out to conserve soil moisture, overcome rainfall shortages and improve soil fertility.

ACKNOWLEDGEMENT

The authors would like to thank the Director-General of MPOB for permission to publish this article.

REFERENCES

Afandi, A M; Khalid, H; Norman, K and Zulkifli, H (2013). Report on irrigation of oil palm at Univanich Palm Oil, Aoluk, Krabi, Southern Thailand. *MPOB Report No 251*. Apr. 24, 2013. 16 pp.

Afandi A M; Zulkifli, H and Norliyana Z Z (2021). Soil erosion and nutrient losses from slopes under oil palm. *Internal Report MPOB Viva No 286/2021*. 25 pp.

Arif, S; Goh, K J and Teo, C H (2003). Temporal soil moisture contents on a hilly slope under oil palm as influenced by soil conservation practices. *Proc. of the Malaysian Society Soil Science Conference 2003*. Malaysian Society of Soil Science, Kuala Lumpur. p. 33-40.

Arifin, T; Tengku Ariff, T A and Mohd, Y A M (2002). Stabilization of upland agriculture under *El Niño* induced climatic risk: Impact assessment and mitigation measures in Malaysia. *CGPRT Centre Working Paper No. 61*. 105 pp.

Burt, C M; Clemmens, A J; Strelkoff, T S; Solomon, K H; Bliesner, R D; Hardy, L A; Howel, T A; and Eisenhauer, D E (1997). Irrigation performance measures: Efficiency and uniformity. *J. Irrig. Drain. Eng., 123(6):* 423-442.

Caliman, J P (1992). Oil palm and water deficit, production, adapted cropping techniques. *Oleagineaux., 47(5)*: 205-216.

Caliman, J P and Southworth, A (1998). Effect of drought and haze on the performance of oil palm, *International Oil Palm Conference*, PT Smart Corporation, Bali, Indonesia. p. 1-20.

Carr, M (2011). The water relations and irrigation requirements of oil palm (*Elaeis guineensis*): A review. *Exp. Agr., 47*: 629-652.

Chaillard, H; Daniel, C; Houeto, V and Ochs, R (1983). Oil palm and coconut irrigation. A 900 ha experiment in the Benin's Republic. *Oleagineux., 38(10)*: 519-533.

Chan, K W (1979). Irrigation of oil palm in Malaysia (Pushparajah, E ed.). *Proc. of the Symp. of Water in Malaysia Agric*. Malaysian Society of Soil Science, Kuala Lumpur. p. 103-116.

Chan, K W; Rajaratnam, J A and Law, I H (1977). Ground cover management and its effects on soil physical properties under oil palm cultivation (Lal, R ed.). *Soil Tillage and Crop Production*. Ibadan, Nigeria. p. 235-246.

Chan, K W; Yee, C B; Lim, K C and Goh, M (1985). Effect of rainfall and irrigation on oil palm yield production (Mok, C K; Lim, K H and Azmi, Mt A eds.). *Proc. of the National Conference on Soil Climate Relationship on Crop Production in Malaysia*. Malaysian Society of Soil Science, Kuala Lumpur. p. 43-67.

Chang, K C and Rao, V (1983). An estimation of the rainfall retention by an oil palm canopy. *PORIM Bulletin., 6*: 12-13.

Cheng-Xu, S; Hong-Xing, C; Hong-Bo, S; Xin-Tao, L and Yong, X (2011). Growth and physiological responses to water and nutrient stress in oil palm. *Afr. J. Biotechnol., 10(51)*: 10465-10471.

Chow, C S (1992). The effects of season, rainfall and cycle on oil palm yield in Malaysia. *Elaeis., 4(1):* 32-43.

Claude, B; Norhazela, S; Shahrakbah, Y; Cheah, S S and Mohamad Nazeeb, A T (2013). An improved method for estimating soil moisture deficit in oil palm (*Elaeis guineensis* Jacq.) areas with limited climatic data. *J. Agric. Sci., 5(8)*: 57-65.

Corley, R H V (1973). Midday closure of stomata in the oil palm in Malaysia. *MARDI Research Bull., 2*: 1-4.

Corley, R H V (1976). Photosynthesis and productivity. *Oil Palm Research* (Corley, R H V; Hardon, J J and Wood, B J eds.). Elsevier Scientific, Amsterdam. p. 55-76.

Corley, R H V (1996). Irrigation of oil palms - A review. *J. Plant. Crops., 24*: 45-52.

Corley, R H V and Hong, T K (1981). Irrigation of oil palm in Malaysia. *Int. Conf. on the Oil Palm in Agriculture in the Eighties (*Pushparajah E and Chew, P S eds.). Incorporated Society of Planters, Kuala Lumpur. p. 343-356.

Corley, R H V and Hong, T K (1982). Irrigation of oil palms in Malaysia. *Oil Palm in Agriculture in the Eighties Vol. 2 (*Pushparajah, E and Chew, P S eds.). Incorporated Society of Planters, Kuala Lumpur. p. 343-356.

Corley, R H V and Tinker, P B (2003). *The Oil Palm.* 5th edition. Wiley-Blackwell Science, Oxford. 680 pp.

Darlan, N H; Siregar, H H and Murtilaksomo, K (2010). Microclimates parameters on oil palm drought region. *International Oil Palm Conference*. Yogyakarta.

Darmosarkoro, W (2010). Facing climate change issue on the oil palm industry. *Proc. of 2010 International Oil Palm Conference*. Yogyakarta. p. 78-89.

DID (1989). Sungai Tekam experimental basin trial report July 1977 - July 1986. *Water Resource Publication No. 20*. Ministry of Agriculture, Kuala Lumpur. 93 pp.

Dislich, C; Keyel, A C; Salecker, J; Kisel, Y; Meyer, K M; Auliya, M and Wiegand, K (2017). A review of the ecosystem functions in oil palm plantations, using forests as a reference system. *Biol. Rev. Camb. Phil. Soc., 49*: 1539-1569.

Dufrene, E (1989). *Photosynthese, consommationeneau et modelisation de la production chez le palmier a huile* (Elaeis guineensis *Jacq*.). These de Docteuren Sciences, Universite Paris-Sud Orsay. 154 pp.

Fairhurst, T H and Hardter, R (2003). *Oil Palm: Management for Large and Sustainable Yields.* Potash and Phosphate Institute (PPI), Potash and Phosphate Institute of Canada (PPIC) and International Potash Institute (IPI). p. 345-348.

Fan, Y; Roupsard, O; Bernoux, M; Le Maire, G; Panferov, O; Kotowska, M M and Knohl, A (2015). A sub-canopy structure for simulating oil palm in the Community Land Model (CLM-Palm): Phenology, allocation and yield. *Geosci. Model. Dev., 8*: 3785-3800.

FAOSTAT (Statistics Division of the FAO) (2011). Food and agricultural commodities production (2013) FAO United Nations. http://faostat.fao.org/site/339/default.aspx, accessed on 7 September 2020.

FASSB (2000). Pengaruh Air ke Atas Penghasilan Sawit. *Kemajuan Penyelidikan Bil. 35*. July, 2000. p. 38.

Feddes, R A and van Dam, J C (2005). *Encyclopaedia of Soils in the Environment*. Elsevier. p. 222-230.

Fleiss, S; Hill, J K; Mcclean, C; Lucey, J M and Reynolds, G (2017). Potential impacts of climate change on oil palm cultivation: A science-for-policy. pp. 1-16. http://www.sensorproject.net/wp-content/uploads/2018/01/Climate-change-reportFINAL.pdf, accessed on 12 September 2021.

Foong, S F and Lee, C H (2000). Increasing oil palm productivity with irrigation – FELDA's experience. *Proc. of the International Planters Conference*. Incorporated Society of Planters, Kuala Lumpur. p. 277-301.

Gawankar, M S; Devmore, J P; Jamadagni, B M; Sagvekar V V and Hameed Khan, H (2003). Effect of water stress on growth and yield of *Tenera* oil palm. *J. Appl. Hort., 5(1)*: 39-40.

Gerritsma, W and Wessel, M (1997). Oil palm: Domestication achieved? *NJAS, 45*:463-475.

Giller, K E and Fairhurst, T (2003). Legume cover plant. *Oil Palm Management for Large and Sustainable Yields* (Fairhurst, T, and Hardter, R eds.). p. 151-161.

Goh, K J (1995). Managing soils for plantation tree crops (part 1) - General soil management. *Soil Survey and Management of Tropical Soils*. *Malaysian Society of Soil Science*. Kuala Lumpur. p. 228-245.

Gurmit, S; Manoharan, S and Toh, T S (1989). United Plantations approach to palm oil mill by-product management and utilization. *International Palm Oil Development Conference*. Kuala Lumpur. p. 225-234.

Hanaa, M D; Celestina, M G P and Jose, M G (2014). Drip *vs.* surface irrigation: A comparison focussing on water saving and economic return using multicriteria analysis applied to cotton. *Biosyst. Eng., 122*: 74-90.

Haniff, M H and Roslan, M M N (2002). Fruit set and oil palm bunch components. *J. Oil Palm Res., 14(2)*: 24-33.

Haniff, M H; Tarmizi, A M; Roslan,M M N; Kushairi, A D; Jusoh, L; Rahima, A S and Ramli, A (2010). Impact of *El Nino* occurrence on oil palm yield in Malaysia. *The Planter, 86*: 837-852.

Hartley, C W S (1988a). *The Oil Palm*. Longman Scientific and Technical, Harlow, England. p. 96-110.

Hartley, C W S (1988b). The preparations of land for oil palm plantations. *The Oil Palm Tropical Agriculture Series* (Wrigley, G ed.). Logman, London. 382 pp.

Henson, I E (1991). Limitations to gas exchange, growth and yield of young oil palm by soil water supply atmospheric humidity. *Soc. Pl. Physiol., 2*: 39-45.

Henson, I E and Chang, K C (1989). Evidence for water as a factor limiting the performance of field palms in West Malaysia. *Proc. of the 1989 International Palm Oil Developments Conference.* PORIM, Bangi. p. 478-498

Henson, I E; Roslan, M M N, Hanif, M H; Zuraidah, Y and Aishah, S N M (2005). Stress development and its detection in young oil palms in North Kedah, Malaysia. *J. Oil Palm Res., 17*: 11-26.

Henson, I (2009). Modelling dry matter production, partitioning and yield of oil palm. OPRODSIM: A mechanistic simulation model for teaching and research. MPOB, Bangi. 92 p.

Hodgson, A S; Constable, G A; Duddy, G R and Daniells, I G (1990). A comparison of drip and furrow irrigated cotton on cracking clay soil. *Irrig. Sci., 11*: 143-148.

Hoekstra, A Y and Chapagain, A K (2007). Water footprints of nations: Water use by people as a function of their consumption pattern. *Water Resour. Manag., 21(1)*: 35-48.

Hoekstra, A Y and Chapagain, A K (2008). *Globalization of Water: Sharing the Planet's Freshwater Resource*. Blackwell Publishing, Oxford, United Kingdom. 220 pp.

Hoekstra, A Y (2003). Virtual water trade. Value of water research report series no.12. *Proc. of the International Expert Meeting on Virtual Water Trade*. Delft, Netherlands. 248 pp.

Hoekstra, A Y; Chapagain, A K; Aldaya, M M and Mekonnen, M M (2011). *The Water Footprint Assessment Manual. Setting the Global Standard.* Earthscan, London. UK. 228 pp.

Hoffmann, M P; Castaneda, V A; van Wijk, M T; Giller, K E; Oberthür, T; Donough, C and Whitbread, A M (2014). Simulating potential growth and yield of oil palm (*Elaeis guineensis*) with PALMSIM: Model description, evaluation and application. *Agric. Syst., 131*: 1-10.

Howell, T A; Meron, M; Davis, K R., Phene, C J and Yamada, H (1987). Water management of trickle

and furrow irrigated narrow row cotton in the San Joaquin Valley. *Appl. Eng. Agric., 3(2)*: 222-227.

Huth, N I; Banabas, M; Nelson, P N and Webb, M (2014). Development of an oil palm cropping systems model: Lessons learned and future directions. *Environ. Model. Softw., 62*: 411-19.

Jazayeri, S M; Méndez, Y D R; Camperos-Reyes, J E; and Romero, H M (2015). Physiological effects of water deficit on two oil palm (*Elaeis guineensis* Jacq.) genotypes. *Agron. Colom., 33(2)*: 164-173.

Kallarackal, J (1996). Water relations and photosynthesis of the oil palm in Peninsular India. *KFRI Research Report 110*. Kerala Forest Institute, Peechi, Thrissur. 94 pp.

Kallarackal, J; Jeyakumar, P and George, S J (2004). Water use of irrigated oil palm at three different arid locations in Peninsular India. *J. Oil Palm Res., 16(1)*: 45-53.

Kee, K K and Chew, P S (1991). Oil palm response to nitrogen and drip irrigation in a wet monsoonal climate in Peninsular Malaysia. *Proc. of the 1991 PORIM International Palm Oil Conference*. PORIM, Bangi. p. 321-339.

Kee, K K; Goh, K J and Chew, P S (2000). Water cycling and balance in mature oil palm agroecosystem in Malaysia. *Proc. of the International Planters Conference*. p. 251-269.

Khalid, H; Zin, Z Z and Anderson, J M (2000a). Soil nutrient dynamics and palm growth performance in relation to residue management practices following replanting of oil palm plantations. *J. Oil Palm Res., 12(1)*: 25- 45.

Khalid, H; Zin, Z Z and Anderson, J M (2000b). Nutrient cycling in an oil palm plantation: The effects of residue management practices during replanting on dry matter and nutrient uptake of young palms. *J. Oil Palm Res., 12(2)*: 29-37.

Khalid, H; Zin, Z Z and Anderson, J M (1996). Management of palm residues using various replanting techniques in oil palm plantations (Ariffin, D; Mohd Basri, W; Rajanaidu, N; Mohd Tayeb, D; Paranjothy, K; Cheah, S C; Chang, K C and Ravigadevi, S eds.). *Proc.of the 1996 PORIM International Palm Oil Congress*. PORIM, Bangi. p. 24 -253.

Kumar, B U (1997). Water management of oil palm at different evapotranspiration replenishment rates under drip irrigation. *Indian Oil Palm J., 6(36)*: 249-252.

Lee, C T; Izwanizam, A and Nga, S K (2008). Water management for oil palm on inland soils in Peninsular Malaysia (Hamdol, J; Goh K. J; Che Fauziah I; Lulie, M; Osumanu, H A; Mahomadu, B J; Alexander, S and Siva, B eds.). *Proc. of the Soil Science Conference of Malaysia 'Peat and other soil factors in crop production'*. Malaysian Society of Soil Science, Kuala Lumpur. p. 233-247.

Lee, C T and Izwanizam, A (2013). Lysimeter studies and irrigation of oil palm in some inland soils of Peninsular Malaysia - FELDA's experience. *The Planter, 89 (1042)*: 15-29.

Lim, K H and Messchalck, G (1979). Moisture conservation and distribution in a soil profile through mulching and their effects on some soil properties and yield of cowpeas (Pushparajah, E ed.). *Proc. of the Symposium on Water in Malaysian Agriculture*. Malaysian Society of Soil Science, Kuala Lumpur. p. 69-87.

Lim, K H; Goh, K J; Kee, K K and Henson, I E (2011). Climatic requirements of oil palm. *Agronomic Principles and Practices of Oil Palm Cultivation* (Goh, K J; Chiu, S B and Paramanathan, S eds). Agricultural Crop Trust, Selangor, Malaysia. p. 1-46.

Lim, K H (1989). Soil erosion control under mature oil palms on slopes (Pushparajah E. and Chin S. L. eds). *Proc. 1988 Int. P.O. Dev. Conf. on Soil Sci. and Agric. Dev. In Malaysia*. Malaysian Society of Soil Science, Kuala Lumpur. p. 307-324.

Ling, A H (1979). Some lysimetric measurements of evapotranspiration of oil palm in central Peninsular Malaysia (Pushparajah, E ed.). *Proc. of the Symp. on Water in Malaysian Agriculture.* Malaysian Society of Soil Science, Kuala Lumpur. p. 89-101.

Mekonnen, M M and Hoekstra, A Y (2010). The green, blue and grey water footprint of crops and derived crop product. *Value of Water Research Report Series No. 47*. UNESCO-IHE, Delft, The Netherlands. 24 pp.

Méndez, Y D R; Chacón, L M; Bayona, C J and Romero, H M (2012). Physiological response of oil palm interspecific hybrids (*Elaeis oleifera* HBK Cortes versus *Elaeis guineensis* Jacq.) to water deficit. *Braz. J. Plant Physiol., 24*: 273-280.

Nordiana, A A; Wahid, O and Tarmizi, A M (2008). MPOB geospatial products and mapping services for oil palm plantation management. *MPOB Information Series No. 448*.

Nordiana, A A: Wahid, O; Esnan, A G; Zaki, A; Tarmizi, A M; Zulkifli H and Norman, K (2013). Land evaluation for oil palm cultivation using geospatial information technologies. *Oil Palm Bulletin, 67*: 17-29.

Norman, K; Tarmizi, A and Kushairi, A (2014). Oil palm cultivation: Enhancing sustainable palm oil production. *Palm Oil Familiarisation Programme*. MPOB, Bangi.

Norizan, M S; Wayayok, A; Abdullah, A F; Mahadi, M and Abd Karim, Y (2021). Spatial variations in water-holding capacity as evidence of the need for precision irrigation. *Water 2021, 13(16):* 2208. DOI: 10.3390/w13162208.

Nur Nadia, K and Syuhadatul Fatimah, O (2016). Climate variability and its impact on the palm oil industry. *Oil Palm Industry Economic Journal, 16(1)*: 18-30.

Ochs, R and Daniels, C (1976). Research on techniques adapted to dry regions. *Oil Palm Research* (Corley, R H V, Hardon, C J J and Wood, B J eds.). Elsevier, Amsterdam. p. 315-330.

Palat, T; Nakharin, C; Clendon, J H and Corley, R H V (2008). A review of 15 years of oil palm irrigation research in Southern Thailand. *Indian National Conference on Oil Palm*. Andhra Pradesh, India. p. 537-545.

Paramanathan, S (2003). Land selection for oil palm. *Oil Palm Management for Large and Sustainable Yields* (Fairhurst, T and Hardter, R eds.). Potash and Phosphate Institute, Atlanta. 362 pp.

Paramanathan, S (2013). Managing marginal soils for sustainable growth of oil palms in the Tropics. *J. Oil Palm Env., 4*: 1-16.

Paramanathan, S (2015). Oil palm plantings at high altitudes. *The Planter,* 443-459.

Paterson, R R M; Kumar, L; Taylor, S and Lima, N (2015). Future climate effects on suitability for growth of oil palms in Malaysia and Indonesia. *Sci. Rep., 5*: 1-11.

Paterson, R R M and Lima, N (2018). Climate change affecting oil palm agronomy, and oil palm cultivation increasing climate change, require amelioration. *Ecol. Evol., 8*: 452-461. DOI: 10.1002/ece3.3610.

Piyanon, K and Shabbir, G (2013). A review of the water footprint of biofuel crop production in Thailand. *J. Sustain. Energy Environ., 4*: 45-52.

PORIM (1993). Existing and potential oil palm areas in Peninsular Malaysia. *PORIM Occasional Paper No. 29*: 25pp.

Ramli, A M; Kumar, K and Yusof, M Z (2016). Harnessing rainwater: Ladang Perlating Jerneh's experience. *The Planter, 92 (1084)*: 445-455.

Rao, C S M; Rao, B N; Vijaya, B V; Suresh, K and Kalpana, S (2018). Influence of different methods and levels of irrigation on photosynthetic pigments in relation to yield of oil palm (*Elaeis guineensis* Jacq.). *Int. J. Curr. Microbiol. App. Sci. 7(02)*: 26-35. DOI: 10.20546/ijcmas.2018.702.005.

Roslan, M M N and Haniff, M H (2004a). Importance of water use efficiency (WUE) in oil palm productivity. *Oil Palm Bulletin, 48*: 24-30.

Roslan, M M N and Haniff, M H (2004b). Water deficit and irrigation in oil palm: A review of recent studies and findings. *Oil Palm Bulletin, 49*: 1-6.

Roslan, M M N; Haniff, M H; Tarmizi, A M; Kushairi, A and Choo, Y M (2013). Water for oil palm: Water management. *The Planter, 89 (1044)*: 171-177.

Roslan, M M N; Haniff, M H and Nur Maisarah, J (2011). Physiological plant stress and responses in oil palm. *Oil Palm Bulletin, 62*: 25-32.

Shahkhirat, M N; Umar, M U M J; Izwanizam, A; Romzi, I and Suhaidi, H (2012). An overview of irrigation approaches implemented FELDA. *Proc. of the 4th National Seminar on Oil Palm Mechanisation.* Bangi, Malaysia.

Shanmuganathan, S; Narayanan, A; Mohamed, M; Ibrahim, R and Khalid, H (2014). A hybrid approach to modelling the climate change effects on Malaysia's oil palm yield at the regional scale. *Adv. Intell. Syst. Comput., (287)*: 335-346.

Shiklomanov, I A (2000). Appraisal and assessment of world water resources. *Water Intl., 25(1)*: 11-32.

Smith, B G (1989). The effects of soil water and atmospheric vapour pressure deficit on stomatal behaviour and photosynthesis in the oil palm. *J. Exp. Bot., 40(215)*: 647-651.

Soon, B B F and Hoong, H W (2002). Agronomic practices to alleviate soil and surface runoff losses in an oil palm. MJSS, *6(Special Ed.)*: 53-64.

Srinivas, K (1996). Plant water relations, yield, and water use of papaya (*Carica papaya* L.) at different

evapotranspiration replenishment rate under drip irrigation. *Trop. Agric. (Trinidad), 73*: 4.

Stephen, M; Henk, W and Jan, V (2007). Biophysical land suitability for oil palm in Kalimantan, Indonesia. *ISRIC Report 2007/01*. 28 pp.

Suharyanti, N A; Mizuno, K and Sodri, A (2020). The effect of water deficit on inflorescence period at palm oil productivity on peatland. *The 1st JESSD Symposium: International Symposium of Earth, Energy, Environmental Science and Sustainable Development Indonesia*. Avenue du Hoggar, France. 23 pp.

Teh, C B S and Cheah, S S (2018). Modelling crop growth and yield in palm oil cultivation. *Achieving Sustainable Cultivation of Oil Palm* (Rival, A ed.). Burleigh Dodds Science Publishing, Cambridge, United Kingdom. p. 183-227.

Tittinutchanon, P; Smith, B G; and Corley, R H V (2000). Irrigation of oil palm in Southern Thailand. *Proc. of the International Planters Conference*. p. 303-315.

Turner, P D (1976). The effects of drought on oil palm yields in Southeast Asia and South Pacific region. *Proc. of the Malaysian Developments in Oil Palm Conference*. Kuala Lumpur. p. 673-694.

Turner, P D and Gillbank, R A (1974). *Oil Palm Cultivation and Management*. Incorporated Society of Planters, Kuala Lumpur. p. 145-213.

Wong, C L; Venneker, R; Uhlenbrook, S; Jamil, A B M and Zhou, Y (2009). Variability of rainfall in Peninsular Malaysia. *Hydrol. Earth Syst. Sci. Discuss.*, *6*: 5471-5503.

Woittiez, L S; Wijk, M T V; Slingerland, M; Noordwijk, M V and Giller, K E (2017). Yield gaps in oil palm: A quantitative review of contributing factors. *Europ. J. Agronomy. 83*: 57-77.

Zulkifli, H; Halimah, M; Vijaya, S and Choo, Y M (2014). Water Footprint: Part 2 - FFB production for oil palm planted in Malaysia. *J. Oil Palm Res. 26(4)*: 282-291.

Journal of Oil Palm Research Vol. 35 (3) September 2023 p. 406-415
DOI: https://doi.org/10.21894/jopr.2022.0041

SURFACE PROPERTIES AND AGGREGATION BEHAVIOUR OF HEXADECYLTRIMETHYLAMMONIUM BROMIDE-PALM-BASED CAPRYLIC ACID MIXED SURFACTANT SYSTEMS

WEN HUEI LIM[1]* and XIOU SHUANG YONG[1,2]

ABSTRACT

Surface properties and aggregation behaviour of mixed surfactant systems with varying molar ratios of hexadecyltrimethylammonium bromide (HTAB) and palm-based caprylic acid (OA) were studied in the present work. The critical micelle concentration (CMC), surface excess concentration (Γ_{max}), minimum area per molecule (A_{min}), surface pressure at CMC (π_{CMC}), zeta potential and particle size were determined using instrumentations (e.g., *surface tensiometer and particle sizer). CMC of HTAB-OA mixed surfactant systems was about 30% (0.532 mM) to 50% (0.359 mM) lower than HTAB single surfactant system (0.787 mM), indicating better surfactant adsorption efficiency. Results also showed that increasing the molar ratio of OA favoured the formation of micelles at low concentration; thus, lowering both CMC and surface tension. However, Γ_{max} of mixed surfactant systems lowered with OA molar ratio, indicating the mixed surfactant systems tend to form stable ion pairs in bulk solution rather than orientating at the air-water interface. CMC values obtained via surface tension measurement were double confirmed by ultraviolet-visible (UV-VIS) absorbance measurement using dye solubilisation. The particle size of mixed surfactant aggregates (250 ± 50 nm) was 50 times larger than the one found in HTAB surfactant (5.6 ± 0.3 nm). Equimolar mixed surfactant system displayed highest colloids stability and aggregates populations. The results suggested the existence of strong synergism when two oppositely charged surfactants are mixed.*

Keywords: critical micelle concentration, mixed surfactant, particle size, surface properties, zeta potential.

Received: 20 February 2022**; Accepted:** 14 June 2022**; Published online:** 27 July 2022.

INTRODUCTION

Surfactant is an amphiphilic molecule that can adsorb onto surfaces or interfaces and results in remarkable changes in surface tension when present at low concentration (Ahmad *et al*., 2007; Bhattarai *et al*., 2021a; 2021b; Lim *et al*., 2000; Rub *et al*., 2021; 2022). Surfactants have various industrial applications such as pharmaceuticals, cosmetics, detergents, paints, agrochemicals, automobiles, and oil recovery. For practical applications, mixed surfactant systems are preferred over single surfactant. Mixed surfactant systems attract much interest due to their ability to self-aggregate into various microstructures. The mixing of cationic and anionic surfactants has a strong synergistic effect as this combination possesses the highest degree of charged difference (Khan and Marques, 1999). Thus, a lot of effort has been made to better understand this phenomenon.

The synergism of mixed surfactant systems is due to the strong attractive interactions between oppositely charged surfactants (Bergström and Bramer, 2008). Therefore, mixed surfactant systems

[1] Malaysian Palm Oil Board,
6 Persiaran Institusi, Bandar Baru Bangi,
43000 Kajang, Selangor, Malaysia.

[2] Faculty of Biotechnology and Biomolecular Sciences,
Universiti Putra Malaysia,
43400 UPM Serdang, Selangor, Malaysia.

* *Corresponding author email: limwen@mpob.gov.my*

offer better surface activity and display complex phase behaviour. Mixed surfactant systems form aggregates at lower concentrations compared to individual surfactants, giving lower critical micelle concentration (CMC) values (Jiang *et al*., 2014; Tsuchiya *et al*., 2007). In general, headgroups of cationic and anionic surfactants in mixed surfactant systems are attracted strongly to each other and closely packed, giving a low minimum area per molecule (A_{min}) with excess surface concentration (Γ_{max}) (Li *et al*., 2008; Mihelj and Tomašić, 2014). This indicates that mixed surfactant systems have higher surfactant adsorption efficiency and effectiveness.

In aqueous, amphiphilic surfactants self-aggregate into complicated aggregates. Self-aggregation of surfactants can be understood as a mechanism for the hydrophobic tail of surfactant to minimise contact with water, while the hydrophilic headgroup presents the balancing force to prevent surfactant from being expelled completely as the separated phase. Different kinds of aggregates like mixed micelles, vesicles and microemulsion are formed from mixed surfactant systems. The most popular microstructure is a vesicle that can act as a vehicle to carry active ingredients in the pharmaceutical industry (Bramer, *et al*., 2007). The potential application of surfactant vesicles in the pharmaceutical industry as drugs, gene delivery systems and even microreactor attracts the attention of researchers worldwide (Caillet *et al*., 2000; Mauryaa *et al*, 2020; Wani *et al*., 2019a; 2020). Studies showed mixed surfactant systems formed vesicles spontaneously in dilute aqueous solutions (Kaler *et al*., 1989; 1992).

Even though mixed surfactant systems possess good surface properties and complex aggregation behaviour, some studies showed mixing of cationic and anionic surfactants tend to form precipitates, especially at an equimolar ratio of cationic and anionic surfactants (Horbaschek *et al*., 2000; Kaler *et al*., 1992). This may affect their subsequent applications. The studies indicated that characteristics of mixed surfactant systems are affected by two major factors, electrostatic interactions of hydrophilic headgroup and hydrophobic interactions between hydrocarbon chains (Kaler *et al*., 1989; Marques *et al*., 2003; Wani *et al*., 2019b). In other words, surfactants self-aggregate to achieve a better balance of double-layer electrostatic interactions and packing properties, resulting in complex phase behaviour. These two factors are influenced by temperature, molar ratios, the structure of surfactant, chain length, co-solvent, ionic strength, *etc*. (Sohrabi *et al*., 2008).

In previous studies, the solubility of mixed surfactant systems was closely related to headgroup chemistry (Tomašić *et al*., 1991) and the packing of hydrocarbon chains (Silva *et al*., 2007). The mixing ratio of surfactants was found to govern self-aggregation behaviour (Kume *et al*., 2008; Zhao *et al*., 2009). Generally, the tendency of micelles formation increased with surfactant concentration and ionic strength (Hao and Hoffmann, 2004). When ethanol was added to mixed surfactant systems, a significant increase in the synergism effect was observed (Aslanzadeh and Yousefi, 2014; Huang *et al*., 1999). Therefore, a desired mixed surfactant system can be modified with the nature of the compounds to give different attractive interactions, molecular size and phase behaviour.

Understanding the physico-chemical properties of mixed surfactant systems is theoretically and practically important as single surfactants are rarely used in industrial applications. In the present work, we focus on the study of mixed surfactant systems with varying molar ratios of hexadecyltrimethylammonium bromide (HTAB) and palm-based caprylic acid (OA). OA is a natural-existing surfactant, and it exhibits better biodegradability compared to synthetic surfactants. OA is known to have low solubility in water. Interestingly, HTAB-OA mixed surfactant systems showed good surface activity, and OA solubility increased in the mixed surfactant system. CMC and surface pressure at CMC (π_{CMC}) of mixed surfactant systems were determined, Γ_{max} and A_{min} were calculated using Rubingh's theory from surface tension data. CMC was found to be closely related to dye solubility. The effect of different molar ratios HTAB and OA on zeta potential and particle size were also studied.

MATERIALS AND METHODS

Materials

The cationic surfactant, HTAB, purity of 99%, was purchased from Sigma-Aldrich, Switzerland. Anionic surfactant, OA derived from palm oil, purity of 99%, was obtained from Wilmar PGEO Edible Oils Sdn. Bhd., Malaysia. ORASOL dye was obtained from Ciba Specialty Chemicals Inc., Switzerland. All chemicals were used without any treatment. Distilled water having 1.6 μS cm^{-1} was used throughout the experiments.

Methods

Sample preparation. A stock solution of HTAB with a concentration above CMC was prepared. Mixed surfactants were prepared by adding the desired amount of OA into the HTAB solution according to molar ratios 5:1, 5:3 and 1:1. The mixed surfactant systems were kept for 24 hr in a water bath at 30°C and prepared in distilled water.

Surface tension measurement. CMC for HTAB and mixed surfactant systems were determined by

surface tension measurement using the du Nouy ring tensiometer (KSV Sigma 70, Helsinki). Surface tension measurements were tested at 25 ± 0.1°C. The concentration of the surfactant was varied by diluting stock surfactant with water using a Hamilton microsyringe. The measured surface tension values were plotted against surfactant concentration. Before every measurement, the ring was flamed clean.

In general, interfacial properties of surfactants at the air-water interface were studied by measuring the surface excess concentration Γ_{max} , mol m^{-2} (Rosen, 1989; Tadros, 2005; Wong *et al*., 2012). The Γ_{max} value is known as surfactant adsorption effectiveness. The concentration of surfactant is usually higher in the surface monolayer compared to the bulk system. Γ_{max} can be calculated from Gibbs isotherm following Equation (1) below:

$$\Gamma_{max} = - \left(\frac{1}{2.3\, nRT} \right) \left(\frac{d\gamma}{d \ln C} \right) \quad (1)$$

where C is the concentration of surfactant, γ is surface tension, R is gas constant (8.314 J mol^{-1} K^{-1}) and T is the absolute temperature. n prefactor is the number of solute species at the interface whose concentration at the interface changes with the value C.

From Γ_{max} values, we can calculate the minimum area per molecule (A_{min}) at the air-water interface from Equation (2) below:

$$A_{min} = \frac{10^{18}}{\Gamma_{max} N_A} \quad (2)$$

where N_A is Avagadro's number and Γ_{max} and A_{min} are expressed in mol m^{-2} and nm^2, respectively.

UV-VIS measurements. A suitable range concentration of surfactants below and above CMC were prepared in distilled water. Highly concentrated dye in ethanol was transferred into a small vial and ethanol was evaporated. Then, a constant volume of different concentration surfactants was added into the vial containing the excess amount of dye and vortex. After being equilibrated for 24 hr, the surfactant was centrifuged to separate the undissolved dye. The supernatant containing surfactant and dissolved dye were measured using a double-beam UV-VIS spectrophotometer (Varian Cary® 50, USA).

Particle size measurement. The size of surfactant aggregates was determined using the dynamic light scattering (DLS) technique (Malvern Zetasizer Nano S, Malvern, Worcestershire, United Kingdom). The sample was loaded into cuvettes and measured at 25.0 ± 0.5°C after 5 min of thermal equilibration. The light-scattering cells were rinsed with acetone prior to use to ensure it was dust-free. Measurement was performed at λ = 638.2 nm, in back-scattering mode, at cell position 4.65 and attenuator 11. A digital correlator analysed the fluctuations of scattered light intensity. Data obtained were analysed using the CONTIN method.

Zeta potential measurement. Laser-Doppler accessory of DLS equipment was used for zeta potential measurement (Tadros, 2005). The sample was loaded into a U-shape cuvette with gold electrodes and measured at 25.0 ± 0.5°C. Zeta potential was related to electrophoretic mobility, μ and calculated from Equation (3) below:

$$\xi = \mu \left(\frac{4 \pi \eta}{\varepsilon'} \right) \quad (3)$$

where η is the viscosity of the solution and ε′ is the static dielectric constant.

RESULTS AND DISCUSSION

Determination of Critical Micelle Concentration (CMC) of Mixed Surfactant Systems

The surface tension of surfactant decreases significantly with increasing concentration of surfactant until a particular concentration known as CMC (Tadros, 2005). When CMC is achieved, surfactant molecules self-aggregate into larger units known as micelles. The most common technique used for the determination of CMC is the break-in surface tension or electrical conductivity *vs.* concentration curve. In the surface tension against concentration plot, the intersection point of two trend lines is generally used to obtain the CMC of a surfactant solution. CMC in aqueous solution can be greatly affected by surfactant concentrations, temperature, pH, chain length of surfactants, mixtures of surfactants, headgroup chemistry of surfactants and their intermolecular interactions (Kume *et al*., 2008; Marques *et al*., 2003).

The surface tension of different molar ratios HTAB:OA mixed surfactant systems is shown in *Figure 1*. When the concentration of surfactants increases, surface tension decreases rapidly until a breakpoint where it remains almost constant. This level-off point surfactant concentration corresponded to CMC. CMC of HTAB was 0.787 mmol dm^{-3}, comparable to previous studies (Murphy and Taggart, 2002; Wong *et al*., 2012; Zhang *et al*., 2015). *Table 1* shows the CMC of different molar ratios of HTAB:OA mixed surfactant systems.

The surface activity of mixed surfactant systems increased with the increasing molar ratio of OA. All HTAB:OA mixed surfactant systems showed approximately 30% to 50% lower CMC compared to conventional single-tailed surfactant HTAB. The equimolar ratio of HTAB:OA exhibited the lowest CMC of 0.359 mmol dm^{-3}. This implied mixed surfactant systems formed micelle easier than HTAB.

This was supported by previous studies that indicated the effective aggregating ability of mixed surfactants (Jurasin *et al.*, 2013; Wong *et al.*, 2012; Zhao *et al.*, 2009). A recent study also showed binary surfactant system achieved lower CMC than the ideal CMC estimated from the Clint equation and deviated negatively from ideal behaviour (Azum *et al.*, 2016). Increasing the concentration of OA generated a driving force for aggregation to occur and therefore lowered the CMC of the system. This special phase behaviour could be explained by synergistic interactions of mixed surfactant systems. Synergism is more favourable for surfactant mixtures with a higher degree of charge difference (Khan and Marques, 1999). When OA was added, electrostatic interaction within the system was disturbed. The addition of anionic OA reduced electrostatic repulsion force between the cationic headgroup of HTAB in micelles, easing micelle formation. This phenomenon could be described as OA lowered surface charge density of micelles by entering the polar area of micelles (Huang *et al.*, 1999). However, the reduction of charge density at the micellar surface was caused by a higher degree of counterion dissociation in mixed surfactant systems as OA was present in micelle (Aslanzadeh and Yousefi, 2014). The hydrophilicity of the surfactant system decreased with increasing OA; the reduction of hydrodynamic radius enables a more energetically favourable aggregation (Perinelli *et al.*, 2016). Subsequently, fewer surfactant molecules were required to orient at the air-water interface, and hence CMC was lowered.

Generally, one of the common ways to discuss the performance of surfactants is surfactant adsorption efficiency. Surfactant adsorption efficiency refers to the surfactant concentration required to produce a given surface tension reduction at experimental conditions. Mixed surfactant systems containing OA displayed lower surface tension; this showed mixed surfactant systems are highly surface-active under experimental conditions. From this experiment, increasing the molar ratio of OA gave a better surfactant adsorption efficiency.

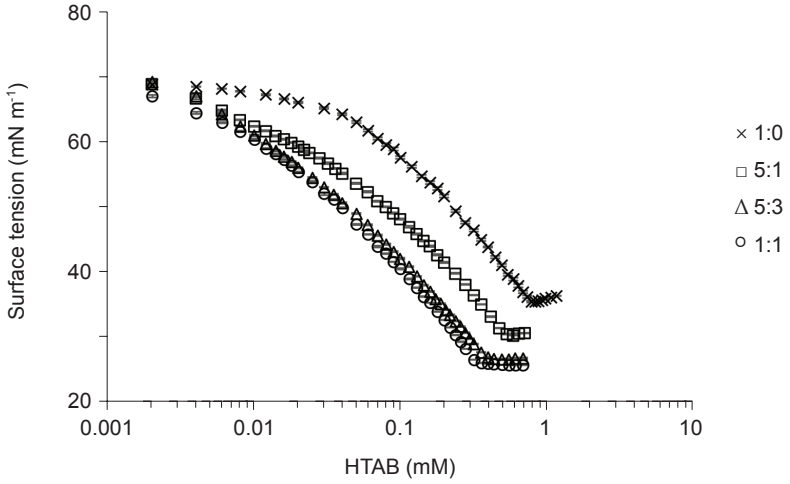

Figure 1. Surface tension measurements of different ratios (cross - 1:0; open square - 5:1; open triangle - 5:3; open circle - 1:1) of HTAB:OA mixed surfactant systems at 25.0 ± 0.5°C.

TABLE 1. CRITICAL MICELLE CONCENTRATION (CMC), SURFACE EXCESS CONCENTRATION (Γ_{MAX}), MINIMUM AREA PER MOLECULE (A_{MIN}) AND SURFACE PRESSURE AT CMC (Π_{CMC}) FOR AQUEOUS HTAB SOLUTION AT DIFFERENT MOLE RATIOS OF OA SYSTEMS AT 25.0 ± 0.1°C

System (HTAB:OA)	CMC (mmol dm^{-3})		$\Gamma_{max} \times 10^{-6}$ (mol m^{-2})	A_{min} ($Å^2$)	$^{\pi}$CMC (mN m^{-1})
	*ST	*A			
1:0	0.787	0.72	2.26	73.54	35.06
5:1	0.532	0.50	2.20	75.58	40.03
5:3	0.396	0.30	2.16	77.04	43.60
1:1	0.359	0.30	2.12	78.17	44.50

Note: *ST and *A* are CMC values obtained from surface tension and absorbance measurements, respectively.

Air/Water Interfacial Properties of Mixed Surfactant Systems

Surfactants lower the surface tension of a solution by forming a monolayer spontaneously at the air-water interface. This is very dependent on the effectiveness of surfactant adsorption, which is another way to discuss the performance of surfactants. Surfactant adsorption effectiveness is defined as the maximum adsorption a surfactant can produce regardless of concentration at given experimental conditions. Γ_{max} and A_{min} were calculated from the Gibbs adsorption equation to determine surfactant adsorption effectiveness. Γ_{max} for all surfactant systems were found to be in the range of 2 to 4 × 10^{-6} mol m^{-2}, which was similar to single-chain surfactant (Tadros, 2005). Hence, all surfactant systems had a high tendency to adsorb onto the air-water interface. All the HTAB-OA mixed surfactant systems have lower Γ_{max} but higher A_{min} than HTAB.

Single-tailed HTAB system showed the highest Γ_{max} of 2.26 × 10^{-6} mol m^{-2} and, consequently, the lowest A_{min}, suggesting HTAB is able to form a more closely packed monolayer at the air-water interface. This is because monomeric tails of HTAB are oriented perpendicularly to the air-water interface in a close-packed arrangement. Increasing OA molar ratio in mixed surfactant systems was followed by a slight decrease in Γ_{max} value, from 2.20 × 10^{-6} mol m^{-2} to 2.16 × 10^{-6} mol m^{-2} and eventually 2.12 × 10^{-6} mol m^{-2} for 5:1, 5:3 and 1:1 of HTAB:OA. The calculated A_{min} values were also in agreement with Γ_{max} values for mixed surfactant systems. A_{min} of mixed surfactant systems increased with the OA molar ratio.

This result further proved the synergistic effect in the HTAB-OA mixed surfactant systems. When the molar ratio of OA increases, OA and HTAB tend to form ion pairs which are stable in bulk solution, reducing the tendency to orient at the air-water interface monolayer. This could be explained in terms of better penetration of the surfactant hydrocarbon molecules chains into the air-water interface (Murphy and Taggart, 2002). Our finding was in parallel with the previous study by Aslanzadeh and Yousefi (2014). A_{min} was found to be higher in the mixed surfactant system, indicating surfactants were closely packed at the air-water interface with an almost perpendicular orientation (Azum *et al.*, 2016). This is, however, in contrast to the previous studies that stated mixed surfactant systems induced effective reduction of A_{min} due to strong interaction between hydrophilic headgroups of cationic and anionic surfactants that are packed densely at the air-water interface (Li *et al.*, 2008; Mihelj and Tomašić, 2014).

Assuming HTAB is arranged perpendicularly to the air-water interface, the effectiveness of adsorption is controlled by the size of the hydrophilic headgroup, especially when the cross-sectional area of the hydrophilic headgroup is larger than that of the hydrophobic chain (Rosen, 1989). More ion pairs formed when the concentration of OA increased. Since cationic and anionic headgroups were held tightly by electrostatic interaction and appeared as a single molecule, the area occupied by the hydrophilic headgroup was larger than a cross-sectional area of the hydrophobic chain. Similarly, as stated earlier, fewer surfactant molecules adsorbed at the surface of saturation, resulting in lower Γ_{max} with higher A_{min}.

π_{CMC} was the reduction of surface tension, closely related to surface tension. Higher π_{CMC} means more reduction of surface tension occurred, so the surfactant was more surface-active. Atoms formed at the outmost layer of the air-water interface play an important role in surface tension. The contribution of the methylene group in surface energy was much greater than the methyl group, resulting in lower π_{CMC}. Even though the area occupied by the methylene group increased more than the methyl group when OA concentration increased, a less compact arrangement of surfactant molecules in a mixed surfactant system leads to a high π_{CMC} value.

From here, we can conclude that the packing and orientation of surfactant molecules at the air-water interface was the main factor affecting the effectiveness of surfactant adsorption. In terms of surfactant adsorption effectiveness, HTAB-OA mixed surfactant systems were less effective as their Γ_{max} is much lower and A_{min} is higher than a single surfactant system.

CMC of Mixed Surfactant Systems from Dye Solubilisation

For several decades, dye solubilisation was used as one of the methods for the determination of CMC (Hartley, 1938). By using UV-VIS spectroscopy, the corresponding absorption peak of dye in the visible light region can be revealed. CMC of surfactants could be obtained by plotting the absorbance of a dye-surfactant solution against surfactant concentration. Similar to surface tension, CMC is the intersection point of two trend lines or the point where absorbance starts to increase. Surfactants with low CMC were generally known to enhance the solubility of hydrophobic compounds, including dye.

CMCs of mixed surfactant systems obtained from absorbance measurement are shown in *Table 1*. The results were in good agreement with CMC obtained from surface tension measurement. CMC of mixed surfactant systems decreased with an increase in OA molar ratio. In the full UV-VIS absorbance spectrum of red dye solubilised in HTAB, the corresponding maximum absorbance (λ_{max}) was 533 nm. All HTAB-OA mixed surfactant

systems had the same red dye solubilisation pattern as HTAB. At concentration below CMC, no solubilisation of red dye occurs and thus, resulting in extremely low absorbance with a plateau trend. When CMC was reached, absorbance increased rapidly with increasing surfactant concentration. This suggested red dye solubilisation took place at the CMC of the surfactant. At CMC, surfactants self-aggregate into micelles, accommodate dye within micelles and dissolve in solution (Tadros, 2005). This clearly indicated that surfactant micelles are responsible for improved dye solubilisation, which had been proven previously (Tehrani-Bagha *et al*., 2013; Tehrani-Bagha and Holmberg, 2013). Decrement of CMC implied more micelles present at constant concentration, and more dye could be accommodated into micelles. Again, the results showed that increased OA concentration in mixed surfactants system improved dye solubilisation, indicating better surface activity.

Determination of Zeta Potential and Particle Size of Mixed Surfactant Systems

Dynamic light scattering measurements were carried out to determine zeta potential and particle size at different molar ratios of HTAB:OA mixed surfactant systems. Zeta potential is one of the commonly used parameters to evaluate the stability of the colloidal system. It is a measure of electrostatic interactions in terms of charge repulsion or attraction between particles. Suspension with low zeta potential is known to be unstable as they aggregate or flocculate readily. Suspension with zeta potential values ± 30 mV or higher is considered to have good colloids stability because the particles tend to repel each other from coagulating. So, zeta potential is the energy barrier that prevents particles from approaching each other.

Results for zeta potential and particle size of different molar ratios HTAB:OA of mixed surfactant systems are shown in *Figure 2-5*. Zeta potential results indicated mixed surfactant systems had greater colloid stability. HTAB cannot form a stable colloid system as it showed low zeta potential. All mixed surfactant systems displayed higher zeta potential than HTAB, but only ratios 5:3 and 1:1 HTAB:OA showed zeta potential higher than 30 mV. The zeta potential of mixed surfactant systems increased with a molar ratio of OA. Therefore, an increase in zeta potential of colloids stability can be attributed to the addition of OA. At a molar ratio 5:1 HTAB:OA, the amount of OA added is still not sufficient to stabilise the colloid system as there are a lot of free HTAB molecules. When more OA was added, more ion pair was formed, and the stability of colloids was enhanced. At the equimolar ratio, zeta potential increased sharply after CMC. This indicates that the aggregates formed were stable. Mixed surfactant systems in the previous study also showed good colloids stability, especially at equimolar ratio (Wu *et al*., 2014).

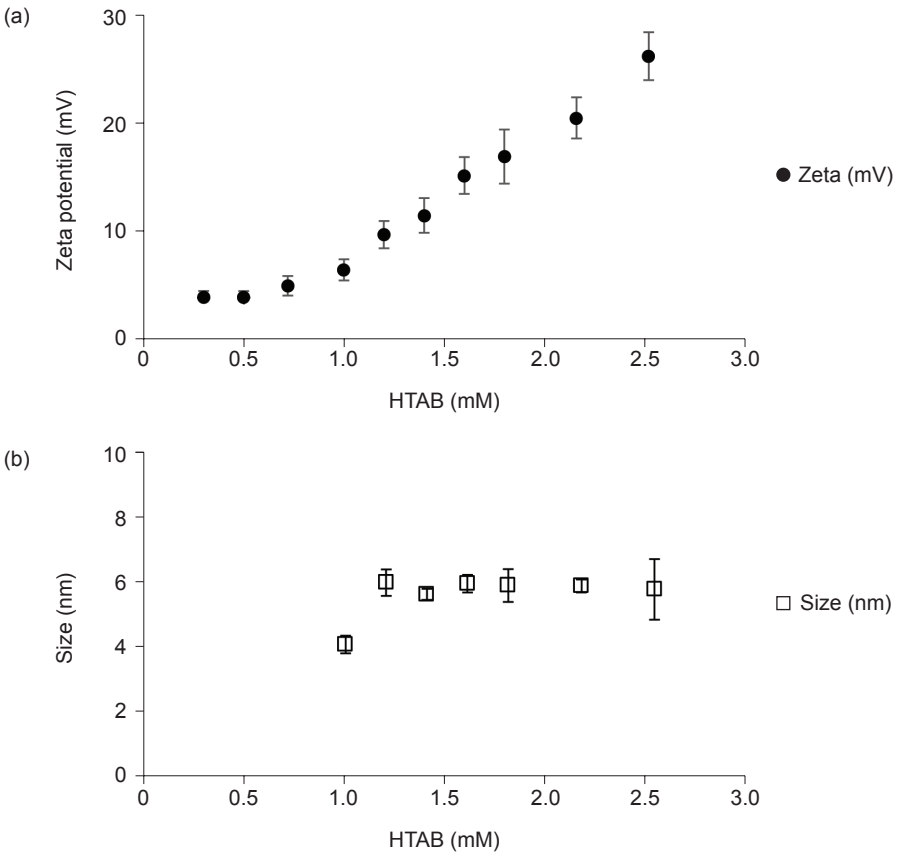

Figure 2. (a) Zeta potential, and (b) particle size measurement of HTAB surfactant solution at 25.0 ± 0.5°C.

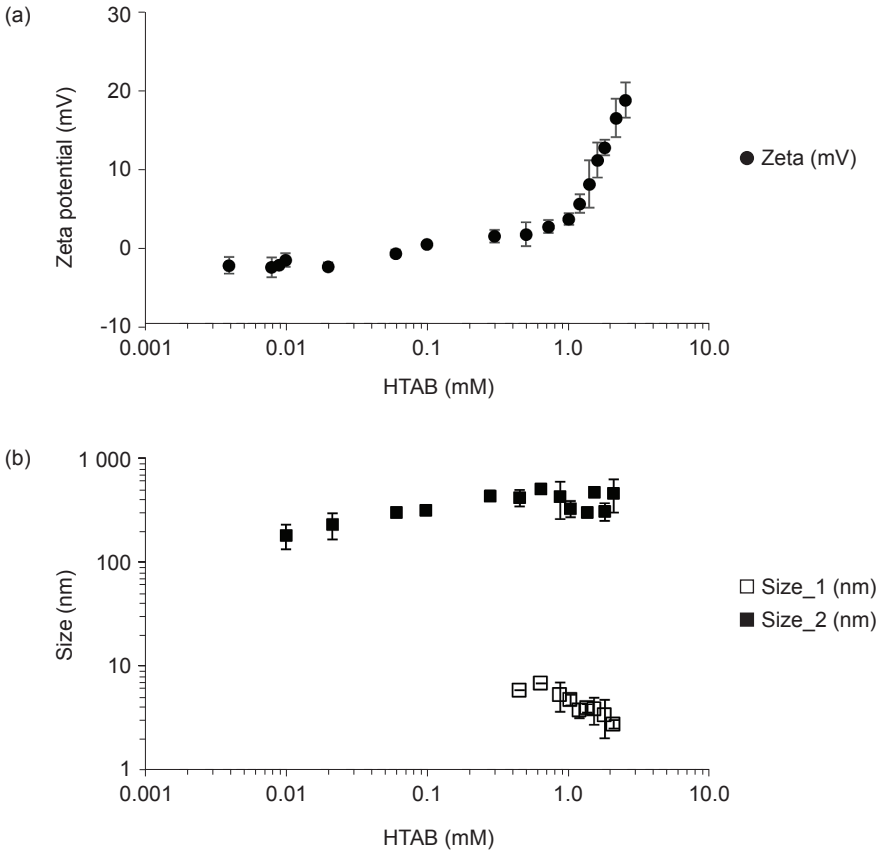

Figure 3. (a) Zeta potential, and (b) particle size measurement of ratio 5:1 of HTAB:OA mixed surfactant systems at 25.0 ± 0.5°C.

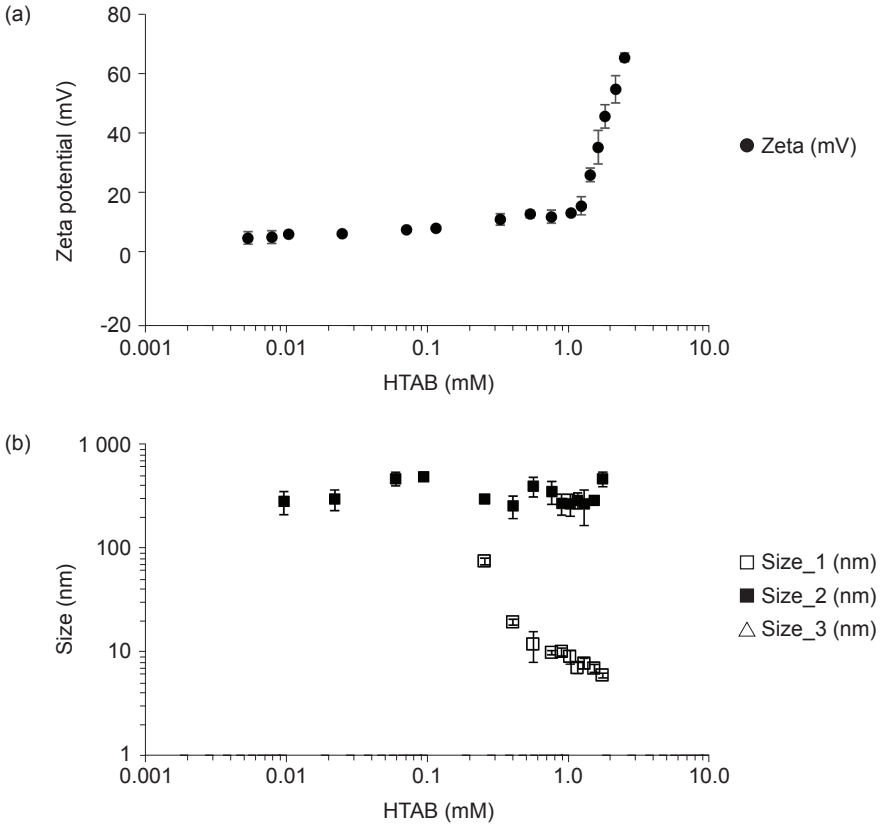

Figure 4. (a) Zeta potential, and (b) particle size measurement of ratio 5:3 of HTAB:OA mixed surfactant systems at 25.0 ± 0.5°C.

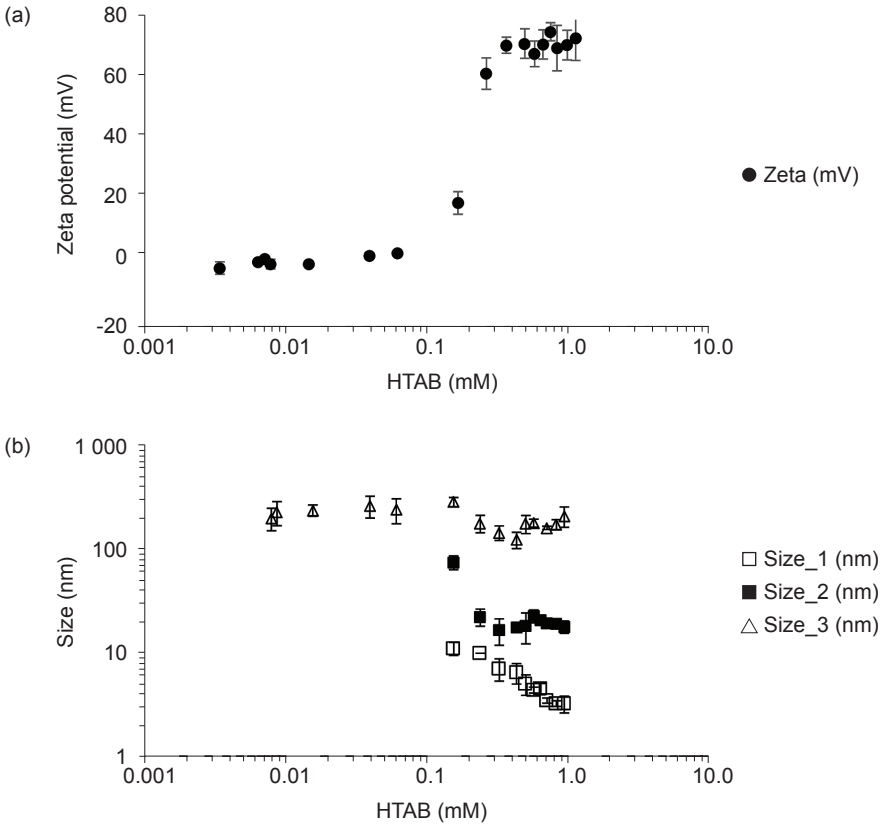

Figure 5. (a) Zeta potential, and (b) particle size measurement of ratio 1:1 of HTAB:OA mixed surfactant systems at 25.0 ± 0.5°C.

For a single HTAB surfactant system, only a type of population was found, and the particle size remained small, less than 10 nm. The particle size increased with increasing of OA. Besides, an increase in OA leads to the appearance of a second population with larger particle size for 5:1 and 5:3 molar ratios HTAB:OA. Interestingly, a third population was discovered with a further increment of OA to equimolar ratio. The previous studies also discovered a second population when the molar ratio of anionic surfactant increased; wide size distribution also implied the existence of phase transition (Aslanzadeh and Yousefi, 2014; Jurasin *et al*., 2013). Other than that, the mixed surfactant system was found to have larger aggregates than simple micelles formed by the pure surfactant system (Nabi *et al*., 2015). We may describe the smallest aggregates as monomer micelles, medium aggregates as unilamellar vesicles and largest aggregates as multilamellar vesicles. This showed that mixed surfactant systems have complex phase behaviour. Herein, we suggested that mixed surfactant systems displayed wider size distribution and colloids stability than HTAB.

CONCLUSION

In this experiment, mixed HTAB-OA surfactant systems exhibited higher surface activity compared to a single surfactant system, HTAB. CMC and surface tension values of the mixed surfactant system decreased with a molar ratio of OA. Interactions within the mixed surfactant systems increased because OA increased the synergism by acting as the driving force for aggregation to occur. In other words, surfactant adsorption efficiency increased with the increasing molar ratio of OA. The mixed surfactant systems with the low CMC enhanced the solubility of hydrophobic dye by accommodating dye molecules into the hydrophobic core of micelles. The mixed surfactant systems exhibited complex phase behaviour with good colloid stability. Among all tested mixed surfactant systems, the equimolar ratio mixed surfactant system was found to have the highest surfactant adsorption efficiency, highest colloids stability and complex phase behaviour (Wani *et al*., 2019b; Wong *et al*., 2012). In conclusion, the addition of OA into the HTAB surfactant system was found to increase the synergism effect of the mixed surfactant system.

ACKNOWLEDGEMENT

The authors would like to thank the Director-General of MPOB for allowing this work to be published and acknowledge the MPOB for the support of this work.

REFERENCES

Ahmad, A; Yeong, S K; Ooi, T L and Ahmad, S (2007). Synergistic effect between sodium lauryl

sulphate and sodium lauryl ether sulphate with alkyl polyglycoside. *J. Oil Palm Res.*, *19(1)*: 332-337.

Aslanzadeh, S and Yousefi, A (2014). The effect of ethanol on nanostructures of mixed cationic and anionic surfactants. *J. Surfactants Deterg., 17(4)*: 709-716.

Azum, N R; Malik, A and Asiri, A M (2016). Micellization and interfacial behavior of binary and ternary mixtures in aqueous medium. *J. Mol. Liq., 216*: 94-98.

Bergström, L M and Bramer, T (2008). Synergistic effects in mixtures of oppositely charged surfactants as calculated from the Poisson-Boltzmann theory: A comparison between theoretical predictions and experiments. *J. Colloid Interface Sci., 322(2)*: 589-595.

Bhattarai, A; Saha, B; Jaffari, Z H; Rub, M A; Alghamdi, Y G and Kumar, D (2021a). Analysis of interaction between glutamic acid and ninhydrin in the presence of acetate buffer solvent: Impact of gemini (twin-headed) surfactants. *Colloids Surf. A: Physicochem. Eng. Asp., 626*: 127061.

Bhattarai, A; Rub, M A; Jaffari, Z H; Saha, B; Thu, H T; Alghamdi, Y G and Kumar, D (2021b). Spectroscopic and conductometric analyses of ninhydrin and threonine reaction in double-headed geminis. *Ind. Eng. Chem. Res., 60(41)*: 14977-14984.

Bramer, T; Dew, N and Edsman, K (2007). Pharmaceutical applications for catanionic mixtures. *J. Pharm. Pharmacol., 59(10)*: 1319-1334.

Caillet, C; Hebrant, M and Tondre, C (2000). Sodium octyl sulfate/cetyltrimethylammonium bromide catanionic vesicles: Aggregate composition and probe encapsulation. *Langmuir, 16(23)*: 9099-9102.

Hao, J and Hoffmann, H (2004). Self-assembled structures in excess and salt-free catanionic surfactant solutions. *Curr. Opin. Colloid Interface Sci., 9(3-4)*: 279-293.

Hartley, G S (1938). The solvent properties of aqueous solutions of paraffin-chain salts. Part I. The solubility of trans-azobenzene in solutions of cetylpyridinium salts. *J. Chem. Soc., 370*: 1968-1975.

Horbaschek, K; Hoffmann, H and Hao, J (2000). Classic Lα phases as opposed to vesicle phases in cationic-anionic surfactant mixtures. *J. Phys. Chem. B., 104(13)*: 2781-2784.

Huang, J B; Mao, M and Zhu, B Y (1999). The surface physico-chemical properties of surfactants in ethanol-water mixtures. *Colloids Surf. A: Physicochem. Eng. Asp., 155(2-3)*: 339-348.

Jiang, Y; Geng, T; Li, Q; Li, G and Ju, H (2014). Phase behavior and phase structure of 1:1 salt-free catanionic surfactant dodecyltrimethylammonium decanoate. *Colloids Surf. A: Physicochem. Eng. Asp., 462*: 27-33.

Jurasin, D; Vincekovic, M; Pustak, A; Smit, I; Bujan, M and Filipovic-Vincekovic, N (2013). Lamellar to hexagonal columnar liquid crystalline phase transition in a catanionic surfactant mixture: Dodecylammonium chloride-sodium bis(2-ethylhexyl) sulfosuccinate. *Soft Matter, 9(12)*: 3349-3360.

Kaler, E W; Murthy, A K; Rodriguez, B E and Zasadzinski, J A (1989). Spontaneous vesicle formation in aqueous mixtures of single-tailed surfactants. *Science, 245(4924)*: 1371-1374.

Kaler, E W; Herrington, K L; Murthy, A K and Zasadzinski, J A N (1992). Phase behavior and structures of mixtures of anionic and cationic surfactants. *J. Phys. Chem., 96(16)*: 6698-6707.

Khan, A and Marques, E F (1999). Synergism and polymorphism in mixed surfactant systems. *Curr. Opin. Colloid Interface Sci., 4(6)*: 402-410.

Kume, G; Gallotti, M and Nunes, G (2008). Review on anionic/cationic surfactant mixtures. *J. Surfactants Deterg., 11(1)*: 1-11.

Li, H; Hao, J and Wu, Z (2008). Phase behavior and properties of reverse vesicles in salt-free catanionic surfactant mixtures. *J. Phys. Chem. B., 112(12)*: 3705-3710.

Lim, W H; Ahmad, S and Ismail, Z (2000). Physico-chemical properties of binary systems of alpha-sulphonated methyl ester derived from palm stearin and nonionic surfactants. *J. Oil Palm Res., 12(2)*: 20-28.

Marques, E F; Regev, O; Khan, A and Lindman, B (2003). Self-organisation of double-chained and pseudodouble-chained surfactants: Counterion and geometry effects. *Adv. Colloid Interface Sci., 100-102*: 83-104.

Mauryaa, N; Imtiyazb, K; Rizvib, M M A; Khedher, K M; Singhe, P and Patel, R (2020). Comparative *in vitro* cytotoxicity and binding investigation of artemisinin and its biogenetic precursors with ctDNA. *RSC Adv., 10*: 24203-24214.

Mihelj, T and Tomašić, V (2014). Amphiphilic properties of dodecylammonium chloride/4-(1-

pentylheptyl) benzene sodium sulfonate aqueous mixtures and study of the catanionic complex. *J. Surfactants Deterg., 17(2)*: 309-321.

Murphy, A and Taggart, G (2002). A comparison of predicted and experimental critical micelle concentration values of cationic and anionic ternary surfactant mixtures using molecular-thermodynamic theory and pseudophase separation theory. *Colloids Surf. A: Physicochem. Eng. Asp., 205(3)*: 237-248.

Nabi, E; Drechsler, M and Gradzielski, M (2015). Phase behaviour and vesicle formation in catanionic mixtures of Na oleate and alkyl trimethyl ammonium bromide and its salt-free version. *Colloid. Polym. Sci., 293(11)*: 3119-3130.

Perinelli, D R; Casettari, L; Cespi, M; Fini, F; Man, D K W; Giorgioni, G and Palmieri, G F (2016). Chemical-physical properties and cytotoxicity of N-decanoyl amino acid-based surfactants: Effect of polar heads. *Colloids Surf. A: Physicochem. Eng. Asp., 492*: 38-46.

Rosen, M J (1989). *Surfactant and Interfacial Phenomena.* 3rd edition. John Wiley and Sons, Inc'. New Jersey. p. 39-122.

Rub, M A; Azum, N; Kumar, D; Arshad, M N; Khan, A; Alotaibi, M M and Asiri, A M (2021). Investigation of solution behavior of antidepressant imipramine hydrochloride drug and non-ionic surfactant mixture: Experimental and theoretical study. *Polymer, 13(22)*: 4025.

Rub, M A; Azum, N; Kumar, D; Alotaibi, M M and Asiri, A M (2022). Impact of numerous media on association, interfacial, and thermodynamic properties of promethazine hydrochloride (PMT) + benzethonium chloride (BTC) mixture of various composition. *J. Mol. Liq., 346*: 118287.

Silva, B F B; Marques, E F and Olsson, U (2007). Lamellar miscibility gap in a binary catanionic surfactant-water system. *J. Phys. Chem. B, 111(48)*: 13520-13526.

Sohrabi, B; Gharibi, H; Tajik, B; Javadian, S and Hashemianzadeh, M (2008). Molecular interactions of cationic and anionic surfactants in mixed monolayers and aggregates. *J. Phys. Chem. B, 112(47)*: 14869-14876.

Tadros, Tharwat F (2005). *Applied Surfactants*: *Principles and Applications.* Wiley-VCH Verlag GmbH & Co. KGaA, Weinheim, Germany. p. 73-84.

Tehrani-Bagha, A R; Singh, R G and Holmberg, K (2013). Solubilisation of two organic dyes by anionic, cationic and nonionic surfactants. *Colloids Surf. A: Physicochem. Eng. Asp., 417*: 133-139.

Tehrani-Bagha, A and Holmberg, K (2013). Solubilisation of hydrophobic dyes in surfactant solutions. *Materials, 6(2)*: 580.

Tomašić, V; Filipović-Vinceković, N; Kojić-Prodić, B and Kallay, N (1991). Precipitation and association in a mixture of dodecylammonium chloride and sodium dodecyl sulfate in aqueous medium. *Colloid Polym. Sci., 269(12)*: 1289-1294.

Tsuchiya, K; Ishikake, J; Kim, T S; Ohkubo, T; Sakai, H and Abe, M (2007). Phase behavior of mixed solution of a glycerin-modified cationic surfactant and an anionic surfactant. *J. Colloid Interface Sci., 312(1)*: 139-145.

Wani, F A; Amaduddin; Aneja, B; Sheehan, G; Kavanagh, K; Ahmad, R; Abid, M and Patel, R (2019a). Synthesis of novel benzimidazolium gemini surfactants and evaluation of their anti-candida activity. *ACS Omega, 4(7)*: 11871-11879.

Wani, F A; Khan, A B; Alshehri, A A; Malik, M A; Ahmad, R and Patel, R (2019b). Synthesis, characterisation and mixed micellisation study of benzene sulphonate based gemini surfactant with sodium dodecyl sulphate. *J. Mol. Liq., 285*: 270-278.

Wani, F A; Behera, K; Padder, R A; Husain, M; Malik, M A; Al-Thabaiti, N S; Ahmad, R and Patela, R (2020). Micellization, anti-proliferative activity and binding study of cationic gemini surfactants with calf thymus DNA. *Colloids Interface Sci. Commun., 34*: 100221.

Wong, S; Lim, W H; Cheng, S F and Chuah, C H (2012). Properties of sodium methyl ester alpha-sulfo alkylate/trimethylammonium bromide mixtures. *J. Surfactants Deterg., 15(5)*: 601-611.

Wu, C J; Kuo, A T; Lee, C H; Yang, Y M and Chang, C H (2014). Fabrication of positively charged catanionic vesicles from ion pair amphiphile with double-chained cationic surfactant. *Colloid. Polym. Sci., 292(3)*: 589-597.

Zhang, S; Ding, S; Yu, J; Chen, X; Lei, Q and Fang, W (2015). Antibacterial activity, *in vitro* cytotoxicity, and cell cycle arrest of gemini quaternary ammonium surfactants. *Langmuir, 31(44)*: 12161-12169.

Zhao, D Y; Li, H G; Song, A X and Hao, J C (2009). Phase behavior and properties of salt-free cationic/anionic surfactant mixtures of oleic acid and stearic acid. *Chin. Sci. Bull., 54(21)*: 3953-3957.

Journal of Oil Palm Research Vol. 35 (3) September 2023 p. 416-425
DOI: https://doi.org/10.21894/jopr.2022.0056

STUDY ON THE EFFECTS OF BLENDING *N*-BUTYL LEVULINATE WITH PALM METHYL ESTER ON THE FUEL PROPERTIES

NUR AAINAA SYAHIRAH RAMLI[1]* and FADZLINA ABDULLAH[1]

ABSTRACT

Alkyl levulinate can be synthesised from renewable levulinic acid and has the potential to be used as a fuel blend component. A variety of compounds can be blended with biodiesel to improve or attain the desired fuel properties. In this study, the effects of blending n-*butyl levulinate (BL) with palm methyl ester (PME) on fuel properties were evaluated. Blends of BL and PME (BL-PMEs) were prepared with 5%, 10% and 15% of BL. The addition of BL has improved the cloud and pour points by 7°C for 15BL-PME. As compared to ASTM D6751 and EN14214 specifications for biodiesel, BL-PMEs revealed properties within the specifications in terms of acid value, flash point, kinematic viscosity (40°C) and oxidative stability. The addition of BL up to 15% increased the acid value and decreased the flash point and kinematic viscosity. The oxidative stability increased slightly upon the addition of BL. The calorific value of BL-PMEs decreased with an increase in BL volume. Up to 10% BL, the calorific value is >35 MJ kg^{-1}. Besides, BL is highly miscible with PME and no phase separation was observed. The present work suggested that BL has potential as a bio-based fuel blend compound for biodiesel.*

Keywords: fuel properties, *n*-butyl levulinate, palm methyl ester.

Received: 9 May 2022**; Accepted:** 2 August 2022**; Published online:** 6 September 2022.

INTRODUCTION

Non-renewable energy generation has compelled the chemical industry to explore alternatives for energy and basic chemical production. Biomass has received significant attention for its potential as an alternative to fossil fuels. One of the promising biomass-derived chemicals is levulinic acid, which can be prepared from biomass through an acid hydrolysis process (Ramli and Amin, 2020). Levulinic acid possesses ketone carbonyl and acidic carboxyl groups which react differently to form a wide range of derivatives, thereby, making levulinic acid an ideal building block chemical.

Alkyl levulinate, or levulinate acid ester, is one of the levulinic acid derivatives, synthesised by direct esterification of levulinic acid with *n*-alcohol (Démolis *et al.*, 2014; Joshi *et al.*, 2011; Unlu *et al.*, 2018; Wang *et al.*, 2017). For instance, *n*-butyl levulinate can be produced from the esterification of levulinic acid with *n*-butanol. Both levulinic acid and *n*-butanol can be obtained from renewable feedstocks, making *n*-butyl levulinate bio-based chemicals. Alkyl levulinates can also be produced by direct conversion of biomass and cellulose; a major component of biomass. For example, the oil palm biomass, such as empty fruit bunch, trunks and oil palm fronds, contains a large amount of cellulose. With cellulose content of 45.2% and 38.2%, theoretical levulinic acid yields of 32.4% and 27.1% could be obtained from oil palm fronds and empty fruit bunch, respectively (Ramli and Amin, 2014). The levulinic acid can be further converted to alkyl levulinate. Alkyl levulinates have the potential to be applied in various areas including as a fuel blend compound, in fragrance and flavour, as a solvent and in the production of fine chemicals (Démolis *et al.*, 2014; Joshi *et al.*, 2011; Ramli and Amin, 2020; Unlu *et al.*, 2018; Wang *et al.*, 2017). Applications of alkyl levulinate have also been explored through their properties as pure fluid and in combination with other compounds (Ramli and Abdullah, 2021).

[1] Malaysian Palm Oil Board,
6 Persiaran Institusi, Bandar Baru Bangi,
43000 Kajang, Selangor, Malaysia.

* *Corresponding author e-mail: aainaa.syahirah@mpob.gov.my*

Biodiesel or fatty acid methyl ester, derived from vegetable oil or animal fat, is a renewable fuel alternative to petroleum diesel fuel. Numerous researches have been conducted on biodiesel production from various feedstocks including palm oil. Comprehensive reviews on palm biodiesel/palm methyl ester (PME) and prospects for the economy, environment, suitability as a bioenergy crop, and its efficiency as a source of renewable fuel can be found in the literature (Mekhilef *et al.*, 2011; Parveez *et al.*, 2021). Some of the less favourable properties of biodiesel are its cold flow properties, such as high cloud and pour points, and low calorific value (Mekhilef *et al.*, 2011; Radhakrishnan *et al.*, 2017). The properties of biodiesel generally depend on the nature of its raw material as well as the technology or process used for its production. The biodiesel standards that are most referred to include European Standard for Biodiesel (EN 14214) and the American Standard Specifications for Biodiesel Fuel (B100) Blend Stock for Distillate Fuels (ASTM D6751) (*Table 1*).

A variety of compounds and additives can be blended with biodiesel to enhance or attain the desired properties (Ali *et al.*, 2014; Cao *et al.*, 2014; Rashedul *et al.*, 2014). Over the years, research has been conducted to produce sustainable and bio-based fuel blend compounds and additives, and investigate their effect on biodiesel properties. As reviewed elsewhere, the compounds can be classified in terms of their point of application such as oxygenated compound, cold flow improver, and cetane number improver (Rashedul *et al.*, 2014). The use of oxygenated compound additives for example alcohol (methanol, butanol, propanol, *etc.*), ether (diethyl ether, diisopropyl ether, *etc.*), and ester (dicarboxylic acid esters and acetoacetic esters) functional groups, is to enhance the combustion quality. The commonly use cold flow improver is vinyl ester co-polymer such as ethylene vinyl acetate, while the cetane number improver includes alkyl nitrates (2-ethyl hexyl nitrate) and peroxides (tertiary butyl peroxide) (Rashedul *et al.*, 2014).

Similar to the oxygenated compounds that are generally used as biodiesel blend components and additives such as alcohol, ether, and ester functional group, alkyl levulinate is also regarded as an oxygenated compound (Christensen *et al.*, 2011b; Rashedul *et al.*, 2014). Several studies have reported the potential of ethyl levulinate to be used as a blend component for biodiesels such as cottonseed oil, poultry fat, canola oil and dairy-washed milk scum biodiesels (Joshi *et al.*, 2011; Srikanth *et al.*, 2017; Unlu *et al.*, 2018). Based on the findings from a previous study, *n*-butyl levulinate (BL) is miscible with diesel when compared to ethyl levulinate with poor solubility thus making the use of ethyl levulinate as a diesel blend component technically challenging (Christensen *et al.*, 2011a). Due to the miscibility factor, BL has been applied as a blend component in fuels containing diesel, gasoline and biodiesel-diesel-butanol-ethanol (Christensen *et al.*, 2011a; 2011b; Hashim *et al.*, 2017). In contrast to the alkyl levulinate with shorter carbon chain lengths such as methyl and ethyl levulinate, *n*-butyl levulinate is expected to have better fuel properties such as higher calorific value and improved low-temperature performance; cloud and pour point. This is supported by the findings of the considerable improvement in low-temperature properties from methyl to butyl for octadecenoic esters, which is explained by the interactions established between the esters (Wang *et al.*, 2020). Nevertheless, no study has been reported about the effect of BL on the neat PME in terms of fuel properties.

Therefore, in the current study, BL is selected for further testing as PME blends. The effect of blending BL with PME on the fuel properties was evaluated. Blends of BL-PMEs were prepared with 5%, 10% and 15% of BL. The effect of BL on acid value, cloud point, pour point, flash point, kinematic viscosity, oxidative stability, and calorific value was determined accordingly. The fuel properties of BL-PMEs were compared with specifications for biodiesel by ASTM D6751 and EN 14214.

TABLE 1. SELECTED SPECIFICATIONS FOR BIODIESEL (ASTM D6751 AND EN 14214)

Property	ASTM D6751		EN 14214	
	Specification[a]	Method	Specification[a]	Method
Flash point, °C	Min. 93	ASTM D93	Min. 101	EN ISO 2719
Kinematic viscosity (40°C), $mm^2 s^{-1}$	1.9–6.0	ASTM D445	3.5–5.0	EN ISO 3104
Density (15°C), kg m^{-3}	-	-	869–900	EN ISO 3675
Cloud point, °C	Report	ASTM D2500	-	EN 23015
Acid value, mg KOH g^{-1}	Max. 0.50	ASTM D664	Max. 0.50	EN 14104
Oxidative stability, hr	Min. 3	EN 14112	Min. 6	EN 14112
Cetane number	Min. 47	ASTM D613	Min. 51	EN ISO 5165

Note: [a] Max. is the maximum value, Min. is the minimum value.

MATERIALS AND METHODS

Materials

Palm methyl ester (PME) or palm-based biodiesel was obtained from Sime Darby Oils, Malaysia. The selected properties of PME are reported in *Table 2*. The commercially available *n*-butyl levulinate (BL) was purchased from Sigma Aldrich, CAS 2052-15-5. The purity of BL (99.4%) has been verified using a gas chromatography-flame ionisation detector (GC-FID) (Ramli and Abdullah, 2021). The materials were of sufficient purity and were used as received without further purification.

TABLE 2. PROPERTIES OF PALM METHYL ESTER (PME)

Parameters	Method	Specification[a]	Value
Water content, mg kg^{-1}	EN ISO 12937	500 max.	257
Acid value, mg KOH g^{-1}	EN 14104	0.50 max.	0.24
Iodine value, g iodine 100 g^{-1}	EN 14111	110 max.	52.68
Ester content, %	EN 14103	96.5 min.	99.89
Density (15°C), kg m^{-3}	EN ISO 12185	860–900	875.2
Flashpoint, °C	EN ISO 2719	120 min.	172
Oxidative stability, hr	EN 14112	10 min.	>15

Note: [a]Max. is the maximum value, Min. is the minimum value.

Methods

Fatty acid profile of PME. The fatty acid methyl esters (FAME) were separated using GC-FID (6890 Agilent) equipped with a capillary column HP-88 (60 m × 250 μm × 0.2 μm). The carrier gas was He at 0.8 mL min^{-1}. The oven temperature was initially held at 150°C, and then programmed to 210°C for 10 min at a rate of 3°C min^{-1}. The injector and detector temperatures were both set at 250°C. The FAME peaks were identified by comparison to known reference standards. Analysis was run in duplicate and mean values were reported.

Preparation of BL-PME blends. Three BL-PME blends were prepared prior to analysis of their properties. The measured quantity of BL was added to PME with constant stirring using a magnetic stirrer for proper mixing. PME was blended with 5%, 10% and 15% of BL. These BL-PMEs were denoted as 5 BL-PME, 10 BL-PME and 15 BL-PME, respectively. Pure samples of BL and PME were kept for control purposes.

Determination of BL, PME and BL-PMEs fuel properties. The properties of BL, PME and BL-PMEs were determined according to standard methods. All analyses were made in duplicate for each sample and the mean value was recorded.

The acid value was determined based on the titration method (mg KOH g^{-1}) according to AOCS Cd 3d-63. The described method is by visual indicator using phenolphthalein, which is similar to EN 14014. The sample was weighed into a conical flask, and 125 mL of the neutralised isopropanol was added, followed by a few drops of phenolphthalein. Complete dissolution of the sample was ensured before titration. The flask was gently swirled while titrated with potassium hydroxide (KOH) standard solution until the appearance of the first permanent pink colour. The acid value was calculated as in Equation (1).

$$\text{Acid value (\%)} = \frac{56.1 \times M \times V}{m} \quad (1)$$

where M is the molarity (M) of KOH solution, V is the volume (mL) of KOH solution and m is the mass (g) of the sample.

Cloud point was determined in accordance with ASTM D2500, using CPP Classic from Normalab (Belgium) to an accuracy of ± 1°C. The sample (50 mL) was cooled in a test jar and was observed at intervals of 1°C decrement. The temperature at which a cloudy structure became visible was noted as the cloud point. The cloud point value was rounded to the nearest whole value (°C).

The pour point was determined in accordance with ASTM D97. Pour point was measured using CPP Classic from Normalab (Belgium) to an accuracy of ±1°C, by placing a test jar containing 50 mL of sample into a cylinder submerged in ethanol (95%) as the cooling medium. The test jar was held in a horizontal position for 5 s at every 3°C decrements and stopped when the sample was no longer flowing within 5 s in a horizontal position. The pour point was taken as 3°C above the temperature at which the sample was no longer flowing. The pour point value was rounded to the nearest whole value (°C).

Flashpoint was determined using Pensky-Martens closed cup method, ASTM D93. The measurement was performed using PMA 5 Automatic Pensky Martens closed-cup flash point tester – Procedure A. The closed-cup tester measures the flash point at the lowest temperature at which the application of an ignition source causes the vapours of a sample to ignite. A test cup is filled with the sample and the lid is then placed on the test cup. Based on the program selected, the sample is heated at 5°C-6°C min^{-1} and stirred at specified rates of 90-120 rpm, and then the ignition source is directed into the test cup.

Kinematic viscosity was obtained using ASTM D445. The test method measures the time

for a volume of liquid to flow under gravity through a calibrated glass capillary viscometer. The measurement was carried out using PMT Tamson NVB Classic (Normalab, France) with a viscometer bath set at 40°C and 100°C. The capillary viscometers and the constant temperature bath were purchased from Cannon Instruments, State College, PA.

The oxidative stability test was performed according to Rancimat method EN 14112 using 743 Rancimat Apparatus (Metrohm, Switzerland). The Rancimat method is an accelerated oxidation test that is run at elevated temperatures and exposes the sample to air. Three grams of sample were heated to 120°C with an airflow rate of 20 L hr^{-1}. The time taken up to the inflection point of conductivity versus the time curve was determined based on the conductimetric method.

The calorific value was determined using a bomb calorimeter Parr 6100 according to ASTM D240. The standardisation of the calorimeter was performed using benzoic acid. The sample was burned in the presence of oxygen inside a sealed container. The heat released from combustion is transferred to a mass of water that surrounds the container. The calorific value represents the gross heat of combustion of the sample.

Data analysis. Data obtained were subjected to analysis of variance (ANOVA) in the IBM SPSS Statistics (Version 23.0). Linear contrasts were used to determine the effects of BL contents on fuel properties using α=0.05. The linear contrast examines whether the BL-PME was significantly different from the control (PME), and whether varying the BL content had a significant effect on the properties. The significance level was accepted at $p \leq 0.05$.

RESULTS AND DISCUSSION

Fatty Acid Composition of PME

The analysis of fatty acid profiles shows that palm methyl ester (PME) contained fatty acids as in *Table 3*. It is reported that biodiesel which contains high saturated fatty acid or low unsaturated fatty acid results in poor cold flow properties; cloud, pour and cold filter plugging point (Lv *et al.*, 2013; Unlu *et al.*, 2018; Verma *et al.*, 2016). In addition, the presence of high unsaturated fatty acid esters makes it prone to autoxidation, which could reduce the oxidation stability. As in the current study, the fatty acid profiles of PME revealed an equal proportion of saturated (49.6%) and unsaturated (50.3%) fatty acids.

TABLE 3. FATTY ACID COMPOSITIONS OF PALM METHYL ESTER (PME)

Fatty acid	Composition (%)
Lauric (C12:0)	0.2
Myristic (C14:0)	1.1
Palmitic (C16:0)	43.5
Palmitioleic (C16:1)	0.2
Margaric (C17:0)	0.1
Stearic (C18:0)	4.3
Oleic (C18:1)	39.8
Linoleic (C18:2)	10.0
Linolenic (C18:3)	0.2
Arachidic (C20:0)	0.4
Eicosenoic (C20:1)	0.1
Others	0.1

Fuel Properties of BL, PME and BL-PMEs

Miscibility is the basic requirement of fuel blends for storage, transportation and utilisation (Wang *et al.*, 2017). In this study, it is implied that *n*-butyl levulinate (BL) is highly miscible with PME. From the visual inspection, no phase separation was observed when blending BL with PME for all fuel blends for more than 72 hr at 25°C-30°C. All samples were stirred well prior to the analysis of each test to ensure the miscibility and homogeneity of BL-PMEs.

As given in *Table 4*, the properties of the control sample PME are within the specified limits by ASTM D6751 and EN 14214 (*Table 1*) for acid value, flash point, kinematic viscosity and oxidative stability. Meanwhile, the properties of BL are within the specifications in terms of acid value, flash point and oxidative stability. The kinematic viscosity of BL did not meet the requirement of EN 14214 but is within the specification of ASTM D6751. The trends and effects of BL addition on BL-PMEs properties are given in the following section.

Effects of BL on Acid Value of BL-PME

Biodiesel composes of fatty acid methyl esters and also small amounts of fatty acids, which are quantified by an acid number, expressed as milligrams of potassium hydroxide required to neutralise 1 g of sample (mg KOH g^{-1}). The high acid value of fuel results in the accumulation of solid particles in the fuel system, which could cause problems in the filters and pumps, and can cause motor corrosion (Unlu *et al.*, 2018).

In this study, the acid value of BL and PME, 0.47 and 0.27 mg KOH g^{-1}, respectively, are within the ASTM D6751 and EN 14214 requirements. As reported in the literatures, the acid value of BL was 0.40 (Christensen *et al.*, 2011a), while the acid value of other alkyl levulinates; ethyl levulinate was 0.16 mg KOH g^{-1} (Lei *et al.*, 2016), 0.36 mg KOH g^{-1} (Joshi *et al.*, 2011) and 0.70 mg KOH g^{-1} (Christensen *et al.*, 2011a). It is presumed that the different

TABLE 4. FUEL PROPERTIES OF BL, PME AND BL-PMES

Vol% BL[a]	Properties[b]						
	AV, mg KOH g^{-1}	CP, °C	PP, °C	FP, °C	KV, mm^2 s^{-1}	OS, hr	CV, MJ kg^{-1}
BL blended with PME[a]							
0	0.27	15	12	174	4.496	13.7	40.3
5	0.28	11	10	159	4.325	14.3	38.7
10	0.31	10	7	151	4.088	14.5	35.1
15	0.33	8	5	143	3.908	14.6	31.4
Control sample[a]							
BL	0.47	<-42	<-42	111	1.997	28.0	27.9
PME	0.27	15	12	174	4.496	13.7	40.3
Contrast[c]							
1[d]	0.011	0.002	0.004	<0.001	0.009	0.001	<0.001
2[e]	0.008	0.047	0.005	<0.001	0.014	0.008	<0.001

Note: [a]BL-*n*-butyl levulinate; PME-palm methyl ester; BL-PMEs-blends of *n*-butyl levulinate with PME; [b]AV-acid value; CP-cloud point; PP-pour point; FP-flash point; KV-kinematic viscosity at 40°C; OS-oxidative stability; CV-calorific value; [c]*p*-value at α=0.05; [d]Whether BL-PME was significantly different from control sample, PME, [e]Whether varying BL from 5% to 15% had significant effect on fuel properties.

acid value reported for alkyl levulinate is due to the residual levulinic acid, as alkyl levulinate is generally prepared from the esterification of levulinic acid (Christensen *et al.*, 2011a). As in this study, BL has been stored prior to testing. This condition may cause oxidation and hydrolysis which resulted in increased acid value (Christensen *et al.*, 2011a). Therefore, the difference in the acid value of BL from this study and literature is possibly due to the partial hydrolysis that occurred during the shelf storage.

The acid value of BL-PMEs was significantly different from PME (p<0.05) and increased visibly as the BL increased from 0% to 15% (*Table 4*). Nevertheless, the maximum addition of 15% BL was found to be within ASTM D6751 and EN 14214. A previous study also reported the increase in acid value on the addition of ethyl levulinate up to 20% in canola oil biodiesel, where a maximum addition of 10% ethyl levulinate was found a suitable amount according to standards for the acid number (Unlu *et al.*, 2018). The increasing trend of acid values may limit the application of the blend component on biodiesel with high acid values (Lawan *et al.*, 2019). However, there is no clear trend in the acid value from the application of ethyl levulinate as a blend component (0%-20%) to cottonseed oil and poultry fat biodiesels (Joshi *et al.*, 2011).

On the other hand, several studies revealed that the addition of a fuel blend component improved the acid value of biodiesel. For example, reduction of acid value by increasing the blend components; ethanol, isopropanol and butanol up to 20% in poultry fat biodiesel (Joshi *et al.*, 2010), 20% of ethyl acetoacetate in waste cooking oil biodiesel (Cao *et al.*, 2014), 20% of ethyl acetoacetate and ethyl levulinate in dairy washed milk-scum biodiesel (Srikanth *et al.*, 2017), and 7% of 1-butanol in palm biodiesel (Ali *et al.*, 2014). It is suggested that the reduction in acid value is because the blend components diluted the free fatty acids present in the biodiesel (Ali *et al.*, 2014; Joshi *et al.*, 2010). From these studies, all blends exhibited acid values that were satisfactory compared to ASTM D6751 and EN 14214.

Effects of BL on Cloud Point and Pour Point of BL-PME

Cloud points and pour points are usually used to assess the cold flow properties of fuels. A cloud point indicates the temperature at which a cloud of wax crystals first appears in a clear liquid product when the liquid is cooled under specified conditions (Hui *et al.*, 2009). The addition of BL to PME generally resulted in lower cloud points (*Table 4*). The BL-PMEs showed a pronounced decrease in cloud point as the BL concentration increased (p<0.05). The BL-PMEs portrayed cloud point reduction of 7°C at 15BL-PME. This may be attributed to the low melting point of BL (<-60°C) (Christensen *et al.*, 2011a), which is much lower compared to the cloud point of PME (15°C).

ASTM D6751 requires cloud point to be reported, while there is no such requirement for cloud point in EN 14214. A similar trend of decreasing cloud points as the blend component's concentration increases has also been reported in various studies. For example, reduction of 15°C for ethyl levulinate-canola oil biodiesel (Unlu *et al.*, 2018), 14°C for ethanol-palm biodiesel (Verma *et al.*, 2016), 9°C for ethyl levulinate- and ethyl acetoacetate-dairy washed milk scum

biodiesel (Srikanth *et al.*, 2017), 6°C-7°C for alcohol (ethanol, isobutanol, propanol), poultry fat biodiesel (Joshi *et al.*, 2010), 4°C for ethyl levulinate-cottonseed oil biodiesel and ethyl acetoacetate-waste cooking oil biodiesel (Cao *et al.*, 2014; Joshi *et al.*, 2011), and 5°C for ethyl levulinate-poultry fat biodiesel (Joshi *et al.*, 2011). The saturated esters are prone to precipitate as the temperature is lowered (Joshi *et al.*, 2011; Srikanth *et al.*, 2017). The decreasing of cloud point with increasing concentration of the blend component is possibly due to the blend component acting as a diluent, which prevented the coagulation of the esters at low temperatures (Cao *et al.*, 2014; Joshi *et al.*, 2011; Srikanth *et al.*, 2017).

As the temperature drops, fuel tends to get solidified until it achieves its pour point; the lowest temperature at which the fuel can flow (Verma *et al.*, 2016). The pour point is not required in ASTM D6751 and EN 14214, but it provides additional information about the cold flow properties of the fuel. It indicates the temperature at which the sample can be cooled without losing its fluidity. The effect on pour point from the addition of BL to PME was similar to the trend elucidated for cloud point. The pour point decreased significantly (p<0.05) with an increasing amount of BL (*Table 4*). The pour point of BL-PMEs decreased by 7°C with an increasing amount of BL added up to 15%. Overall, the trend suggested that the cold flow properties; cloud and pour point of BL contributed to the improvement of the cold flow properties of BL-PME.

A similar trend for cloud and pour points was also reported in the previous studies. The significant reduction of pour points is due to the low freezing temperature of the blend component, which is substantially below the temperature at which biodiesel typically undergoes solidification (Ali *et al.*, 2014). For instance, the freezing point of 1-butanol is -90°C, resulting in the decrease of the pour point from 16°C to 9°C by increasing the 1-butanol content up to 7% (Ali *et al.*, 2014). Besides, ethyl levulinate with a freezing point <-79°C resulted in a reduction of pour point by 3°C to 6°C (Joshi *et al.*, 2011; Srikanth *et al.*, 2017). It is proposed that the application of the blend compounds and the appropriate blending amount should be evaluated based on the application conditions. This is because, neither the ASTM D6751 nor EN 14214 specification state the maximum or minimum requirements of fuel temperature properties, including cloud and pour point, since it is the location and seasonal dependant.

Effects of BL on Flash Point of BL-PME

The flash point of a fuel is defined as the minimum ignition temperature at which fuel produces enough vapour to cause ignition leading to flame generation (Arbab *et al.*, 2013). The flash point is related to the safety requirements for handling and storage of fuel (Kaisan *et al.*, 2020). Higher flash point makes fuel safer for handling and storage and could prevent unexpected ignition during combustion. Most biodiesels possess higher flash points than that diesel (Arbab *et al.*, 2013). For a compound with a very low flash point, its use as a standalone fuel blend component could potentially deteriorate the safe storage criterion of the fuel (Mohammadi *et al.*, 2014).

Varying the BL content from 5% to 15%, the flash point decreased significantly (p<0.001), which is due to the lower flash point of BL. Nevertheless, the flash point of 5-, 10- and 15BL-PME are all still within the specifications of ASTM D6751; minimum of 93°C, and EN 14214; minimum of 101°C. The findings from previous studies also reported a similar trend. In previous studies on the effect of ethyl levulinate and ethyl acetoacetate as a blend component to cottonseed oil, poultry fat, dairy-washed milk scum and waste cooking oil biodiesels, the flash point for all samples were above the ASTM D6751 limit, but the 20% blends reported flash point below 101°C (Cao *et al.*, 2014; Joshi *et al.*, 2011; Srikanth *et al.*, 2017).

Furthermore, a significant reduction in flash points was observed as alcohols (ethanol, isopropanol and butanol) were blended with biodiesel (Cao *et al.*, 2014; Joshi *et al.*, 2011; Srikanth *et al.*, 2017). This is due to the low flash point of the respective alcohols. Nevertheless, a further increase of the alcohol content from 5% to 20% has minimal effect on the flash point (Joshi *et al.*, 2010). In terms of alcohol, biodiesel blended with longer carbon chain alcohol gives better flash points, which is due to their higher flash point. For example, the flash point for 50% of pentanol blended with *Calophyllum inophyllum* biodiesel is within ASTM D6751 specification, while 50% of butanol blend did not meet the specification (Nanthagopal *et al.*, 2018). Even though the flash points of biodiesel due to the addition of fuel blend component were within the limits suggested by ASTM D6751 and EN 14214, the variations in the flash points could limit the utilisation of the respective blend component on other biodiesels with relatively lower flash points (Lawan *et al.*, 2019).

Effects of BL on Kinematic Viscosity of BL-PME

Biodiesel has a higher viscosity than petroleum diesel as reflected in the relevant standards, which are 1.9–6.0 $mm^2\ s^{-1}$ and 3.5–5.0 $mm^2\ s^{-1}$ according to ASTM D6751 and EN 14214, respectively, for biodiesel, and 1.9–4.1 $mm^2\ s^{-1}$ according to EN 590 for petroleum diesel (Smith *et al.*, 2010). Fuels with high kinematic viscosity increase fuel consumption and cause poor fuel spray and atomisation (Arbab *et al.*, 2013). In terms of combustion and emission,

fuel with lower kinematic viscosity enhances the contact between air and fuel during combustion and lower NOx emissions (Radhakrishnan *et al*., 2017). Nevertheless, fuel with both low and high viscosities, which exceeds the upper and lower limit of the specification, can hurt fuel performance. For example, fuel with low viscosity does not provide sufficient lubrication (Isioma *et al*., 2013).

In contrast to PME, the kinematic viscosity of BL-PME was significantly different (p<0.05) (*Table 4*). As the percentage of BL increased, a decrease in kinematic viscosity was observed (p<0.05), which is due to the lower kinematic viscosity of BL than that of PME. In previous studies, with considerably lower kinematic viscosities for ethyl levulinate (1.50 $mm^2 s^{-1}$) and ethyl acetoacetate (1.63 $mm^2 s^{-1}$) compared to biodiesel, the kinematic viscosity of fuels containing these compounds did not meet the EN 14214. For instance, 20% of ethyl levulinate in cottonseed oil, poultry fat and canola oil biodiesels (Joshi *et al*., 2011; Unlu *et al*., 2018), 15% of ethyl levulinate and ethyl acetoacetate in dairy-washed milk scum biodiesel (Srikanth *et al*., 2017), and 20% of ethyl acetoacetate in waste cooking oil biodiesel (Cao *et al*., 2014). Meanwhile, as butanol and pentanol possess higher kinematic viscosity (2.6-2.9 $mm^2 s^{-1}$), the addition of these compounds to *C. inophyllum* and palm biodiesels also caused lower kinematic viscosity of the fuel blends (Nanthagopal *et al*., 2018; Radhakrishnan *et al*., 2017). Nevertheless, the kinematic viscosities are within ASTM D6751 and EN 14214 for butanol and pentanol addition up to 60% (Nanthagopal *et al*., 2018).

Effects of BL on Oxidative Stability of BL-PME

Oxidative stability affects the stability of biodiesel during extended storage. Biodiesel with a higher percentage of saturated fatty acid possesses higher oxidation stability (Srikanth *et al*., 2017). The requirement of oxidative stability for biodiesel is a minimum of 3 and 6 hr for ASTM D6751 and EN 14214, respectively. Meanwhile, a more stringent limit was set by the Malaysian Standard for PME, MS 2008, which is 10 hr minimum. The use of antioxidants; natural and synthetic, is effective to tackle the oxidative stability challenges for biodiesel (Lawan *et al*., 2019). Antioxidants are components which prevent auto-oxidation of oils and fats by giving their hydrogen to free radicals formed in the initiation and propagation stages of autoxidation (Lawan *et al*., 2019).

In the current study, the initial oxidative stability of the PME sample was 30.4 hr (*Table 2*). The PME has been stored after the procurement and before the preparation of BL-PMEs and the determination of oxidative stability. The decrease in oxidative stability of PME is due to the prolonged storage period. During the time of analysis, the oxidative stability of control samples BL and PME are 28.0 and 13.7 hr, respectively. The increase in BL from 5% to 15% increased the oxidative stability of BL-PME (p<0.05) from 14.3 to 14.6 hr. Even though the oxidative stability of BL is higher compared to PME with a difference of 1.04 times, the addition of BL did not result in substantial improvement of the oxidative stability of BL-PMEs. The oxidation stability which is defined by the induction period is the time elapsed between the start of the analysis and the time when the formation of oxidation products begins to increase rapidly. The results suggested that oxidation will occur faster in PME compared to BL and BL-PMEs. The oxidative stability of all BL-PMEs along with the neat BL and PME were within the acceptable limit according to ASTM D6751, EN 14214 and MS 2008.

It is suggested that the oxidation reactions of oils and fats involving the free radicals mechanism start with a dehydrogenation reaction to produce carbon-based free radicals (Wang *et al*., 2020). Among the indicators used to evaluate the tendency of the dehydrogenation reaction to occur is the C-H bond dissociation energy, where a compound with lower bond dissociation energy is easier to oxidise, and thus possesses lower oxidative stability (Wang *et al*., 2020). The C-H bond in PME is weaker compared to BL due to the presence of unsaturated fatty acids in PME. In addition, as described in the reaction kinetics of alkyl levulinates, due to the ketone carbonyl group and alkyl ester contributions, the bond dissociation energies around the carbonyl groups of alkyl levulinate are higher (Tian *et al*., 2017). It is presumed that the absence of unsaturated components in BL makes it more stable than the unsaturated fatty acid chains in PME. Unlike antioxidants, it is presumable that the change of oxidative stability of BL-PMEs does not correspond to BL acting to prevent the auto-oxidation of oils like antioxidants. The oxidative stability of BL-PMEs is influenced by the oxidative stability property of BL itself as the number of BL increases in the blends.

A similar trend in the slight increase of oxidative stability for different biodiesel blends such as cottonseed oil biodiesel and dairy-washed milk-scum biodiesel has been reported on the use of oxygenated compounds; ethyl levulinate and ethyl acetoacetate, respectively, with both compounds possessing comparable oxidative stability >20 hr (Cao *et al*., 2014; Joshi *et al*., 2011). In contrast, a slight decrease in oxidative stability was reported in the addition of ethyl levulinate from 2.5% to 20.0% to poultry fat biodiesel, and the addition of ethyl levulinate and ethyl acetoacetate from 5.0% to 20.0% each to waste cooking oil biodiesel (Joshi *et al*., 2011; Srikanth *et al*., 2017). The different trends anticipated from the addition of oxygenated compounds on the oxidative stability of biodiesel blends are possibly related to the different unsaturation fatty acids

present in these biodiesels. Further assessments are necessary to inspect the relationship between the unsaturation of fatty acid with different functional groups of the additives towards the oxidative stability of fuel blends.

Effects of BL on Calorific Value of BL-PME

Calorific value is the amount of heat released per unit quantity of fuel when burned completely and the products of combustion are cooled back to the temperature of the combustible mixture (Arbab *et al.*, 2013). A higher calorific value of a fuel is preferred since the heat release during combustion is facilitated (Arbab *et al.*, 2013). The calorific value of biodiesel is usually lower than that of diesel due to its oxygen content (Kaisan *et al.*, 2020; Wang *et al.*, 2017). The heating value is not specified in ASTM D6751 and EN 14214 but is prescribed in EN 14213 (biodiesel for heating purposes) with a minimum of 35 MJ kg^{-1} (Ali *et al.*, 2014). The calorific value of BL-PMEs was significantly different from PME (p<0.001). As the amount of BL increased from 5% to 15%, the calorific value of BL-PMEs decreased significantly to p<0.001 (*Table 4*). The calorific value of the BL-PME is within the requirement of EN 14213 for blending of BL up to 10%.

It was stated that the calorific value of fuel would be lower if the fuel had more oxygen content (Nanthagopal *et al.*, 2018). As alkyl levulinate is regarded as an oxygenated compound with oxygen content higher than that of diesel and biodiesel (Wang *et al.*, 2017), the decrease in calorific value of BL-PMEs is due to the increase in oxygen content of the fuel blends. A similar trend has been reported in previous studies on the addition of oxygenated compounds such as alcohols. This includes the addition of 1-butanol and 1-pentanol in *C. inophyllum* biodiesel (Nanthagopal *et al.*, 2018), pentanol in palm oil biodiesel (Radhakrishnan *et al.*, 2017), and ethyl levulinate and 1-butanol in diesel-biodiesels (Wang *et al.*, 2017). Since the addition of oxygenated compounds increases the oxygen content of the resultant fuels, a reduction in NOx and smoke emissions were observed (Nanthagopal *et al.*, 2018; Radhakrishnan *et al.*, 2017). Further study on the impact of BL on emission characteristics of BL-PME is necessary to truly assess its efficacy as a PME blend compound.

CONCLUSION

The effect of blending *n*-butyl levulinate (BL) at different amounts; 5%, 10% and 15%, with palm methyl ester (PME) on the fuel properties was evaluated. The BL-PMEs of all blending ranges satisfy the requirements of ASTM D6751 and EN 14214 for biodiesel in terms of acid value, flash point, and kinematic viscosity at 40°C. The cold flow characteristic of BL; low pour and cloud points, contributed to the enhancement of the BL-PME fuel properties. The addition of BL up to 15% has improved both cloud and pour points by 7°C. The high oxidative stability of BL increased the oxidative stability of BL-PMEs. Meanwhile, the calorific value of the BL-PME up to 10% BL is within the requirement of EN 14213, a minimum of 35 MJ kg^{-1}. The BL-PMEs properties were significantly different from PME (p<0.05). The properties were affected visibly (p<0.05) as the BL content increased. From the analysis, BL appears to be acceptable to be blended with biodiesel.

ACKNOWLEDGEMENT

The authors would like to thank the Director-General of MPOB for the permission to publish this article. The authors would also like to acknowledge the analysts of AOTD and E&P, MPOB for technical assistance in completing this study.

REFERENCES

Ali, O M; Mamat, R and Faizal, C K M (2014). Influence of 1-butanol additives on palm biodiesel fuel characteristics and low-temperature flow properties. *Appl. Mech. Mater., 465-466*: 130-136. DOI: 10.4028/www.scientific.net/AMM.465-466.130.

Arbab, M I; Masjuki, H H; Varman, M; Kalam, M A; Imtenan, S and Sajjad, H (2013). Fuel properties, engine performance and emission characteristic of common biodiesels as a renewable and sustainable source of fuel. *Renew. Sustain. Energy Rev., 22*: 133-147. DOI: 10.1016/j.rser.2013.01.046.

Cao, L; Wang, J; Liu, K and Han, S (2014). Ethyl acetoacetate: A potential bio-based diluent for improving the cold flow properties of biodiesel from waste cooking oil. *Appl. Energy, 114*: 18-21. DOI: 10.1016/j.apenergy.2013.09.050.

Christensen, E; Williams, A; Paul, S; Burton, S and McCormick, R L (2011a). Properties and performance of levulinate esters as diesel blend components. *Energy Fuels, 25(11)*: 5422-5428. DOI: 10.1021/ef201229j.

Christensen, E; Yanowitz, J; Ratcliff, M and McCormick, R L (2011b). Renewable oxygenate blending effects on gasoline properties. *Energy Fuels, 25(10)*: 4723-4733. DOI: 10.1021/ef2010089.

Démolis, A; Essayem, N and Rataboul, F (2014). Synthesis and applications of alkyl levulinates. *ACS*

Sustain. Chem. Eng., 2(6): 1338-1352. DOI: 10.1021/sc500082n.

Hashim, H; Narayanasamy, M; Yunus, N A; Shiun, L J; Muis, Z A and Ho, W S (2017). A cleaner and greener fuel: Biofuel blend formulation and emission assessment. *J. Cleaner Prod., 146*: 208-217. DOI: 10.1016/j.jclepro.2016.06.021.

Hui, L W; Lye, O T and K, H H (2009). Study on low temperature properties of palm oil methyl esters-petrodiesel blends. *J. Oil Palm Res., 21*: 683-692.

Isioma, N; Muhammad, Y; Sylvester, O D; Innocent, D and Linus, O (2013). Cold flow properties and kinematic viscosity of biodiesel. *Univers. J. Chem., 1(4)*: 135-141. DOI: 10.13189/ujc.2013.010402.

Joshi, H; Moser, B R; Toler, J; Smith, W F and Walker, T (2010). Effects of blending alcohols with poultry fat methyl esters on cold flow properties. *Renew. Energy, 35(10)*: 2207-2210. DOI: 10.1016/j.renene.2010.02.029.

Joshi, H; Moser, B R; Toler, J; Smith, W F and Walker, T (2011). Ethyl levulinate: A potential bio-based diluent for biodiesel which improves cold flow properties. *Biomass Bioenergy, 35(7)*: 3262-3266. DOI: 10.1016/j.biombioe.2011.04.020.

Kaisan, M U; Anafi, F O; Nuszkowski, J; Kulla, D M and Umaru, S (2020). Calorific value, flash point and cetane number of biodiesel from cotton, jatropha and neem binary and multi-blends with diesel. *Biofuels, 11(3)*: 321-327. DOI: 10.1080/17597269.2017.1358944.

Lawan, I; Zhou, W; Garba, Z N; Zhang, M; Yuan, Z and Chen, L (2019). Critical insights into the effects of bio-based additives on biodiesels properties. *Renew. Sustain. Energy Rev., 102*: 83-95. DOI: 10.1016/j.rser.2018.12.008.

Lei, T; Wang, Z; Chang, X; Lin, L; Yan, X; Sun, Y; Shi, X; He, X and Zhu, J (2016). Performance and emission characteristics of a diesel engine running on optimized ethyl levulinate–biodiesel–diesel blends. *Energy, 95*: 29-40. DOI: 10.1016/j.energy.2015.11.059.

Lv, P; Cheng, Y; Yang, L; Yuan, Z; Li, H and Luo, W (2013). Improving the low temperature flow properties of palm oil biodiesel: Addition of cold flow improver. *Fuel Process. Technol., 110*: 61-64. DOI: 10.1016/j.fuproc.2012.12.014.

Mekhilef, S; Siga, S and Saidur, R (2011). A review on palm oil biodiesel as a source of renewable fuel. *Renew. Sustain. Energy Rev., 15(4)*: 1937-1949. DOI: 10.1016/j.rser.2010.12.012.

Mohammadi, P; Tabatabaei, M; Nikbakht, A M and Esmaeili, Z (2014). Improvement of the cold flow characteristics of biodiesel containing dissolved polymer wastes using acetone. *Biofuel Res. J., 1(1)*: 26-29. DOI: 10.18331/brj2015.1.1.6.

Nanthagopal, K; Ashok, B; Saravanan, B; Patel, D; Sudarshan, B and Aaditya Ramasamy, R (2018). An assessment on the effects of 1-pentanol and 1-butanol as additives with *Calophyllum inophyllum* biodiesel. *Energy Convers. Manag., 158*: 70-80. DOI: 10.1016/j.enconman.2017.12.048.

Parveez, G K A; Tarmizi, A H A; Sundram, S; Kheang, L S; Ong-Abdullah, M; Palam, K D P; Salleh, K M; Ishak, S M and Idris, Z (2021). Oil palm economic performance in Malaysia and R&D progress in 2020. *J. Oil Palm Res., 33(2)*: 181-214. DOI: 10.21894/jopr.2021.0026.

Radhakrishnan, S; Devarajan, Y; Mahalingam, A and Nagappan, B (2017). Emissions analysis on diesel engine fueled with palm oil biodiesel and pentanol blends. *J. Oil Palm Res., 29(3)*: 380-386. DOI: 10.21894/jopr.2017.2903.11.

Ramli, N A S and Abdullah, F (2021). Study of density, surface tension, and refractive index of binary mixtures containing alkyl levulinate and *n*-alcohol from 298.15 to 323.15 K. *J. Chem. Eng. Data, 66(5)*: 1856-1876. DOI: 10.1021/acs.jced.0c00694.

Ramli, N A S and Amin, N A S (2020). Catalytic conversion of carbohydrate biomass in ionic liquids to 5-hydroxymethyl furfural and levulinic acid: A review. *BioEnergy Res., 13(3)*: 693-736. DOI: 10.1007/s12155-020-10125-8.

Ramli, N A S and Amin, N A S (2014). Catalytic hydrolysis of cellulose and oil palm biomass in ionic liquid to reducing sugar for levulinic acid production. *Fuel Process. Technol., 128*: 490-498. DOI: 10.1016/j.fuproc.2014.08.011.

Rashedul, H K; Masjuki, H H; Kalam, M A; Ashraful, A M; Ashrafur Rahman, S M and Shahir, S A (2014). The effect of additives on properties, performance and emission of biodiesel fuelled compression ignition engine. *Energy Convers. Manag., 88*: 348-364. DOI: 10.1016/j.enconman.2014.08.034.

Smith, P C; Ngothai, Y; Dzuy Nguyen, Q and O'Neill, B K (2010). Improving the low-temperature properties of biodiesel: Methods and consequences. *Renew. Energy, 35(6)*: 1145-1151. DOI: 10.1016/j.renene.2009.12.007.

Srikanth, H V; Venkatesh, J; Godiganur, S; Venkateswaran, S and Manne, B (2017). Bio-based diluents improve cold flow properties of dairy washed milk-scum biodiesel. *Renew. Energy, 111*: 168-174. DOI: 10.1016/j.renene.2017.03.092.

Tian, M; McCormick, R L; Luecke, J; de Jong, E; van der Waal, J C; van Klink, G P M and Boot, M D (2017). Anti-knock quality of sugar derived levulinic esters and cyclic ethers. *Fuel, 202*: 414-425. DOI: 10.1016/j.fuel.2017.04.027.

Unlu, D; Boz, N; Ilgen, O and Hilmioglu, N (2018). Improvement of fuel properties of biodiesel with bioadditive ethyl levulinate. *Open Chem. J., 16(1)*: 647. DOI: 10.1515/chem-2018-0070.

Verma, P; Sharma, M P and Dwivedi, G (2016). Evaluation and enhancement of cold flow properties of palm oil and its biodiesel. *Energy Rep., 2*: 8-13. DOI: 10.1016/j.egyr.2015.12.001.

Wang, W; Li, F and Li, Y (2020). Effect of biodiesel ester structure optimization on low temperature performance and oxidation stability. *J. Mater. Res. Technol., 9(3)*: 2727-2736. DOI: 10.1016/j.jmrt.2020.01.005.

Wang, Z; Lei, T; Lin, L; Yang, M; Li, Z; Xin, X; Qi, T; He, X; Shi, J and Yan, X (2017). Comparison of the physical and chemical properties, performance, and emissions of ethyl levulinate–biodiesel–diesel and *n*-butanol–biodiesel–diesel blends. *Energy Fuels, 31(5)*: 5055-5062. DOI: 10.1021/acs.energyfuels.6b02851.

Journal of Oil Palm Research Vol. 35 (3) September 2023 p. 426-436
DOI: https://doi.org/10.21894/jopr.2023.0006

ANTIPROLIFERATIVE EFFECTS OF PALM OIL IN THE PRESENCE OF PHOTOBIOMODULATION AGAINST K562 CANCER CELLS

AZADEH HEKMAT[1]*; KIMIA FAROKHI BAHAR[1] and ZAHRA HAJEBRAHIMI[2]

ABSTRACT

Palm oil (PO) is utilised for food such as cooking oil and non-food such as for making creams, soaps and detergents. It contains various unsaturated and saturated fats, vitamin E and β-carotenes. This study aimed to clarify the influence of PO plus photobiomodulation (PBM) on leukaemia (K562 cells) proliferation. Cells were treated with various concentrations of PO, PBM at wavelength 655 nm with 1, 2, 3 and 6 J/cm^2, and PO in pre- and post-irradiation with PBM. The proliferation of cells was investigated by MTT assay, morphologic microscopy and flow cytometry. The amount of reactive oxygen species (ROS) was also determined. Cells were subjected to PO and then PBM in the presence of NAC (N-acetylcysteine) to assess the involvement of ROS in cell growth. PO can diminish the viability of K562 cells significantly. PBM did not have a remarkable effect on the viability of cells. Pre-treatment with PO and then irradiation with 1 J/cm^2 energy could induce apoptosis through intracellular ROS generation and had effective antiproliferative impacts on cells compared to those which acquired separate treatments with laser irradiated alone or PO alone. Thus, our research offers new strategies to utilise PO in combination with PBM in cancer treatment.

Keywords: flow cytometry analysis, K56 leukaemiaia cells, MTT assay, palm oil, photobiomodulation (PBM).

Received: 10 April 2022; **Accepted:** 31 October 2022; **Published online:** 24 February 2023.

INTRODUCTION

Organic compounds found in natural sources (microorganisms, animals, as well as plants) have been an inspiration for drug development. Various plant-derived compounds have been utilised as anticancer agents, for example, paclitaxel (PTX) was found in *Taxus brevifolia* and *T. baccata* (Pashah *et al*., 2019). *Elaeis*, a genus of palms, contains three accepted species. The first two, *Elaeis oleifera* (also named *E. melanococca*), and *E. guineensis* are the American and African palms, respectively. The third species, *E. odora*, is not cultivated and there is little information about it (Godswill *et al*., 2016). *Elaeis* originated from the Greek word erlaion, meaning oil. Palm oil (PO) is obtained from the fleshy mesocarp of the fruit which contains 45%-55% oil, however, the colour varies from orange-red to light yellow. PO melts at 25°C and is utilised for cooking and making creams and soaps, and administered as a poison antidote (Owoyele and Owolabi, 2014; Parveez *et al*., 2021). It is also utilised with various other herbs as a lotion for skin diseases (Ahmad *et al*., 2021). It is well-known to be effective against various forms of intestinal disorders, particularly dysentery in infants and diarrhea (Owoyele and Owolabi, 2014). PO contains various unsaturated and saturated fats in the forms of palmitate (44.0%, saturated), oleate (39.0%, monounsaturated), linoleate (10.0%, polyunsaturated), stearate (5.0%, saturated), myristate (1.0%, saturated), alpha-linolenate (0.3%, polyunsaturated), and glyceryl laurate (0.1%, saturated) (Owoyele and Owolabi, 2014). It also offers a rich source of vitamin E and β-carotenes, such as tocotrienols and tocopherols which are recognised nutritional antioxidants that behave as scavengers of free radicals or the oxygen atom. Previous studies have confirmed the antioxidant, anti-diabetic, anti-bacterial, anti-cancer and anti-inflammatory effects

[1] Department of Biology, Science and Research Branch, Islamic Azad University, Tehran, Iran.

[2] A&S Research Institute, Ministry of Science Research and Technology, Tehran, Iran.

* *Corresponding author e-mail: hekmat@ut.ac.ir*

of PO (Owoyele and Owolabi, 2014). It has been shown that PO phenolics enhanced the growth of BHK normal cells (Syrian Baby Hamster Kidney) (Sekaran *et al.*, 2010). However, more *in vitro* findings have revealed that the lipid-soluble compounds found in PO, particularly tocotrienols, can induce apoptosis and inhibit proliferation in different human cancer cells including lung (Ji *et al.*, 2012), melanoma (Komarasamy and Sekaran, 2012), pancreatic (Ji *et al.*, 2015), breast (Sekaran *et al.*, 2010) and prostate (Kumar *et al.*, 2006) cancers. Correspondingly, in animal models, it was discovered that PO phenolics can reduce tumour growth (Sambanthamurthi *et al.*, 2011; Sekaran *et al.*, 2010).

Photobiomodulation (PBM) therapy also known as low-level laser (LLL) therapy is a fast-growing technology utilised to modify cellular behaviours or tissue regeneration. The PBMT mechanism is hinged directly on the biomodulation effect or biostimulation, implying that irradiation at a certain wavelength could modify cellular behaviours (Kara and Orbak, 2009). PBMT can induce reactive oxygen species (ROS) in a cancer cell (Kara and Orbak, 2009). It has been known that wavelengths in the range of 390-600 nm can be utilised to treat superficial tissue, and longer wavelengths in the range of 600-1100 nm, which penetrate further, can apply to treat deeper-seated tissues (Avci *et al.*, 2013).

Chronic Myelogenous Leukaemia (CML) and several other types of cancer are recognised to develop resistance to existing drugs through numerous resistance mechanisms, such as drug efflux caused by poor drug permeability and P-glycoproteins, deregulation of mismatch repair mechanism, mutations, variations in the metabolic pathways as well as alternative drug export pumps (Robey *et al.*, 2018). Resistance to antitumor drugs and their harmful adverse effects on cancer patients, induced the scientific community to design novel cancer treatments. Consequently, we were motivated to clarify the influence of PO in the presence of PBM at a wavelength of 655 nm on chronic myelogenous leukaemia (K562 cells) proliferation by MTT assay, morphologic microscopy and flow cytometry. The amount of ROS was also determined. Cells were also subjected to PO and then PBM in the presence of NAC (*N*-acetylcysteine) to assess the involvement of ROS in K562 cell growth. All of the evidence acquired from this research could offer an advantageous and innovative clinical strategy for cancer therapy in the future.

MATERIALS AND METHODS

Materials

The K562 human chronic myeloid leukaemia cell line (ATCC No. CCL-243™) was acquired from the Iranian Biological Resource Center, Iran. MTT (3-[4,5-Dimethylthiazol-2-yl]-2, 5-diphenyltetrazolium bromide), DCFH-DA (2′,7′-Dichlorodihydrofluorescein diacetate), and DAPI (4′-6-Diamidino-2-phenylindole) were acquired from Sigma Aldrich Co., USA. PO produced by Mewah Oils & Fats Pte. Ltd. Co., Malaysia, bought from Behshahr Industrial Co., Iran. The fetal bovine serum (FBS) and RPMI-1640 medium were prepared from Gibco, USA. Dimethylsulfoxide (DMSO) and NAC were obtained from Merck, Germany. Streptomycin and penicillin were obtained from Bio-idea, Iran. The Annexin FITC kit was obtained from IQ product, Netherlands.

Palm Oil Sample Preparation

The stock solution was prepared by dissolving 500 µg of palm oil in 1 mL ethanol (70% v/v) then the solution was shaken gently in a shaker for 15 min. For cell viability measurements, ROS level measurements, and NAC treatment, 1 µL from stock solution was taken and diluted to 99 µL culture medium and obtained the first dilution contained 5 µg/mL of palm oil. In the same way, dilutions containing 10, 25, 50, 75 and 100 µg/mL of palm oil were prepared. For each concentration of palm oil, 10 samples were prepared and tested. For cell morphological observation and flow cytometry method, 6 µL from stock solution was taken and diluted to 599 µL culture medium and obtained the first dilution containing 5 µg/mL of palm oil. In the same way, dilutions containing 10, 25, 50, 75 and 100 µg/mL of palm oil were prepared. All sample solutions were sterilised by filtration through a filter (0.22 µm pore size). All solutions obtained were transferred to amber bottles and kept until use. To investigate the biological effects of ethanol (used for dissolving palm oil), 1, 2, 5, 10, 15 and 20 µL of 70% v/v ethanol were diluted with a medium to prepare 100 µL of 0.7%, 1.4%, 3.5%, 7.0%, 10.5% and 14.0% v/v ethanol, respectively.

In vitro Laser Irradiation

In this study, for *in vitro* laser applications, a "red" diode laser (PFA 23847V, Pooya Far Azma Co., Iran) with a wavelength of 655 nm and a cooling system were utilised under the following irradiation parameters: Power 220 V, frequency 50/60 Hz, continuous wave mode, and 1 µm beam radius. Plates with 96 wells each were utilised, and the cells were seeded at an initial density of 5×10^4 cells/cm^2 in wells. Irradiation was cautiously measured and performed in a dark laminar flux hood. Furthermore, to prevent any overlapping of the irradiated light caused by scattering K562 cells were seeded separately and a black plate was utilised

as a background to diminish specular reflection. A schematic representation of the 96-well plates made for cell proliferation and PBM applications is demonstrated in *Figure 1*. After 24 hr, the cells were exposed to laser irradiation. The effective power was measured in cell culture plate wells utilising an advanced laser power meter (Pooya Far Azma Co.). The energy intensity applied to cells was adjusted to approximately 1, 2, 3 and 6 J/cm^2 by applying 30 mW power for 30, 60, 90 and 180 s, respectively. The irradiating probe was kept vertically over each well at a total distance of 1 cm above the cells.

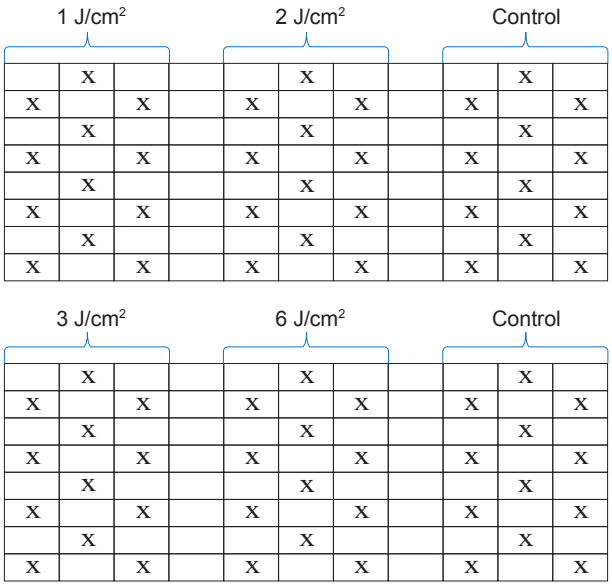

Figure 1. The schematic representation of the 96- well plates for PBM applications.

Cell Culture and Treatment

Cells were cultured in RPMI 1640 medium including FBS (10%, heat-inactivated) and 1% Pen Strep (10 000 units/mL Penicillin and 10 mg/mL Streptomycin) in a humidified incubator including 5% CO_2 at 37°C. Upon reaching more than 90% confluence, cells were subcultured. The K562 cells were divided into five groups randomly, including one control group and four experimental groups. The experimental groups were (1) cells irradiated with 1, 2, 3 and 6 J/cm^2 for 30, 60, 90 and 180 s, respectively, (2) cells treated with the sterilised PO in various concentrations (5, 10, 25, 50, 75 and 100 µg/mL) for 24 hr, (3) cells were irradiated with 655 nm (1 J/cm^2; for 30 s) after that treatment with the PO (5 µg/mL) for 24 hr, (4) cells were treated with the PO (5 µg/mL) for 24 hr then exposed to PBM (1 J/cm^2; for 30 s).

Measurement of Cell Viability

After 24 hr treatment of K562 cells (control and experimental groups), 0.5 mg/mL MTT (20 µL) was added to each well of 96-well plates. Subsequently, the cells were incubated for 3 hr in a CO_2 incubator at 37°C. Later, the insoluble formazan formed was dissolved in 100 µL of DMSO and mixed (Dashtaki *et al.*, 2020; Ibrahim *et al.*, 2021). The OD (optical density) of each well at 570 nm, was measured against a reagent blank with an ELISA reader, ELx808, BioTek Instruments, Inc., USA. All trials were repeated four times.

Cell Morphological Changes/Fluorescence Imaging

Observation of morphological variations of K562 cells was done according to the previous method (Rahman *et al.*, 2013). After 24 hr of treatment of K562 cells with PO and/or PBM, the medium of each cultured cell was removed and washed once with 2 mL of cold PBS buffer (0.01 M, pH 7.4). Consequently, the cells were imaged utilising an inverted microscope, INV100; BEL Engineering, Italy. For DAPI staining, 4×10^5 cells/well were seeded in 24-well plates and treated with PO and/or PBM. Then, the cells were washed with cold PBS. DAPI solution was added to the cell suspension at a final concentration of 100 µg/mL. The cellular morphology was evaluated via fluorescence microscopy, Axoscope 2 plus, ZEISS, Germany.

Determination of Intracellular ROS Production

An oxidation-sensitive fluorescent probe, DCFH-DA, was employed to determine the formation of ROS based on the ROS-dependent oxidation of DCFH-DA to DCF (2′7′-dichlorofluorescein). Consequently, K562 cells were exposed to PBM (1 J/cm^2 for 30 s) (first experimental group); then cells were treated with the sterilised PO (5 µg/mL) for 24 hr (second experimental group). The other group was pre-treated with the sterilised PO (5 µg/mL) for 24 hr and then exposed to PBM. After that, the cell culture medium was picked up and the cells were incubated with 2 µM DCFH-DA for 45 min at 37°C. Later, the cells were washed with PBS and the OD of each well at 530 nm, was measured against a reagent blank with an ELISA reader, Elx808, BioTek Instruments, Inc., USA. All trials were repeated three times.

Antioxidant (NAC) Treatment

The impact of PO in the presence of the PBM on ROS generation in the absence or presence of NAC was investigated. NAC powder was solved in RPMI 1640, and then K562 cells were pre-treated with 4 mM NAC for 3 hr in a CO_2 incubator at 37°C. Later the cells were pre-treated with the sterilised PO (5 µg/mL) for 24 hr and then exposed to PBM. After 24 hr of treatment of cells, 0.5 mg/mL MTT

(20 µL) was added to each well of 96-well plates. The cell viability was examined according to the MTT assay as mentioned earlier.

Flow Cytometry Method

The Annexin V binding was utilised via the Annexin FITC kit. K562 cells were seeded into 6-well plates (10^6 cells/well) for 24 hr, then, treated with PO and/or PBM. Afterwards, the cells were collected through centrifugation for 5 min at 1000 g and washed twice with PBS buffer (0.01 M, pH 7.4). Then, the cells were suspended in 100 µL of Annexin V binding buffer (HEPES/NaOH (10 mM, pH 7.4), NaCl (140 mM), and 2.5 mM $CaCl_2$). Afterward, the cells were double-stained with a 5 µL solution of PI (Propidium iodide) and a 5 µL solution of FITC-labelled Annexin V. All trials were incubated for 30 min in the darkness at room temperature and later analysed via flow cytometry, BD FACSCalibur™, BD Biosciences Inc., USA.

Statistical Analysis

FlowJo software (Version 7.6.1.) was utilised for the analysis of flow cytometry data. Significant differences were evaluated by a t-test of GraphPad Prism Software (Version 8.4.3, GraphPad Software Inc., San Diego, USA). GraphPad Prism also was utilised for plotting graphs. All data were stated as the mean ± the standard deviation (SD). The $p<0.05$ [signified by a single asterisk (*)] was cidered statistically significant while $p<0.01$ [symbolised by a double asterisk (**)] and $p<0.001$ [symbolised by a triple asterisk (***)] were considered as statistically highly significant.

RESULTS AND DISCUSSION

Growth Rates of K562 Cells in the Presence of PO or/and PBM

As mentioned earlier, PO is rich in phytonutrients, and in folklore medicine, it is utilised in the treatment and management of cancer (Loganathan *et al*., 2017). In this study, since cell cultures are one of the best biological systems utilised to discover the impact of toxic compounds or drugs on the rate of cell proliferation, at first, the MTT assay was utilised to measure the influence of PO in the presence of pre- and post-exposed to PBM on K562 cells growth. At first, the effects of PO in various concentrations were examined on the growth of K562 cells under dark conditions. As demonstrated in *Figure 2a*, the relative viability of K562 cells decreased significantly. Thus, our data demonstrate that PO (particularly at higher concentrations) has the potential ability to restrain the proliferation of chronic myeloid leukaemia. This observation is consistent with previous *in vitro* and *in vivo* studies, which demonstrate that PO and its derived product have a significant role against cancer cells (Absalome *et al*., 2020; Loganathan *et al*., 2021; Sambanthamurthi *et al*., 2011). The underlying process of cell death caused by PO has been evaluated by some researchers. For example, Ji *et al*. (2015) reported that PO phenolics could generate apoptosis in pancreatic cancer cell lines (BxPC-3 and PANC-1) by suppression of the NF-κB pathway, *i.e.*, with increased expression of cleaved PARP, and caspase-9, and caspase-3 with a reduction in expressions of Bcl-xL and survivin. PO contains vitamin E which is a fat-soluble antioxidant and contains two major categories, the tocotrienols, and the tocopherols (Abdullah *et al*., 2021). The anticarcinogenic ability of α-, β-, γ- and δ-tocotrienols has been shown in various cancers. These antitumor properties of tocotrienols were once presumed to owe to their antioxidant properties, however, recent data indicated that tocotrienols can influence numerous signalling pathways (Abdullah *et al*., 2021). Thus, although the mode of action of PO on cancer cells is not fully clear, however, possible routes of action for PO are via modulating antioxidants balance and oxidative stress within the cancer cells as well as influencing signalling pathways.

Even though nearly all solvents are toxic to cancer cells *in vitro*, they are still required for dissolving drug agents for biological assays. Hence, it is required to verify the most suitable concentrations of solvents to utilise in biological assays. Accordingly, since the stock solution was prepared by dissolving PO in ethanol, the effects of ethanol on K562 cells were investigated at the concentration of 0.7%, 1.4%, 3.5%, 7.0%, 10.5% and 14.0% (v/v). As shown in *Figure 2b*, ethanol showed non-toxic effects at concentrations of 0.7%, 1.4%, 3.5% and 7.0% (v/v). However, ethanol diminished K562 cell proliferation at higher concentrations (10.5%, and 14.0% (v/v)) considerably. Thus, the antiproliferative properties of PO at higher concentrations are influenced by concentrations of ethanol. Hence, in the follow-up research, PO at 5 µg/mL concentration (including 0.7% (v/v) ethanol) was selected.

PBM can define the variations in cellular activity in response to irradiation with light under particular conditions. PBM has offered an exciting new frontier in oncology (Tam *et al*., 2020). From the previous studies, it is apparent that exposure to various doses and wavelengths of laser can generate stimulation, inhibition, or even no effects at all in both cancerous and normal cells (Tam *et al*., 2020). Thus, in the next experiments, the impact of various laser irradiation energies at 655 nm on cells was investigated (*Figure 2c*). The results of the MTT assay showed that only at higher radiation energy (6 J/cm^2) and longer time of irradiation (180 s), cell survival was reduced slightly, *i.e.*, lower energy level (1 J/cm^2)

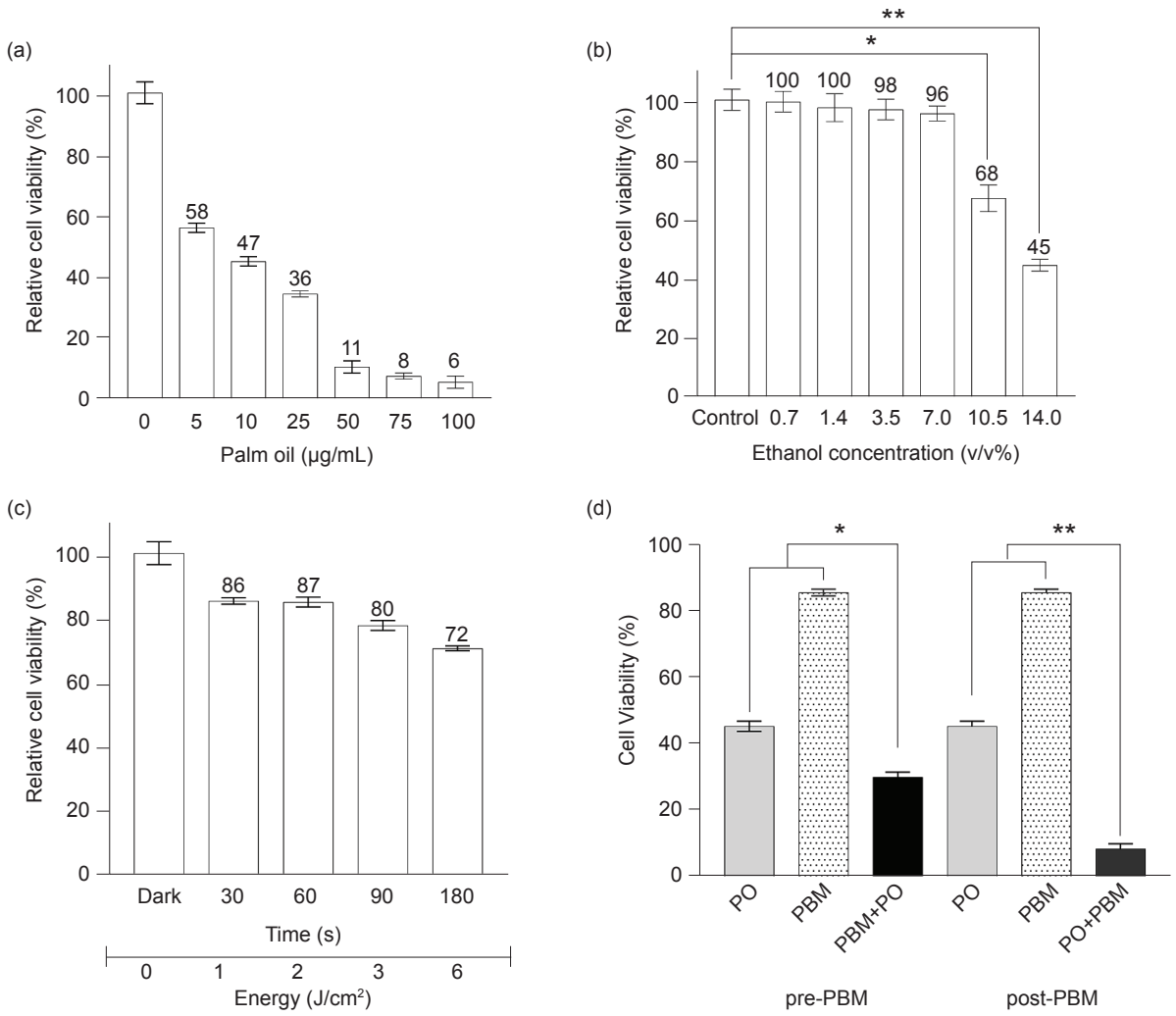

*Figure 2. MTT assay of K562 cells after treatment with (a) various concentrations of PO, (b) ethanol at the various concentrations (v/v%), (c) PBM in different duration of time, and (d) PO in pre- and post-exposed to PBM. Values are mean ± standard deviation; * and ** indicate* $p<0.05$ *and* $p<0.01$*, respectively.*

did not have a remarkable effect on the viability of K562 cells. Numerous laboratory experiments have reported that dosage, tissue types and laser properties are important parameters in PBM. It has been also observed that the probability of getting a response in cells obtaining higher doses is larger compared to those obtaining lower doses (Tam *et al*., 2020). Accordingly, this study displayed that PBM (655 nm, energy densities from 1 to 6 J/cm^2) alone is not capable of killing human chronic myeloid leukaemia cells (K562 cell line) significantly. Our observation is similar to the results of AlGhamdi *et al*. (2012) who published that lower doses of PBM (632.8 nm, energy densities from 0.5 to 4.0 J/cm^2, and power densities from 1-500 mW) did not have negative effects on the cell proliferation rate and other cellular functions. Our result is also consistent with the findings of Dastanpour *et al*. (2015) who found that lower energy densities (5 and 10 J/cm^2) did not exhibit any considerable variations in KG-1a cell proliferation. Even though several studies had been conducted, the full impact of PBM on cell life processes has not been identified completely. However, it has been shown that PBM can increase ATP production in cell cultures and also can induce mitochondrial retrograde signalling (Rola *et al*., 2022). Furthermore, based on the current state of knowledge, only higher energy density can promote apoptotic processes (Rola *et al*., 2022).

In the follow-up research, the cytotoxicity impact of PO in the presence of pre- and post-exposed to PBM was assessed (*Figure 2d*). Accordingly, PO at a concentration of 5 µg/mL and PBM with an energy level of 1 J/cm^2 were selected for the remaining experiments. It should be noted that, even though PBM at the energy level of 1 and 2 J/cm^2 generated the same variation in the cell viability, 1 J/cm^2 was chosen for the combined treatment owing to its minimum power to avoid any undesirable heat generation. Also, as miniated earlier the antiproliferative properties of PO at this concentration were not influenced by concentrations

of ethanol. When K562 cells were pre-exposed to PBM and then treated with PO for 24 hr, 30% cell growth was observed ($p<0.05$). However, when cells were treated with PO for 24 hr and then post-exposed to PBM only 5% cell growth was observed ($p<0.01$). Hence, our study demonstrated that although PBM alone is not capable of killing K562 cells significantly, however, the application of PBM can somehow enhance the cellular penetration of K562 cells into PO. Therefore, the anticancer effect of PO improves, significantly. It could be proposed that in the presence of red-light irradiation, phototoxic reactions sensitised tumour cells to PO and therefore, diminished the cell viability. Our results are similar to the results of Lee *et al.* (2020) who explored the influence of PBM (25 mW and 30 s irradiation time) combined with phloroglucinol on fibrosis inhibition *in vitro*.

K562 Cells Morphological Analysis

The K562 cells were evaluated for any altered morphology after being subjected to PO, PBM, and PO in combination with PBM utilising a light microscope. As seen in *Figure 3a*, control cells were round. Furthermore, the morphology of K562 cells treated with PBM with radiation energy of 1 J/cm^2 did not change (*Figure 3b*). However, the morphologies of cells treated with PO (under dark conditions) changed remarkably (*Figure 3c*). After being pre-treated with PO and then exposed to PBM, the number of cells remarkably reduced, cells were aggregated, and apoptotic bodies and parts of the condensed cytoplasm and nucleus were observable (*Figure 3d*). These results revealed the occurrence of apoptosis in the treated cells. According to these observations, it is clear that pre-treatment with PO and then irradiation with LLL can promote mortality of cells besides those mortality effects generated via PO alone.

To acquire a better insight into the influences of pre-treatment with PO and then irradiation, cell morphology was evaluated through the treatment of K562 cells with DAPI stain. The binding of DAPI with Thymine-Adenine bases in the minor groove of DNA can generate almost 20-fold fluorescence enhancement. As displayed in *Figure 4*, the viable cells are uniformly blue, while cells that were pre-treated with PO and then irradiated with 1 J/cm^2 are blue and contain bright blue dots in their nuclei, because of the nuclear fragmentation. This observation showed that pre-treatment with PO and then irradiation with LLL can induce nuclear fragmentation in K562 cells, which is a sign of apoptosis. This observation is in good agreement with MTT assay investigations as mentioned above.

Estimated ROS in K562 Cells After Treatments

Here we hypothesised that pre-treated with the sterilised PO and then exposed to PBM can alter ROS levels in cells. In this direction, the intracellular ROS level was analysed by the DCFH-DA probe. In *Figure 5*, K562 cells exhibited ROS production. The level of ROS increased significantly during treatment with the PO ($p<0.01$). However, the level of ROS produced using a 655 nm laser was not much higher than the non-irradiated cells. Nevertheless, the level of ROS significantly increased during pre-treated with PO and then exposed to PBM ($p<0.001$). It has

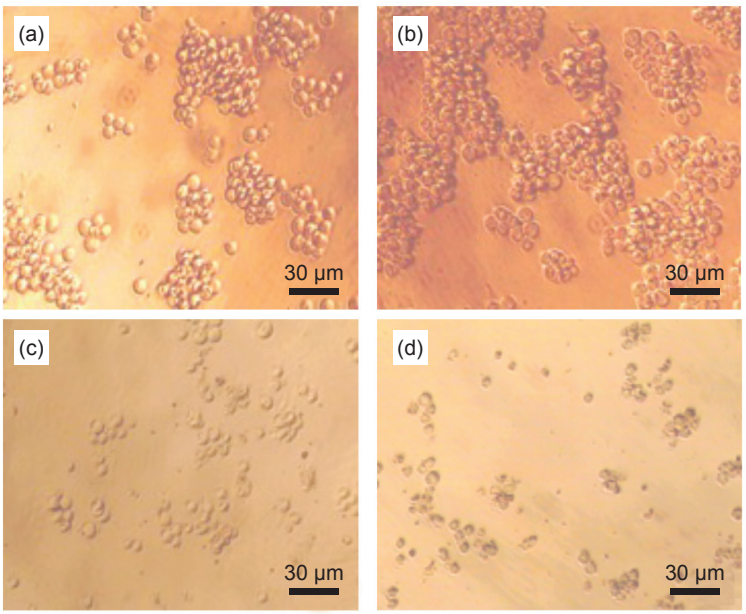

Figure 3. Morphological analysis of K562 cells: (a) control cells, (b) cells exposed to PBM (1 J/cm^2), (c) cells treated with PO (5 µg/mL), and (d) cells treated with PO in post-exposed to PBM (magnification 40x).

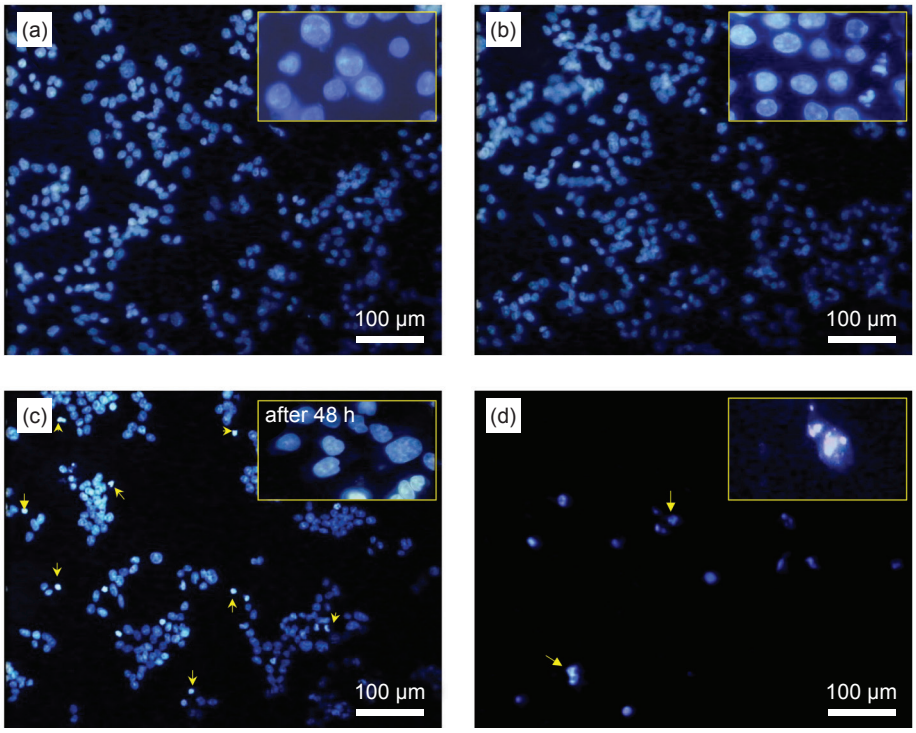

Figure 4. Fluorescence microscopic examination of K562 cells: (a) control cells, (b) cells exposed to PBM (1 J/cm²), (c) cells treated with PO (5 µg/mL), and (d) cells treated with PO in post-exposed to PBM. The cells were stained with DAPI. The yellow arrows point to destroyed chromatin in apoptotic cells.

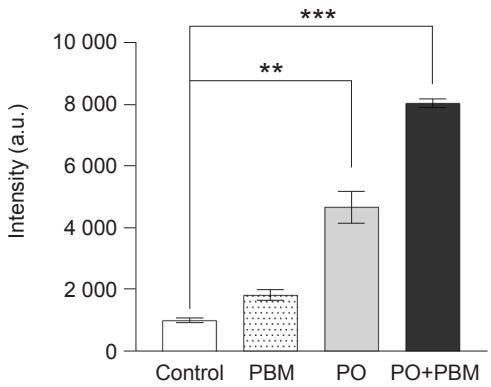

*Figure 5. ROS production level. K562 cells were pretreated with PO, PBM, and pre-treated with PO and then exposed to PBM. Values are mean ± standard deviation; ** and *** indicate* p<0.01 *and* p<0.001.

been shown that ROS can promote both extrinsic and intrinsic pathways of apoptosis in malignant cells. Most chemotherapeutic agents (such as doxorubicin, cisplatin, daunorubicin, topotecan and oxaliplatin) can produce ROS and altered redox homeostasis in malignant cells (Nakamura and Takada, 2021). Furthermore, several natural anticancer compounds (such as naringenin, epicatechin and catechin) can inhibit the protein kinase C signalling pathway and increase ROS generation which consequently causes ROS-mediated apoptosis (Bekhet *et al.*, 2021). Collectively, our results indicate that ROS is one of the effectors in the death mechanism of K562 cells by PO in the presence of PBM. At first sight, this observation seems to be in contrast to the proposed antioxidant role of PO (Arai *et al.*, 2022; Owoyele and Owolabi, 2014). However, as indicated by several studies, antioxidant compounds (such as resveratrol, campesterol and quercetin) can display prooxidant activity in cancer cells at higher concentrations (Bekhet *et al.*, 2021). Hence, although experiments have reported on the ROS scavenging capacity of PO, however, we observed that PO could increase ROS production in K562 cells, and an increase in ROS production intensified in the presence of PMB.

Effect of NAC on Proliferation of PO+LLLI-Treated Cells

To discover whether oxidative stress could play a part in the cytotoxicity of PO and PBM, K562 cells were subjected to PO for 24 hr and then subjected to PBM in the presence of NAC. As indicated in *Figure 6*, compared with the control, pre-treatment with NAC eliminated the cytotoxicity of pre-treated with PO and then irradiated with LLL in K562 cells, noticeably (p<0.001). Although NAC (as an antioxidant) cannot scavage O_2 (superoxide radicals), however, can scavenge directly OH (hydroxyl radicals), HOCl (hypochlorous acid), and H_2O_2 (hydrogen peroxide). Furthermore, consistent with the literature, NAC can only scavenge intracellular ROS (Yan *et al.*, 2017). Therefore, even though the exact mechanisms are still unclear, our results imply that ROS is one of the effectors in

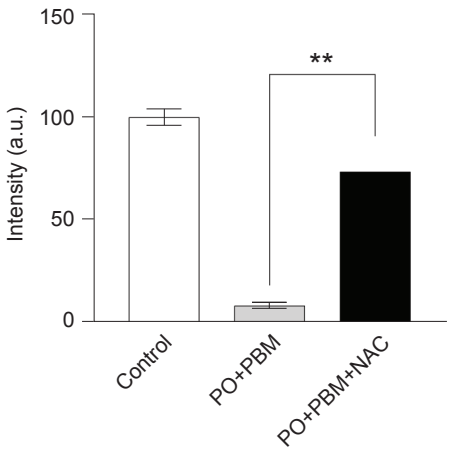

*Figure 6. Effect of NAC on PO+PBM-treated cells. K562 cells were pretreatment with NAC then 475 pre-treated with PO and later exposed to PBM. Values are mean ± standard deviation; **476 indicates* $p<0.01$.

the death mechanism of K562 cells by PO in the presence of PBM, *i.e.*, K562 cells undergo ROS-dependent cell death in response to irradiation and treatment with PO. ROS can generate the activation of various biological pathways, causing apoptosis, differentiation or cell proliferation. Further increment in intracellular ROS can lead to DNA structure modification, protein function alternation and changes in mitochondrial function (Perillo *et al.*, 2020). This observation is in good agreement with the result of ROS level estimation as mentioned above.

Influence of PO in the Presence of PBM on Necrosis or Apoptosis of K562 Cells

Apoptosis or programmed cell death is a significant mechanism to protect tissues and organs from several kinds of cell destruction and stress. Unlike necrosis, apoptosis does not initiate an inflammatory response, thus apoptosis induction in cancer therapy is very valuable (Hattori *et al.*, 2015). Flow cytometry is an appropriate instrument for the simultaneous assessment of apoptosis and necrosis in cells. Accordingly, the K562 cells were treated with PO, and PBM, as well as pre-treated with PO and then irradiated with PBM. Subsequently, the early-stage apoptosis, necrosis and late-stage apoptosis rates of cells were identified utilising the flow cytometry and Annexin V/PI double staining method (*Figure 7*). PI stains cells can only be identified in necrosis or late apoptosis, while Annexin V can be identified in both the late and early stages of apoptosis. Accordingly, living cells (Annexin V^-/PI^-, bottom left quadrant), early apoptotic cells (Annexin V^+/PI^-, bottom right quadrant), late apoptotic cells (Annexin V^+/PI^+, top right quadrant) and necrotic cells (Annexin V^-/PI^+, top left quadrant) were classified (Marasini and Aryal, 2022). As observed in *Figure 7b*, when cells were treated with PO, an increase in the content of both early and late apoptotic cells was observed (30.8% and 18.8%, respectively). However, the proportions of necrotic cells were 5.1%. On the contrary, no cytotoxic effect of PBM (1 J/cm^2) was observed in cells in comparison to the dark group, which agrees with the morphological and MTT cytotoxic results (*Figure 7c*). In contrast, after pre-treated cells with PO and then irradiated with LLL, a considerable increase in the content of both early and late apoptotic cells (56.7% and 25.5%, respectively) was detected (*Figure 7d*). It should be noted that compared with control cells no obvious necrotic cell death was identified in the culture. These data correlate with those of Razzaghi *et al.* (2021) who observed that the number of pre-apoptotic cells in A375 cells treated with liposomal doxorubicin (DOX) and then exposed to laser irradiation (λ=655 nm, 5 J/cm^2) was higher than that of cells treated with only liposomal DOX. More interestingly, our result correlates with those of Seragel-Deen *et al.* (2020) who have proved that higher apoptotic cells were observed in HEp-2 cells after pre-treatment with cisplatin and then irradiated with 190.91 J/cm^2 laser irradiation compared to those which acquired separate treatments with laser irradiated alone or cisplatin alone.

Taken together, based on our results, the cell death mechanisms of PO could be potentiated by utilising PBM possibly through ROS production and apoptosis induction. Pre-treatment of K562 cells with PO is thought to represent the initial signal to apoptosis, after that PBM floods the cell with ROS that further sensitizes the K562 cells to react to PO apoptotic stimuli. According to the literature, higher ATP levels would be consumed in apoptosis processes (Diniz *et al.*, 2020; Lee *et al.*, 2020). Hence the extra energy derived from PBM can increased the level of apoptosis in K562 cells. Therefore, PO in the presence of PBM could introduce a novel treatment for leukaemia. It is important to mention that even though cell culture is an essential method for understanding the probable cell reactions to treatment, however, one should be careful before generalising *in vitro* results, because cell behaviour and cell-matrix interactions in the complex environments of tissues can generate unexpected reactions. Thus, although the present *in vitro* study offers encouraging data, the exact mechanism remains undiscovered and ought to be clarified.

CONCLUSION

Briefly, we proved that pre-treatment with PO and then irradiated with 1 J/cm^2 energy could induce apoptosis through intracellular ROS generation and had effective antiproliferative impacts on the K562 cells compared to those which acquired separate treatments with laser irradiated alone or PO alone.

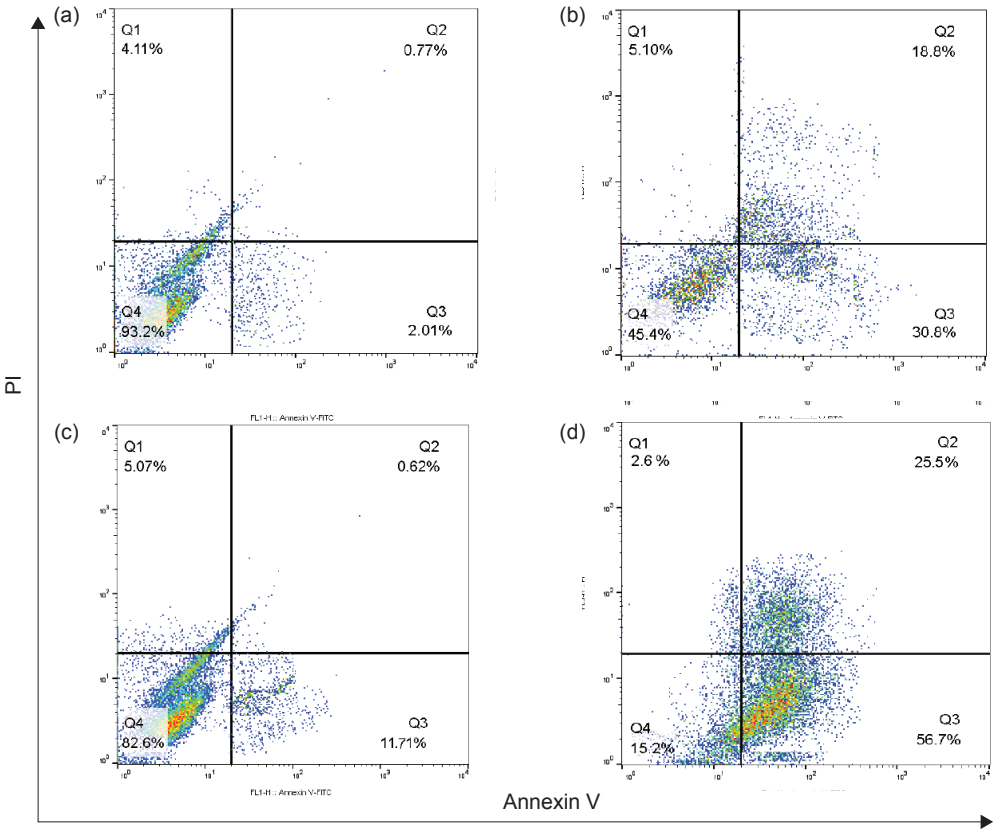

Figure 7. Flow cytometry analyses of K562 cells: (a) control cells, (b) cells treated with 5 µg/mL PO, (c) cells exposed to PBM (1 J/cm^2) and (d) cells pre-treated with PO and then exposed to PBM.

Thus, even though further experiments are vital, our research offers new strategies to utilise PO in combination with PBM in cancer treatment.

ACKNOWLEDGEMENT

The authors appreciate and acknowledge all the people who helped us do this project.

REFERENCES

Abdullah, A; Atia, A; Alrawaiq, N S; Yusof, M K M and Rusli, M F (2021). Palm oil tocotrienols in cancer chemoprevention and treatment. *Elaeis guineensis* (Kamyab, H ed.) IntechOpen, London. p. 1-28. DOI: 10.5772/intechopen.98199.

Absalome, M A; Massara, C C; Alexandre, A A; Gervais, K; Chantal, G G A; Ferdinand, D and Brigitte, T (2020). Biochemical properties, nutritional values, health benefits and sustainability of palm oil. *Biochimie, 178*: 81-95. DOI: 10.1016/j.biochi.2020.09.019.

Ahmad, N; Hasan, Z A A and Bilal, S H (2021). Stability and performance of palm-based transparent soap with oil palm leaves extract. *J. Oil Palm Res., 33(4)*: 724-731. DOI: 10.21894/jopr.2021.0024.

AlGhamdi, K M; Kumar, A and Moussa, N A (2012). Low-level laser therapy: A useful technique for enhancing the proliferation of various cultured cells. *Lasers Med. Sci., 27(1)*: 237-249. DOI: 10.1007/s10103-011-0885-2.

Arai, W; Kameya, H; Hashim, R; Sulaiman, O; Arai, T; Sudesh, K and Kosugi, A (2022). Reactive oxygen species scavenging capacities of oil palm trunk sap were evaluated using the electron spin resonance spin trapping method. *Ind. Crops Prod., 182*: 1-9. DOI: 10.1016/j.indcrop.2022.114887.

Avci, P; Gupta, A; Sadasivam, M; Vecchio, D; Pam, Z; Pam, N and Hamblin, M R (2013). Low-level laser (light) therapy (LLLT) in skin: Stimulating, healing, restoring. *Semin. Cutan. Med. Surg., 32(1)*: 41-52.

Bekhet, O H and Eid, M E (2021). The interplay between reactive oxygen species and antioxidants in cancer progression and therapy: A narrative review. *Transl. Lung Cancer Res., 10(9)*: 4196-4206. DOI: 10.21037/tcr-21-629.

Dashtaki, A; Mahjoub, S; Zabihi, E and Pourbagher, R (2020). The effects of pre-treatment and

post-treatment of thymol against tert-butyl hydroperoxide (t-BHP) cytotoxicity in MCF-7 cell line and fibroblast derived foreskin. *Rep. Biochem. Mol. Biol., 9(3)*: 338-347. DOI: 10.29252/rbmb.9.3.338.

Dastanpour, S; Beitollahi, J M and Saber, K (2015). The effect of low-level laser therapy on human leukemic cells. *J. Lasers Med. Sci., 6(2)*: 74-79.

Diniz, I M; Souto, G R; Freitas, I D; de Arruda, J A A; da Silva, J M; Silva, T A and Mesquita, R A (2020). Photobiomodulation enhances cisplatin cytotoxicity in a culture model with oral cell lineages. *Photochem. Photobiol., 96(1)*: 182-190. DOI: 10.1111/php.13152.

Godswill, N N; Frank, N E G; Walter, A N; Edson, M Y J; Kingsley, T M; Arondel, V and Emmanuel, Y (2016). *Oil Palm: Breeding Oilseed Crops for Sustainable Production* (Gupta, S K ed.). Academic Press, San Diego. p. 217-273.

Hattori, N; Yamada, S; Torii, K; Takeda, S; Nakamura, K; Tanaka, H and Nakayama, G (2015). Effectiveness of plasma treatment on pancreatic cancer cells. *Int. J. Oncol., 47(5)*: 1655-1662. DOI: 10.3892/ijo.2015.3149.

Ibrahim, N E S; Morsy, H and Abdelgwad, M (2021). The comparative effect of nisin and thioridazine as potential anticancer agents on hepatocellular carcinoma. *Rep. Biochem. Mol. Biol., 9(4)*: 452-462. DOI: 10.52547/rbmb.9.4.452.

Ji, X; Usman, A; Razalli, N H; Sambanthamurthi, R and Gupta, S V (2015). Oil palm phenolics (OPP) inhibit pancreatic cancer cell proliferation via suppression of NF-κB pathway. *Anticancer Res., 35(1)*: 97-106.

Ji, X; Wang, Z; Geamanu, A; Goja, A; Sarkar, F H and Gupta, S V (2012). Delta-tocotrienol suppresses Notch-1 pathway by upregulating miR-34a in nonsmall cell lung cancer cells. *Int. J. Cancer, 131(11)*: 2668-2677. DOI: 10.1002/ijc.27549.

Kara, C and Orbak, R (2009). Comparative evaluation of Nd: YAG laser and fluoride varnish for the treatment of dentinal hypersensitivity. *J. Endod., 35(7)*: 971-974. DOI: 10.1016/j.joen.2009.04.004.

Komarasamy, T V and Sekaran, S D (2012). The anti-proliferative effects of a palm oil-derived product and its mode of actions in human malignant melanoma MeWo cells. *J. Oleo Sci., 61(4)*: 227-239. DOI: 10.5650/jos.61.227.

Kumar, K S; Raghavan, M; Hieber, K; Ege, C; Mog, S; Parra, N and Toles, R (2006). Preferential radiation sensitization of prostate cancer in nude mice by nutraceutical antioxidant γ-tocotrienol. *Life Sci., 78(18)*: 2099-2104. DOI: 10.1016/j.lfs.2005.12.005.

Lee, Y; Kim, H; Hong, N; Ahn, J C and Kang, H W (2020). Combined treatment of low-level laser therapy and phloroglucinol for inhibition of fibrosis. *Lasers Surg. Med., 52(3)*: 276-285. DOI: 10.1002/lsm.23131.

Loganathan, R; Selvaduray, K R; Nesaretnam, K and Radhakrishnan, A K (2021). Palm tocotrienols cause cleavage of poly-(adp)-ribose polymerase enzyme and down-regulation of cyclooxygenase-2 protein level in human breast cancer cells. *J. Oil Palm Res., 33(1)*: 119-128. DOI: 10.21894/jopr.2020.0082.

Loganathan, R; Subramaniam, K M; Radhakrishnan, A K; Choo, Y M and Teng, K T (2017). Health-promoting effects of red palm oil: Evidence from animal and human studies. *Nutr. Rev., 75(2)*: 98-113. DOI: 10.1093/nutrit/nuw054.

Marasini, R and Aryal, S (2022). Indocyanine-type infrared-820 encapsulated polymeric nanoparticle-assisted photothermal therapy of cancer. *ACS Omega, 7(14)*: 12056-12065. DOI: 10.1021/acsomega.2c00306.

Nakamura, H and Takada, K (2021). Reactive oxygen species in cancer: Current findings and future directions. *Cancer Sci., 112(10)*: 3945–3952. DOI: 10.1111/cas.15068.

Owoyele, B V and Owolabi, G O (2014). Traditional oil palm (*Elaeis guineensis* Jacq.) and its medicinal uses: A review. *TANG, 4(3)*: 16.11-16.18. DOI: 10.5667/tang.2014.0004.

Parveez, G K A; Tarmizi, A H A; Sundram, S; Loh, S K; Ong-Abdullah, M; Palam, K D P and Idris, Z (2021). Oil palm economic performance in Malaysia and R&D progress in 2020. *J. Oil Palm Res., 33*(2): 181-214. DOI: 10.21894/jopr.2021.0026.

Pashah, Z; Hekmat, A and Hesami Tackallou, S (2019). Structural effects of diamond nanoparticles and paclitaxel combination on calf thymus DNA. *Nucleosides Nucleotides Nucleic Acids., 38(4)*: 249-278. DOI: 10.1080/15257770.2018.1515440.

Perillo, B; Di Donato, M; Pezone, A; Di Zazzo, E; Giovannelli, P; Galasso, G and Migliaccio, A (2020). ROS in cancer therapy: The bright side of the moon. *Exp. Mol. Med., 52(2)*: 192-203. DOI: 10.1038/s12276-020-0384-2.

Rahman, S N S A; Wahab, N A and Abd Malek, S N (2013). *In vitro* morphological assessment of apoptosis induced by antiproliferative constituents from the rhizomes of *Curcuma zedoaria*. *Evid.*

Based Complement. Alternat. Med., 2013: 1-14. DOI: 10.1155/2013/257108.

Razzaghi, M R; Ghazimoradi, M H; Afzali, S; Kamani, E; Mohajerani, E; Shirkavand, A and Farivar, S (2021). Effect of a low-level laser on liposomal doxorubicin efficacy in a melanoma cell line. *J. Lasers Med. Sci., 12:* 1-5. DOI: 10.34172/jlms.2021.28.

Robey, R W; Pluchino, K M; Hall, M D; Fojo, A T; Bates, S E and Gottesman, M M (2018). Revisiting the role of efflux pumps in multidrug-resistant cancer. *Nat. Rev. Cancer, 18(7)*: 452-464. DOI: 10.1038/s41568-018-0005-8.

Rola, P; Włodarczak, S; Lesiak, M; Doroszko, A and Włodarczak, A (2022). Changes in cell biology under the influence of low-level laser therapy. *Photonics, 9(7)*: 502. DOI: 10.3390/photonics9070502.

Sambanthamurthi, R; Tan, Y; Sundram, K; Hayes, K C; Abeywardena, M; Leow, S S and Sinskey, A J (2011). Positive outcomes of oil palm phenolics on degenerative diseases in animal models. *Br. J. Nutr., 106(11)*: 1664-1675. DOI: 10.1017/S0007114511002133.

Sekaran, S D; Leow, S S; Abobaker, N; Tee, K K; Sundram, K; Sambanthamurthi, R and Wahid, M B (2010). Effects of oil palm phenolics on tumor cells *in vitro* and *in vivo*. *Afr. J. Food Sci., 4(8)*: 495-502. DOI: 10.5897/AJFS.9000113.

Seragel-Deen, F; Ghani, S A A; Baghdadi, H M and Saafan, A M (2020). Combined cisplatin treatment and photobiomodulation at high fluence induces cytochrome c release and cytomorphologic alterations in HEp-2 cells. *Open Access Maced. J. Med. Sci., 8(A)*: 366-373. DOI: 10.3889/oamjms.2020.4561.

Tam, S Y; Tam, V C; Ramkumar, S; Khaw, M L; Law, H K and Lee, S W (2020). Review on the cellular mechanisms of low-level laser therapy use in oncology. *Front. Oncol., 10*: 1255. DOI: 10.3389/fonc.2020.01255.

Yan, D; Cui, H; Zhu, W; Nourmohammadi, N; Milberg, J; Zhang, L G and Keidar, M (2017). The specific vulnerabilities of cancer cells to the cold atmospheric plasma-stimulated solutions. *Sci Rep., 7(1)*: 1-12. DOI: 10.1038/s41598-017-04770-x.

Journal of Oil Palm Research Vol. 35 (3) September 2023 p. 437-447
DOI: https://doi.org/10.21894/jopr.2022.0058

HIGH YIELD AND QUALITY CHARCOAL FROM OIL PALM KERNEL SHELL WITH AN IMPROVED PILOT-SCALE CONTINUOUS CARBONISATION SYSTEM

Z NAHRUL HAYAWIN[1]*; A A ASTIMAR[1]; M F IBRAHIM[2]; A W NOORSHAMSIANA[1] and M ROPANDI[1]

ABSTRACT

The present study compared the production, quality, and yield of charcoal manufactured from oil palm kernel shell (OPKS) via an improved pilot-scale continuous carbonisation system, the pilot rotary kiln (PRK), with a batch conventional carbonisation approach, the Taki carbonisation system (TCS). Previous investigations demonstrated that the PRK was highly energy-efficient at 55% compared to 38% in TCS. Furthermore, the PRK attained a higher OPKS-charcoal yield at 30 ± 2.4% than TCS, which produced 22 ± 1.7%. The improved system was a self-sustaining carbonisation process that could continuously run for 8 hr, whereas the TCS required 72 hr to convert the same amount of OPKS into charcoal. A good quality charcoal (83.7 ± 2.0% fixed carbon, 10.2 ± 1.4% volatile matter, 6.1 ± 1.2% ash, and 33.1 ± 1.8 MJ kg^{-1} higher heating value) was also acquired via the PRK. The present study also demonstrated that the PRK approach was more financially feasible than TCS as it was projected to require lower capital cost and a higher benefit-to-cost ratio (B:C), which palm oil mill operators could achieve.

Keywords: charcoal, continuous system, conventional system, oil palm biomass, oil palm kernel shell.

Received: 23 March 2022; **Accepted:** 7 August 2022; **Published online:** 21 September 2022.

INTRODUCTION

Charcoal is a porous carbon-rich solid generated through pyrolysis with little or no oxygen (O_2) at moderate temperatures, between 350°C-700°C (Chen *et al.*, 2019). In developing countries, charcoal is primarily employed as domestic fuel, an energy source in power plants, in soil amendments, and an ingredient in chemical products (Fan *et al.*, 2022; Heberlein *et al.*, 2022; Kamali *et al.*, 2022), while activated carbon is utilised in water and air treatment. Moreover, charcoal mitigates global warming by reducing greenhouse gas (GHG) emissions (Basalirwa *et al.*, 2020; Nahrul *et al.*, 2020).

Charcoal is advantageous over coal and coke as it is easier to store, cheaper, lighter, cleaner, safer, free from sulphur and mercury, and possessed a higher heating value (Lan *et al.*, 2019; Tymoszuk *et al.*, 2019). Charcoal could be acquired from lignocellulosic material, including agricultural biomass composed of high carbon content, an essential characteristic of charcoal production (Sangsuk *et al.*, 2020). Converting agricultural biomass to charcoal also aids in reducing the accumulation of agricultural wastes, making it environmentally friendly (Awasthi *et al.*, 2020).

In Malaysia, the palm oil business is the largest agricultural industry that generates an abundant amount of oil palm biomass yearly in the form of oil palm empty fruit bunch (OPEFB), oil palm mesocarp fibre (OPMF), oil palm kernel shell (OPKS), an oil palm frond (OPF), and oil palm trunk (OPT) (Kushairi *et al.*, 2018). The OPEFB, OPF, and OPT are returned to plantations for mulching purposes. Approximately 30% of 454 Malaysian palm oil mills utilise oil palm biomass to produce biofertiliser, biogas, and wood products (Mahlia *et al.*, 2019). Presently, OPKS is directly employed as a solid fuel boiler for steam and energy generation (Vijaya *et al.*, 2008).

[1] Malaysian Palm Oil Board,
6 Persiaran Institusi, Bandar Baru Bangi,
43000 Kajang, Selangor, Malaysia.

[2] Department of Bioprocess Technology,
Faculty of Biotechnology and Biomolecular Sciences,
Universiti Putra Malaysia, 43400 Serdang,
Selangor, Malaysia.

* *Corresponding author: nahrul.hayawin@mpob.gov.my*

According to Idris *et al.* (2015), transforming OPKS, OPMF, and OPEFB into charcoal and selling it as an energy resource would be 3.0 to 3.5 times more profitable, which could be included in the Malaysian renewable energy (RE) policy. Moreover, Malaysia aims to achieve between 2080 and 4000 MW of installed RE capacity by 2030 (Hamzah *et al.*, 2019). The energy content of oil palm biomass is at a minimum of 65.0% of the low-rank coal range of 17-24 MJ kg^{-1}. Consequently, oil palm biomass could be utilised as a solid fuel for boiler alone or mixed with charcoal. Moreover, oil palm biomass contains low sulphur (0.2%), preventing SOx production during combustion (Harimi *et al.*, 2005).

Producing charcoal from agricultural biomass is achievable through various carbonisation technologies. Due to their simplicity, low capital, and operational cost, traditional carbonisation methods, such as brick kilns, earth pits, and earth mounds, are still operating (Santos *et al.*, 2017); an example is the Taki carbonisation system (TCS) (Astimar *et al.*, 2012). Nonetheless, the major drawback of the traditional technologies is that they are batch systems. Furthermore, the techniques require over seven days to obtain charcoal with a low yield, while the gases produced are released directly into the atmosphere (Kammen and Lew, 2005).

A metal rotary kiln was developed to shorten the carbonisation process and produce a higher charcoal yield (Bailis *et al.*, 2013; Sangsuk *et al.*, 2018; Tavakkol *et al.*, 2021). Subsequently, the method was further improved for a continuous carbonisation system that manufactures increased charcoal yield with good HHV and low gaseous emission. Furthermore, the gases emitted during the process are treated before releasing them into the atmosphere. In the current study, OPKS-charcoal was manufactured via the pilot rotary kiln (PRK) to evaluate the performance of the new continuous carbonisation technology. The method was also compared to the traditional batch carbonisation technique, the TCS.

MATERIALS AND METHODS

Sample Preparation

The present study obtained OPKS samples from the Ulu Kanchong Palm Oil Mill, Negeri Sembilan, Malaysia. On average, the diameter of the kernel shells was approximately 15 mm. The samples were prepared according to the methodology outlined by Nahrul Hayawin *et al.* (2018). First, the OPKS was sun-dried for two weeks to allow the moisture content to be under 10%. Subsequently, the dried OPKS was measured with a thermogravimetric analyser (TGA) for proximate analysis before the carbonisation process.

Carbonisation via TCS

The TCS is an earthen kiln categorised under the traditional carbonisation system. The method utilises tropical wood residues from wood industries as a fuel. A TCS consisting of two furnace kilns that could carbonise a total of 2.24 t of OPKS per batch was employed in the present study. The furnace kilns were made from bricks laid with clay (wall thickness = 0.24 m) and 5.8 × 3 × 3.3 m in length, width, and height, respectively (*Figure 1*). Each kiln comprised a door to load the raw materials and the system was equipped with an 8 m chimney connected to a wood vinegar collecting tank (diameter = 1 m, height = 2.1 m). The whole system was located in a plant that covered an area of 240 m^2.

The TCS was operated with 1.5 t of tropical wood residues cut to 1.5 m long as fuel loaded vertically at the back of the furnace kilns. Subsequently, 1.1 t of OPKS were weighed and loaded into the drums (diameter = 0.58 m, height = 0.85 m). All loaded drums were arranged in the furnaces after their lids were closed. Tropical wood residues loaded at the back of the kilns were then ignited before closing the furnace door to block the air intake. Subsequently, the carbonisation temperatures inside the furnaces were recorded. The fire was extinguished after 72 hr and the system was allowed to cool for five days. The resulting OPKS-charcoal was collected and stored at the charcoal-making centre, while the wood vinegar from the TCS system was collected from the collecting tank, stored, and kept in 150 L plastic drums.

Carbonisation with PRK

Figure 2 illustrates the schematic diagram representation of the continuous carbonisation system, PRK, designed and built by a local engineer. The carbonisation reactor was 4 m long with outer and inner diameters of 508 and 476 mm and could withstand temperatures over 900°C. Furthermore, an alternative door was added at the end of the reactor to prevent the charcoal from being stuck. An automatic pressure valve system was also attached to the top of the reactor to prevent pressure from exceeding the limit.

The PRK could carbonise up to 2 t of raw material per day. Since the system was continuous, it could run for 24 hr without stopping once it started. The system employed diesel to ignite the burner, operating between 178 and 356 kW power and approximately 10 135 mbar pressure. A scrubber was also employed to capture the smoke and treat the gas released during the carbonisation process. The SS400/Rubber scrubber possessed a 0.25 m^3 capacity, compatible with the chemical and physical properties of the gas stream. A cyclone

separator with approximately 0.25 m^3 capacity was also attached to separate particulates from the by-product. Moreover, the PRK was attached to two condenser units, each at 1.5 × 1 × 2 m (height × width × length) and 0.25 m^3 capacity.

The system was initiated by igniting the burner and heating for 2 hr until the optimum temperature of 700°C was obtained. Subsequently, the burner was turned off pre-OPKS with less than 10% moisture content was fed into the screw feeder. The self-burning raw material (exothermic process) moved horizontally in the reactor for approximately an hour and turned into charcoal at the end of the process. Hourly, 80 kg OPKS was introduced until all 1.2 t were processed and the charcoal was collected by loading it in the tightly closed drum to avoid air intake. The smoke produced during the carbonisation was channelled to a scrubber, while the wood vinegar was collected at the outlet pipe placed before the chimney, stored, and kept in a closed 150 L plastic drum.

Analytical Procedures

The current study analysed the lignocellulosic compositions of the OPKS and OPKS-charcoal according to the TAPPI Test Method (T 203 om-83 and T 222 om-83). Additionally, the proximate (volatile matter, fixed carbon, and moisture and ash contents) and ultimate [carbon (C), hydrogen (H), nitrogen (N), and sulfur (S)] analyses were performed according to ASTM D7582-10 and ASTM E775-778, respectively, with thermogravimetric analyser (TGA) [(Mettler Toledo, TGA/SDTA 851, United States of America (USA)] and an elemental analyser (CHNS/O Perkin Elmer 2400, Series 2, USA).

The chemical compositions of the wood vinegar obtained in the present study were assessed with gas chromatography-mass spectrometry (GC-MS) (Shimadzu GCMS–QP2010Plus, Japan) on a TG-WAXMS capillary column (60 m × 0.25 mm × 0.25 μm). The sampling was managed at a split

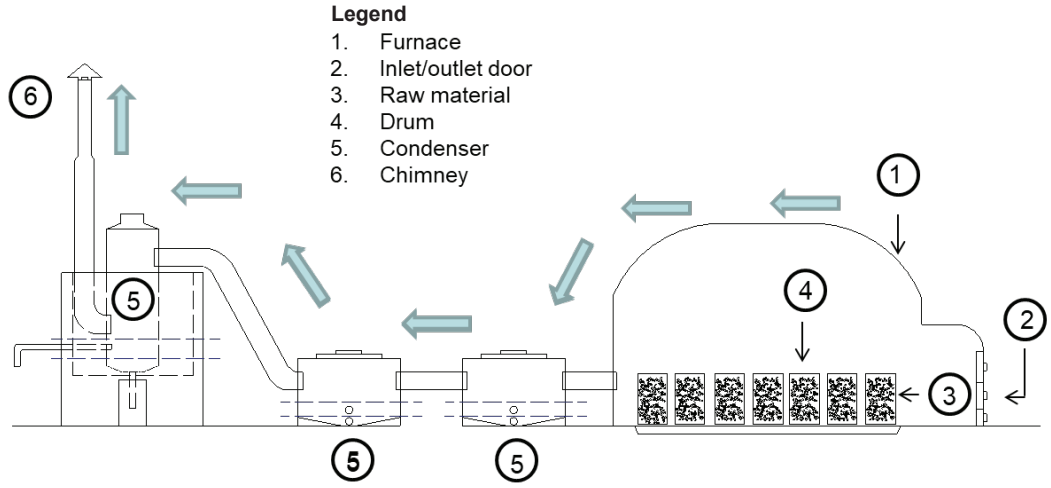

Figure 1. The schematic diagram of the TCS system.

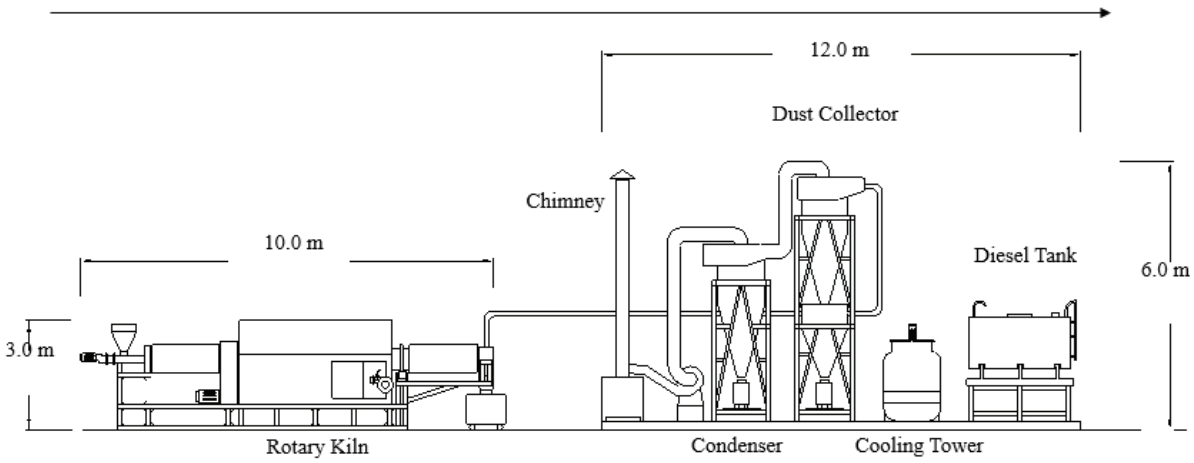

Figure 2. The schematic diagram of the PRK system.

rate of 80:1 with 1 µL of the wood vinegar injected into the column. The injection port temperature was 260°C, while the column temperature was maintained at 60°C for 2 min. Subsequently, the temperature was programmed to rise to 240°C at 10°C min^{-1} for 10 min. Helium was employed as the carrier gas at a flow rate of 1.2 mL min^{-1}. Mass spectrometry was performed with an electron impact (EI) source at 70 eV electron energy, 280°C ion source temperature, and a mass scanning range of 45-550 amu s^{-1}.

The composition of the gas released during the carbonisation process was quantitatively measured with a gas chromatography GC (GC Agilent Technologies 6890N) equipped with thermal conductivity (TCD) analyser and flame ionisation detector (FID). Furthermore, the higher heating value (HHV) of the charcoal obtained in the current study was analysed with a Parr 1261 bomb calorimeter (ISO 18125:2017). All assessments were repeated thrice.

Energy Balance Calculation

The input and output energy of the present study was considered for energy balance calculation (Kodera and Kaiho, 2016). First, Equation (1) was employed to calculate the input energy from the calorific contents of the raw materials. Subsequently, the calorific content of the charcoal recovered was determined with Equation (2), and the heat required to evaporate water was calculated with Equations (3), (4), and (5). Finally, Equation (6) determined the net heat loss due to convection radiation.

$$\text{Calorific content of raw material} = \text{Raw material (dry basis)} \times \text{alorific of value raw material} \quad (1)$$

$$\text{Calorific content of charcoal} = \text{Charcoal (dry basis)} \times \text{calorific value of charcoal} \quad (2)$$

$$\text{Heat required to evaporate water (liquid)} = C`p \times n \times (373\text{-}Trt) \quad (3)$$

$$\text{Heat required to evaporate water (gas)} = Cp \times n \times (Tp\text{-}373) \quad (4)$$

$$\text{Total heat required to evaporate water} = \text{Heat required to evaporate water (liquid)} + \text{heat required to evaporate water (gas)} \quad (5)$$

$$\text{Net heat loss by convection radiation} = \text{Input energy} - \text{output energy} \quad (6)$$

where C'p represents the heat capacity of water (J $mol.K^{-1}$), n is water in mol, Trt denotes room temperature (K), Cp is the heat capacity of steam (J $mol.K^{-1}$), and Tp denotes the temperature of the product (K).

RESULTS AND DISCUSSION

The Production of OPKS-biochar via the PRK and TCS Systems

Carbonisation profile. The OPKS were characterised prior to producing biochar through the PRK and TCS systems to ensure that the raw material employed in the current study has a consistent composition. Compared to other types of oil palm biomass, raw OPKS contains higher lignin and fixed carbon contents and a low ash percentage, making OPKS an excellent material for producing charcoal with higher yield and good quality (*Table 1*).

In TCS, the temperature rose slowly from 150°C to 300°C in the central region of the carbonisation chamber during the initial 5-10 hr of operation. The temperature was then increased rapidly to approximately 700°C after 12 hr before slowly decreasing towards the end of the process, which took approximately 75 hr (*Figure 3a*). Meanwhile, the PRK took 3 hr during the pre-carbonisation process to reach the highest temperature, 700°C, which was maintained throughout the process *Figure 3b*. The burner in the PRK system was automatically turned off when the temperature inside the kiln reached 700°C. The temperature was kept constant for approximately 6 hr for self-burning before it naturally dropped.

The results demonstrated that the PRK was a better carbonisation system that could increase the temperature faster and complete the carbonisation process in a shorter duration than TCS. During the carbonisation process, more volatile compounds were released due to the thermal decomposition of the OPKS. The hemicellulose component decomposed at 250°C to 300°C, followed by cellulose at an average temperature between 350°C and 400°C. At temperatures above 400°C, lignin started to degrade, similar to the report by Chen *et al.* (2016).

The Production Yield and Quality of the OPKS-charcoal

Table 2 summarises the performance comparisons of different carbonisation systems employed in producing OPKS-charcoal. The PRK system was developed with a high-quality metal to prevent heat loss to the environment, resulting in a faster carbonisation process, thus shortening the retention time. Consequently, the technique required a shorter process duration, 8 hr, than other systems, including heat distribution pipe kiln (HDP), transportable metal kin (TPI), and TCS.

The PRK system is also a continuous operation that utilises a suitable amount of raw material during the carbonisation process that continuously loads, carbonises, and collects. The approach

TABLE 1. CHARACTERISTICS COMPARISON BETWEEN THE RAW OPKS EMPLOYED IN THE CURRENT STUDY AND OTHER TYPES OF OIL PALM BIOMASS UTILISED IN CHARCOAL PRODUCTION

Properties	OPKS (present study)	OPKS	OPEFB	OPF	OPT
HHV (MJ kg^{-1})	17.9 ± 0.5	18.3	17.9	17.3	19.3
Cellulose	27.7 ± 0.1	30.1	50.0	56.0	41.0
Hemicellulose	21.6 ± 0.4	21.4	30.0	27.0	32.0
Lignin	44.0 ± 1.0	47.3	17.0	21.0	25.0
Proximate analysis					
Volatile matter	71.0 ± 0.1	77.4	83.9	72.5	79.8
Moisture content	-	-	6.8	7.4	8.34
Fixed carbon	26.3 ± 1.0	20.0	8.9	5.81	13.3
Ash	2.6 ± 0.2	2.59	7.08	14.3	6.9
Ultimate analysis					
C	60.9 ± 1.2	43.6	45.6	38.4	43.8
H	12.8 ± 0.8	4.92	6.19	5.53	6.2
N	0.66 ± 0.1	0.49	0.35	2.3	0.44
S	0.19 ± 0.1	-	ND	0.09	0.09

Source: Goh *et al.* (2012); Nahrul Hayawin *et al.* (2017); Nipattummakul *et al.* (2012); Nyakuma *et al.* (2014); Oh *et al.* (2016); Purwanto *et al.* (2018) and Trangkaprasith, (2011).

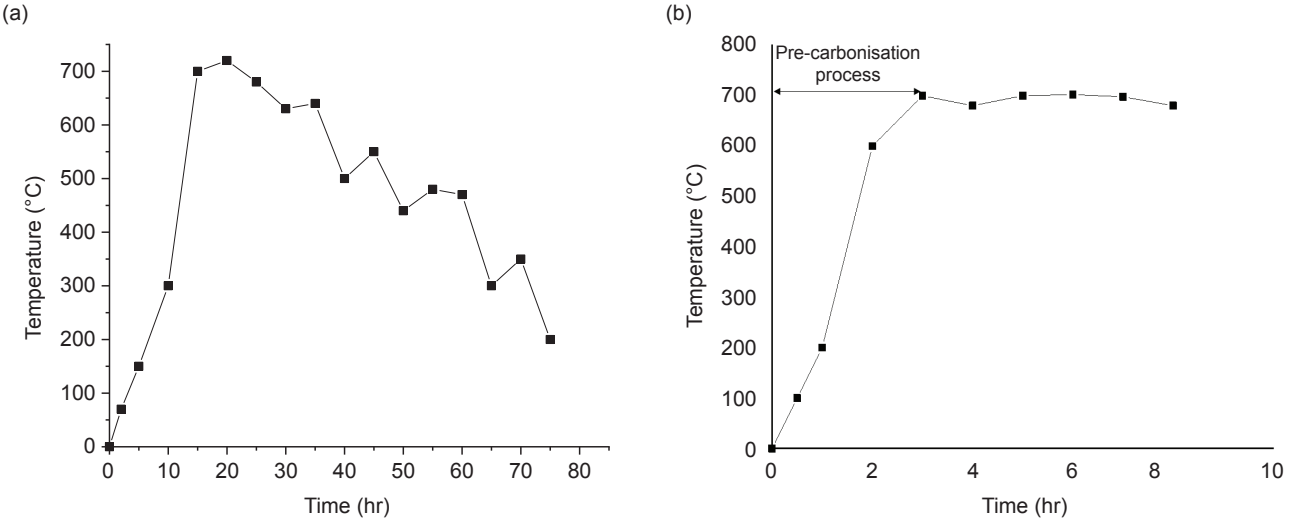

Figure 3. The temperature profile of the OPKS-charcoal production in the (a) TCS, and (b) PRK systems.

accomplishes faster carbonisation, prevents the over-burning of raw material into ash, and thus, increases the quality of OPKS-charcoal compared to TCS and other batch kiln systems. Conversely, low OPKS-charcoal yield (22 ± 1.7%) was produced with TCS due to a longer carbonisation process, burning more OPKS into ash.

A conventional earth kiln system requires a high temperature, 500°C, to reduce volatile matters and tar due to its material structures, hence decreasing the quality and yield of the charcoal obtained (Sangsuk *et al.*, 2018). In the PRK system, more liquids and tar were removed from the raw material during carbonisation at 400°C-700°C, resulting in increased fixed carbon (Arami-niya *et al.*, 2010). Moreover, exothermic decomposition started within the temperature range, which involved the breakdown and devolatilisation of the OPKS that released mixed gases, vapours, and tars, therefore contributing to higher fixed carbon content (Wang *et al.*, 2017). Consequently, the PRK produced OPKS-charcoal with high yield and fixed carbon content at 30 ± 2.4% and 83.7 ± 2.0%, respectively.

The OPKS-charcoal acquired through the PRK documented higher HHV than those obtained via TCS, kiln-HDP, and TPI kiln. The increased HHV of the PRK-produced OPKS-charcoal was due to faster heat distribution throughout the kiln, resulting in efficient heat transfer to materials in the reactor. Conversely, a thermal gradient was generated in the TCS from the hot surfaces of the char particles to its interior, leading to difficulties in caloric transport (Alslaibi *et al.*, 2013). The observations supported the findings reported by Parikh *et al.* (2005), which correlated HHV with the fixed carbon, volatile

matter, and ash content of the charcoal. Moreover, the high ash content of the OPKS-charcoal acquired through TCS also contributed to the low HHV. Overall, the OPKS-charcoal produced via the PRK approach documented higher quality and yield than batch systems (TCS, kiln HDP, and TPI kiln). The system also produced OPKS-charcoal that met the United Kingdom (UK) standard quality specifications for imported charcoal (Paddon and Harker, 1979).

Energy Efficiency

The heat in the distribution pipe in the kiln of the PRK system was rotated, resulting in perfectly carbonised materials, producing OPKS-charcoal with elevated HHV. The uniformity during the carbonisation process in the PRK approach resulted in its high efficiency (55%) compared to the TCS (38%) (*Table 3*). Furthermore, increased mass yield and HHV supplied highly efficient energy-conversion charcoal. Charcoal efficiency is classified into four categories, (1) 8%-12% for the conventional or traditional kiln, (2) 12%-17% for improved conventional or traditional kiln, (3) 14%-20% for industrial technology, and (4) 25%-33% for new high yield technology (Energypedia, 2019), where the PRK method is classified under the fourth category.

By-products

The carbonisation of OPKS into biochar produces two main by-products, wood vinegar and gases. In the current study, the wood vinegar from the PRK method was collected during carbonisation before being analysed with GC. Nevertheless, the vinegar collected from TCS was not evaluated as it was mixed with the vinegar from the firewood employed during carbonisation. *Table 4* lists approximately

TABLE 2. COMPARISONS BETWEEN THE TCS AND PRKS-PRODUCED CHARCOAL AND THE UK SPECIFICATIONS FOR IMPORTED CHARCOAL

Item	TCS (present study)	PRK (present study)	Metal kiln-heat distribution pipe (HDP) (Sangsuk *et al.*, 2018)	Transportable metal kiln (TPI) (Paddon and Harker, 1979)	UK specification (Paddon and Harker, 1979)
Carbonisation duration (hr)	72	8	27	34	-
Moisture content of raw material (%)	9.55 ± 0.7	9.55 ± 1.0	30	38	-
HHV of raw material (MJ kg^{-1})	17.9 ± 0.9	17.9 ± 0.9	18.5	21.7	-
Moisture content of OPKS-charcoal (%)	-	-	8.5	3.5	< 5
Volatile matter of OPKS-charcoal (%, dry basis)	12.5 ± 1.0	10.2 ± 1.4	7.7	13.3	< 13
Fixed carbon of OPKS-charcoal (%, dry basis)	80.1 ± 2.0	83.7 ± 2.0	81	81.1	> 80
Ash content of the OPKS-charcoal (%, dry basis)	7.4 ± 0.1	6.1 ± 1.2	11.3	2.10	< 3
HHV of OPKS-charcoal (MJ kg^{-1}, dry basis)	30.9 ± 0.9	33.1 ± 1.8	30.4	32.5	> 30
OPKS-charcoal yield (%)	22 ± 1.7	30 ± 2.4	24	21	-
Cost per system (USD)	45 761	102 963	9 300	1 000 (Austin and Kohn, 1990)	-

TABLE 3. THE ENERGY BALANCE OF THE OPKS-CHARCOAL PRODUCED VIA THE TCS AND PRK APPROACHES

Energy	TCS	PRK
Input		
Raw material (OPKS)	160.6 × 10^6 kJ	1 032.7 × 10^6 kJ
Raw material firewood	33.7 × 10^6 kJ	-
Diesel	-	0.14 × 10^6 kJ
Scrubber	-	7.3 × 10^6 kJ
Total input	194.3 × 10^6 kJ	1 040.1 × 10^6 kJ
Output		
OPKS-charcoal	60.9 × 10^6 kJ	572.1 × 10^6 kJ
Wood vinegar	42.5 × 10^6 kJ	510.5 × 10^6 kJ
Total output	103.4 × 10^6 kJ	1 082.6 × 10^6 kJ
Heat required to evaporate water (gas)	6.64 × 10^5 kJ	5.40 × 10^5 kJ
Total heat required to evaporate water	8.25 × 10^5 kJ	7.01 × 10^5 kJ
Total output energy	8.3 × 10^6 kJ	17.9 × 10^6 kJ
Net heat loss by convection radiation/exhaust	45.9 × 10^6 kJ	16.2 × 10^6 kJ
Net-energy ratio	0.53	1.04
Energy efficiency = [(yield OPKS-charcoal × HHV OPKS-charcoal)/ (HHV OPKS)] × 100	38%	55%

33 chemical compounds detected in the OPKS-wood vinegar collected from the PRK system. The chemicals were from furan and pyran derivatives, phenol and its derivatives, organic acids, ketones, amides, and alcohols.

The highest compounds in the OPKS-wood vinegar were phenols and their derivatives, accounting for 41.9% of the total composition. The major compounds present in the group were 3-amino-1, 2-propanediol (23.0%) and phenol (18.8%), followed by organic acids (38.2%), primarily hexadecanoic acid. Other compounds (18.9%), amide (18.5%), furan and pyran derivatives (11.8%), alcohols (9.3%), and ketones (1.91%) were also detected. Phenols and furans were derived from the decomposition of lignin and hemicellulosic components in woody materials, including oil palm biomass (Mathew and Zakaria, 2015), while amide, alcohols, and ketones were produced from the decomposition of cellulose during the carbonisation process (Stefanidis *et al.*, 2014).

According to Suresh *et al.* (2019), the antifungal activities and some preservative effects of the OPKS are attributable to the phenols, ketones, and organic acids. Moreover, the organic acids and phenols in the OPKS-wood vinegar were correlated with strong bacteria inhibition (Ma *et al.*, 2013). The organic acids in wood vinegar also improved the nutritional quality of fruits due to enhanced soil nutrients, such as NH_4^+-N, NO_3^-, N, and Mg, that are essential for plant growth (Zhang *et al.*, 2020). Consequently, carbonising OPKS produces good quality charcoal and wood vinegar for various applications.

In the current study, gaseous pollutants released during OPKS carbonisation with TCS and PRK were examined at 700°C, the temperature at which high HHVcharcoal was produced (*Table 5*). Primarily, H_2, CO, and CH_4 gases were recorded at approximately 74.0% and 51.2% of the total volume in the PRK and TCS systems. According to Wu *et al.* (2019), H_2 was primarily produced from the secondary tar cracking reaction and dehydrogenation of cellulose. The CO was contributed from the carbonyl functional group, while an unstable intermediate decomposition product formed CH_4 during the OPKS carbonisation. The gases could be captured and comprehensively converted to synthesise hydrogen and natural gases, hence considered one of the most promising fossil fuel alternatives in the future (Zhang *et al.*, 2016).

The CO_2 compounds were principally derived from oxygenated organic and inorganic components in OPKS (Adam, 2009). Conventional carbonisation, such as the TCS and traditional charcoal systems, produce the highest CH_4 and CO_2. Nevertheless, the emission of CH_4 gas has more notable greenhouse effects than CO_2 as the gas was from biomass burning. Accordingly, introducing an environmentally efficient rotary kiln or PRK could significantly reduce the harmful gaseous emissions.

TABLE 4. THE COMPOUNDS IDENTIFIED IN THE OPKS-WOOD VINEGAR PRODUCED DURING THE CARBONISATION PROCESS WITH THE PRK SYSTEM

No.	Compound	Retention time (min)	Relative content (%)
	Furan and pyran derivatives		**11.8**
1	Pyridine	7.47	5.13
2	Paromomycin	14.5	1.5
3	Pyridine	14.5	2.17
4	Cystine	15.7	2.96
	Phenol and derivatives		**41.8**
5	3-Amino-1,2-propanediol	9.54	23.0
6	Phenol	20.2	18.8
	Organic acids		**38.2**
7	Acetic acid	10.3	1.56
8	Hexadecanoic acid	19.8	36.6
	Ketones *(1.91)*		**1.91**
9	Butyrolactone	14.2	1.91
	Amide *(18.57)*		**18.5**
10	Acetamide	8.18	4.46
11	Benzeneethanamine	8.37	1.25
12	N-Methoxy-1-ribofuranosy l-4-imidazolecarboxylic amide	9.18	12.8
	Alcohols		**9.30**
13	Ethanol	11.6	9.30
	Others		**18.9**
14	D-Mannoheptulose	9.36	12.3
15	d-Glycero-d-ido-heptose	13.8	2.85
16	Deoxyspergualin	14.2	3.81

TABLE 5. THE COMPOSITIONS OF THE GASEOUS PRODUCTS FROM OPKS CARBONISATION AT 700°C VIA DIFFERENT SYSTEMS

Gas (wt%)	TCS	PRK	Giudicianni *et al.* (2017)
H_2	5.04 ± 1.0	36.8 ± 3.4	0.3-4.8
CH_4	24.1 ± 5.0	16.7 ± 2.2	0.3-5.3
CO_2	45.7 ± 3.5	16.7 ± 2.8	74.2-87.7
CO	22.1 ± 1.9	20.4 ± 0.9	7.6-19.4
C_2	2.98 ± 0.9	5.96 ± 1.8	-
Others	-	3.24 ± 1.7	-

Comparison and Economic Analysis

The economic analysis of the TCS and PRK systems assessed in the current study is summarised in *Table 6*. The estimated fixed cost to acquire OPKS-charcoal via TCS and PRK was RM12 318 and RM35 077 respectively. The payback period for the TCS was projected at 4.46 years, which was longer than the PRK, requiring 0.26 years. The findings were due to the lower internal rate of return (IRR) of TCS, 48%, compared to PRK at 65%, contributed by a higher benefit to cost ratio (B:C) of 1.18 compared to 0.85 by the TCS.

Since the B:C of the PRK employed in the present study was >1, the net present value (NPV) was positive, and the IRR was greater than the opportunity cost of capital, the investment for the approach was more financially feasible than TCS. Furthermore, the economic attainability of PRK would be more profitable if the system is installed near palm oil millers and utilises the OPKS produced by the mills. The approach could reduce the cost of transportation for raw materials, while excess energy and steam produced internally by the mills could be redirected to operate the PRK.

CONCLUSION

Harvesting OKPS-charcoal at 700°C carbonisation temperature utilising raw materials from OPKS via the PRK, a continuous carbonisation technology, produced the highest charcoal and energy efficiency at 38% and 55%, respectively. In the current study, the OPKS-charcoal acquired through the PRK and TCS systems recorded 33.1 and 30.9 MJ kg^{-1} HHV, respectively. The OPKS-charcoal with the high yield, HHV, and low gaseous emissions was considerable to the palm oil industry as it offered value-added

TABLE 6. ECONOMICS ANALYSIS OF THE TCS AND PRK PRODUCED OPKS-CHARCOAL IN A PILOT-PLANT CAPACITY (RM1 = USD0.23)

Item	Cost involved in the TCS system	Cost involved in the PRK system
Capital cost (building, TCS system, and infrastructure)	RM300 000	RM500 000
Operating cost (per month) (A)		
Electricity	RM15	RM2 550
Water	RM15	RM20
Transportation	RM600	RM600
Labour	RM6 000	RM3 600
Raw material, OPKS	RM2 688	RM17 280
Firewood/Diesel*	RM3 000	RM11 027*
Total production cost (A)	RM12 318	RM35 077
Average charcoal and vinegar sale (per month) (B)		
Charcoal price (RM3 kg^{-1})	RM5 913.60 Charcoal produced was 1 971.20 kg $month^{-1}$ = RM3 × 1 971.20 kg	RM51 840 Charcoal produced was 17 280 kg $month^{-1}$ = RM3 × 17 280 kg
Price of wood vinegar (RM10 L^{-1})	RM12 000 Wood vinegar produced was 1 200 L $month^{-1}$ = RM10 × 1 200 L	RM144 000 Wood vinegar produced was 14 400 L $month^{-1}$ = RM10 × 14 400 L
Total sales per month (B)	RM17 913.60	RM195 840.00
Net profit per month (B – A)	RM5 595.60 ≈ USD1 274.91	RM160 763 ≈ USD36 628.63
Payback period = per year	4.46 years	0.26 years

products and a zero-waste operation. Furthermore, manufacturing OPKS-charcoal with the continuous PRK approach could generate higher profit than conventional carbonisation technologies, therefore suitable for utilisation in commercial settings.

ACKNOWLEDGEMENT

The authors would like to extend gratitude to the Director-General of MPOB for the permission to publish this article.

REFERENCES

Adam, J (2009). Improved and more environmentally friendly charcoal production system using a low-cost retort-kiln (Eco-charcoal). *Renew. Energy*, *34(8)*: 1923-1925.

Alslaibi, T; Abustan, I; Ahmad, M and Foul, A (2013). A review: Production of activated carbon from agricultural by-products via conventional and microwave heating. *J. Chem. Technol. Biotechnol.*, *88(7)*: 1183-1190.

Arami-niya, A; Mohd, W; Wan, A and Mjalli, F (2010). Using granular activated carbon prepared from oil palm shell by ZnCl 2 and physical activation for methane adsorption. *J. Anal. Appl. Pyrolysis*, *89(2)*: 197-203.

Astimar, A; Ropandi, M; Norfaizah, J; Nahrul Hayawin, Z and Zawawi, I (2012). The production of oil palm-based activated charcoal and pyroligneous acid (wood vinegar). *MPOB Information Series, TT No. 515, (June)*: 1-2.

Austin, J E and Kohn, T O (1990). *Strategic Management in Developing Countries: Case Studies.* Free Press, USA. 691 pp.

Awasthi, M K; Duan, Y; Awasthi, S K; Liu, T and Zhang, Z (2020). Influence of bamboo biochar on mitigating greenhouse gas emissions and nitrogen loss during poultry manure composting. *Bioresour. Technol.*, *303(February)*: 122952.

Bailis, R; Rujanavech, C; Dwivedi, P; Oliveira, A De; Chang, H; Carneiro, R and Miranda, D (2013). Energy for sustainable development innovation in charcoal production: A comparative life-cycle assessment of two kiln technologies in Brazil. *Energy Sustain. Dev.*, *17(2)*: 189-200.

Basalirwa, D; Sudo, S; Wacal, C; Akae, F; Oo, A Z; Koyama, S; Sasagawa, D; Yamamoto, S; Masunaga, T and Nishihara, E (2020). Assessment of crop residue and palm shell biochar incorporation on greenhouse gas emissions during the fallow and crop growing seasons of broccoli (*Brassica oleracea* var. *italica*). *Soil Tillage Res.*, *196(October 2019)*: 104435.

Chen, D; Chen, X; Sun, J; Zheng, Z and Fu, K (2016). Pyrolysis polygeneration of pine nut shell: Quality of pyrolysis products and study on the preparation of activated carbon from biochar. *Bioresour. Technol.*, *216*: 629-636.

Chen, W H; Wang, C W; Ong, H C; Show, P L and Hsieh, T H (2019). Torrefaction, pyrolysis and two-stage thermodegradation of hemicellulose, cellulose and lignin. *Fuel*, *258*: 116168.

Energypedia (2019). Charcoal production. GIZ HERA cooking energy compedium. https://energypedia.info/wiki/Charcoal_Production, assessed on 6 January 2021.

Fan, X; Wang, X; Cai, Y; Xie, H; Han, S and Hao, C (2022). Functionalized cotton charcoal/chitosan biomass-based hydrogel for capturing Pb^{2+}, Cu^{2+} and MB. *J. Hazard. Mater.*, *423*: 127191.

Goh, C S; Tan, H T and Lee, K T (2012). Pretreatment of oil palm frond using hot compressed water: An evaluation of compositional changes and pulp digestibility using severity factors. *Bioresour. Technol.*, *110*: 662-669.

Hamzah, N; Tokimatsu, K and Yoshikawa, K (2019). Solid fuel from oil palm biomass residues and municipal solid waste by hydrothermal treatment for electrical power generation in Malaysia: A review. *Sustainability*, *11:* 1060.

Harimi, M; Megat Ahmad, M; Sapuan, S and Idris, A (2005). Numerical analysis of emission component from incineration of palm oil wastes. *Biomass and Bioenergy*, *28*: 339-345.

Heberlein, S; Chan, W P; Veksha, A; Giannis, A; Hupa, L and Lisak, G (2022). High temperature slagging gasification of municipal solid waste with biomass charcoal as a greener auxiliary fuel. *J. Hazard. Mater.*, *423*: 127057.

Idris, J; Shirai, Y; Andou, Y; Mohd Ali, A; Othman, M; Ibrahim, I and Hassan, M (2015). Self-sustained carbonisation of oil palm biomass produced an acceptable heating value charcoal with low gaseous emission. *J. Clean. Prod.*, *89*: 257-261.

Kamali, M; Sweygers, N; Al-Salem, S; Appels, L; Aminabhavi, T M and Dewil, R (2022). Biochar for soil applications-sustainability aspects, challenges and future prospects. *Chem. Eng. J.*, *428*: 131189.

Kammen, D M and Lew, D J (2005). Review of technologies for the production and use of charcoal. *Renewable and Appropriate Energy Laboratory Report*, 1-19.

Kodera, Y and Kaiho, M (2016). Model calculation of heat balance of wood pyrolysis. *J. Jpn. Inst. Energy*, *95(10)*: 881-889.

Kushairi, A; Loh, S K; Azman, I; Hishamuddin, E; Ong-Abdullah, M; Izuddin, Z B M N; Razmah, G; Sundram, S and Parveez, G K A (2018). Oil palm economic performance in Malaysia and R&D progress in 2018. *J. Oil Palm Res.*, *30(2)*: 163-195.

Lan, W; Chen, G; Zhu, X; Wang, X; Wang, X and Xu, B (2019). Research on the characteristics of biomass gasification in a fluidized bed. *J. Energy Inst.*, *92*: 613-620.

Ma, C; Song, K; Yu, J; Yang, L; Zhao, C; Wang, W; Zu, G and Zu, Y (2013). Pyrolysis process and antioxidant activity of pyroligneous acid from *Rosmarinus officinalis* leaves. *J. Anal. Appl. Pyrolysis*, *104*: 38-47.

Mahlia, T M I; Ismail, N; Hossain, N; Silitonga, A S and Shamsuddin, A H (2019). Palm oil and its wastes as bioenergy sources: A comprehensive review. *Environ. Sci. Pollut. Res.*, *26(15):* 1-18.

Mathew, S and Zakaria, Z A (2015). Pyroligneous acid-the smoky acidic liquid from plant biomass. *Appl. Microbiol. Biotechnol.*, *99(2)*: 611-622.

Nahrul Hayawin, Z; Astimar, A A; Idris, J; Mamat, R; Hassan, M A; Bahrin, E K and Suraini Abd-Aziz (2017). Microwave-assisted pre-carbonisation of palm kernel shell produced charcoal with high heating value and low gaseous emission. *J. Clean. Prod.*, *142*: 2945-2949.

Nahrul Hayawin, Z; Astimar, A A; Idris, J; Nor Faizah, J; Ropandi, M; Mohamad Faizal, I; Hassan, M A and Abd Aziz, S (2018). Reduction of POME final discharge residual using activated bioadsorbent from oil palm kernel shell. *J. Clean. Prod.*, *182*: 830-837.

Nahrul Hayawin, Z; Ibrahim, M F; Norfaizah, J; Ropandi, M; Astimar, A A; Noorshamsiana, A W and Abd Aziz, S (2020). Palm oil mill final discharge treatment by a continuous adsorption system using oil palm kernel shell activated carbon produced from two-in-one carbonisation activation system reactor. *J. Water Process Eng.*, 101262.

Nipattummakul, N; Ahmed, I I; Kerdsuwan, S and Gupta, A K (2012). Steam gasification of oil palm trunk waste for clean syngas production. *Appl. Energy, 92:* 778-782.

Nyakuma, B B; Johari, A; Ahmad, A and Abdullah, T A T (2014). Comparative analysis of the calorific fuel properties of empty fruit bunch fiber and briquette. *Energy Procedia*, *52*: 466-473.

Oh, S J; Choi, G G and Kim, J S (2016). Characteristics of bio-oil from the pyrolysis of palm kernel shell in a newly developed two-stage pyrolyzer. *Energy, 113*: 108-115.

Paddon, A R and Harker, A P (1979). The production of charcoal in a portable metal kiln. *Tropical Products Institute, 12*: 17.

Parikh, J; Channiwala, S A and Ghosal, G K (2005). A correlation for calculating HHV from proximate analysis of solid fuels. *Fuel*, *84(5)*: 487-494.

Purwanto, H; Zakiyuddin, A M; Rozhan, A N; Mohamad, A S and Salleh, H M (2018). Effect of charcoal derived from oil palm empty fruit bunch on the sinter characteristics of low grade iron ore. *J. Clean. Prod.*, *200*: 954-959.

Sangsuk, S; Suebsiri, S and Puakhom, P (2018). The metal kiln with heat distribution pipes for high quality charcoal and wood vinegar production. *Energy Sustain. Dev.*, *47*: 149-157.

Santos, S de F de O M; Piekarski, C M; Ugaya, C M L; Donato, D B; Braghini, A; de Francisco, A C and Carvalho, A M M L (2017). Life cycle analysis of charcoal production in masonry kilns with and without carbonisation process generated gas combustion. *Sustainability*, *9(9)*: 1-20.

Stefanidis, S D; Kalogiannis, K G; Iliopoulou, E F; Michailof, C M; Pilavachi, P A and Lappas, A A (2014). A study of lignocellulosic biomass pyrolysis via the pyrolysis of cellulose, hemicellulose and lignin. *J. Anal. Appl. Pyrolysis*, *105*: 143-150.

Suresh, G; Pakdel, H; Rouissi, T; Brar, S K; Fliss, I and Roy, C (2019). *In vitro* evaluation of antimicrobial efficacy of pyroligneous acid from softwood mixture. *Biotechnology Research and Innovation*, *3(1)*: 47-53.

Tavakkol, S; Zirwes, T; Denev, J A; Jamshidi, F; Weber, N; Bockhorn, H and Trimis, D (2021). An Eulerian-Lagrangian method for wet biomass carbonisation in rotary kiln reactors. *Renew. Sust. Energ. Rev.*, *139*: 110582.

Trangkaprasith, K (2011). Heating value enhancement of fuel pellets from frond of oil palm. *Int. Conf. Biol. Environ. Chem. IPCBEE Vol.1. IACSIT Press. Singapore*, *1*: 302-306.

Tymoszuk, M; Mroczek, K; Kalisz, S and Kubiczek, H (2019). An investigation of biomass grindability. *Energy*, *183*: 116-126.

Vijaya, S; Ma, A N; Choo, Y M and Nik Meriam, N S (2008). Life cycle inventory of the production of crude palm oil - A gate to gate case study of 12 palm oil mills. *J. Oil Palm Res.*, *20(2)*: 484-494.

Wang, Q; Han, K; Gao, J; Li, H and Lu, C (2017). The pyrolysis of biomass briquettes: Effect of pyrolysis temperature and phosphorus additives on the quality and combustion of bio-char briquettes. *Fuel*, *199*: 488-496.

Wu, Z; Li, Y; Xu, D and Meng, H (2019). Co-pyrolysis of lignocellulosic biomass with low-quality coal: Optimal design and synergistic effect from gaseous products distribution. *Fuel*, *236*: 43-54.

Zhang, S; Chen, Z; Cai, Q and Ding, D (2016). The integrated process for hydrogen production from biomass: Study on the catalytic conversion behavior of pyrolytic vapor in gase solid simultaneous gasification process. *Int. J. Hydrog. Energy*, *41(16)*: 6653-6661.

Zhang, Y; Wang, X; Liu, B; Liu, Q; Zheng, H; You, X; Sun, K; Luo, X and Li, F (2020). Comparative study of individual and co-application of biochar and wood vinegar on blueberry fruit yield and nutritional quality. *Chemosphere*, *246*: 125699.

Journal of Oil Palm Research Vol. 35 (3) September 2023 p. 448-455
DOI: https://doi.org/10.21894/jopr.2022.0065

THERMOPHYSICAL PROPERTIES OF OIL PALM EMPTY FRUIT BUNCH PEDUNCLE FOR USE AS A MULCHING MATERIAL

SUNDAY EDET ETUK[1], UBONG WILLIAMS ROBERT[2] and OKECHUKWU EBUKA AGBASI[3]*

ABSTRACT

The choice of mulching or topsoil covering material for the retardation of soil water loss through evaporation requires a good knowledge of thermal properties of the material. Peduncle of oil palm empty fruit bunch was obtained from some local oil palm processing units in Uyo, soaked in water and air-dried completely before shaping and subjecting samples to various laboratory tests. The bulk density, water absorption, thermal conductivity, specific heat capacity, volumetric heat capacity, thermal diffusivity, thermal effusivity and solar radiation absorptivity of the sample were found to be (332.59 ± 0.65) kg m^{-3}, (269.54 ± 1.28)%, (0.078 ± 0.001) W m^{-1} K^{-1}, (1552.56 ± 1.56) J kg^{-1} K^{-1}, (0.516 ± 0.001) MJ m^{-3} K^{-1}, (1.51 ± 0.01) 10^{-7} m^2 s^{-1}, (200.42 ± 1.33) J m^{-2} K^{-1} $s^{-1/2}$ and (15.54 ± 0.05) m^{-1} respectively in the longitudinal direction whereas the respective values were found to be (332.54 ± 0.68) kg m^{-3}, (269.51 ± 1.27)%, (0.042 ± 0.001) W m^{-1} K^{-1}, (1553.38 ± 0.44) J kg^{-1} K^{-1}, (0.517 ± 0.001) MJ m^{-3} K^{-1}, (0.82 ± 0.01) 10^{-7} m^2 s^{-1}, (147.98 ± 1.57) J m^{-2} K^{-1} $s^{-1/2}$ and (21.06 ± 0.18) m^{-1} in the transverse direction. The results of the tests favour the peduncle as a potential mulching material for retardation of soil water loss through evaporation and a slow response to changes in its thermal environment.

Keywords: bulk density, evaporation, mulching material.

Received: 10 May 2022; **Accepted:** 17 August 2022; **Published online:** 3 October 2022.

INTRODUCTION

Plants are photoautotrophs. They are grown on soils which have all the elements needed for the preparation of their food, including water, employing solar energy. A plant absorbs light from the solar system, water from the ground, and carbon dioxide gas derived from the atmosphere for the preparation of its food (Garg and Garg, 2018). A plant absorbs only part of the energy from the solar system, whereas the remaining part of the energy from the solar system is lost as heat and fluorescence. The photon energy that is within the range of light wavelength suitable for photosynthesis, is designated as photosynthetically active radiation (PAR) (Etuk *et al*., 2016a; 2016b; Liu and van Iersel, 2021; Mõttus *et al*, 2012; Ross and Suler, 2000).

It is expedient to point out that solar energy is a requirement for the sustenance of plant life, which depends on seasons, latitude and cloud cover, among other factors. The majority of this energy is ineffective for plants and instead heats the earth, atmosphere, and, in some cases, reflects from the earth (Garg and Garg, 2018). The proportion of solar energy which heats the earth gives rise to evapotranspiration of soil water, arising from crop transpiration and soil evaporation. Evaporation of soil water in non-irrigated areas has some adverse effects on plants. This situation calls for adequate

[1] Department of Physics,
University of Uyo, Uyo, Nigeria.

[2] Department of Physics,
Akwa Ibom State University,
Ikot Akpaden, Mkpat Enin, Nigeria.

[3] Department of Physics,
Michael Okpara University of Agriculture,
Umudike, Nigeria.

* *Corresponding author: agbasi.okechukwu@gmail.com*

mulching to reduce or slow down the rate of soil evaporation for the nourishment of plant life, during dry season (Kakaire *et al*., 2015). The rate of heat transport through the mulching material(s) should be considered when selecting the material(s). More so, high temperatures are known to hasten the ripening, senescence and withering of crops. A long duration of severe heat energy is capable of causing some crops to go into dormancy. This, coupled with the evaporation of soil water, will result in moisture stress, which may cause perpetual dormancy (FAO, 1998). This research, therefore, seeks to examine some thermophysical properties of oil palm empty fruit bunch (EFB) peduncle to establish its mulching suitability against evaporation during the dry season in non-irrigated farmlands. The peduncle of EFB is obtained from oil palm tree, scientifically named *Elaeis guineensis*. The oil palm tree belongs to Arecaceae palm family in the Plantae kingdom of Arecales order. The plant has Africa as its origin (Verheye, 2010) and it is said to originate from the tropical rainforest zone. Indonesia is said to be the largest exporter of palm oil (Murphy, 2007; Ziaei and Ali, 2021).

Theoretical Considerations

Ekpe and Akpabio (1994) stated that several factors, including geographic and site characteristics as well as thermophysical properties, would determine the soil temperature. Evapotranspiration is a combination of the evaporation of water from the soil and the transpiration of water from leaves. It is determined by environmental soil and air conditions. According to the report of the Food and Agriculture Organization of the United Nations (FAO, 1998), the crop coefficient changes with the variations in ground cover, during the crop growing period. The evaporating power of the atmosphere affects the initial crop coefficient. Transpiration in some plants happens to be very low because such plants close their stomata during the day and open them at night. In such situations, transpiration is low whereas losses of water are mainly from the evaporation of the soil. Hence, the bulk of crop evapotranspiration under standard conditions from such plants is through evaporation from the soil. A typical example of a plant with such behaviour is pineapple. It is only with a full ground cover that soil evaporation can be reduced, leading to a single crop coefficient for mid-season. This mid-season crop coefficient value would be lower than at the initial stage, since it occurs during full ground cover.

Ekpe and Akpabio (1994) and Keunbo *et al*. (2020) attributed that the changes in temperature of soil with depth are due to various factors, including the quantum of radiant energy that gets to the surface of the soil, thermal properties of the soil, and colour of the soil. The amount of absorbed radiant energy leads to changes in soil temperature. Heating the air above the soil would raise the surface temperature, heating the interior layers of soil and radiating to the atmosphere, which may occur as a result of absorbed soil surface energy. Robert *et al*. (2020a) expressed the heat budget as Equation (1):

Heat flow through the soil = Absorbed solar radiation + Heat absorbed from the atmosphere - Re-emitted radiant energy (1)

The heat balance equation above, in one dimension, can be expressed as Equation (2) (Khaty *et al*., 1978):

$$-k\left(\frac{\partial T}{\partial x}\right)_{x=0} = h(T_{atm} - T_{x=0}) + \alpha I - \varepsilon \Delta R \quad (2)$$

where k is soil thermal conductivity, T is soil temperature, h is surface heat transfer coefficient, T_{atm} is air temperature in the atmosphere, α is solar radiation absorptivity at the soil surface, I is solar radiation intensity, ε is long-wave emissivity of the soil surface, and ΔR is the difference between the incident long-wave radiation and the soil surface emitted radiation.

Giving solar temperature, T_s as Equation (3):

$$T_s = T_{atm} + \left(\frac{\alpha I}{h}\right) - \left(\frac{\varepsilon \Delta R}{h}\right) \quad (3)$$

Considering the above equation, Sohda *et al*. (1979) and Moustafa *et al*. (1981) expressed:

$$T(x,t) = \alpha_0 + \sum_{m=1}^{\alpha} \{\alpha_m \, exp[i(m\omega t + \alpha_m x]\} \quad (4)$$

as a general solution to one-dimensional heat conduction

Equation (4) results in Equation (5):

$$T(x,t) = \alpha_0 + \sum_{m=1}^{\alpha} \{\alpha_m \exp(-\alpha_m x) \, Cos \, (m\omega t - \alpha_m x)\} \quad (5)$$

as its real part, with $\alpha_m = (^{m\omega pc}/_{2k})^{\frac{1}{2}} (1-i)$

where $\omega = 2\pi/\text{period}$.

With the modification of Equation (5), a more convenient expression showing the variation of soil temperature with thickness of soil yields, as Equation (6):

$$T(x,t) = T_m - A_s \exp(-ax) \, Cos\{w(t - t_0 - {}^{ax}/_{w})\} \quad (6)$$

where A_s is daily temperature amplitude (in °C at $x = 0$), x is thickness of the soil, t is time of the day (in hours), t_0 is time corresponding to the minimum temperature at the soil surface (in hours). T_m can be computed from the hourly soil surface temperature

average, T_{hss} on a 24-hour period in °C employing, Equation (7):

$$T_m = \sum_{m=1}^{24} (T_{hss}/_{24}) \quad (7)$$

This results in the expression of Equation (8):

$$T(x,t) = T_m - A_s \exp(-ax)\, Cos\{(\pi/_{12})[t=t_0-(^{12ax}/_{\pi})]\} \quad (8)$$

MATERIALS AND METHODS

Materials Collection and Sample Preparation

Several undecayed EFBs of oil palm were collected from some local oil palm processing units in Uyo Local Government Area, Akwa Ibom State, Nigeria. The peduncle was removed from each bunch (*Figure 1*) before being sorted. Those wider than 114 mm in diameter were chosen for use in this study. The selected ones were then soaked in cold water for 48 hr to remove any accompanying impurities. The soaked peduncles were removed from the water after 48 hr and each of them was suspended with a string to hang freely to dry in the atmosphere. Circular pieces were prepared from longitudinal and transverse sections of the peduncles. The pieces were identical, with a thickness of 9 mm and a diameter of 110 mm. In all, five of such pieces were prepared each from the longitudinal section and transverse section. They were then sun-dried completely, coded (for ease of identification), and then used as test samples in this work.

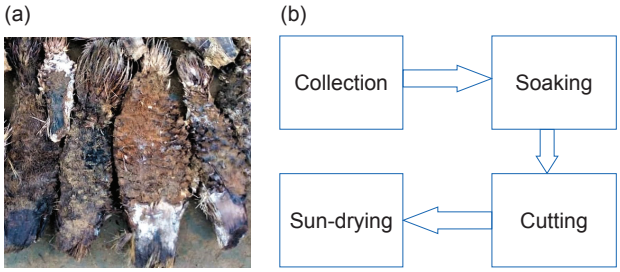

Figure 1. (a) Peduncles of oil palm empty fruit bunch, and (b) steps of sample preparation.

Property Tests

The thermal conductivity of each test sample was determined by using Modified Lee–Charlton's Disc Apparatus Technique as described in details elsewhere by Robert *et al*. (2021a) and obtained based on the relation in Equation (9):

$$k = \left(\frac{Mcx}{A\Delta\theta}\right)\frac{dT}{dt} \quad (9)$$

where M is mass of the disc, c is specific heat capacity of the disc, x is test sample's thickness, A is cross-sectional area of the sample, $\Delta\theta$ is temperature across the test sample's thickness and $\frac{dT}{dt}$ is rate of cooling of the disc.

After that, the samples were cut into reasonable sizes and shapes required for other tests. The modified water displacement method, proposed by Robert *et al.* (2019) was used for the bulk density test. The mass of each sample was measured using a digital weighing balance (S. METTLER - 600 g) after which its value was divided by that of bulk volume (Etuk *et al.*, 2018; Robert *et al.*, 2021b; 2021c) to obtain the required bulk density. The samples were then weighed for water absorption investigation. Then, 10 identical vessels were filled with equal volumes of water, initially at 28°C, and the samples were immersed separately in water. They were removed from the water after 24 hr and allowed to surface-dry. The samples were then re-weighed and water absorption was calculated using the formula (Robert *et al.*, 2020b).

$$WA = \left(\frac{M_w - M_d}{M_d}\right) 100\% \quad (10)$$

where M_d is mass before immersion, M_w is mass after immersion, and WA is water absorption.

Specific heat capacity was measured for each sample with the aid of SEUR'S Apparatus (Etuk *et al.*, 2020). In this study, the device was designed with a central square cavity measuring 60 × 60 × 14 mm for heat exchange. The heat exchange plates were aluminium, test samples, and plywood materials each of which was cut to a square of almost similar dimensions (for length and width) as the cavity but with a consistent thickness of about 8 mm. During heat exchange, the hot aluminium plate was sandwiched between the test sample and plywood plate until the system attained thermal balance. Temperature monitoring and measurements were conducted by using three digital thermometers (Model 305, calibrated and equipped with a Type-K probe). The obtained data were then used to compute the value of specific heat capacity, C based on the relation in Equation (11):

$$C = \frac{Q_a - Q_p}{M_s \delta T} \quad (11)$$

where Q_a is quantity of heat lost by the aluminium plate, Q_p is quantity of heat gained by the plywood, M_s is mass of the sample, δT is rise in temperature of the sample.

Corresponding volumetric heat capacity, was determined for the test samples from the values of bulk density and specific heat capacity as suggested by Robert *et al.* (2022):

$$C_v = \rho C \quad (12)$$

where ρ is bulk density.

Thermal diffusivity value, was computed using the equation (Cengel *et al*., 2012; Etuk *et al*., 2010; Rajput, 2015; Welty *et al*., 2001):

$$\lambda = \frac{k}{\rho C} \quad (13)$$

Solar radiation absorptivity and thermal effusivity were computed using the values for other related parameters already obtained. The value of solar radiation absorptivity, α was computed on a 24 hr periodic basis employing the equation expressed by several authors, including Ekpe and Akpabio (1994) and Robert *et al*. (2020a) as:

$$a = \sqrt{\frac{w}{2\lambda}} \quad (14)$$

whereas thermal diffusivity value, was calculated using the formula:

$$e = \sqrt{k\rho C} \quad (15)$$

RESULTS AND DISCUSSION

The experimental values determined per test carried out on the test samples are expressed in *Table 1*. It can be seen from the table that the bulk density of the test samples ranges from 331.65 to 333.24 kg m^{-3} while that of soil samples was reported to be between 1000.00 kg m^{-3} and 2000.00 kg m^{-3} (Birkeland, 1984; Blake and Hartge, 1986; Purser 1988), indicating that samples were far less dense than soil samples. This also shows that the degree of compactness of particles is equally far less compared to that of any soil sample. Hence, it allows for good aeration and supports permeability, a situation that accounts for a higher percentage of water absorption. Measurement of bulk density is vital in quantitative studies relating to soil, as it is a necessary parameter for computing soil moisture movement within a profile. Variation in bulk density of soil is attributable to the relative proportion and density of solid organic particles as well as porosity. It is plausible that the test sample if applied as a mulching material, will make the soil less dense.

The results clearly show thermal conductivity values of 0.074 ± 0.001 W m^{-1} K^{-1} for the test sample when subjected to heat flow in the longitudinal direction, and 0.042 ± 0.001 W m^{-1} K^{-1} when in the transverse. This can be explained in terms of the low bulk density value and availability of a high degree of still air space, which equally accounts for the low bulk density. Bulk density has a direct relationship with the thermal conductivity of the samples. This is because, the more the percentage of dead air space (still air volume) in the samples, the bulk density will be lower and hence, lower their thermal conductivity since air is a good heat insulant. Our finding is supported by the report of the United State

TABLE 1. EXPERIMENTAL RESULTS OF THE PROPERTY TESTS PERFORMED ON THE OIL PALM EMPTY FRUIT BUNCH PEDUNCLE

Tests section	Sample code	Bulk density (kgm^{-3})	Water absorption (%)	Thermal conductivity (Wm^{-1} K^{-1})	Specific heat capacity (Jkg^{-1} K^{-1})	Volumetric heat capacity (MJm^{-3} K^{-1})	Thermal diffusivity (10^{-7} m^2 s^{-1})	Thermal effusivity (Jm^{-2} K^{-1} $s^{-1/2}$)	Solar radiation absorptivity (m^{-1})
Longitudinal	SL1	332.93	268.88	0.078	1556.76	0.518	1.50	201.06	15.57
	SL2	330.78	272.01	0.076	1550.24	0.513	1.48	197.41	15.68
	SL3	333.14	269.43	0.079	1552.33	0.517	1.53	202.12	15.42
	SL4	331.99	271.76	0.076	1545.41	0.513	1.48	197.47	15.68
	SL5	334.02	265.61	0.080	1558.04	0.520	1.54	204.04	15.37
	Mean ± Std error	332.59 ± 0.65	269.54 ± 1.28	0.078 ± 0.001	1552.56 ± 1.56	0.516 ± 0.001	1.51 ± 0.01	200.42 ± 1.33	15.54 ± 0.05
Transverse	ST1	331.79	271.83	0.042	1554.03	0.516	0.81	147.16	21.19
	ST2	332.83	269.13	0.043	1553.61	0.517	0.83	149.11	20.93
	ST3	334.13	265.74	0.044	1554.33	0.519	0.85	151.17	20.68
	ST4	330.71	272.10	0.040	1552.83	0.514	0.78	143.32	21.59
	ST5	333.25	268.75	0.043	1552.11	0.517	0.83	149.14	20.93
	Mean ± Std error	332.54 ± 0.68	269.51 ± 1.27	0.042 ± 0.001	1553.38 ± 0.44	0.517 ± 0.001	0.82 ± 0.01	147.98 ± 1.57	21.06 ± 0.18

Department of Agriculture (USDA) Forest Products Laboratory on thermal conductivity of wood, which shows that density and grain direction, among other factors, affect the thermal conductivity of a wood sample. The thermal conductivity value obtained either in the longitudinal or transverse direction indicates that the sample as a ground cover or mulching material retards heat transport on the soil it covers. However, the transverse sample exhibits more pronounced heat retardation compared to the longitudinal sample. Thermal conductivity is very important as far as thermal transport is involved (Incropera and De Witt, 1990). The values of thermal conductivity for straw and sawdust were reported as 0.0576 W $m^{-1} K^{-1}$ for straw and 0.0649 W $m^{-1} K^{-1}$ for sawdust (Perry and Green, 2007; Powell and Childs, 1972; Sayigh, 1978). It can be inferred that, transversely, the sample has a mean thermal conductivity value which is 27% less than the thermal conductivity value of straw and 35% less than that of sawdust. However, the mean thermal conductivity value of the sample is higher than that of straw by 22% and that of sawdust by 12% when considered in a longitudinal direction to the flow of heat.

The mean specific heat capacity of about 1552.56 J $kg^{-1} K^{-1}$ was obtained for the samples in the longitudinal direction whereas 1553.38 J $kg^{-1} K^{-1}$ was recorded for the ones selected for transverse observation. This suggests that the test sample has an approximate specific heat capacity of 1550 J $kg^{-1} K^{-1}$. This specific heat capacity result is comparable with the observation of Kodeŝovā *et al*. (2013) on the specific heat capacity of soil organic matter reported as being 1900 J $kg^{-1} K^{-1}$. Theirs was a little higher than ours, possibly because of the presence of soil particles in soil organic matter. It can be adjudged from the results that about 0.516 MJ needs to be added in the form of heat to one unit of volume of the test sample to cause an increase of one unit of its temperature, as shown in its volumetric heat capacity value. Comparatively, the result of the volumetric heat capacity of the sample was far less than the value reported for *Miscanthus* biochar, as 2.3348 MJ $m^{-3} K^{-1}$; switchgrass biochar, as 2.2232 MJ $m^{-3} K^{-1}$ and wood chip biochar, as 0.00939 MJ $m^{-3} K^{-1}$ (Behazin, 2016).

The thermal diffusivity of plant-based materials is generally much smaller than that of other materials like stone, metals and others. For the studied samples, the mean thermal diffusivity value was 1.51×10^{-7} $m^2 s^{-1}$ in the longitudinal direction and 0.82×10^{-7} $m^2 s^{-1}$ in the transverse direction. The low thermal diffusivity expresses how sluggish the test sample can absorb heat from its surroundings. Thermal diffusivity is the ratio of thermal conductivity to the product of bulk density and specific heat capacity. Herewith, the low thermal conductivity, coupled with the moderate mean bulk density and specific heat capacity of the sample, enable the thermal diffusivity value of the sample to be lower than that of wood chip biochar, which was 2.9426 ± 0.1437 $m^2 s^{-1}$ (Behazin, 2016). Thermal diffusivity is an important indicator of thermal insulating behaviour. Since the test sample exhibits low thermal diffusivity, which was even lower than that reported for soil samples, it therefore suggests that it can be very useful as a retardant of soil water evaporation during the summer or dry season.

A material's thermal effusivity (also known as the thermal inertia or thermal responsivity of a material) is a measure of its ability to exchange thermal energy with its surroundings. In the longitudinal direction, the samples have a thermal effusivity value of about 200 J $m^{-2} K^{-1} s^{-1/2}$. The thermal effusivity values of the samples in this research are within the range for wood samples. Wood has a low thermal effusivity value in J $m^{-2} K^{-1} s^{-1/2}$ whereas metals have high thermal effusivity values in kJ $m^{-2} K^{-1} s^{-1/2}$. This is supportive of the test sample as a potential mulching material. Considering solar radiation absorptivity, the sample has a mean value of 15.54 m^{-1} in the longitudinal direction to the flow of heat, whereas a mean value of 21.06 m^{-1} was obtained in the transverse direction. The results yield about 26.16% decrements in the value of solar radiation absorptivity in longitudinal as compared with transverse. As far as solar radiation absorptivity is concerned, the mean value suggests that the test sample is better in the transverse direction than in the longitudinal direction.

Variation in soil temperature, as aforementioned, is influenced by the amount of solar radiation that reaches and is absorbed by the soil. Since the test sample is expected to receive solar radiation when applied as a soil surface cover, it implies that the variation of the sample's temperature will depend on the quantum of solar radiation it receives and absorbs. Now, revisiting our Equation (8), and substituting the mean values of solar radiation absorptivity into it gives rise to the following models:

For application of the sample in the longitudinal direction,

$$T(x,t) = T_m - A_s \exp(-15.54x) Cos \{(0.262)[t - t_0 - (59.35x)]\} \quad (16)$$

For application of the sample in the transverse direction,

$$T(x,t) = T_m - A_s \exp(-21.06x) Cos \{(0.262)[t - t_0 - (80.43x)]\} \quad (17)$$

These can be applied to predict temperature variation of peduncle of oil palm empty fruit bunch in a chosen direction of placement taking into

consideration its thickness, x at any time, t of the day.

According to Shafiquzzaman and Naher (2017), oil palm fibres are easily degraded, environmentally friendly, and nutrient-rich, once formed. They also posited that bio compost, apart from being a good biofertiliser, is a good biocontrol agent against soil-borne pathogens. Their report and that of Baharuddin *et al*. (2009) show that soils that were initially slightly acidic were found to be alkaline with an electrical conductivity range of between 40.10 S cm^{-1} and 50.40 mS cm^{-1} with improved C:N ratio, percentage nitrogen (N), phosphorus (P), and potassium (K), causing the bio composting of oil palm fibres to exhibit great potential as soil micronutrient enhancers and improve plant growth performance and crop yield production. The above is supported by the report of Kavitha *et al*. (2013) that suggests an empty oil palm fruit bunch demonstrates an improved C:N ratio with an increase in the macronutrients such as NPK as well as micronutrients including zinc (Zn), iron (Fe), copper (Cu) and manganese (Mn). Hence, oil palm EFB has a positive effect in terms of nutrients in the soil and plant growth (Liew *et al*., 2010; Tao *et al*., 2018; Trisakti *et al*., 2017; Zaharah and Lim, 2000). The above are added advantages to the test sample as a potential mulching material. Apart from the retardation of water evaporation from the soil, this means that the test sample is degradable in nature, very rich in soil nutrients, and improves the pH of the soil. This is supported by the report of Triyono and Haryanto (2019). *Figure 2* shows that the soil mulched with our test sample enhances the growth of a crop planted on it.

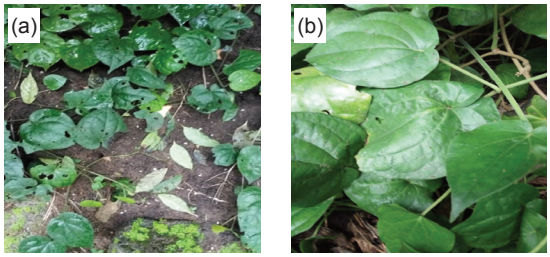

Figure 2. The crop grown on soil (a) without the peduncle, and (b) mulched with the peduncles.

TABLE 2. THERMODYNAMIC AND TRANSPORT PROPERTIES OF SOME RELATED SOIL MATERIALS (at 20°C)

Soil component	Density (Mg m^{-3})	Specific heat (kJ kg^{-1} K^{-1})	Volumetric heat capacity (MJ m^{-3} K^{-1})
Soil minerals (average)	2.6500	0.73	1.9000
Soil organic matter (average)	1.3000	1.90	2.5000
Water	1.0000	4.18	4.1800
Air	0.0012	1.00	0.0012

Source: Van Wijk and De Vries (1963).

For comparison with the results obtained in this study, the values of thermal transport and thermodynamic properties of some related materials are adopted as presented in *Table 2*. As shown, the specific heat capacity of the test samples was greater than the values reported for soil minerals and air. Also, the samples were observed to be lighter than any of the materials listed in *Table 2*.

CONCLUSION

This research work was aimed at investigating the thermophysical properties of the peduncle of an oil palm empty fruit bunch for the purpose of among others, using it as mulching material for retardation of soil water loss by evaporation; protecting soils from wind, water, and traffic-induced compaction and erosion; conserving soil moisture; increasing water detention capacity; providing for good aeration and supporting permeability. The results of thermophysical properties, as well as density, are indications that the test sample can slow down heat flow, respond sluggishly to changes in its thermal environment and render storage of thermal energy difficult, therefore, retarding soil water loss. Generally, it was found that the sample is a potential mulching material suitable for soil cover for enhancement of crop performance and production. Herewith, we recommend that the peduncle of the oil palm empty fruit bunch can be used by farmers as a mulching material for topsoil covering which will address the problem of environmental pollution as a result of the usage of inorganic fertilisers.

ACKNOWLEDGEMENT

We would wish to thank the editor and reviewer(s) for their inputs.

REFERENCES

Behazin, E; Ogunsona, E; Rodriquez-Uribe, A; Mohanty, A K; Misra, M and Anyia, A O (2016). Mechanical, chemical, and physical properties of wood and perennial grass biochars for possible composite applications. *BioRes., 11(1)*: 1334-1348.

Blake, G R and Hartge, K H (1986). Bulk density. *Methods of Soil Analysis Part 1: Physical and Mineralogical Methods* (Klute, A ed.). 2nd edition. American Society of Agronomy, Agronomy Monographs. Madison, Wisconsin. 1188 pp.

Baharuddin, A S; Wakisaka, M; Shivai, Y; Abd Aziz, S; Abdul Rahman, N A and Hassan, M A (2009). Co-

composting of empty fruit bunches and partially treated palm oil mill effluents in pilot scale. *Int. J. Agr. Res*., *4(2)*: 69-78.

Birkeland, P W (1984). *Soils and Geomorphology*. Oxford University Press, New York. p. 14-15.

Cengel, Y A; Cimbala, J M and Turner, R H (2012). *Fundamentals of Thermal-Fluid Sciences*. 4th edition. McGraw-Hill, Singapore. p. 23, 40 and 642.

Ekpe, S D and Akpabio, G T (1994). Comparison of the thermal properties of soil samples for passively cooled building design. *Turk. J. Phy*., *18*: 117-122.

Etuk, S E; Agbasi, O E and Nwokolo, C S (2016a). Modelling and estimating photosynthetically active radiation from measured global solar radiation at Calabar, Nigeria. *Phy. Sci. Int. J., 12(2)*: 1-2.

Etuk, S E; Nwokolo, C S; Agbasi, O E and John-Jaja, A (2016b). Analysis of photosynthetically active radiation over six tropical ecological zones in Nigeria. *J. Geog. Env. Earth Sci. Int., 7(4)*: 1-15.

Etuk, S E; Agbasi, O E; Abdulrazzaq, Z T and Robert, U W (2018). Investigation of thermophysical properties of alates (swarmers) termite wing as potential raw material for insulation. *Intl. J. Sci. World*, *6(1)*: 1-7. DOI: 10.14419/ijsw.v6i1.8529.

Etuk, S E; Robert, U W and Agbasi, O E (2020). Design and performance evaluation of a device for determination of specific heat capacity of thermal insulators. *Beni-Suef Univ. J. Bas. App. Sci*., *9(34)*: 1-7. DOI: 10.1186/s43088-020-0062-y.

Etuk, S E; Akpabio, L E and Akpan, I O (2010). Comparative study of thermal transport in *Zea mays* straw and *Zea mays* heartwood (cork) boards. *Ther. Sci., 14(1)*: 31-38.

FAO (1998). *Food and Agriculture Organization of the United Nations. Crop Evapotranspiration Guidelines for Computing Crop Water Requirements*. FAO Irrigation and Drainage Paper 56. p. 8-19.

Garg, S K and Garg, R (2008). *Environmental Studies and Green Technologies*. Khana Publishers, Delhi. p. 67.

Incropera, F P and De Witt, D P (1990). *Fundamental of Heat and Mass Transfer.* 3rd edition. John Wiley and Sons, New York. p. 45-51, 57.

Jain, R K and Rao, S S (2011). *Industrial Safety, Health and Environment Management Systems.* 3rd edition. Khana Publishers, New Delhi. p. 929.

Kakaire, J; Makokha, G L; Mwanjalolo, M; Mensah, A K and Menya, E (2015). Effects of mulching on soil hydro-physical properties in Kibnale sub-catchment, South Central Uganda. *App. Ec. Env. Sci., 3(5)*: 127-135.

Kavitha, B; Jothimani, P and Rajannan, G (2013). Empty fruit bunch - A potential organic manure for agriculture. *Int. J. Sci., Env. Tech*., *2(5)*: 930-937.

Keunbo, P; Kim, Y; Lee, K and Kim, D (2020). Development of a shallow-depth soil temperature estimation model based on air temperatures and soil water contents in a permafrost area. *Appl. Sci. 10(3)*: 1058. DOI: 10.3390/app10031058.

Khaty, A B; Sodha, M S and Malik, M A S (1978). Periodic variation of ground temperature with depth. *Solar Ene., 30*: 425-427.

Kodeŝovā, R; Viasakova, M; Fēr, M; Tepla, D; Jakŝik, O; Neuberger, P and Adamovsky, R (2013). Thermal properties of representative soils of Czech Republic. *Soil Water Res*., *4*: 141-150.

Liew, V K; Rahman, Z A; Musa, M H and Hessein, A (2010). Empty fruit bunch application and oil palm root proliferation. *J. Oil Palm Res*., *22*: 750-757.

Liu, J and van Iersel, M W (2021). Photosynthetic physiology of blue, green, and red light: Light intensity effects and underlying mechanisms. *Front. Plant Sci., 12*: 619987. DOI: 10.3389/fpls.2021.619987.

Mõttus, M; Sulev, M; Baret, F; Lopez-Lozano, R and Reinart, A (2012). Photosynthetically active radiation: Measurement and modeling. *Encyclopedia of Sustainability Science and Technology* (Meyers, R A eds.). Springer, New York. DOI: 10.1007/978-1-4419-0851-3_451.

Moustafa, S; Jarra, D; El-Manay, H; Al-Shaini, H and Brusewitz, G (1981). Arid soil temperature model. *J. Soil Ener., 27*: 83-88.

Murphy, D J (2007). Future progress for oil palm in the 21st century: Biological and related challenges. *Eur. J. Lipid Sci Tech., 109*: 1-11.

Perry, R H and Green, D W (2007). *Perry's Chemical Engineering Handbook*. 8th edition. McGraw-Hill Companies, New York. p. 7-12.

Powell, R I and Childs, G E (1972). *American Institute of Physics Handbook*. (Gray, D E ed.). 3rd edition. McGraw-Hill New York. p. 7-11.

Purser, M D (1988). *The impact of clearcut logging with high-lead yarding on spatial distribution and variability*

of infiltration capacities on a forest hillslope. Masters Thesis, University of Washington.

Rajput, E R E (2015). *Heat and Mass Transfer*. 6th edition. S. Chand and Company Pvt. Ltd, New Delhi. p. 27-31.

Robert, U W; Etuk, S E and Agbasi, O E (2019). Modified water displacement method and its use for determination of bulk density of porous materials. *J. Renew. Ener. Mech., 1(1)*: 1-16. DOI: 10.25299/rem.2019.vol1(01).2292.

Robert, U W; Etuk, S E; Agbasi, O E and Umoren G P (2020a). Comparison of clay soils of different colors existing under the same conditions in a location. *Imam J. App. Sci., 5(2)*: 68-73. DOI: 10.4103/ijas.ijas_35_19.

Robert, U W; Etuk, S E; Iboh, U A; Umoren, G P; Agbasi, O E and Abdulrazzaq, Z T (2020b). Thermal and mechanical properties of fabricated plaster of paris filled with groundnut seed coat and waste newspaper materials for structural application. *Építőanyag - J. Sil. Based Comp. Mat., 72(2)*: 72-78. DOI: 10.14382/epitoanyag-jsbcm.2020.12.

Robert, U W; Etuk, S E; Agbasi, O E and Okorie, U S (2021a). Quick determination of thermal conductivity of thermal insulators using a modified Lee-Charlton's disc apparatus technique. *Int. J. Thermophys., 42(8)*: 113. DOI: 10.1007/s10765-021-02864-3.

Robert, U W; Etuk, S E; Agbasi, O E; Umoren, G P and Inyang, N J (2021b). Investigation of thermophysical and mechanical properties of board produced from coconut (*Cocos nucifera*) leaflet. *Environ. Technol. Innov., 24(1)*: 101869. DOI: 10.1016/j.eti.2021/101869.

Robert, U W; Etuk, S E; Agbasi, E O; Ekong, S A; Abdulrazzaq, Z T and Anonaba, A U (2021c). Investigation of thermal and strength properties of composite panels fabricated with plaster of paris for insulation in buildings. *Intl. J. Thermophys., 42(2)*: 1-18. DOI: 10.1007/s10765-020-02780-y.

Robert, U W; Etuk, S E; Emah, J B; Agbasi, O E and Iboh, U A (2022). Thermophysical and mechanical properties of clay-based composites developed with hydrothermally calcined waste paper ash nanomaterial for building purposes. *Intl. J. Thermophys., 43(5)*: 74. DOI: 10.1007/s10765-022-02995-1.

Ross, J and Suler, M (2000). Sources of errors in measurements of PAR. *Agric. Meteorol., 100*: 103-125.

Sayigh, A A M (1978). The technology of flat plate collector. *Solar Energy Conversion, an Introductory Course.* University of Waterloo, Onlario, Canada. 108 pp.

Shafiquzzaman, S and Naher, L (2017). Effective composting of empty bunches using potential *Trichoderma* strains. *Biotech. Rep., 13*: 1-7.

Sohda, M S; Goyal, I C; Kaushik, S C; Tiwari, G N; Seth, A K and Malik, M A S (1979). Periodic heat transfer with temperature dependent thermal conductivity. *Int. J. Heat Mass Trans., 22(5)*: 777-781.

Tao, H; Snaddon, J L; Slade, E M; Henneron, L; Caliman, L and Willis, K J (2018). Application of oil palm empty fruit bunch effects on soil biota and function: A study in Sumatra Indonesia. *Agr. Ecosyst. Enviro., 256*: 105-113.

Trisakti, B; Lubis, J and Husaini, T (2017). Effect of turning frequency on composting of empty fruit bunches mixed with activated liquid organic fertilizer. *IOP Conference Series: Mat. Sci. Eng., 180(1)*: 012150.

Triyono, S and Haryanto, A (2019). Cultivation of straw mushroom (*Volvariella volvacea)* on oil palm empty fruit bunch growth media. *Int. J. Recyc. Organ. Wast. Agr., 8*: 381-392.

Van Wijk, W R and De Vries, D A (1963). Periodic temperature variations in a homogenous soil. *Physics of Soil Environment* (Van Wijk, W R ed.). North-Holland Publishing Company, Amsterdam. p. 102-143.

Verheye, W H (2010). Soils, plant growth and production of oil palm. *Land Use, Land Cover and Soil Sciences* (Verheye W ed.). Encyclopedia of Life Support system (EOLSS) UNESCO-EOLSS55 Publishers. Oxford UK. 290 pp.

Welty, J R; Wicks, C E; Wilson, R E and Rorrer, G (2001). *Fundamental of Momentum, Heat and Mass Transfer*. 4th edition. John Wiley and Sons Inc. Hoboken. p. 552.

Zaharah, A R and Lim, K C (2000). Oil palm empty fruit bunch as a source of nutrients. *Mal. J. Soil Sci., 4*: 51-66.

Ziaei, S M and Ali, I (2021). Commodity exports and macroeconomic performance: The case of palm oil in Malaysia. *Cogent Econ. Finance, 9*: 1. DOI: 10.1080/23322039.2021.1901388.

Journal of Oil Palm Research Vol. 35 (3) September 2023 p. 456-466
DOI: https://doi.org/10.21894/jopr.2022.0060

INTEGRATED MICROWAVE-STEAM STERILISATION OF LOOSE OIL PALM FRUITS: ENHANCED HEATING UNIFORMITY, CRUDE PALM OIL QUALITY AND ENERGY SAVINGS

SYED MOHAMMAD AHSAN SHAH[1]; ARSHAD ADAM SALEMA[1,2]*; NIK SUHAIMI MAT HASSAN[3]; YOSRI MOHD SIRAN[3] and SYAHRIL ANUAR MD REJAB[3]

ABSTRACT

Loose oil palm fruits are often left uncollected in large quantities while harvesting fresh fruit bunches, which incurs considerable losses in crude palm oil yield. Although the free fatty acid content in loose fruits is undesirably high, microwave sterilisation is known to reduce it significantly. The present study enhanced microwave sterilisation using a new integrated microwave-steam method in which steam exiting the fruits during vaporisation is entrapped and used to complement the heat treatment process. The effect of this new method on the heating uniformity, drying rate, oil extraction rate, crude palm oil quality and energy consumption/cost was investigated. Results showed that up to 25.7% and 13.6% reduction in temperature non-uniformity and energy consumption/cost was achieved with MW-steam heating. Moreover, sterilisation duration was reduced by up to 11.6%. The stacked arrangement of fruits improved microwave absorption efficiency, reducing temperature non-uniformity by up to 45.0% and energy consumption by up to 19.2%. MW-steam sterilisation achieved up to a 10.5% increase in oil extraction rate. Crude palm oil with excellent hydrolytic and oxidative stability was acquired, thus, boosting oil value that can facilitate post-processing in palm oil mills.

Keywords: energy, microwave, oil palm, stacking, sterilisation.

Received: 17 May 2022; **Accepted:** 22 August 2022; **Published online:** 22 September 2022.

INTRODUCTION

Malaysia's oil palm sector is a significant contributor to its economy (Mumtaz *et al.*, 2010) and it is of utmost importance that the palm oil produced is of excellent quality and stability. A major cause of oil quality deterioration is the rise of free fatty acids (FFA) catalysed by lipase enzymes (Morcillo *et al.*, 2013). To inactivate lipase enzyme and halt FFA production, fresh fruit bunches (FFB) undergo sterilisation in palm oil mills (Omar *et al.*, 2018). However, large quantities of loose oil palm fruits detach from these bunches during harvesting and transportation and end up uncollected and left to rot, resulting in substantial losses to the crude palm oil (CPO) yield. Loose oil palm fruits account for up to 4% to 6% of the total FFB harvested and could contribute to an additional 1% to 2% in the oil extraction rate (OER) (Henson, 2012). Loose fruits are mostly damaged and bruised due to the handling practices in palm oil mills and thus, have a very high amount of FFA content which increases rapidly upon abscission and continues to increase with time (Ali *et al.*, 2014). Although the sterilisation

[1] Mechanical Engineering Discipline, School of Engineering, Monash University Malaysia, Bandar Sunway 47500, Selangor, Malaysia.

[2] Monash Industry Palm Oil Research Platform (MIPO), School of Engineering, Monash University Malaysia, 47500 Bandar Sunway, Selangor, Malaysia.

[3] Research and Development Centre, Sime Darby Research Sdn. Bhd., 42960 Carey Island, Selangor, Malaysia.

* *Corresponding author e-mail: arshad.salema@monash.edu*

of loose fruits (high FFA content) together with FFB (low FFA content) offsets the overall FFA content to a certain degree, FFA content should be as low as possible to maximise CPO quality and minimise the refining costs (Chong, 2012). Moreover, the current conventional steam sterilisation method practised in palm oil industries gives rise to highly polluting effluent, which must undergo rigorous and expensive treatment before disposal (Madaki and Seng, 2013).

The conventional steam sterilisation method typically involves the use of horizontal or vertical sterilisers. Other oil palm sterilisation technologies include continuous sterilisers, dry (oven) heating and microwave (MW) heating (Vincent *et al*., 2014). Although these technologies have proven effective in halting FFA production in oil palm fruits, MW sterilisation is known to cease and reduce the FFA content drastically (Tang *et al*., 2017). According to Kanjanapongkul (2021), no significant increase in FFA content was detected even 8 weeks after MW sterilisation. Since no steam and water is utilised, MW heating has been termed a clean and dry technology for CPO production with no effluent discharge (Cheng *et al*., 2011). Moreover, MW heating allows the retention of vital nutrients in CPO, such as carotenoids (Sarah, 2018). However, MW heating has been associated with non-uniform heating in foods which causes incomplete microbial inactivation and overheating (Vadivambal and Jayas, 2010). Heating uniformity can be improved by improving the electric field inside the cavity or the uniformity of MW absorption by the dielectric material (Bae *et al*., 2017). Recently proposed methods to improve electric field uniformity required sophisticated modifications to the MW cavity, such as the use of rotary waveguides (He *et al*., 2020), multiple waveguides (Ahn *et al*., 2020), and MW cavity with adjustable geometry (Wu *et al*., 2020). Other researchers have proposed increasing the MW absorption in a material by minimising the reflections either by optimising the load position (Requena-Perez *et al*., 2004) or by surrounding the load with dielectric layers (Monzó-Cabrera *et al*., 2004).

Previous studies on MW heating of oil palm fruits have primarily focused on the quality of CPO produced, with little emphasis on improving heating uniformity and energy consumption. According to Shehu *et al.* (2019), researchers have attributed the non-adoption of MW heating for oil palm sterilisation in industries to non-uniform heating and a lack of techno-economic experimental data such as energy analysis. Moreover, the effect of MW heating on trace contaminants in CPO such as iron and phosphorus is also not present in the literature. The novel integrated MW-steam sterilisation method is a clean alternative approach to enhance the sterilisation of loose oil palm fruits in terms of temperature uniformity, CPO quality and energy consumption without requiring additional resources (water or chemicals) or making sophisticated modifications to the MW system. The technique involves enclosing oil palm fruits inside a closed container and subjecting them to MW irradiation. In doing so, the steam exiting the fruits from moisture vaporisation is prevented from escaping into the atmosphere and is trapped inside the container instead. The overall heat treatment process would thereby enhance due to the concurrent influence of MW heating, and convective heating from the entrapped steam. The method differs from hybrid steam-MW sterilisation in which steaming and MW heating are done separately (Hock *et al*., 2020).

The present study investigates the integrated MW-steam sterilisation method at the laboratory scale; the effect on heating uniformity, moisture drying, CPO quality and energy consumption was explored. The investigation seeks to establish the feasibility of implementing integrated MW-steam sterilisation in palm oil industries in the future to add value to high FFA loose oil palm fruits, eliminate effluent discharge and maximise oil recovery. Although industrial MW systems (waveguide perpendicular to sample; belt conveyer system) differ significantly in operation compared to domestic MW systems (waveguide adjacent to sample; turntable system), it is crucial to realise the effectiveness of MW-steam sterilisation at a smaller scale as a proof of concept prior to its application to a larger scale.

MATERIALS AND METHODS

Loose oil palm fruits (*Tenera* variety) were collected 24-36 hr post-harvest from the grounds of a local oil palm plantation in Selangor, Malaysia. The accumulation was a mixture of bruised: bruise-free fruits with a ratio of 4:1. The sterilisation of loose oil palm fruits was carried out in a domestic MW system (Model: ME711K, Samsung, Korea) at a continuous power of 800 W. Experimental parameters included the number of fruit layers (single layer and two stacked layers), heating time (1, 2, 3, 4 and 5 min), and sterilisation method (MW sterilisation and MW-steam sterilisation). The fruits were loaded inside an MW safe polypropylene container in a single layer (~125 g) or stacked layers (~250 g). The United States Food and Drug Administration (FDA) has approved polypropylene for food contact applications; its high heat tolerance (melting point of 160°C) prevents chemical leaching, making it an inexpensive and ideal option for the MW heating of foodstuff (Marsh and Bugusu, 2007). The MW-steam sterilisation involved fastening the container with a lid. A container lid was pierced with two holes

(~2 mm diameter) to allow adequate venting of steam produced from moisture vaporisation and prevent explosion due to excessive pressure build-up. The percentage loss in the moisture of oil palm fruits upon MW heating was calculated on a wet basis using Equation (1):

$$M_l = \frac{(m_i - m_f)}{m_i} \times 100 \quad (1)$$

where M_l is the moisture loss (%), m_i is the initial mass (g) before MW heating, and m_f is the final mass (g) after MW heating. The residual moisture content (M) in fruits upon MW heating was then calculated by deducting moisture loss (M_l) from the initial moisture content in fruits.

The initial moisture content of oil palm fruits was determined using the drying oven method (Ahn *et al*., 2014) in a Venticell LSIS-B2V/VC111 laboratory oven (MMM Group, Germany) in which the fruit samples were subjected to successive heating at 105°C with 24 hr intervals until a steady-state mass was reached.

Temperature Analysis

The internal (mesocarp) and surface (skin) temperatures of up to four oil palm fruits were recorded immediately after each experimental run. Glass fibre insulated type K thermocouples (RS Components Ltd., Malaysia) linked with a TC-08 data logger (Pico Technology, United Kingdom) were used to measure and record the internal temperatures (~3 mm depth) at ± 0.5°C accuracy. The surface temperature readings were taken using an infrared thermometer (DigiTech, Australia).

Quality and Energy Analysis

CPO was extracted using a hydraulic press with a compressive force of 15 MPa, then centrifuged (Model: Centrifuge 5810 R, Eppendorf, Germany) for 5 min at 4000 rpm to separate the oil from sludge and emulsion. The recovered oil was weighed on a mass balance to determine the OER of CPO using Equation (2):

$$\text{OER } (\%) = \frac{\text{Mass of recovered oil (g)}}{\text{Initial sample mass (g)}} \times 100 \quad (2)$$

The CPO was then subjected to quality analysis: the FFA content (as palmitic acid), moisture and volatile matter (MV) content, *p*-anisidine value (AnV), total oxidation in ultraviolet light (UV TOTOX), iron content, phosphorus content, iodine value (IV), carotene content and DOBI of CPO was determined based on the MPOB Methods p2.5:2004, p2.1:2004, p2.4:2004, p2.12:2004, p2.10: 2004, p2.8 Part2: 2004, p3.2:2004, p2.6:2004 and p2.9: 2004 (Kuntom *et al*., 2005). The energy consumption of the MW system was assessed using a Power-Mate Lite power meter (Hypertec, Australia).

RESULTS AND DISCUSSION

Effect on Temperature Distribution

Table 1 shows the temperature distribution in a single layer of oil palm fruits during MW heating and MW-steam heating. The geometry and position of the dielectric sample inside the cavity are among the factors that influence temperature distribution (Rattanadecho and Makul, 2016). Temperature non-uniformity was quantified by calculating the coefficient of variance (CV). On average, the CV of internal temperatures was 21.1% lower in MW-steam heating (0.15) than MW heating (0.19) through a heating period of 5 min. In contrast, the CV of surface temperatures was on average 30.0% lower in MW-steam heating (0.14) than in MW heating (0.20). Hence, enhancement in internal and surface temperature uniformity was attained with MW-steam heating. The occurrence is possibly due to convective heat transfer from the entrapped vapours inside the closed container to the fruits, enhancing the overall heat distribution. As opposed to volumetric heating from MW irradiation, convective heating involves heat transfer between the steam and the solid surface, which may justify the greater influence of MW-steam heating in improving the uniformity of surface temperatures than internal temperatures. The combination of MW heating and convective heating from the trapped steam played an essential role in enhancing the sterilisation process of oil palm fruits.

Table 2 shows the temperature distribution in stacked layers of oil palm fruits during MW heating and MW-steam heating. On average, the CV of internal temperatures was 27.2% lower in MW-steam heating (0.08) than MW heating (0.11) through a heating period of 5 min. In comparison, the CV of surface temperatures was 10.0% lower with MW-steam heating (0.09) than MW heating (0.10). Although improved temperature uniformity with MW-steam heating was apparent from our earlier discussion, the constructive effect of MW-steam heating in improving the uniformity of surface temperatures was not as influential in stacked fruits as compared to a single layer of fruits. Nevertheless, stacking of fruits significantly improved temperature uniformity, with the average CV more than 33.0% lower for internal temperatures and 50.0% lower for surface temperatures, as compared to a single layer. The impact of the stacked arrangement of fruits was discovered to be more effective in achieving a more uniform heating pattern and temperature distribution than the effect of MW-steam heating.

Shah *et al*. (2022) investigated the effect of stacking oil palm fruits in layers under intermittent MW heating and reported enhanced heating uniformity.

Effect on Heating Rate and Sterilisation

The mean internal temperature in a single layer of oil palm fruits leapt rapidly during the first minute of MW heating and MW-steam heating at a heating rate of ~1.1°C/s (*Table 1*). However, the heating rate deteriorated by more than 81% after 1 min (~0.2°C/s). An initial heating rate of ~1.2°C/s was reported by Cheng *et al*. (2011) at the same power level (800 W), dropping to as low as ~0.2°C/s as heating continued. Similarly, the mean surface temperature in a single layer initially rose at a rate of ~0.9°C/s but decreased by more than 60% (~0.3°C/s) after 1 min (*Table 1*). MW heating involves rapid agitation of water molecules and charged ions inside a dielectric material for fast heat generation (Tang and Resurreccion, 2009). Due to the low specific heat capacity (2816 J/kg·K) and thermal conductivity

TABLE 1. TEMPERATURE DISTRIBUTION IN A SINGLE LAYER OF LOOSE OIL PALM FRUITS AFTER MW HEATING AND MW-STEAM HEATING

(a) MW heating	Heating time (min)									
	1		2		3		4		5	
Temperature	Internal	Surface	Internal	Surface	Internal	Surface	Internal	Surface	Internal	Surface
T1 (°C)	113.9	87.7	125.9	133.8	145.7	141.6	150.6	173.0	153.9	196.3
T2 (°C)	68.0	62.5	89.8	88.0	101.0	110.3	104.1	116.5	116.3	123.8
T3 (°C)	87.7	93.7	100.1	109.4	117.9	118.6	118.3	147.8	137.9	155.3
Mean (°C)	89.8	81.3	105.3	110.4	121.6	123.6	124.4	145.8	136.0	158.5
SE (°C)	13.3	9.6	10.7	13.2	13.0	9.4	13.7	16.3	10.9	21.0
CV	0.26	0.20	0.18	0.21	0.19	0.13	0.19	0.19	0.14	0.26
(b) MW-steam heating	**Heating time (min)**									
	1		2		3		4		5	
Temperature	Internal	Surface	Internal	Surface	Internal	Surface	Internal	Surface	Internal	Surface
T1 (°C)	97.2	83.0	110.1	100.5	133.1	115.3	141.1	157.4	155.1	189.0
T2 (°C)	78.6	64.3	89.1	76.0	95.1	94.1	98.5	112.8	111.5	147.3
T3 (°C)	91.4	73.0	98.8	92.9	103.6	98.5	110.1	124.9	119.0	160.9
Mean (°C)	89.1	73.4	99.3	89.8	110.6	102.6	116.6	131.7	128.5	165.7
SE (°C)	5.5	5.4	6.1	7.2	11.5	6.5	12.7	13.3	13.5	12.3
CV	0.11	0.13	0.11	0.14	0.18	0.11	0.19	0.18	0.18	0.13

Note: SE - Standard error; CV - Coefficient of variance.

TABLE 2. TEMPERATURE DISTRIBUTION IN STACKED LAYERS OF LOOSE OIL PALM FRUITS AFTER MW HEATING AND MW-STEAM HEATING

(a) MW heating	Heating time (min)									
	1		2		3		4		5	
Temperature	Internal	Surface	Internal	Surface	Internal	Surface	Internal	Surface	Internal	Surface
T1 (°C)	89.1	74.2	96.9	96.3	108.9	113.6	111.6	120.7	118.1	126.9
T2 (°C)	68.9	67.4	91.8	88.1	104.3	104.4	105.5	111.7	106.9	113.9
T3 (°C)	65.2	58.7	85.8	83.3	97.5	98.9	100.8	106.0	101.5	108.0
T4 (°C)	58.7	53.6	77.1	77.1	87.3	91.5	92.2	98.2	92.9	102.3
Mean (°C)	70.5	63.5	87.9	86.2	99.5	102.1	102.5	109.2	104.9	112.8
SE (°C)	6.6	4.6	4.3	4.1	4.7	4.7	4.1	4.8	5.3	5.3
CV	0.19	0.14	0.10	0.10	0.10	0.09	0.08	0.09	0.10	0.09
(b) MW-steam heating	**Heating time (min)**									
	1		2		3		4		5	
Temperature	Internal	Surface	Internal	Surface	Internal	Surface	Internal	Surface	Internal	Surface
T1 (°C)	85.1	81.6	98.3	98.8	100.4	105.4	102.4	111.9	108.8	116.1
T2 (°C)	81.1	65.9	93.7	91.2	98.1	101.5	100.2	104.8	103.1	111.4
T3 (°C)	66.7	61.7	88.7	87.1	95.7	98.0	97.4	99.8	98.3	105.3
T4 (°C)	60.3	53.9	82.0	79.2	89.2	91.9	90.2	96.8	92.1	93.3
Mean (°C)	73.3	65.8	90.7	89.1	95.9	99.2	97.6	103.3	100.6	106.5
SE (°C)	5.9	5.8	3.5	4.1	2.4	2.9	2.7	3.3	3.6	5.0
CV	0.16	0.18	0.08	0.09	0.05	0.06	0.06	0.06	0.07	0.09

Note: SE - Standard error; CV - Coefficient of variance.

(0.458 W/m·K) of oil palm mesocarp, less energy per kg is required to incur a temperature change, and a rapid surge in temperature is exhibited (Dogan *et al*., 2014; Law *et al*., 2019). However, the decline in heating rate is likely due to reduced MW absorbance as dielectric properties in oil palm fruits weaken during moisture drying. The same phenomenon applies to stacked layers of oil palm fruits, where the mean internal temperature increased rapidly at a rate of ~0.8°C/s during the first min of MW heating and MW-steam heating and subsequently dropped to as low as ~0.1°C/s (*Table 2*). The mean surface temperature in stacked layers increased at ~0.7°C/s during the first min of heating before dropping to ~0.1°C/s (*Table 2*). Despite a 100% increase in mass, the internal and surface heating rate was only 31% and 23% lower in stacked layers than in a single layer due to the enhanced effect of stacking fruits on MW absorption efficiency (Shah *et al*., 2022). Since MW heating involves volumetric heating, the internal temperatures were initially higher than the surface. The rapid moisture evaporation resulted in a significant pressure-driven flow of vapour transferring heat to fruit surfaces by convection. Ultimately, the surface temperatures exceeded the internal temperatures as the heating was prolonged in both single (*Table 1*) and stacked layers (*Table 2*). The fruit's outer skin being less permeable than its inner flesh may also deter the escape of vapours and confine the heat near the surface.

Figure 1 shows that MW-steam heating (dashed lines) had marginally faster drying rates as compared to MW heating (solid lines). The vapours entrapped inside the container in MW-steam heating escalated the collision frequency between vapour molecules and the container walls, exerting pressure. Consequently, the increase in the average kinetic energy of the molecules allowed faster vaporisation (Connors, 1990). When vapour molecules saturate the air inside a closed container, the vapour condenses to the liquid phase (Wellbeloved, 2020). In the present study, the vapours condensed to liquid onto the container walls and lid. If measures for adequate steam venting are overlooked, the unrestricted build-up of pressure inside the container could result in an explosion resulting in steam burns or injuries from the spilling of hot liquid.

Oil palm fruits are sterilised to inactivate the lipase enzyme, and soften the fruit mesocarps while preserving the kernel condition (Vincent *et al*., 2014). The initial moisture content of loose oil palm fruits was determined to be 32 wt.% on average. The moisture content should be lowered to at least 15 wt.% to inactivate lipase (Okolo and Adejumo, 2014). Yoosa *et al*. (2018) advised that residual moisture content of 15 wt.% helps preserve fruits from fungi, and halts FFA from increasing while preserving the kernel condition. Shah *et al*. (2022) reported a ~70% reduction in fruit hardness with a residual moisture content of 15 wt.%. From *Figure 1*, the optimum sterilisation duration to reduce the moisture content to 15 wt.% was determined. With MW heating, the requisite heating duration to achieve sterilisation was determined to be 2.8 min for a single layer and 4.4 min for stacked layers. MW-steam heating took 2.5 min of heating for a single layer and 4.2 min of heating for stacked layers for sterilisation. Sample temperatures during optimal sterilisation durations were well below the melting point of polypropylene (160°C) in both single (*Table 1*) and stacked layers (*Table 2*), implying sufficient thermal resistance of the container under MW irradiation. Interestingly, doubling the sample size (number of layers) does not necessarily double the requisite heating time; only a 57% and 68% increase in heating time was required for stacked fruits with MW heating and MW-steam heating, respectively, possibly due to the constructive effect of stacking/dielectric layering on the MW absorption which was earlier discussed. MW heating required ~13% (20 s) and ~7% (16 s) longer heating time than MW-steam heating for single and stacked layers, respectively. It is evident that combining the stacking of fruits with integrated MW-steam heating can reduce sterilisation duration.

Figure 2 shows the appearance of sterilised loose oil palm fruits after MW and MW-steam heating. Raw fruits had vibrant yellowish-orange mesocarps and white kernels. Upon sterilisation, the mesocarps deepened in colour with oil discharges, white kernels, and a caramel-type odour. Excessive moisture removal resulted in brown and dry mesocarp fibres and dark kernels. Similar observations were reported by Cheng *et al.* (2011). No noticeable difference in physical appearance was observed between single and stacked layers. However, the mesocarps of MW-steam sterilised fruits were visibly uniform in appearance throughout (both away and near the surface), likely due to the constructive influence of steam on fruit surfaces.

Effect on Oil Extraction Rate and Crude Palm Oil Quality

Table 3 lists the OER, and quality characteristics of CPO produced from MW and MW-steam sterilisation of loose oil palm fruits. An OER of up to 25.6% was achieved with integrated MW-steam sterilisation. An 8.5% to 10.5% increase in OER was recorded with MW-steam sterilisation in a single layer and stacked layers, respectively, as compared to regular MW sterilisation. The improved heating uniformity with MW-steam sterilisation was likely influential in enhancing the OER. However, the OER is also reliant on the method of oil extraction. Cheng *et al.* (2011) obtained an OER of 21.2% from MW-sterilised oil palm fruits using solvent extraction. Whereas Yoosa *et al*. (2022) reported an OER of 30.3% from MW-sterilised oil palm fruits (15 wt.%

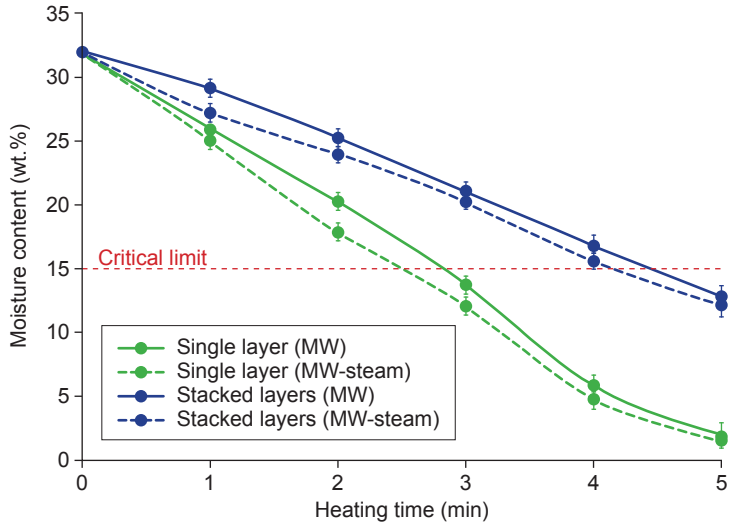

Figure 1. Drying curves of loose oil palm fruits during MW heating and MW-steam heating.

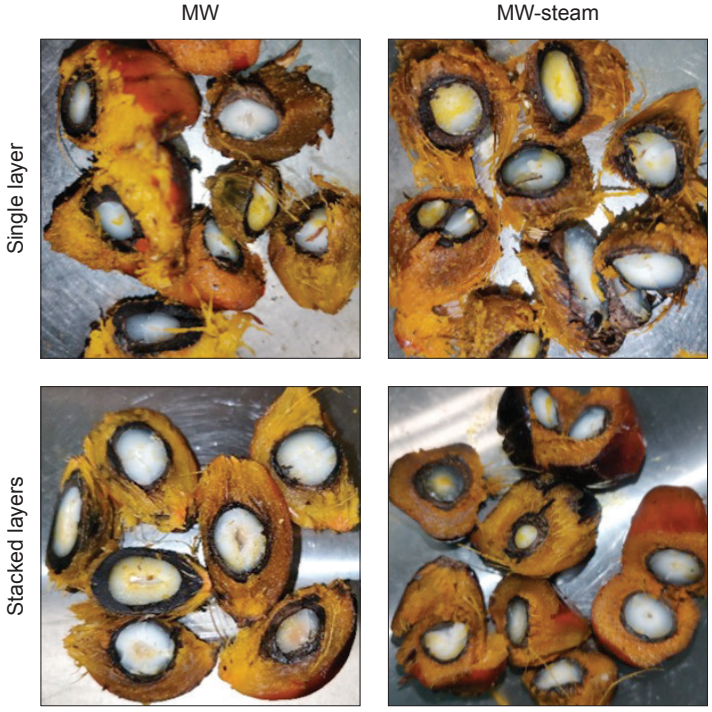

Figure 2. The physical appearance of sterilised oil palm fruits after MW heating and MW-steam heating.

residual moisture content) using an automatic palm oil presser. Although they reported an additional ~3.5% in OER with a lower residual moisture content of 5 wt.%, the requisite sterilisation duration and consequently the energy consumption/cost increased significantly by up to 58.0%. The total OER in Malaysian palm oil mills was 20.0% in the year 2021 (Parveez, 2002).

The quality of CPO extracted from the sterilised oil palm fruits (M = 15 wt.%) was well within the commercial standards (*Table 3*). The FFA content in non-sterilised fruits was determined to be 16.4%, which is undesirably high and unfit for human consumption. *Table 3* shows that MW sterilisation caused a significant drop in the FFA content of oil palm fruits. According to Tang *et al*. (2017), MW heating significantly reduces the FFA content in oil palm fruits. Recently, Shah *et al*. (2022) reduced the FFA content in oil palm fruits by ~94 using intermittent MW heating. In another study, Nokkaew and Punsuvon (2014) reduced the FFA content in oil palm fruits from 38.0% to 3.0% using

TABLE 3. THE OER AND QUALITY OF CPO EXTRACTED FROM STERILISED LOOSE OIL PALM FRUITS

Quality parameter	Single (MW)	Single (MW-steam)	Stacked (MW)	Stacked (MW-steam)	Standard quality CPO*
OER (%)	23.60 ± 1.10	25.60 ± 1.30	22.80 ± 0.90	25.20 ± 1.80	-
FFA (%)	1.2 ± 1.3	1.1 ± 1.0	1.3 ± 1.1	1.0 ± 0.8	5.0 (max)
MV (%)	0.08 ± 0.00	0.08 ± 0.00	0.07 ± 0.01	0.07 ± 0.00	0.25 (max)
AnV	0.54 ± 0.04	0.15 ± 0.90	0.74 ±1.11	0.39 ± 0.20	5.0 (max)
UV TOTOX	0.86 ± 0.08	0.91 ± 0.08	0.91 ± 0.10	0.97 ± 0.02	1.80 (max)
Iron (µg/g)	1.4 ± 4.7	1.8 ± 3.1	2.8 ± 2.1	2.1 ± 1.1	5.0 (max)
Phosphorus (µg/g)	10.5 ± 3.2	15.0 ± 0.8	11.8 ± 2.5	12.3 ± 1.7	20.0 (max)
IV (g/100g)	52.9 ± 0.5	52.6 ± 0.1	51.9 ± 1.2	53.7 ± 0.2	50.4-53.7
Carotene (mg/kg)	535 ± 44	485 ± 62	479 ± 39	503 ± 17	474-689
DOBI	5.2 ± 0.5	4.6 ± 0.9	4.7 ± 0.4	4.4 ± 0.9	2.3 (min)

Source: Farah *et al*. (2019).

MW heating. Recently, Kanjanapongkul (2021) achieved an FFA content of 1.5% using combined ohmic and MW heating. In the present study, the FFA content was well below the critical limit of 5.0% across all CPO samples, even superior to special quality CPO (FFA: 2.5%). MW heating samples experienced the maximum FFA content of 1.2% and 1.3% in single and stacked layers. CPO samples from MW-steam heating had ~10.5% lower FFA content than MW heating, indicating added improvement in oil quality, possibly due to enhanced sterilisation as a result of improved heating uniformity.

The MV content of CPO extracted from non-sterilised loose oil palm fruits (M = 32 wt.%) was determined to be 0.48%. Since lipase is a hydrolase, minimising moisture is of utmost importance to prevent lipid hydrolysis to produce CPO that is fit for storage. In the current study, the MV content was drastically reduced by more than 83.0% in the CPO samples and was way below the standard limit of 0.25%. Up to 5.4%, lower MV was obtained with MW-steam heating than with regular MW heating. Moreover, stacked fruits had 10.8% lower MV than a single layer, hinting at the constructive effect of the stacked arrangement on moisture drying due to increased MW absorption (Shah *et al*., 2022). The combined effect of MW-steam heating and stacking produced CPO with 15.7% lower MV content than from a single layer with regular MW heating.

AnV is the amount of the secondary oxidation products (aldehydes and ketones) broken down from the primary products (lipid peroxides and hydroperoxides) and responsible for the oil's rancid taste and smell (Yang and Boyle, 2016). The AnV was well below the critical limit of 5 for all samples, implying excellent secondary oxidative stability of CPO obtained through MW sterilisation. Moreover, MW-steam heating further augmented oxidative stability as AnV was 72.9% and 47.1% lower in single and stacked layers. CPO with a high AnV has a reduced shelf life and is also unhealthy for consumption. Tan *et al*. (2017) produced CPO with an AnV of 2.2 using MW heating, whereas the AnV recorded in the present study was significantly lower (0.15 to 0.74), especially using MW-steam heating. The specific extinctions at wavelengths 233 nm and 269 nm in ultraviolet light were also used to detect the presence of primary and secondary oxidation products in CPO, respectively. The ultraviolet total-oxidation or UV TOTOX (E233 + E269) was below 1 for all oil samples, indicating better oxidative stability than standard quality CPO.

A pro-oxidant metal such as iron catalyses lipid oxidation in CPO causing oxidative instability and poor bleachability (Bustamam *et al*., 2020). It is essential that the iron content in CPO is minimal and does not exceed 5.0 µg/g. The iron content was below 3.0 µg/g in all cases. Moreover, iron content was 22% (single layer) to 25% (stacked layers) lower in CPO extracted from MW-steam heated samples than MW heated (*Table 3*). Phosphorus is another trace contaminant in CPO that should not exceed 20 µg/g for better bleaching properties. The phosphorus content was well below the critical limit for all CPO samples in the present study and did not exceed 15 µg/g. However, CPO produced from fresh oil palm fruits with low FFA content has a significantly lower amount of phosphorus (2 µg/g) (Hassan *et al*., 2021).

The IV was consistent with the standard quality CPO requirement (50.4 g/100g-53.7 g/100 g) for all cases. Hassan *et al*. (2021) reported a similar IV (52.3 g/100 g) for CPO extracted from fresh oil palm fruits sterilised using the conventional steam method. However, Tripathi and Yadav (2021) reported an IV of 46.1 g/100 g in CPO after 10 min of MW heating, declining further when exposure was prolonged; hence, optimal sterilisation duration is necessary to maintain IV within the desired range. IV is yet another indicator of

oxidative stability of CPO as it reveals the degree of fatty acid unsaturation in oil (Noor *et al*., 2020). Since unsaturated compounds in the oil are very reactive toward halogens like iodine, they are more prone to oxidation; hence, IV must be controlled within the recommended range. In a recent study, MW treatment effectively reduced the unsaturated fatty acid to saturated fatty acid ratio and IV in milk thistle seed oil (Fathi-Achachlouei *et al*., 2019).

Carotenoids are vital phytonutrients and potent antioxidants that provide oxidative stability to palm oil. The carotene content (as β-carotene) of all four oil samples was within the standard CPO quality range (474-689 mg/kg), inferring adequate carotene retention. Prolonged heating at temperatures above 60°C can degrade carotenoids; hence, it was advisable to use low temperatures (low MW power level) or low heating periods for sterilisation (Sarah, 2018). The present results were closer to the lower limit, possibly due to heating at a high MW power setting (800 W) with maximum sterilisation temperatures topping 100°C in all cases (*Table 1* and 2). Carotene content also reduces with an increase in storage time (Ali *et al*., 2014), which was more than 24 hr in the present study. Nevertheless, Sarah *et al*. (2018) produced red palm oil (high carotene content) at an 800 W power level using freshly harvested oil palm fruits.

DOBI is a critical CPO quality characteristic expressed as the ratio of carotene concentration to the secondary oxidation products (Basyuni *et al*., 2017). The DOBI value for all oil samples was above 4.00, which is superior to that of standard CPO quality (DOBI: 2.30). A high DOBI indicates facilitation in the refining process, particularly bleaching. Remarkably, DOBI was as high as 5.16 (single layer) and 4.73 (stacked layers); CPO with a DOBI above 3.00 is recognised to be of premium quality (Nokkaew *et al*., 2019). The results for MW-steam heated samples (4.40-4.60) were comparable to that of CPO obtained using the combined MW and oven drying method (3.89-4.61) in a study by Tapanwong *et al*. (2020).

Effect on Energy Consumption/Cost

The electricity consumption in palm oil mills for FFB processing is 0.02 kWh/kg, excluding costs of fuel, water, chemicals and refining (Norfaradila *et al*., 2014). With MW-steam sterilisation, CPO of commercial standards was produced, simplifying the palm oil milling process to only two major steps: Sterilisation and oil extraction. The reduced sterilisation duration due to MW-steam heating and stacking allowed significant energy savings. *Figure 3* presents the energy consumption data calculated in this study using the E1 tariff (0.337 MYR/kWh) of Tenaga Nasional Berhad, Malaysia (TNB) utility company. In a single layer, electricity consumption was 0.44 kWh/kg with MW heating (*Figure 3a*), and 0.38 kWh/kg with MW-steam heating (*Figure 3b*). In stacked layers, consumption was 0.35 kWh/kg with MW heating (*Figure 3c*), and 0.32 kWh/kg with MW-steam heating (*Figure 3d*). Using MW-steam heating, energy consumption was 13.6% lower in a single layer and 8.6% lower in stacked layers as compared to regular MW heating. Moreover, 19.2% and 17.9% lower energy consumption/costs were attained by stacking under MW and MW-steam heating, respectively, as compared to a single layer. To the best of the author's knowledge, MW-steam heating combined with stacking (0.32 kWh/kg) is the lowest energy consumption process for MW sterilisation of oil palm fruits. Kanjanapongkul (2021) reported energy consumption of 0.38 kWh/kg using combined ohmic and MW heating of oil palm fruits, but at the expense of CPO quality with poor carotene retention (438 mg/kg). Recently, Yoosa *et al.* (2022) attained a similar energy consumption of 0.38 kWh/kg using regular MW sterilisation.

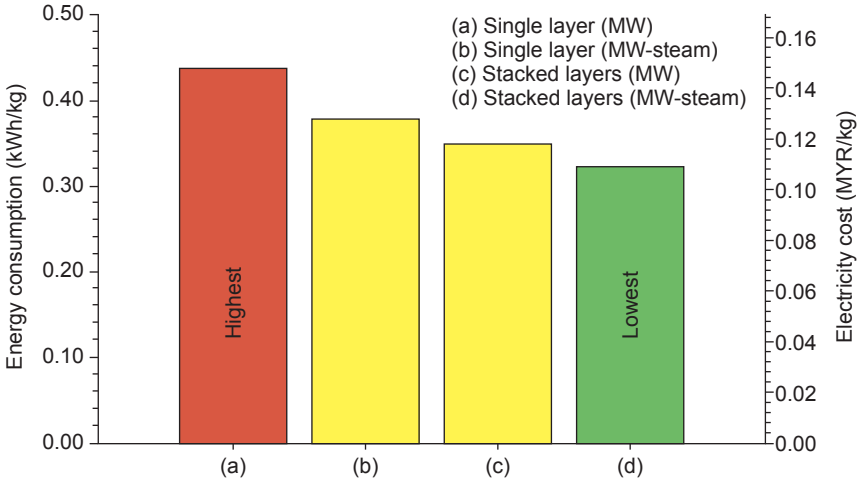

Figure 3. Energy consumption and energy cost to sterilise per kg of loose oil palm fruits using MW heating and MW-steam heating.

CONCLUSION

A significant improvement in temperature uniformity in both internal and surface temperature distributions was discovered with MW-steam heating. The stacked arrangement of fruits was also influential in enhancing heating uniformity. MW-steam heating had no significant effect on MW absorbance; however, stacking fruits enhanced the absorption efficiency significantly. CPO extracted from MW and MW-steam sterilised fruits met commercial standards: While the IV and carotene content were comparable to standard CPO quality, the FFA content, MV, PV, AV, UV TOTOX, iron and phosphorus were superior to standard CPO. Moreover, MW-steam heating boosted the oil extraction rate and augmented the CPO quality, particularly the FFA, MV and AV. The reduction in energy consumption and cost for sterilisation was noteworthy: Stacking reduced energy consumption by up to 19.2%, while MW-steam heating reduced it by up to 13.6%. It can be concluded with certainty that MW sterilisation of oil palm fruits was enhanced using the integrated MW-steam sterilisation method allowing improved temperature uniformity, a faster drying rate, increased oil extraction rate, superior CPO quality and lower energy consumption. In doing so, the value was added to high FFA loose fruits to minimise oil yield losses by increasing the OER. The findings of the present research work intend to serve as a prologue to incorporating integrated MW-steam heating in industrial MW systems to enhance the sterilisation process. Although food industries could readily adopt the technique due to its minimalism, experimental work in an industrial MW system is crucial to truly realise the effectiveness of MW-steam sterilisation on a larger scale.

ACKNOWLEDGEMENT

The authors thankfully acknowledge the financial support received in the form of a seed grant (award No. 2018/MIPO/ILSS/10) from Monash Industry Palm Oil Research Platform (MIPO), Monash University Malaysia. We also acknowledge Sime Darby Research Sdn. Bhd., Carey Island, Selangor, Malaysia for their services and persistent support.

REFERENCES

Ahn, J Y; Kil, D Y; Kong, C and Kim, B G (2014). Comparison of oven-drying methods for determination of moisture content in feed ingredients. *Asian-Australas. J. Anim. Sci., 27(11)*: 1615. DOI: 10.5713/ajas.2014.14305.

Ahn, S H; Jeong, C H; Lim, D M and Lee, W S (2020). Kilowatt-level power-controlled microwave applicator with multiple slotted waveguides for improving heating uniformity. *IEEE Trans. Microw. Theory Tech., 68(7)*: 2867-2875. DOI: 10.1109/TMTT.2020.2977645.

Ali, F S; Shamsudin, R and Yunus, R (2014). The effect of storage time of chopped oil palm fruit bunches on the palm oil quality. *Agric. Sci. Procedia*, *2*: 165-172. DOI: 10.1016/j.aaspro.2014.11.024.

Bae, S H; Jeong, M G; Kim, J H and Lee, W S (2017). A continuous power-controlled microwave belt drier improving heating uniformity. *IEEE Microw. Wirel. Compon. Lett., 27(5)*: 527-529. DOI: 10.1109/LMWC.2017.2690849.

Basyuni, M; Amri, N; Putri, L A P; Syahputra, I and Arifiyanto, D (2017). Characteristics of fresh fruit bunch yield and the physicochemical qualities of palm oil during storage in North Sumatra, Indonesia. *Indones. J. Chem., 17(2)*: 182-190. DOI: 10.22146/ijc.24910.

Bustamam, F K A; Sulaiman, N; Beng, Y C and Khairuddin, N S K (2020). A snapshot on the iron content in Malaysian crude palm oil. *Malaysian J. Anal. Sci., 24(6)*: 855-861.

Cheng, S F; Nor L M and Chuah, C H (2011). Microwave pretreatment: A clean and dry method for palm oil production. *Ind. Crops Prod., 34(1)*: 967-971. DOI: 10.1016/j.indcrop.2011.03.002.

Chong, C L (2012). Measurement and maintenance of palm oil quality. *Palm Oil* (Lai, O M; Tan C P and Akoh, C C eds.). AOCS Press, Illinois, USA. p. 431-470.

Connors, K A (1990). Introduction to chemical kinetics. *Chemical Kinetics: The Study of Reaction Rates in Solution*. 1st edition. VCH Publishers, Weinheim, Germany. p. 1-16.

Dogan, H H; Yücel, P and Halkman, A (2014). Non-thermal processing|microwave. *Encyclopedia of Food Microbiology*. 2nd edition. Academic Press, Oxford. p. 962-965.

Farah, K A B; Yeoh, C B and Najwa, S (2019). Revision of the Malaysian standard for palm oil-specification MS 814: 2007, (second revision) amendment 1: 2018-What's new? *Palm Oil Developments*, *71*: 18-32.

Fathi-Achachlouei, B; Azadmard-Damirchi, S; Zahedi, Y and Shaddel, R (2019). Microwave pretreatment as a promising strategy for increment of nutraceutical content and extraction yield of oil

from milk thistle seed. *Ind. Crops Prod.*, *128*: 527-533. DOI: 10.1016/j.indcrop.2018.11.034.

Hassan, N S M; Hossain, M; Balakrishnan, V; Zuknik, M H; Mustaner, M; Easa, A M and Yahaya, A N A (2021). Influence of fresh palm fruit sterilization in the production of carotenoid-rich virgin palm oil. *Foods*, *10(11)*: 2838. DOI: 10.3390/foods10112838.

He, J; Yang, Y; Zhu, H; Li, K; Yao, W and Huang, K (2020). Microwave heating is based on two rotary waveguides to improve efficiency and uniformity by gradient descent method. *Appl. Therm. Eng.*, *178*: 115594. DOI: 10.1016/j.applthermaleng.2020.115594.

Henson, I E (2012). Ripening, harvesting and transport of oil palm bunches. *Palm Oil: Production, Processing, Characterization and Uses* (Lai, O; Tan, C and Casimir, C eds.). AOCS Press, Urbana, USA. p. 137-162.

Hock, T K; Chala, G T and Cheng, H H (2020). An innovative hybrid steam-microwave sterilization of palm oil fruits at atmospheric pressure. *Innov. Food Sci. Emerg. Technol.*, *60*: 102289. DOI: 10.1016/j.ifset.2020.102289.

Kanjanapongkul, K (2021). Single and combined effects of ohmic and microwave heating on crude palm oil quality and stability. *Agr. Nat. Resour.*, *55(2)*: 177-186.

Kuntom, A; Aini, I N; Amri, I N; Thin, S M; Wai, L S and Yew, A T (2005). *MPOB Test Methods.* A compendium of test on palm oil products, palm kernel products, fatty acids, food related products and others. MPOB. Kuala Lumpur. 414 pp.

Law, M C; Chang, J S L; Chan, Y S; Pui, D Y and You, K Y (2019). Experimental characterisation and modelling of microwave heating of oil palm kernels, mesocarps and empty fruit bunches. *Dry. Technol.*, *37(1)*: 69-91. DOI: 10.1080/07373937.2018.1439057.

Madaki, Y S and Seng, L (2013). Palm oil mill effluent (POME) from Malaysia palm oil mills: Waste or resource. *Int. J. Environ. Sci. Technol.*, 2: 1138-1155.

Marsh, K and Bugusu, B (2007). Food packaging - roles, materials and environmental issues. *J. Food Sci., 72(3)*: R39-R55. DOI: 10.1111/j.1750-3841.2007.00301.x.

Monzó-Cabrera, J; Escalante, J; Díaz-Morcillo, A; Martínez-González, A and Sánchez-Hernández, D (2004). Load matching in multimode microwave-heating applicators based on the use of dielectric-layer moulding with commercial materials. *Microw. Opt. Technol. Lett.*, *41(5)*: 414-417.

Morcillo, F; Cros, D; Billotte, N; Ngando-Ebongue, G F; Domonhédo, H; Pizot, M and Arondel, V (2013). Improving palm oil quality through identification and mapping of the lipase gene causing oil deterioration. *Nat. Commun.*, *4(1)*: 1-8. DOI: 10.1038/ncomms3160.

Mumtaz, T; Yahaya, N A; Abd-Aziz, S; Abdul Rahman, N; Yee, P L; Shirai, Y and Hassan, M A (2010). Turning waste to wealth-biodegradable plastics polyhydroxyalkanoates from palm oil mill effluent - A Malaysian perspective. *J. Cleaner Prod.*, *18(14)*: 1393-1402. DOI: 10.1016/j.jclepro.2010.05.016.

Nokkaew, R and Punsuvon, V (2014). Sterilization of oil palm fruits by microwave heating for replacing steam treatment in palm oil mill process. *Adv. Mat. Res.*, *1025*: 470-475. DOI: 10.4028/www.scientific.net/AMR.1025-1026.470.

Nokkaew, R; Punsuvon, V; Inagaki, T and Tsuchikawa, S (2019). Determination of carotenoids and DOBI content in crude palm oil by spectroscopy techniques: Comparison of RAMAN and FT-NIR spectroscopy. *Int. J. GEOMATE*, *16(55)*: 92-98. DOI: 10.21660/2019.55.4813.

Noor, M A M; Musa, H and Ghazali, R (2020). Uncertainty of iodine value determination in palm olein. *Malaysian J. Anal. Sci., 24(4)*: 511-518.

Norfaradila, J; Norela, S; Salmijah, S and Ismail, B S (2014). Life cycle assessment (LCA) for the production of palm biodiesel: A case study in Malaysia and Thailand. *Malays. Appl. Biol.*, *43(1)*: 53-63.

Okolo, J and Adejumo, B (2014). Effect of bleaching on some quality attributes of crude palm oil. *IOSR J. Eng.*, *04*: 25-28. DOI: 10.9790/3021-041203025028.

Omar, A M; Norsalwani, T T; Asmah, M S; Badrulhisham, Z Y; Easa, A M; Omar, F M; Hossain, M S; Zuknik, M H and Norulaini, N N (2018). Implementation of the supercritical carbon dioxide technology in oil palm fresh fruits bunch sterilization: A review. *J. CO_2 Util.*, *25*: 205-215. DOI: 10.1016/j.jcou.2018.03.021.

Parveez, A (2022). Overview of the Malaysian oil palm industry 2021. https://bepi.mpob.gov.my/images/overview/Overview2021.pdf.

Rattanadecho, P and Makul, N (2016). Microwave-assisted drying: A review of the state-of-the-art. *Dry. Technol.*, *34(1)*: 1-38. DOI: 10.1080/07373937.2014.957764.

Requena-Perez, M E; Pedreno-Molina, J L; Pinzolas-Prado, M; Monzo-Cabrera, J; Diaz-Morcillo, A and Sanchez-Hernandez, D (2004). Load matching in multimode microwave-heating applicators by load location optimisation. *34th European Microwave Conference 2004*. p. 1549-1552.

Sarah, M (2018). Carotenoids preservation during sterilization of palm fruit using microwave irradiation. *ARPN J. Eng. Appl. Sci.*, *13(3)*: 1009-1014.

Sarah, M; Widyastuti, S and Ningsih, D (2018). Red palm oil production by microwave irradiation. *IOP Conf. Ser.: Mater. Sci. Eng., 309(1)*: 012091. DOI: 10.1088/1757-899X/309/1/012091.

Shah, S M A; Shen, Y J; Salema, A A; Lee, Y Y; Balan, P; Hassan, N S M; Siran, Y M and Rejab, S A M (2022). Enhanced productivity, quality and heating uniformity by stacking oil palm fruits under microwave irradiation. *Int. J. Therm. Sci.*, *179*: 107634. DOI: 10.1016/j.ijthermalsci.2022.107634.

Shehu, U E; Mokhtar, M N; Mohd Nor, M Z; Baharuddin, A S and Nawi, N M (2019). A study on the use of water as a medium for the thermal inactivation of endogenous lipase in oil of palm fruit. *Energies*, *12(20)*: 3981. DOI: 10.3390/en12203981.

Tan, J C; Chuah, C H and Cheng, S F (2017). A combined microwave pretreatment/solvent extraction process for the production of oil from palm fruit: Optimisation, oil quality and effect of prolonged exposure. *J. Sci. Food Agric.*, *97(6)*: 1784-1789. DOI: 10.1002/jsfa.7975.

Tang, J and Resurreccion, F (2009). Electromagnetic basis of microwave heating. *Development of Packaging and Products for Use in Microwave Ovens*. Woodhead Publishing, Wood Lane, London, UK. p. 3-37.

Tang, M; Xia, Q; Holland, B J; Wang, H; Zhang, Y; Li, R and Cao, H; (2017). Effects of different pretreatments to fresh fruit on chemical and thermal characteristics of crude palm oil. *J. Food Sci.*, *82(12)*: 2857-2863. DOI: 10.1111/1750-3841.13972.

Tapanwong, M; Nokkaew, R and Punsuvon, V (2020). Effect of combination microwave and oven drying on the chemical properties of different ripeness crude palm oil. *Int. J. GEOMATE*, *18(67)*: 27-32. DOI: 10.21660/2020.67.5567.

Tripathi, P and Yadav, N (2021). Changes in fats quality parameters after thermal processing of selected oils/fats primarily consumed in India. *J. Adv. Food Sci. Technol.*, *8(1)*: 10-23.

Vadivambal, R and Jayas, D S (2010). Non-uniform temperature distribution during microwave heating of food materials - A review. *Food Bioprocess Technol.*, *3(2)*: 161-171. DOI: 10.1007/s11947-008-0136-0.

Vincent, C J; Shamsudin, R and Baharuddin, A S (2014). Pre-treatment of oil palm fruits: A review. *J. Food Eng.*, *143*: 123-131. DOI: 10.1016/j.jfoodeng.2014.06.022.

Wellbeloved, M (2020). Humidification and the HME filter. *South. Afr. J. Anaesth. Analg.*, *26(6)*: 161-163. DOI: 10.36303/SAJAA.2020.26.6.S3.2564.

Wu, Y; Yan, B; Yang, Y; Zhu, H and Huang, K (2020). Accordion microwave oven for uniformity and efficiency heating. *Int. J. RF Microw. Comput.-Aided Eng.*, *30(6)*: 22190. DOI: 10.1002/mmce.22190.

Yang, X and Boyle, R A (2016). Sensory evaluation of oils/fats and oil/fat-based foods. *Oxidative Stability and Shelf Life of Foods Containing Oils and Fats* (Hu, M and Jacobsen, C eds.). AOCS Press, Illinois, USA. p. 157-185.

Yoosa, P; Hattha, E and Tantanawat, T (2018). The effects of controlling the residual moisture content in oil palm fruits under microwave sterilisation, *J. Adv. Agric. Technol., 5(1)*: 63-68. DOI: 10.18178/joaat.5.1.63-68.

Yoosa, P; Srimongkol, S and Yuttawiriya, R (2022). The effect moisture residue in oil palm fruits with microwave technique: Quantifying the significant factor of residual moisture as the process parameter for commercial sterilization. *J. Adv. Agric. Technol.*, *9(1)*: 1-8.

Journal of Oil Palm Research Vol. 35 (3) September 2023 p. 467-475
DOI: https://doi.org/10.21894/jopr.2022.0071

CO-SOLVENT SELECTION FOR TOCOTRIENOL EXTRACTION FROM PALM FATTY ACID DISTILLATE USING SUPERCRITICAL CARBON DIOXIDE

NAJWA OTHMAN[1]; CHONG GUN HEAN[1,2]; EZZAT MOHAMAD AZMAN[1] and NORHIDAYAH SULEIMAN[1,2]*

ABSTRACT

A predictive model was devised for the estimation of the Kamlet-Taft (KT) dipolarity/polarisability (π) parameter for binary mixtures of supercritical carbon dioxide ($scCO_2$) and co-solvent. The model allows the selection of the best co-solvent for the extraction of tocotrienols from palm fatty acid distillate (PFAD). Ethanol, acetone and isopropanol were separately used as co-solvents in the range of 0.05 - 0.15 mL/g for the experimental set-up at 20 MPa and 53°C for 300 min and a CO_2 flow rate of 32 ± 5 g/min. The model's estimations of π* for all these binary mixtures followed the trends for the extraction of tocotrienols. The π* values increased with the concentration of co-solvent in the binary system and tocotrienol extraction was directly proportional to the π* value, but only up to a particular value. Of the three co-solvents tested, ethanol was predicted to be the best to enhance tocotrienol extraction. With a 0.075 mL/g of ethanol, the extraction yield was 30.03^a ± 0.03 mg/g, more than that achieved with pure $scCO_2$ (16.45^b ± 2.02 mg/g).*

Keywords: co-solvents, Kamlet-Taft, palm fatty acid distillate, supercritical fluid extraction, tocotrienols.

Received: 25 February 2022; **Accepted**: 5 September 2022; **Published online**: 7 November 2022.

INTRODUCTION

Agricultural by-products are essential sources of natural antioxidants. Palm fatty acid distillate (PFAD) is a by-product of refining crude palm oil. While PFAD is commonly used as a fatty acid for non-food industries, it is also a source of various bioactive compounds for the food and health industries, such as tocopherols, tocotrienols, squalene, sterols and others.

Both tocopherols and tocotrienols belong to the vitamin E family and are components of palm oil (Colombo, 2010). Tocotrienols have more excellent neuroprotective, anticancer and cholesterol-lowering effects than tocopherols (Colombo, 2010). They exist as four different isomers: α-, β-, γ- and δ-tocotrienol. All except β-tocotrienol exhibit more incredible health benefits than α-tocopherol. Colombo (2010) reported that a nanomolar concentration of α-tocotrienol could prevent neurodegeneration.

Supercritical carbon dioxide ($scCO_2$) extraction has been extensively used to extract bioactive compounds and lipids (Brunner, 2005). The development of $scCO_2$ technology is in line with the environmental sustainability issues. Efficient extraction of $scCO_2$ is due to the low viscosity, density and high diffusivity of $scCO_2$ to interact with the solute in the sample. Altering the main operating conditions of the $scCO_2$ system, such as pressure and temperature, will directly impact the physical properties, including the density of $scCO_2$. For instance, increasing pressure at a constant temperature will increase the solvent's density and solvating power. Thus, the consideration of the density at the supercritical region is necessary since the pressure and temperature of $scCO_2$ significantly impact it.

[1] Department of Food Technology,
Faculty of Food Science and Technology,
Universiti Putra Malaysia,
43400 UPM Serdang, Selangor, Malaysia.

[2] Supercritical Fluid Centre (SFC),
Faculty of Food Science and Technology,
Universiti Putra Malaysia,
43400 UPM Serdang, Selangor, Malaysia.

* *Corresponding author e-mail: su_hidayah@upm.edu.my*

Nevertheless, $scCO_2$ is a nonpolar solvent with high selectivity for nonpolar to moderately polar compounds. This makes $scCO_2$ less efficient for the extraction of high polarity compounds. The addition of co-solvents (modifiers or entrainers) in the $scCO_2$ system improves extraction and fractionation, especially in food and pharmaceutical applications. Sato *et al.* (2017) reported that using a co-solvent resulted in a higher yield of compounds such as saccharides and cinnamic acid, which also have antioxidant properties. Jafarian *et al.* (2020) reported an increase in the amount of phytosterol (67% by weight) extracted from rapeseed oil deodoriser distillates through the addition of 5% (v/v) ethanol to the $scCO_2$ process at 35 MPa and 313 K. Lima *et al.* (2019) reported that the addition of methanol (5% v/v) to the $scCO_2$ process enhanced the yield of oil extracted from *Piper klotzschianum* leaves to approximately 40%. De O Silva *et al.* (2019) demonstrated the $scCO_2$ extraction of oil from pomegranate seeds with alcohol (ethanol, methanol, or isopropanol) as a co-solvent that produces speciality oils rich in conjugated linolenic acid, phenolics and tocopherols.

Polar co-solvents are commonly used in the $scCO_2$ extraction process, at concentrations of 5%-20%, to increase the solubility of the compounds of interest, reducing the main operating condition such as pressure and carbon dioxide (CO_2) consumption, hence, increasing the separation process (Duereh *et al.*, 2020b; Tirado *et al.*, 2019). Co-solvents can modify the characteristics of the supercritical solvent, such as its polarity. Technically, CO_2 has a non-specific interaction with the solute of interest, via dispersion. The presence of a co-solvent can improve the extraction process by creating a specific interaction with polar solutes, via hydrogen bonding. Nevertheless, a greater understanding of the actions of a co-solvent is necessary to optimise the extraction of the compounds of interest.

Extraction of palm oil waste under supercritical conditions has been conducted either by using co-solvent or without the aid of co-solvent. However, a full investigation on estimating the effect of co-solvent on the tocotrienols extract from PFAD using the predictive model of Kamlet-Taft (KT) Dipolarity/Polarisability has been partially reported. The KT parameters provide detailed information on a solvent's characteristics, particularly its modes of action and solubility (Islam *et al.*, 2020). In this regard, KT solvatochromic dipolarity/polarisability (π^*) can predict the effect of a solvent on the separation of a target compound; hence, knowledge of this parameter enables the best co-solvent to be selected for a particular separation or extraction process. Therefore, the purpose of this study was to use KT (π^*) to predict the best co-solvent for $scCO_2$ to achieve the selective extraction of tocotrienols from PFAD. The work included a study of the extraction of PFAD using three polar co-solvents, ethanol, acetone and isopropanol.

MATERIALS AND METHODS

Materials

PFAD was procured from Jomalina-Sime Darby (Teluk Panglima Garang, Selangor, Malaysia). For supercritical fluid extraction, liquid carbon dioxide at 99.99% (food grade) purity was purchased from Alpha Gas Solution Sdn. Bhd., Shah Alam, Malaysia. All solvents used were either analytical grade or high-performance liquid chromatography (HPLC) grade, and were purchased from Sigma Aldrich (Kappelweg, Schnelldorf, Germany).

Dissolution of PFAD in Co-solvents

The solubility of PFAD in the co-solvents was tested using the same method as Lee *et al.* (2019). Preliminary experiments were carried out visually to identify the best co-solvents for the $scCO_2$ extraction and the ability of PFAD to dissolve in the mixed co-solvent. In a test tube, about 0.2 g PFAD was added to 4 mL of various solvents (ethanol, isopropanol, or acetone), and the mixture was heated to varying temperatures (40°C to 60°C) in a water bath, with continuous stirring for 5 min. The dissolution of PFAD was evaluated visually. This led to the identification of ethanol, isopropanol and acetone as potentially good co-solvents for extracting tocotrienols from PFAD as tabulated in *Table 1*.

Supercritical Carbon Dioxide ($scCO_2$) Extraction Process

The extraction of tocotrienols from PFAD was conducted using laboratory-scale $scCO_2$ extraction with a 1 L extractor (dimension in meters: 0.21H x 0.08D) equipped with a CO_2 recirculating system. A fixed 100 g of pre-treated PFAD was weighed and loaded into the extractor vessel packed with glass beads and glass wool. Several methods have been suggested for the introduction of the co-solvent to the $scCO_2$ system, such as (1) directly adding the co-solvent to the sample, (2) pre-mixing the $scCO_2$ and co-solvent, and (3) using a secondary pump to add the co-solvent to the system (Putra *et al.*, 2018). Herein, PFAD was manually mixed with different amounts of the co-solvent (0.050, 0.075, 0.100 and 0.150 mL/g).

Dynamic extractions were continuously carried out for 6 hr at a flow rate of 32 ± 5 g/min, and extracts were collected at the separator in amber glass. Any residual co-solvent in the extracts was removed using a rotary evaporator (IKA RV 10 and IKA HB

10 control, Staufen, Germany) before the collected samples were stored at -20°C for further analysis.

Quantification of Tocotrienols

High-performance liquid chromatography (HPLC) was performed using an Agilent Technologies 1200 Series instrument with a diode-array detector (Agilent Technologies, United States) to identify and quantify the tocotrienol content of the PFAD extracts. As a standard for the tocotrienol quantification, a commercial tocotrienol product, Gold Tri. E 50 (99% pure), procured from Sime Darby, Malaysia, was used. A Kinetex PFP column with 150 x 4.6 mm i.d. and 5 μm particle diameter (Phenomenex, United States) was used for analysis. The injection volume was set at 6 μL, and the tocotrienol isomers were detected at the maximum absorption wavelength, 290 nm. The tocotrienol isomers separated from the extract at a flow rate of 0.6 mL/min with 85% (v/v) methanol in water for 50 min.

A Predictive Model of Kamlet-Taft (KT) Dipolarity/ Polarisability

Duereh *et al*. (2019) developed a predictive framework to estimate the KT dipolarity/ polarisability parameter of the binary liquid mixture, $\Delta\pi^{*,N}_{mix}$. This model was proposed based on the linear relationship between the relative normalised dipolarity/ polarisability $\Delta\pi^{*,N}_{mix}$ of binary liquid polar-nonpolar mixtures which have a linear relationship and gas phase dipole moments. The predictive framework is used with the function of the Wilson thermodynamic excess function without considering the density dependency since the π* values of binary liquid mixtures do not significantly change with the density.

A modification to the predictive framework has been made by Duereh *et al*. (2020b) to predict the π* values of $scCO_2$-cosolvent binary mixtures. In this modification, density-dependent via a correction function ($g(\rho_{co_2})$) is added to the predictive framework. This is because a remarkable deviation between the experimental and predicted π* values using the previous predictive framework (Duereh *et al*., 2019) of $scCO_2$-cosolvent at 50°C and 10 MPa (supercritical region) were found. This suggested that density is another significant factor affecting the π* values at the supercritical phase instead of the dipole moment. The modification of the predictive framework as shown in Equation (1):

$$\Delta\pi^{*,N}_{mix} = \mu_2 [-x_1 \ln (x_1 + 1.981x_2) - x_2 \ln (x_2 + 0.181x_1)] \; x \; g(\rho_{co_2}) \quad (1)$$

where $\Delta\pi^{*,N}_{mix}$ is KT dipolarity/polarisability parameter of the $scCO_2$-cosolvent, μ_2 is dipole moment of cosolvent, x_1 is a composition of CO_2, x_2 is a composition of cosolvent, and $g(\rho_{co_2})$ is local density enhancement.

Four correction functions of local density enhancement have been evaluated by Duereh, *et al.* (2020b) using the fluorescence method, UV method, Raman method and molecular dynamics simulations. Based on the plot of correction functions of local density enhancement as a function of pure density (ρ_{co_2}), which was estimated using Span and Wagner equation, the UV method was chosen since it sowed the smallest value of local density enhancement and almost symmetric shape compared to the other methods. The correction function using UV (g^{UV} (ρ_{co_2})) is as defined in Equation (2):

$$g^{UV}(\rho_{co_2}) = 1 + \{[0.937\ X\ (1 - \exp(-3.916(\rho_{co_2}))] - 0.884\ \rho_{co_2}\} \quad (2)$$

The predictive framework with the modification of local density enhancement using the UV method is shown in Equation (3):

$$\Delta\pi^{*,N}_{mix} = \mu_2 [-x_1 \ln (x_1 + 1.981x_2) - x_2 \ln (x_2 + 0.181x_1)] \; x \; \{1 + \{[0.937\ X\ (1 - \exp(-3.916\ \rho_{co_2}))] - 0.884\ \rho_{co_2}\}\} \quad (3)$$

RESULTS AND DISCUSSION

Dissolution of PFAD in Various Co-solvents

To extend the $scCO_2$ solvating power and improve the affinity for polar compounds, adding small volumes of a (polar) co-solvent with the appropriate chemical and physical properties is necessary. The KT parameters dipolarity/ polarisability (π*), hydrogen-bond basicity (β), and hydrogen-bond acidity (α) effectively characterise potential solvents. Herein, three types of co-solvents (ethanol, isopropanol, and acetone) were chosen. The co-solvents were selected based on gas phase dipole moment and the function of the co-solvent as hydrogen bond donor or hydrogen bond acceptor. This is necessary to investigate the influence of dipole moment on the KT dipolarity/ polarisability and the available specific interactions that can be formed between co-solvent and solute.

Table 1 explains that full PFAD dissolution was achieved with solvents that have α, β, and π* values in the range 0.08 to 0.86, 0.43 to 0.84 and 0.48 to 0.71, respectively. The dissolution tests of PFAD in ethanol, acetone and isopropanol at different temperatures are also shown in *Table 1*, with 4 mL of solvent mixed with 0.2 g PFAD for 5 min of stirring. It was found that PFAD was highly soluble in all three solvents at 40°C to 60°C. Increasing the temperature caused the viscosity of solvents to decrease, which

gave high dissolution rates of the PFAD (Lee *et al.*, 2019). Since PFAD was highly soluble in the three solvents tested, they were all used as co-solvents in the $scCO_2$ extraction.

TABLE 1. KAMLET-TAFT (KT) PARAMETERS AND DISSOLUTION OF PFAD IN DIFFERENT CO-SOLVENTS

Solvent	Kamlet-Taft (KT) parameters			Solubility characteristics
	α	β	π^*	
Acetone	0.08	0.43	0.71	Full dissolution at 40°C, 50°C and 60°C
Ethanol	0.86	0.75	0.54	Full dissolution at 40°C, 50°C and 60°C
Isopropanol	0.76	0.84	0.48	Full dissolution at 40°C, 50°C and 60°C

Note: α - hydrogen bond donor; β - hydrogen bond acceptor; π^* - dipolarity; Kamlet-Taft parameters adapted from Weerachanchai *et al.* (2014).

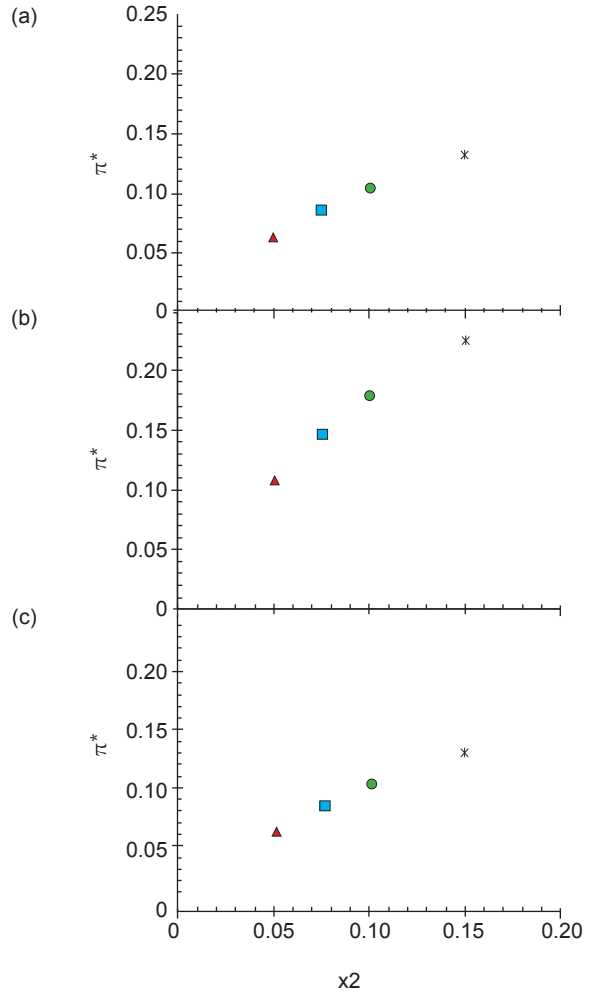

Figure 1. Kamlet-Taft (KT) dipolarity/polarisability (π) at 50°C and 20 MPa for (a) CO_2 (1)- C_2H_5OH (2), (b) CO_2 (1)- C_3H_6O (2), (c) CO_2 (1)- C_3H_8O (2) as a function of the amount of component 2. Symbol lists: ▲ = 0.05 mL/g, ■ = 0.075 mL/g, ● = 0.1 mL/g, and ⁎ = 0.15 mL/g.*

KT Dipolarity/Polarisability of CO_2 and Co-solvent Mixtures

Figure 1 shows the $\Delta\pi^{*,N}_{mix}$ values for the binary mixtures of $scCO_2$ and various co-solvent (ethanol, acetone, and isopropanol) as estimated using the predictive model of KT dipolarity/polarisability to describe the co-solvent effects. Herein, the focus is only on the co-solvent composition and dipole moment towards the $\Delta\pi^{*,N}_{mix}$ values of the binary $scCO_2$-co-solvent system. π^* increases as the co-solvent added in the $scCO_2$ system increases. Acetone (C_3H_6O) has higher π^* values relatively compared to ethanol (C_2H_5OH) and isopropanol (C_3H_8O). This is because acetone has a higher dipole moment (2.88). The dipole moment governs the specific dipolarity/polarisability interactions between target compounds and the co-solvent in the supercritical state (Duereh *et al.*, 2020b). The molecular dynamics simulations showed the specific interactions that appeared between solute and co-solvent (Frolov and Kiselev, 2014; Gurina *et al.*, 2017). Hence, improve the solubility of target compounds in $scCO_2$ via the interactions. This has been proven by the infrared spectroscopic analyses (Lalanne *et al.*, 2004; Reilly *et al.*, 1995) and theoretical investigations (Danten, 2002; Saharay and Balasubramanian, 2006) whereby CO_2 can form the electron donor-acceptor interactions with the oxygen atom in alcohol co-solvent since CO_2 can act as a weak Lewis acid via electron deficiency in the carbon atom. Consequently, the π^* values plotted in *Figure 1* follow the trend in values of the dipole moment of the co-solvents (*Table 2*).

TABLE 2. THE DIPOLE MOMENTS OF THE CO-SOLVENTS

Solvent	Dipole moment, μ
Ethanol	1.69
Acetone	2.88
Isopropanol	1.66

Note: Adapted from Duereh *et al.*, 2020a; 2020b.

In addition, the polarity can be estimated via π^* to quantify the effect of co-solvent in the separation of the target compound in the sample. *Figure 2* depicts the relationship between the amount of tocotrienol extracted from PFAD and the estimated π^* values of the solvent mixtures. The amount of tocotrienol extracted tended to increase linearly up to the particular value of π^* but then started to decline as the estimated value of π^* increased further for all mixtures of CO_2-C_2H_5OH, CO_2-C_3H_6O, and CO_2-C_3H_8O. Technically, during the extraction process, it is restricted by the equilibrium solubility of the solute in the solvent. Thus, the outer layer of solute is completely extracted by solvent. However, the extraction rate starts to decrease because many solutes have been extracted at the equilibrium

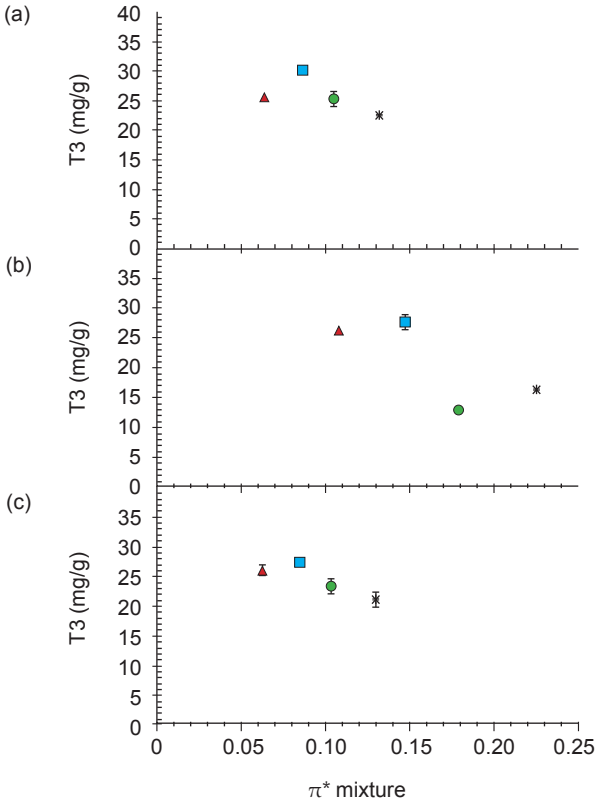

Figure 2. Tocotrienols extraction (mg/g) from PFAD as a function of Kamlet-Taft (KT) dipolarity/polarisability (π) of the mixtures of $scCO_2$ and (a) C_2H_5OH, (b) C_3H_6O and (c) C_3H_8O. Symbol lists: ▲ = 0.05 mL/g, ■ = 0.075 mL/g, ● = 0.1 mL/g, and ✱ = 0.15 mL/g.*

control phase. It can be noted that the extraction rate is reduced as the mass transfer decreases due to the free solute in the sample being depleted.

A more remarkable yield recovery is expected with the addition of co-solvent due to the polarity of tocotrienols. Instead of having only non-specific interaction via dispersion between CO_2 and solutes, the presence of co-solvent will create a more specific interaction via hydrogen bonding with the solute of interest, hence, improving the polarity. In the final stage of the extraction process, the diffusion control phase will take place, whereby the extraction of solute depends on the diffusion rate and ability of the solvent to penetrate deep into the sample to extract the remaining solutes. The addition of a co-solvent increases the density of the fluid mixture ($scCO_2$-cosolvent) around the solute, which causes the solid particles to swell, helping to break the chemical bonds and releases the soluble compounds, thus, enhancing the internal diffusion and solubilisation of interest compounds (Coelho *et al.*, 2020; Monroy *et al.*, 2016).

However, Machado *et al.* (2015) reported that a large amount of co-solvent will produce insufficient energy to break the bonds between the solvent molecules, and consequently, the solubility of polar compounds decreases. Besides, the saturation occurs between CO_2 and co-solvent when a higher amount of co-solvent is added to the system, leading to several phases such as liquid and gas phases will appear in the system (Yao *et al.*, 1994; Yoon *et al.*, 1994). It is important to note that the $scCO_2$ system should be maintained as a single homogenous phase. Other than that, a higher amount of co-solvent in the system will contribute to the solvent-solvent interactions in competition for the solvation of solutes, thus decreasing the recovery (Porto *et al.*, 2014). According to molecular dynamics simulations (Skarmoutsos *et al.*, 2010) and spectroscopic NMR (Maiwald *et al.*, 2007; Schnabel *et al.*, 2007), there is a possible self-hydrogen bonding interaction of alcohol co-solvents that appeared in a $scCO_2$-cosolvent system rather than forming the electron donor-acceptor interactions between CO_2 and alcohol co-solvents.

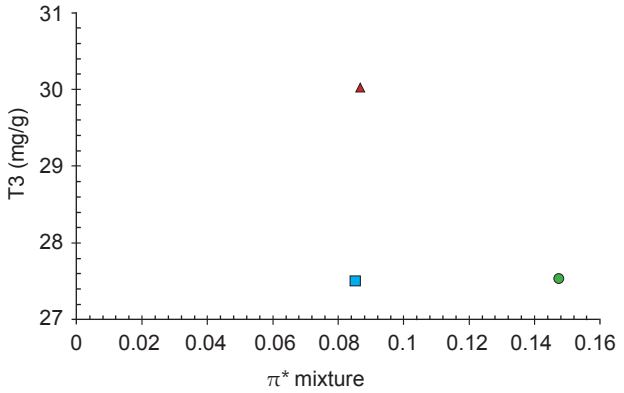

Figure 3. Recovery of tocotrienols from PFAD using $scCO_2$ with three different co-solvents (0.075 mL/g) at 50°C and 20 MPa as a function of Kamlet-Taft (KT) dipolarity/polarisability (π) of the CO_2- co-solvent mixtures in the supercritical state. Symbol list: ▲ = CO_2-C_2H_5OH, ■ = CO_2- C_3H_8O, and ● = CO_2-C_3H_6O.*

Figure 3 shows the recovery of tocotrienols from PFAD using $scCO_2$ with the addition of the different co-solvents. There is no significance different (p-value <0.05) between tocotrienols concentration among the three co-solvents, as depicted in *Table 3*. The most significant amount of tocotrienols extracted was 30.03 mg/g, with ethanol as the co-solvent in the $scCO_2$ system; the estimated value of π* for that mixture was 0.086. In principle, the dipole moment is an important factor influencing the π* value. As mentioned before, acetone had the highest π* value due to a large number of dipole moments. The change in π* values will create a specific interaction via hydrogen bonding between co-solvent and solute. However, the type of co-solvent is also another important factor. For instance, only one molecule in acetone will be involved in forming hydrogen bonding compared to ethanol. Thus, this is the limiting factor in the solubility of tocotrienols in the $scCO_2$-acetone system.

Ethanol can be considered a polarity-modifying solvent in $scCO_2$ extraction (Díaz-Reinoso *et al.*,

2020). As reported by Duereh and Smith (2018), the presence of ethanol at the supercritical state can increase both KT-polarisability and KT-basicity. Theoretically, CO_2 has low KT-basicity and dipolarity/polarisability. The KT-parameter can be changed over a narrow range of values (0-0.2) in the supercritical region. The addition of co-solvent such as ethanol may increase both KT-polarisability and KT-basicity, inducing the formation of both interactions (dispersion and hydrogen bonding), which enhance the solubility of the solute. More significant amounts of tocotrienols are extracted in the presence of ethanol because of the increase in the polarity of the solvent. Since tocotrienols contain hydroxyl groups (Coelho *et al.*, 2020), adding ethanol allows H-bonding between the co-solvent and the solute molecule, which increases the solubility of the compounds of interest in the $scCO_2$ phase (Coelho *et al.*, 2020). Furthermore, adding ethanol leads to swelling of the solid matrix, which facilitates the transport of the solute and so reduces the extraction time (Trevisani Juchen *et al.*, 2019). Several studies have evaluated $scCO_2$ with the addition of a co-solvent (Porto *et al.*, 2014; Sato *et al.*, 2017; Sookwong *et al.*, 2016).

Comparative Study of $scCO_2$, $scCO_2$ + Co-solvents, and Soxhlet Extraction

Three extraction techniques were compared, with Soxhlet extraction as a benchmark against evaluating the $scCO_2$ process. The extraction of tocotrienol using $scCO_2$ was significantly (p-value <0.05) higher than that achieved by Soxhlet extraction (*Table 3*). This is due to the thermo-sensitivity of tocotrienols becoming important at the higher operating temperature of Soxhlet extraction (Ribeiro *et al.*, 2019). According to Othman *et al*. (2022), the tocotrienol extract increases when the temperature rises from 40°C to 50°C. However, a further increase in temperature may result in a reduction in tocotrienol extracts. Similarly, Zhao and Zhang (2014) found that the amount of 1,8-cineole extracted from Eucalyptus leaf oil was less with Soxhlet extraction than with $scCO_2$ extraction, and Jafarian *et al*. (2020) found that the extraction of phytosterols and tocopherols from rapeseed oil waste was greater with $scCO_2$ than with Soxhlet extraction.

$scCO_2$ has been categorised as a poor solvent for high molecular weight or hydrophilic compounds due to zero dipole moment (Zhang *et al.*, 2002). Significant changes of CO_2 π^* over a narrow range of value in the supercritical region leads to the interaction between CO_2 and many solutes through dispersion forces (Duereh and Smith, 2018). Nevertheless, the polarity of CO_2 can be switched since it is Lewis acid. Adding co-solvents to the $scCO_2$ increases the recovery of tocotrienols because the co-solvents polarity increases the dissolution of tocotrienols in PFAD. Tocotrienol extraction was approximately doubled with the addition of ethanol to the $scCO_2$ system compared with pure $scCO_2$, due to both specific (hydrogen bonding) and non-specific (dispersion) interactions between the co-solvent and the solute molecule, which increase the solubility of the tocotrienols in the solvent phase. According to and Waśkiewicz (2020), ethanol is generally employed in supercritical mixtures to improve the dissolvability of polar molecules and the selectivity of $scCO_2$. However, the main limitation of introducing co-solvent in the supercritical state is the phase equilibrium since it can reach saturation with excessive co-solvent presence in the $scCO_2$ system.

CONCLUSION

In this work, a predictive framework based on the values of CO_2 density, co-solvent dipole moment, and π^* of the pure components is proposed that allows estimation of the value of π^* for binary mixtures of $scCO_2$ and co-solvent (here, under the operating conditions of 20 MPa and 53°C). The estimates of π^* increase as the co-solvent in the binary mixture increases. Moreover, the extraction yield of tocotrienols was directly proportional to the π^* values of the binary mixtures as estimated using the predictive framework, but only up to a particular value of π^* after which it decreased as π^* increased

TABLE 3. EFFECT OF EXTRACTION CONDITIONS ON TOCOTRIENOLS CONCENTRATIONS (mg/g) IN PFAD EXTRACTS

Extraction condition		Tocotrienols (mg/g)
$scCO_2$		$16.45^{b} \pm 2.02$
$scCO_2$ + co-solvent	Ethanol	$30.03^{a} \pm 0.03$
	Acetone	$27.55^{a} \pm 1.44$
	Isopropanol	$27.51^{a} \pm 0.01$
Soxhlet extraction		$10.45^{c} \pm 0.57$

Note: Means that do not share superscript letters are significantly different (p-value < 0.05).

further. According to the predictive framework, ethanol is the best co-solvent for extracting tocotrienols from PFAD. This is due to the capability of ethanol to form more specific interactions with tocotrienols, which enhances the dissolution of tocotrienols in the $scCO_2$. The presence of ethanol as a co-solvent nearly doubled the extraction of tocotrienols (to 30.03 ± 0.03 mg/g) compared with that achieved by pure $scCO_2$ (16.45 ± 2.02 mg/g), and ethanol was slightly better in this respect than the other two co-solvents tested. This suggests that ethanol has excellent potential to be used to enhance the $scCO_2$ extraction of tocotrienols from PFAD.

ACKNOWLEDGEMENT

This research was conducted under the financial support of a research grant (GP-IPM/2017/9577900) from Universiti Putra Malaysia. The authors would like to thank Sime Darby for providing the PFAD sample.

REFERENCES

Brunner, G (2005). Supercritical fluids: Technology and application to food processing. *J. Food Eng.*, *67(1-2)*: 21-33. DOI: 10.1016/j.jfoodeng.2004.05.060.

Coelho, J P; Filipe, R M; Paula Robalo, M; Boyadzhieva, S; Cholakov, G S and Stateva, R P (2020). Supercritical CO_2 extraction of spent coffee grounds. Influence of co-solvents and characterization of the extracts. *J. Supercrit. Fluids*, *161*: 104825. DOI: 10.1016/j.supflu.2020.104825.

Colombo, M L (2010). An update on vitamin E, tocopherol and tocotrienol-perspectives. *Molecules*, *15(4)*: 2103-2113. DOI: 10.3390/molecules15042103.

Danten, Y (2002). Vibrational spectra of CO_2-electron donor-acceptor complexes from ab initio. *J. Phys. Chem. A*, *106(48)*: 11831-11840. DOI: 10.1021/jp021598v.

de O Silva, L; Ranquine, L G; Monteiro, M and Torres, A G (2019). Pomegranate (*Punica granatum* L.) seed oil enriched with conjugated linolenic acid (cLnA), phenolic compounds and tocopherols: Improved extraction of a specialty oil by supercritical CO_2. *J. Supercrit. Fluids.*, *141*: 126-137. DOI: 10.1016/j.supflu.2019.02.019.

Díaz-Reinoso, B; Moure, A and Domínguez, H (2020). Ethanol-modified supercritical CO_2 extraction of chestnut burs antioxidants. *Chem. Eng. Process. - Process Intensification*, *156*(*August*): 108092. DOI: 10.1016/j.cep.2020.108092.

Duereh, A; Guo, H; Sato, Y and Inomata, H (2020a). Local composition models for predicting Kamlet-Taft dipolarity/polarisability of nonaqueous binary and ternary mixtures. *J. Mol. Liq.*, *304*: 112691. DOI: 10.1016/j.molliq.2020.112691.

Duereh, A; Sugimoto, Y; Ota, M; Sato, Y and Inomata, H (2020b). Kamlet-taft dipolarity/polarisability of binary mixtures of supercritical carbon dioxide with cosolvents: Measurement, prediction, and applications in separation processes. *Ind. Eng. Chem. Res.*, *59(27)*: 12319-12330. DOI: 10.1021/acs.iecr.0c01251.

Duereh, A; Guo, H; Sato, Y; Smith, R L and Inomata, H (2019). Predictive framework for estimating dipolarity/polarisability of binary nonpolar-polar mixtures with relative normalised absorption wavelength and gas-phase dipole moment. *Ind. Eng. Chem. Res.*, *58(41)*: 18986-18996. DOI: 10.1021/acs.iecr.9b04319.

Duereh, A and Smith, R L (2018). Strategies for using hydrogen-bond donor/acceptor solvent pairs in developing green chemical processes with supercritical fluids. *J. Supercrit. Fluids.*, *141*: 182-197. DOI: 10.1016/j.supflu.2017.11.004.

Frolov, A I and Kiselev, M G (2014). Prediction of cosolvent effect on solvation free energies and solubilities of organic compounds in supercritical carbon dioxide based on fully atomistic molecular simulations. *J. Phys. Chem. B*, *118(40)*: 11769-11780. DOI: 10.1021/jp505731z.

Gurina, D L; Antipova, M L; Odintsova, E G and Petrenko, V E (2017). The study of peculiarities of parabens solvation in methanol- and acetone-modified supercritical carbon dioxide by computer simulation. *J. Supercrit. Fluids*, *126*: 47-54. DOI: 10.1016/j.supflu.2017.02.008.

Islam, T; Sarker, Z I; Uddin, A B M H; Yunus, B; M, R P D; Mia, A R and Ferdosh, S (2020). Kamlet Taft parameters: A tool to alternate the usage of hazardous solvent in pharmaceutical and chemical manufacturing/synthesis - A gateway towards green technology. *Anal. Chem. Lett.*, *10(5)*: 550-561. DOI: 10.1080/22297928.2020.1860124.

Jafarian Asl, P; Niazmand, R and Yahyavi, F (2020). Extraction of phytosterols and tocopherols from rapeseed oil waste by supercritical CO_2 plus co-solvent: A comparison with conventional solvent extraction. *Heliyon*, *6(3)*: e03592. DOI: 10.1016/j.heliyon.2020.e03592.

Lalanne, P; Tassaing, T; Danten, Y; Cansell, F; Tucker, S C and Besnard, M (2004). CO_2-ethanol interaction studied by vibrational spectroscopy in supercritical CO_2. *J. Phys. Chem. A*, *108(14)*: 2617-2624. DOI: 10.1021/jp037802b.

Lee, W J; Ng, C C; Ng, J S; Smith, R L; Kok, S L; Hee, Y Y; Lee, S Y; Tan, W K; Zainal Abidin, N H; Halim Lim, S A and Chong, G H (2019). Supercritical carbon dioxide extraction of α-mangostin from mangosteen pericarp with virgin coconut oil as co-extractant and *in-vitro* bio-accessibility measurement. *Process Biochem., 87:* 213-220. DOI: 10.1016/j.procbio.2019.09.009.

Lima, R N; Ribeiro, A S; Cardozo-Filho, L; Vedoy, D and Alves, P B (2019). Extraction from leaves of *Piper klotzschianum* using supercritical carbon dioxide and co-solvents. *J. Supercrit. Fluids*., *147*: 205-212. DOI: 10.1016/j.supflu.2018.11.006.

Machado, B A S; De Abreu Barreto, G; Costa, A S; Costa, S S; Silva, R P D; Da Silva, D F; Brandao, H N; Da Rocha, J L C; Nunes, S B; Umsza-Guez, M A and Padilha, F F (2015). Determination of parameters for the supercritical extraction of antioxidant compounds from green propolis using carbon dioxide and ethanol as co-solvent. *PLoS ONE*, *10(8)*: 1-26. DOI: 10.1371/journal.pone.0134489.

Maiwald, M; Li, H; Schnabel, T; Braun, K and Hasse, H (2007). On-line 1H NMR spectroscopic investigation of hydrogen bonding in supercritical and near critical CO_2-methanol up to 35 MPa and 403 K. *J. Supercrit. Fluids*, *43(2)*: 267-275. DOI: 10.1016/j.supflu.2007.05.009.

Monroy, Y M; Rodrigues, R A F; Sartoratto, A and Cabral, F A (2016). Influence of ethanol, water, and their mixtures as co-solvents of the supercritical carbon dioxide in the extraction of phenolics from purple corn cob (*Zea mays* L.). *J. Supercrit. Fluids*, *118*: 11-18. DOI: 10.1016/j.supflu.2016.07.019.

Othman, N; Chong, G H; Azman, E M and Suleiman, N (2022). Effect of process variables in supercritical carbon dioxide extraction of tocotrienols from hydrolysed palm fatty acid distillate (PFAD). *J. Food Process. Preserv.*, *46(5)*: 1-10. DOI: 10.1111/jfpp.16533.

Porto, C D A; Natolino, A and Decorti, D (2014). Extraction of proanthocyanidins from grape marc by supercritical fluid extraction using CO_2 as solvent and ethanol – water mixture as co-solvent. *J. Supercrit. Fluids*, *87(September 2012)*: 59-64. DOI: 10.1016/j.supflu.2013.12.013.

Putra, N R; Yian, L N; Nasir, H M; Binti Idham, Z and Yunus, M A C (2018). Effects of process parameters on peanut skins extract and CO_2 diffusivity by supercritical fluid extraction. *IOP Conf. Ser.: Mater. Sc. Eng., 334:* 0.12057. DOI: 10.1088/1757-899X/334/1/012057.

Reilly, J T; Bokis, C P and Donohue, M D (1995). An experimental investigation of Lewis acid-base interactions of liquid carbon dioxide using Fourier Transform Infrared (FT-IR) spectroscopy. *Int. J. Thermophys.*, *16(3)*: 599-610. DOI: 10.1007/BF01438845.

Ribeiro, P P C; E Silva, D M de L; Dantas, M M; Ribeiro, K D da S; Dimenstein, R and Damasceno, K S F da S C (2019). Determination of tocopherols and physicochemical properties of faveleira (*Cnidoscolus quercifolius*) seed oil extracted using different methods. *Food Sc. Technol., 39(2):* 280-285. DOI: 10.1590/fst.24017.

Saharay, M and Balasubramanian, S (2006). Electron donor-acceptor interactions in ethanol-CO_2 mixtures: An ab-initio molecular dynamics study of supercritical carbon dioxide. *J. Phys. Chem. B*, *110(8)*: 3782-3790. DOI: 10.1021/jp053839f.

Sato, T; Fukuda, F; Nihei, K ichi and Itoh, N (2017). Effect of temperature and pressure on the extraction of strawberry receptacles with a mixture of supercritical carbon dioxide and entrainers. *J. Supercrit. Fluids, 130(June)*: 23-29. DOI: 10.1016/j.supflu.2017.07.011.

Schnabel, T; Srivastava, A; Vrabec, J and Hasse, H (2007). Hydrogen bonding of methanol in supercritical CO_2: Comparison between 1H NMR spectroscopic data and molecular simulation results. *J. Phys. Chem. B*, *111(33)*: 9871-9878. DOI: 10.1021/jp0720338.

Skarmoutsos, I; Guardia, E and Samios, J (2010). Hydrogen bond, electron donor-acceptor dimer, and residence dynamics in supercritical CO_2-ethanol mixtures and the effect of hydrogen bonding on single reorientational and translational dynamics: A molecular dynamics simulation study. *J. Chem. Phys.*, *133(1):* 014504. DOI: 10.1063/1.3449142.

Sookwong, P; Suttiarporn, P; Boontakham, P; Seekhow, P; Wangtueai, S and Mahatheeranont, S (2016). Simultaneous quantification of vitamin E, γ-oryzanols and xanthophylls from rice bran essences extracted by supercritical CO_2. *Food Chem.*, *211*: 140-147. DOI: 10.1016/j.foodchem.2016.05.001.

Tirado, D F; Rousset, A and Calvo, L (2019). The selective supercritical extraction of high-

value fatty acids from *Tetraselmis suecica* using the Hansen solubility theory. *Chem. Eng. Trans.*, *75*(*March 2018*): 133-138. DOI: 10.3303/CET1975023.

Trevisani, J P; Nolasco Araujo, M; Hamerski, F; Corazza, M L and Pedersen Voll, F A (2019). Extraction of parboiled rice bran oil with supercritical CO_2 and ethanol as co-solvent: Kinetics and characterisation. *Ind. Crops Prod., 139*: 111506. DOI: 10.1016/j.indcrop.2019.111506.

Uwineza, P A and Waśkiewicz, A (2020). Recent advances in supercritical fluid extraction of natural bioactive compounds from natural plant materials. *Molecules, 25(17)*: 3847. DOI: 10.3390/molecules25173847.

Weerachanchai, P; Lim, K H and Lee, J M (2014). Influence of organic solvent on the separation of an ionic liquid from a lignin-ionic liquid mixture. *Biores. Technol., 156*: 404-407. DOI: 10.1016/j.biortech.2014.01.077.

Yao, S; Guan, Y and Zhu, Z (1994). Investigation of phase equilibrium for ternary systems containing ethanol, water and carbon dioxide at elevated pressures. *Fluid Phase Equilib.*, *99*(*C*): 249-259. DOI: 10.1016/0378-3812(94)80035-9.

Yoon, J H; Lee, H and Chung, B H (1994). High-pressure three-phase equilibria for the carbon dioxide-ethanol-water system. *Fluid Phase Equilib.*, *102(2)*: 287-292. DOI: 10.1016/0378-3812(94)87081-0.

Zhang, X; Han, B; Hou, Z; Zhang, J; Liu, Z; Jiang, T; He, J and Li, H (2002). Why do co-solvents enhance the solubility of solutes in supercritical fluids? New evidence and opinion. *Chem. Eur. J.*, *8(22)*: 5107-5111. DOI: 10.1002/1521-3765(20021115)8:22<5107::AID-CHEM5107>3.0.CO;2-0.

Zhao, S and Zhang, D (2014). Supercritical CO_2 extraction of Eucalyptus leaves oil and comparison with Soxhlet extraction and hydro-distillation methods. *Sep. Purif. Technol.*, *133*: 443-451. DOI: 10.1016/j.seppur.2014.07.018.

Journal of Oil Palm Research Vol. 35 (3) September 2023 p. 476-490
DOI: https://doi.org/10.21894/jopr.2022.0038

GENETIC VARIABILITY OF MPOB-CAMEROON OIL PALM GERMPLASM BASED ON MORPHOLOGICAL TRAITS USING MULTIVARIATE ANALYSIS

WAN NOR SALMIAH TUN MOHD SALIM[1]; ZULKIFLI YAAKUB[1]*; SUZANA MUSTAFFA[1]; NOR AZWANI ABU BAKAR[1]; FATIN MOHD NASIR[1]; MARHALIL MARJUNI[1]; MOHD DIN AMIRUDDIN[1] and MEILINA ONG-ABDULLAH[1]

ABSTRACT

Understanding genetic variability and its distribution among breeding materials is a prerequisite to improve conservation programmes and design breeding strategies. In this study, 31 populations of dura *palms from MPOB-Cameroon oil palm germplasm were evaluated for 21 quantitative traits. Data retrieved from the MPOB Breeding Information System (MPOB-BIS™) was investigated for genetic variability using principal component analysis (PCA) and cluster analysis (CA). The first six principal components (PC1-PC6) with eigenvalue >1.0, accounted for 91.89% of the total variability. The first principal component, PC1 which accounted for 38.35% of the total variation was the largest, contributed by oil yield and total economic product. Whilst PC2 with 16.86% total variation was positively associated with bunch index, bunch number and kernel yield. Population CMR 03 is considered extremely distinct and most positive along PC1 as it performed well in most of bunch quality traits. Population CMR 13 is most positive towards PC2 and among the most negative towards PC1 due to good performance in some vegetative traits studied. CA revealed greater variation among the materials evaluated. Complementing this study with molecular analysis provides the impetus for leveraging new genetic resources in future oil palm improvements and more tractable conservation of oil palm germplasm.*

Keywords: cluster analysis, core collection, genetic resources, morphological characteristics, principal component analysis.

Received: 6 December 2021; **Accepted:** 26 May 2022; **Published online:** 8 July 2022.

INTRODUCTION

Oil palm has been recognised as the highest oil-producing tropical perennial crop. It is one of the key sources of vegetable oils in the world. Malaysia and Indonesia contribute more than one-third of the global vegetable oil production (OECD/FAO, 2019). Palm oil offers great potential in food and non-food applications such as cooking, production of shortening, soap, surfactant, *etc*. Global population growth, with rapidly improving living standards and dietary customs, has led to a gradual increase in market demand for palm oil consumption (Verheye, 2010). This is also reflected in Malaysia's oil palm plantation areas, which have grown exponentially from 54 700 ha in 1960 to 5.90 million hectares in 2019 (MPOB, 2020).

Oil palm (*Elaeis guineensis* Jacq.) is native to West Africa where the oil palm belt runs through Sierra Leone, Liberia, Ivory Coast, Ghana, Cameroon, Nigeria and the Democratic of Congo (formerly known as Zaire) (Hartley, 1988). The highest allelic diversity was identified among the Nigerian oil palm populations, suggesting the possible centre of oil palm origin (Bakoumé *et al*., 2015; Zeven,

[1] Malaysian Palm Oil Board,
6 Persiaran Institusi, Bandar Baru Bangi,
43000 Kajang, Selangor, Malaysia.

* *Corresponding author e-mail: zulkifly@mpob.gov.my.*

1964). In Southeast Asia, the African oil palm was initially introduced with four seedlings planted in Bogor Botanical Gardens, Indonesia in 1848, giving rise to the Deli *dura* populations. It was brought into Malaysia in 1878 and has become the backbone of oil palm planting materials in the country (Rajanaidu *et al*., 2013). Due to the extremely narrow genetic base of oil palm caused by the restriction in a number of ancestral progenitors, researchers from the Malaysian Palm Oil Board (MPOB) have mounted a series of prospection exercises throughout the oil palm belt in Africa and America to explore new genetic resources for future breeding programmes (Corley and Tinker, 2016; Rajanaidu, 1994).

Oil palm germplasm was collected from 11 African countries including Nigeria, Cameroon, Zaire, Angola, Ghana, Guinea, Gambia, Madagascar, Sierra Leone, Senegal and Tanzania to form the largest *ex-situ* conservation programme (Rajanaidu *et al*., 2013). This is imperative to broaden the genetic base of current oil palm materials to improve yield potential, enhance nutritional qualities and tackle future challenges in the oil palm industry. In 1984, through scientific collaboration efforts between MPOB and Pamol, Unilever successfully amassed oil palm materials from the Western and Eastern parts of Cameroon of West Africa (Rajanaidu, 1986). One to 15 open-pollinated palms were collected from 32 different sites in Cameroon, to cover the entire country as much as possible within the available time frame. A total of 58 *dura* bunches were sampled during the prospection and the data was recorded *in situ*. Bunch weight, stalk weight, fruit diameter, nut diameter and mean fruit weight showed a significant difference between the sites. In terms of material quality, the Cameroon *duras* had a mean bunch weight of 16.83 kg, a mean fruit weight of 10.33 g and a mesocarp to the fruit of 39.69% (Rajanaidu, 1986).

Currently, oil palm genetic resources in MPOB are maintained in the form of field genebank to safeguard the long term interest of the Malaysian oil palm industry. Despite being readily available for use, conservation in the form of field genebank necessitates large space and high maintenance costs. Aside from that, it is also a labour and time-intensive effort. Understanding and assessing the genetic diversity of oil palm germplasm is a key pillar for establishing a core collection and crop improvement. According to Frankel *et al*. (1984), a core collection is a small number of accessions that represent the genetic diversity of a crop species and wild relatives with the least amount of repetition. Morphological (Sapey *et al*., 2017), biochemical (Hayati *et al*., 2004), cytological (Castilho *et al*., 2000) and molecular techniques (Zulkifli *et al*., 2012) were employed to gauge germplasm diversity, with morphological traits being commonly evaluated as they are direct, rapid and inexpensive (Suzana *et al*., 2020).

Plant breeders frequently measure a large number of variables, some of which may lack sufficient discriminatory power for germplasm evaluation, characterisation and evaluation (Das *et al*., 2017). In this case, multivariate analysis enables discrimination by eliminating variables that are difficult to measure and contribute little to explaining variation (Arandas *et al*., 2017). Over the years, the use of multivariate analysis in evaluating the genetic diversity of various crops such as tomato (Evgenidis *et al*., 2011), rice (Sohrabi *et al*., 2012), wheat (Ahmad *et al*., 2014), groundnut (Jonah *et al*., 2014), cauliflower (Aleem *et al*., 2021), bean (Girgel, 2021) has increased as they help to explain variations among the genotypes. Among the multivariate tools, principal component analysis (PCA) and cluster analysis (CA) are widely utilised to assess genetic divergence and classify germplasm materials (Li-Hammed *et al*., 2016). PCA is a data reduction technique by transforming the multi-correlated variables into another set of uncorrelated variables for further study, whilst CA is an exploratory data analysis method for grouping accessions based on phenotypic performance and depicts the pattern of relatedness between genotypes (Bhandari *et al*., 2017). In this study, these techniques are adopted to assess the genetic variability in the MPOB-Cameroon oil palm germplasm. Various researches have been conducted on MPOB oil palm germplasm, however, these studies have yet to cover the entire population of MPOB-Cameroon germplasm. The findings from this study may provide important information for oil palm conservation and breeding strategies.

MATERIALS AND METHODS

Planting Materials

A total of 3590 open-pollinated palms collected from 32 sites throughout Cameroon (*Figure 1*) were planted in MPOB Kluang Research Station Johor, Malaysia in 1986. A total of 1800 palms were laid down in two replicates using the Randomised Complete Block Design (RCBD) and named Trial 0.218 while another 1790 palms were grown using Complete Randomised Design (CRD) with two replications planted in Trial 0.219. All populations were planted at both trials. The palms at each site represent populations labelled as CMR (Cameroon) 01-32, hence a total of 32 populations were made. Population CMR 06, however no longer exists in both trials.

Data Collection

A total of 21 quantitative traits were recorded for all accessions and their replications. Yield data collection of individual palms was conducted from

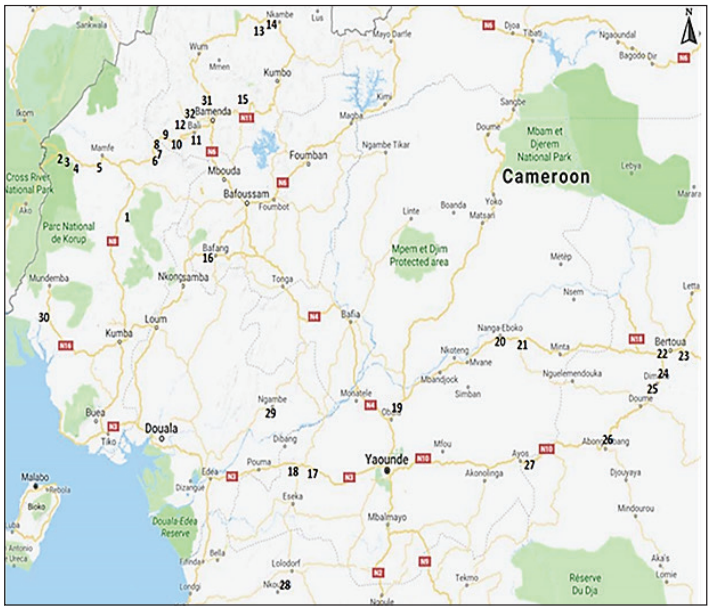

Site No.	Area
1	30 km from Nguti
2	11 km from Eyumojok
3	Near to Site 2
4	16 km from Eyumojok
5	6 km South of Mamfe
6	Kendem - 43 km from Mamfe
7	Mbeme - 50 km from Mamfe
8	Numba - 64 km from Mamfe
9	Widikum
10	Batibo
11	8 km from Bali
12	Teze-Andek
13	Kikangko - 20 km from Miseje
14	Kamine - 16 km from Nkambe
15	Babessie - 40 km North of Ndop
16	12 km from Bafang
17	12 km from Yaounde-Douala Road
18	15 km from Yaounde-Douala Road
19	6 km from Obala-Bertoua Road
20	Nanga Eboko
21	At the junction of Betoua
22	20 km from Bertoua
23	14 km from Bertoua
24	39 km from Betoua
25	Obila
26	13 km from Abang Mbang
27	7 km from Ayos
28	101 km from Ebolowa
29	Ngambe
30	Ndian
31	Bafut - 18 km from Bamenda
32	Mbengwi

Figure 1. Collection sites in Cameroon.

1990 until 1995 (Rajanaidu *et al*., 2017). The traits related to yield were fresh fruit bunch (FFB), bunch number (BNO) and average bunch weight (ABWT). Bunch quality components were evaluated from 1991-1993 by using the bunch analysis method developed by Blaak *et al.* (1963). Twelve bunch traits parameters were measured such as mean fruit weight (MFW), mean nut weight (MNW), mesocarp to fruit (MTF), kernel to fruit (KTF), shell to fruit (STF), oil to dry mesocarp (OTDM), fruit to bunch (FTB), oil to bunch (OTB), kernel to bunch (KTB), oil yield (OY), kernel yield (KY) and total economic product (TEP). Vegetative measurement was carried out in 1995 using a protocol developed by Corley and Breure (1981). Six parameters measured for vegetative traits were frond production (FP), petiole cross-section (PCS), rachis length (RL), height increment (HI), leaf area index (LAI) and bunch index (BI).

Statistical Analysis

A dataset of 31 populations consisting of 2633 *dura* palms was systematically extracted from MPOB Breeding Information System (MPOB-BIS™) (Mohd Din *et al*., 2012) and the population means were calculated using Microsoft Excel version 14.0. The mean data were converted into a new dataset with a mean of zero and a standard deviation of one to remove all biases due to the different scales of variables (Bhandari *et al*., 2017). Correlation, coefficient of variation (CV) and multivariate analyses of PCA and CA were conducted using SAS version 9.4 (SAS Inc). In SAS software, the PRINCOMP procedure was used to execute a PCA, while the PRINQUAL method was applied to perform a multidimensional preference analysis. Average linkage cluster analysis known as the Unweighted Pair-Group Method with Arithmetic average (UPGMA) was employed to construct phylogenetic relationships among the populations from a distance matrix (Sokal and Michener, 1958).

RESULTS AND DISCUSSION

Performance of Yield, Bunch Quality Components and Vegetative Traits

Among the 31 *dura* populations, CMR 19 produced the highest FFB yield (125.99 kg palm^{-1} yr^{-1}) with a CV of 31%, attributed to the high BNO (15.69 bunches palm^{-1} yr^{-1}) and moderate ABWT (8.22 kg palm^{-1} yr^{-1}) (*Figure 2a*). In contrast, CMR 26 produced the lowest FFB yield (75.51 kg palm^{-1} yr^{-1}) due to low BNO (8.22 bunches palm^{-1} yr^{-1}) despite its high ABWT (9.37 kg palm^{-1} yr^{-1}).

On the other hand, even with the highest BNO (16.19 bunches palm^{-1} yr^{-1}), CMR 02 was not among the top FFB yielders due to its low ABWT (7.26 kg palm^{-1} yr^{-1}), which is below the grand mean (8.61 kg palm^{-1} yr^{-1}). These results suggest that high BNO together with moderate ABWT may contribute to high FFB yields as observed by Noh *et al.* (2012). As the selection of high-yielding palms is important for breeding purposes, the selection of CMR palms can be based on high BNO and moderate ABWT as these two traits are associated with high FFB yields. Therefore, CMR 19, CMR 12 and CMR 07 performed the best in terms of FFB, BNO and ABWT with CV values between 21%-35%. A CV of 20%-30% is tolerable for bunch yield traits of perennial crops, such as the oil palm (Hartley, 1988).

For bunch quality traits, population CMR 01 in Western Cameroon had the highest MFW (10.45 g) and MNW (5.93 g) (*Figure 2b*). Similarly, CMR 28 sourced from the South Province of Cameroon showed the same trend, with MFW and MNW values that were not significantly different from CMR 01. KTF varied from 10.93% to 15.47% with a trial mean of 12.55%, meanwhile, KTB ranged from 6.73% to 9.31% with a trial mean of 7.83%. The highest KTF and KTB were observed in CMR 13, with 15.47% and 9.31% respectively (*Figure 2d*). The highest FTB value was also recorded in CMR 01 (70.49%) and the lowest was found in CMR 14 (61.01%) (*Figure 2e*). As an indicator of pollination efficiency, high FTB is necessary to produce high OTB (Myint *et al.*, 2019; Noh *et al.*, 2010). It is interesting to note that the average FTB for MPOB-Cameroon germplasm (65.55%) is comparable with other MPOB-*dura* germplasm collections from Nigeria, Zaire and Angola with the range of 65.39% to 67.85% (Rajanaidu *et al.*, 2017). OY was highest in CMR 03 (*Figure 2f*) due to its high OTB (15.69%) (*Figure 2e*) and MTF (46.80%) (*Figure 2c*), which also contributed to the highest TEP (24.96 kg palm^{-1} yr^{-1}) (*Figure 2f*) observed in this MPOB-Cameroon germplasm.

Vegetative traits can be an important character for the improvement of oil palm. Among the populations, CMR 18 and CMR 14 exhibited the highest FP of 30.49 and 30.41 fronds palm^{-1} yr^{-1} respectively, which have the potential to produce high yields (*Figure 2g*). Besides FP, smaller PCS and shorter RL are favoured characters to increase yield per unit area as they can be planted at higher density (Noh *et al.*, 2010). In this study, the PCS ranged from 12.67 cm^2 to 23.89 cm^2 whereas the RL varied from 4.08 m to 5.17 m. The smallest PCS and shortest RL were observed in populations CMR 13 and CMR 14, respectively (*Figures 2g, 2h*). The mean values of PCS (19.66 cm^2) and RL (4.75 m) of Cameroon *dura* materials were 49.32% and 16.67% respectively, lower than the DxP standard cross. The mean value for HI of this germplasm (24.42 cm yr^{-1}) is comparable to the DxP standard cross (24.46 cm yr^{-1}). With the lowest HI (20.43 cm yr^{-1}) and highest BI (0.46) (*Figures 2g, 2h*), CMR 02 is the best population for future breeding programmes not only for better yields but also in reducing harvesting costs. Among the MPOB germplasm collections, the *dura*s from Cameroon showed a high BI (trial mean of 0.42) in addition to Nigeria, Tanzania and Angola with a value ranging from 0.48 to 0.55 (Rajanaidu *et al.*, 2017). This was corroborated by Fadila *et al.* (2016) with regard to *dura*s from Cameroon.

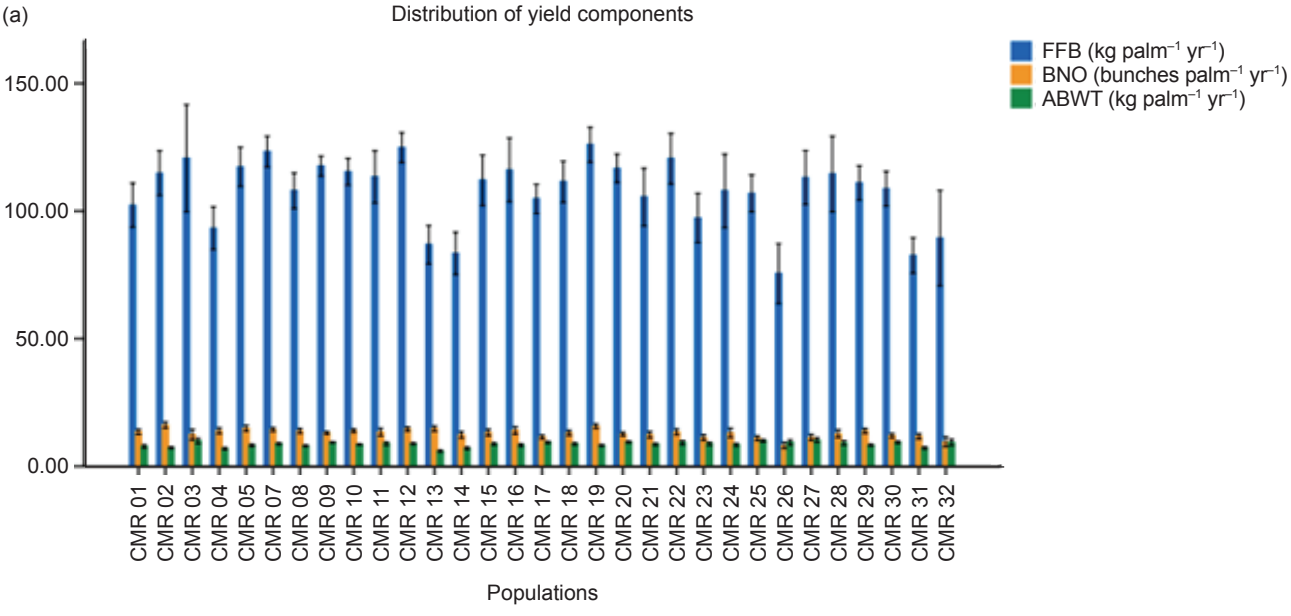

(b) Distribution of bunch quality traits (I)

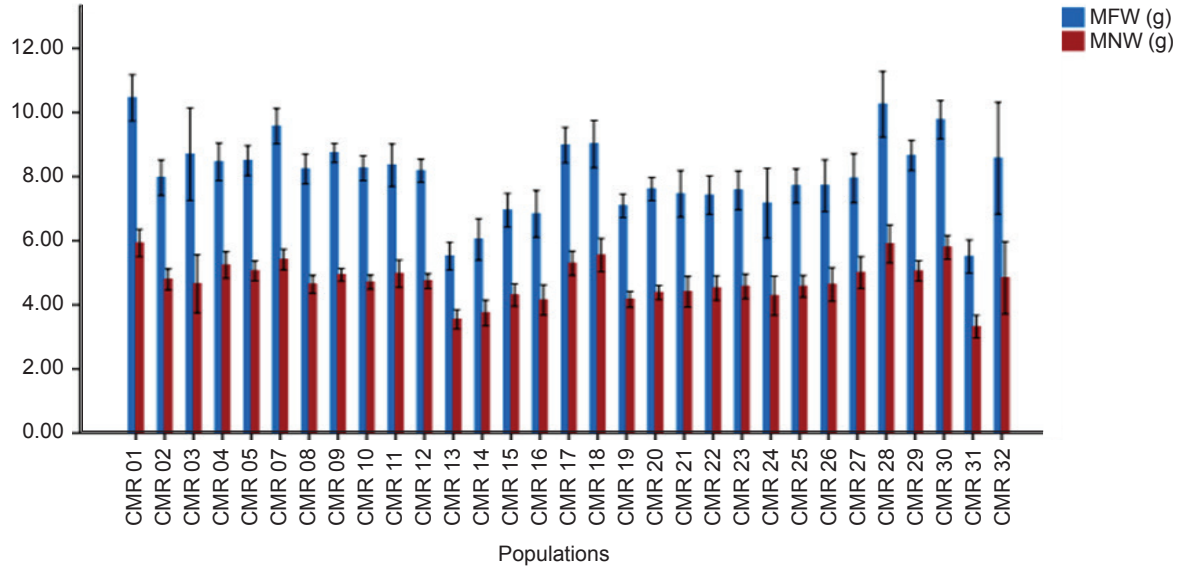

(c) Distribution of bunch quality traits (II)

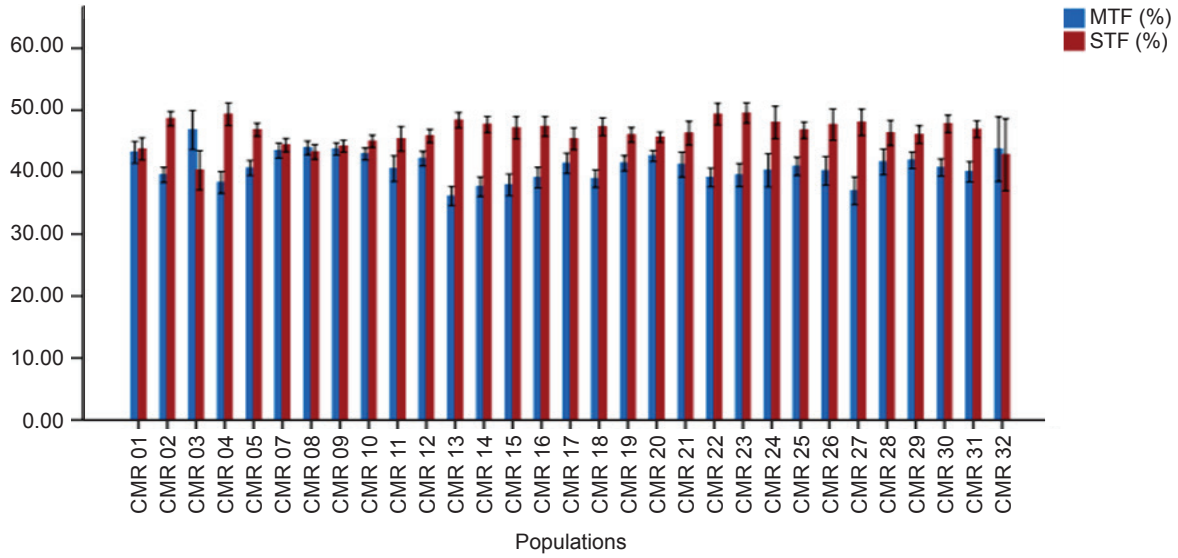

(d) Distribution of bunch quality traits (III)

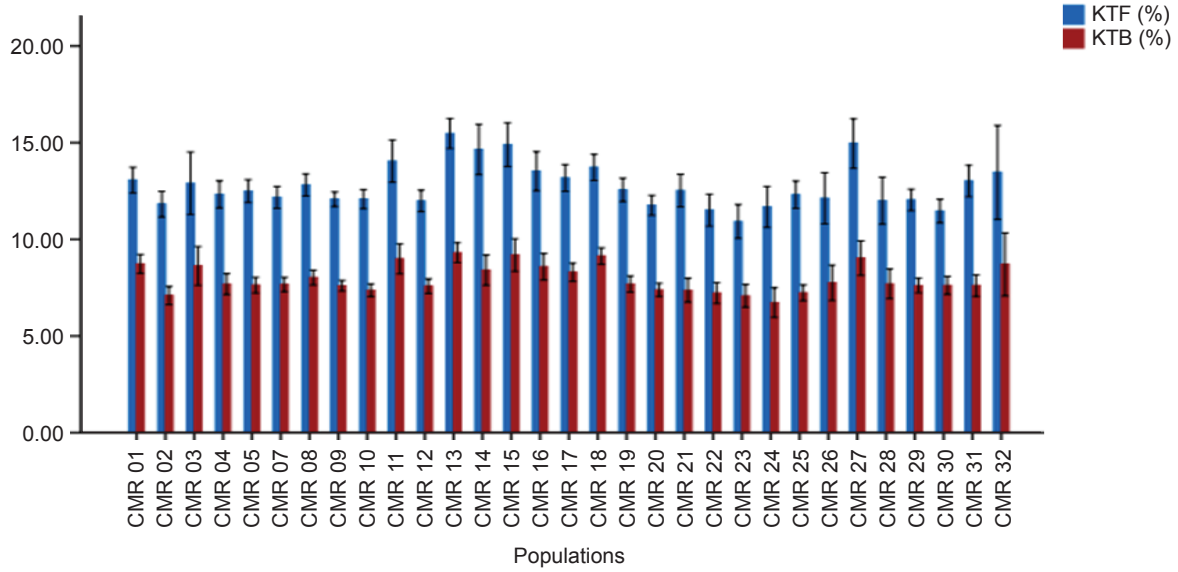

(e) Distribution of bunch quality traits (IV)

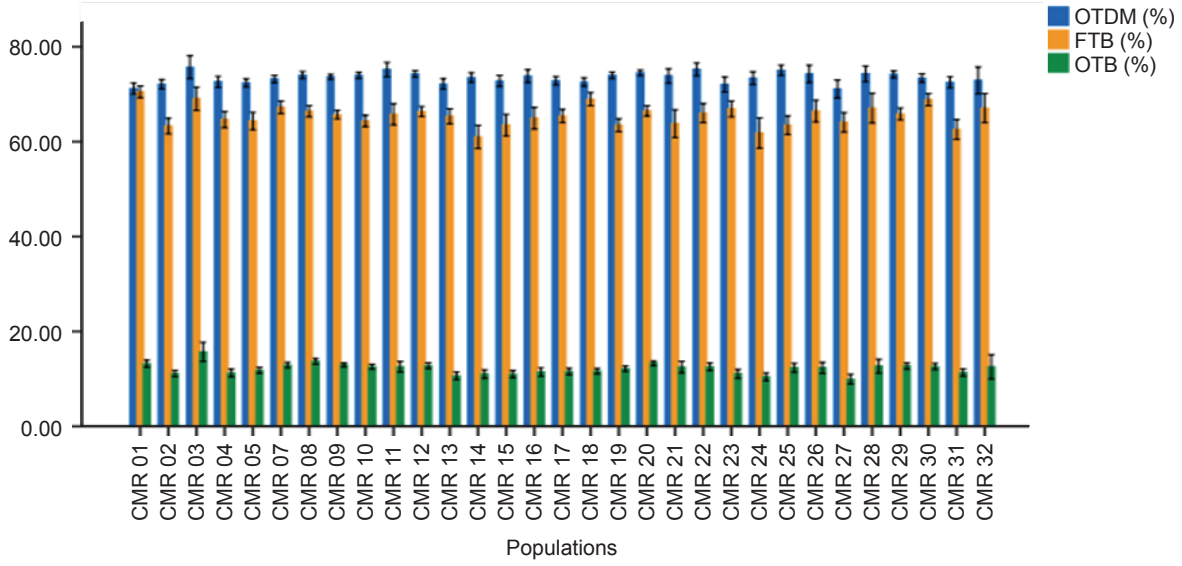

(f) Distribution of bunch quality traits (V)

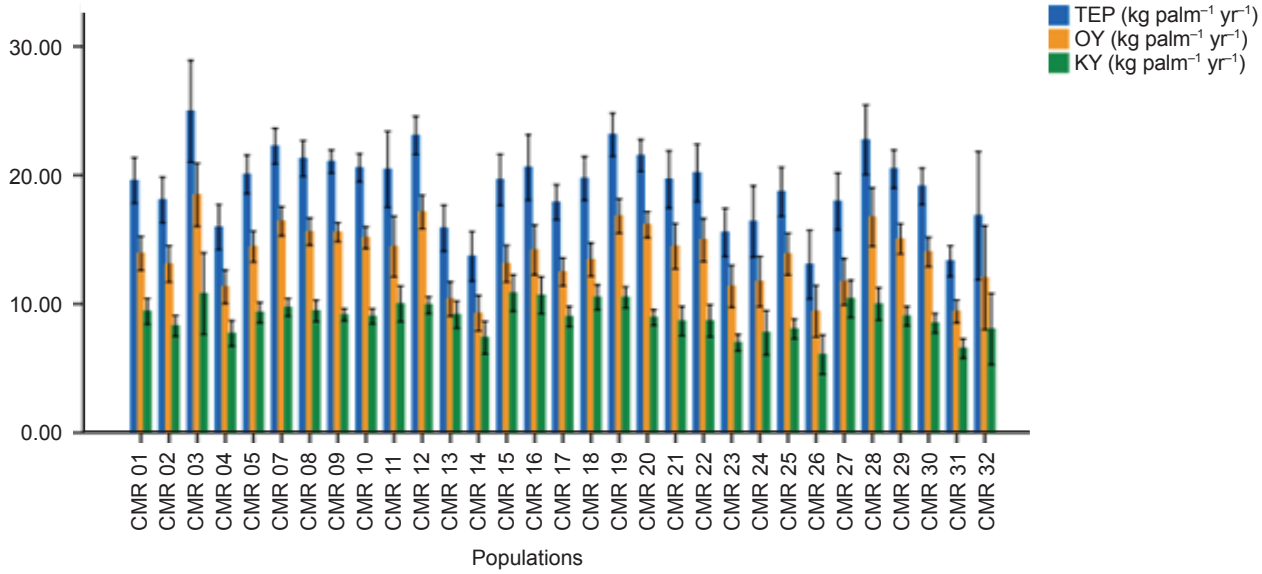

(g) Distribution of vegetative traits (I)

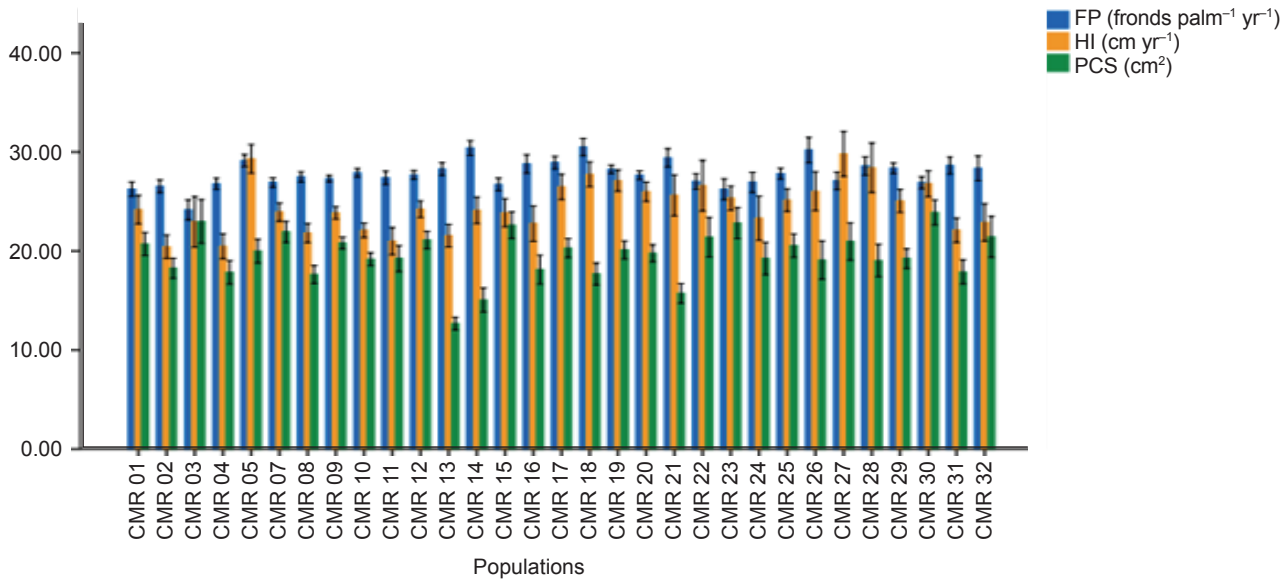

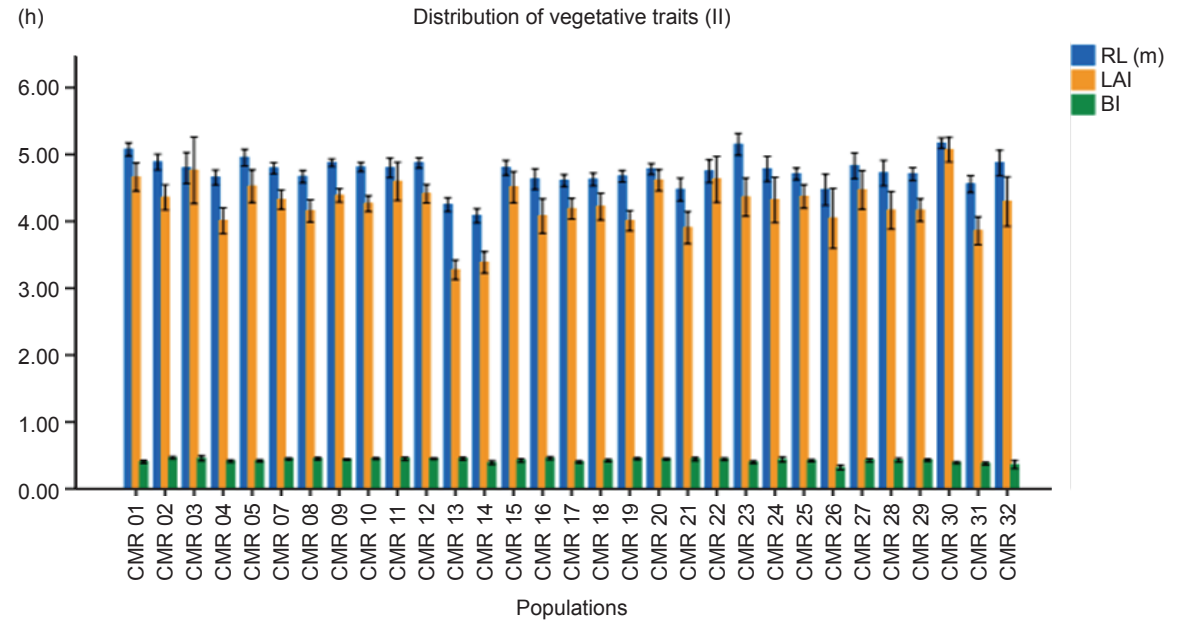

Figure 2. Performance of MPOB-Cameroon dura*s germplasm. (a) Population mean of yield and its component, (b-f) population mean of bunch quality traits and (g-h) population mean of vegetative traits.*

Correlation between Morphological Traits

Correlation analysis was computed to study the relationships between 21 traits among the 31 populations of Cameroon oil palm germplasm (*Table 1*). The correlations between yield-related traits were weak to moderate. FFB was positively correlated to both BNO (r=0.58, $p\leq0.01$) and ABWT (r=0.41, $p\leq0.05$). As expected, BNO was negatively correlated to ABWT (r=-0.50, $p\leq0.01$). This result is in agreement with Suzana *et al*. (2020) who reported a negative correlation between BNO and ABWT as well for MPOB-Tanzania oil palm germplasm (r=-0.42). Okwuagwu *et al*. (2008) showed moderate (r=0.67) to strong (r=0.86) correlation between FFB-BNO while low (r=0.20) correlation between FFB-ABWT in their populations studied. These results indicated that an increase in BNO and ABWT likely corresponds to higher FFB yields. In contrast, BNO and ABWT seemed to be negatively correlated, usually considered antagonistic, as reported in several studies (Corley and Tinker, 2016; Marhalil *et al*., 2013). Henson and Mohd Tayeb (2003) reported that the mean ABWT increased with palm age while reducing the BNO.

The quality of bunches is also important to breeders as this characteristic is highly associated with the quality of palm oil. Strong positive correlations were observed between OY-TEP (r=0.98, $p\leq0.01$) and MFW-MNW (r=0.97, $p\leq0.01$). It is interesting to note that STF is negatively correlated with all bunch analysis traits and the highest correlation was observed between STF and MTF (r=-0.88, $p\leq0.01$). Shi *et al*. (2019) reported that STF was negatively correlated to MTF (r=-0.96) and KTF (r=-0.50). This strong negative relationship between STF and MTF suggests that an increase in shell thickness would associate with a reduced mesocarp content and *vice versa*. While for vegetative traits, the LAI was positively and highly correlated to RL (r=0.86, $p\leq0.01$) and PCS (r=0.85, $p\leq0.01$), whereby both traits are important for palm compactness. A positive significant correlation between PCS-RL (r=0.39) and PCS-LAI (r=0.65) was also observed by Marhalil *et al.* (2013) in the evaluation of elite germplasm of MPOB-Nigerian *dura* × AVROS *pisifera* progenies. The MPOB-Cameroon germplasm thus, showed stronger relationships between LAI and RL, as well as with PCS. An increase in LAI promotes better photosynthetic capability in the crop, thus, enhancing yield production (Noor and Harun, 2004). In addition, FP was negatively correlated with all other vegetative traits except HI (r=0.31, $p>0.05$). Correlation between traits is indispensable for breeders to select vital characters from the studied traits (Sohrabi *et al*., 2012).

PCA Indicating CMR 03 and CMR 13 Potential for Breeding Programme

PCA is a powerful tool for data compression and is capable of providing an overview of complex multivariate data (Bro and Smilde, 2014). PCA's task is to reduce the dimension of the data while retaining most of its original information. The PCA indicated that about 91.89% of the total variation of all studied traits is accounted for from the first six principal components (PCs) with eigenvalues of >1.0 (*Table 2*). As highlighted by Kaiser (1960), PCs with eigenvalues of >1.0 should be retained as it is

TABLE 1. THE CORRELATION COEFFICIENT ANALYSIS OF MPOB-CAMEROON OIL PALM GERMPLASM BETWEEN 21 TRAITS

	Bunch yield			Bunch quality												Vegetative measurement					
	FFB	**BNO**	**ABWT**	**MFW**	**MNW**	**MTF**	**KTF**	**STF**	**OTDM**	**FTB**	**OTB**	**KTB**	**OY**	**KY**	**TEP**	**FP**	**PCS**	**RL**	**HI**	**LAI**	**BI**
FFB	1.00																				
BNO	0.58**	1.00																			
ABWT	0.41*	-0.50**	1.00																		
MFW	0.38*	-0.01^{ns}	0.44**	1.00																	
MNW	0.33^{ns}	-0.01^{ns}	0.39*	0.97**	1.00																
MTF	0.36*	-0.04^{ns}	0.44*	0.54**	0.32^{ns}	1.00															
KTF	-0.27^{ns}	-0.02^{ns}	-0.26^{ns}	-0.36*	-0.29^{ns}	-0.44**	1.00														
STF	-0.26^{ns}	0.06^{ns}	-0.31^{ns}	-0.41*	-0.20^{ns}	-0.88**	-0.05^{ns}	1.00													
OTDM	0.31^{ns}	-0.07^{ns}	0.38*	0.00^{ns}	-0.11^{ns}	0.43*	-0.30^{ns}	-0.31^{ns}	1.00												
FTB	0.17^{ns}	-0.14^{ns}	0.33^{ns}	0.71**	0.66**	0.48**	-0.19^{ns}	-0.43*	0.04^{ns}	1.00											
OTB	0.35*	-0.01^{ns}	0.38*	0.49**	0.30^{ns}	0.88**	-0.35^{ns}	-0.79**	0.62**	0.60**	1.00										
KTB	-0.15^{ns}	-0.08^{ns}	-0.08^{ns}	-0.02^{ns}	0.03^{ns}	-0.22^{ns}	0.89**	-0.24^{ns}	-0.25^{ns}	0.26^{ns}	-0.07^{ns}	1.00									
OY	0.87**	0.44**	0.41*	0.50**	0.37*	0.68**	-0.35*	-0.56**	0.53**	0.40*	0.73**	-0.15^{ns}	1.00								
KY	0.75**	0.49**	0.23^{ns}	0.30^{ns}	0.28^{ns}	0.18^{ns}	0.35*	-0.38*	0.11^{ns}	0.28^{ns}	0.25^{ns}	0.50**	0.68**	1.00							
TEP	0.89**	0.48**	0.39*	0.48**	0.37*	0.60**	-0.19^{ns}	-0.55**	0.45**	0.40*	0.65**	0.01^{ns}	0.98**	0.80**	1.00						
FP	-0.38*	-0.21^{ns}	-0.18^{ns}	-0.25^{ns}	-0.17^{ns}	-0.34^{ns}	0.23^{ns}	0.25^{ns}	-0.03^{ns}	-0.28^{ns}	-0.32^{ns}	0.09^{ns}	-0.37*	-0.22^{ns}	-0.36*	1.00					
PCS	0.44**	-0.21^{ns}	0.71**	0.50**	0.45**	0.43*	-0.41*	-0.26^{ns}	0.11^{ns}	0.41*	0.34^{ns}	-0.15^{ns}	0.40*	0.18^{ns}	0.37*	-0.57**	1.00				
RL	0.46**	0.07^{ns}	0.44**	0.59**	0.57**	0.38*	-0.50**	-0.15^{ns}	-0.16^{ns}	0.47**	0.24^{ns}	-0.24^{ns}	0.39*	0.17^{ns}	0.36*	-0.62**	0.80**	1.00			
HI	0.24^{ns}	-0.24^{ns}	0.53**	0.27^{ns}	0.34^{ns}	-0.10^{ns}	-0.10^{ns}	0.16^{ns}	-0.07^{ns}	0.15^{ns}	-0.07^{ns}	-0.04^{ns}	0.14^{ns}	0.18^{ns}	0.16^{ns}	0.31^{ns}	0.29^{ns}	0.15^{ns}	1.00		
LAI	0.56**	-0.04^{ns}	0.67**	0.60**	0.57**	0.43*	-0.41*	-0.25^{ns}	0.16^{ns}	0.50**	0.43*	-0.14^{ns}	0.50**	0.28^{ns}	0.48**	-0.59**	0.85**	0.86**	0.24^{ns}	1.00	
BI	0.77**	0.77**	-0.06^{ns}	-0.02^{ns}	-0.07^{ns}	0.14^{ns}	-0.01^{ns}	-0.15^{ns}	0.25^{ns}	-0.08^{ns}	0.18^{ns}	-0.06^{ns}	0.66**	0.66**	0.70**	-0.38*	-0.09^{ns}	0.08^{ns}	-0.19^{ns}	0.11^{ns}	1.00

Note: FFB - fresh fruit bunch; BNO - bunch number; ABWT - average bunch weight; MFW - mean fruit weight; MNW - mean nut weight; MTF - mesocarp to fruit ratio; KTF - kernel to fruit; STF - shell to fruit ratio; OTDM - oil to dry mesocarp ratio; FTB - fruit to bunch ratio; OTB - oil to bunch ratio; KTB - kernel to bunch ratio; OY - oil yield; KY - kernel yield; TEP - total economic product; FP - frond production; PCS - petiole cross section; RL - rachis length; HI - height increment; LAI - leaf area index; BI - bunch index.

*, **, and ns indicate significant at $p \leq 0.05$, $p \leq 0.01$ and not significant, respectively.

one of the criteria for principal component selection, also known as Kaiser's criterion or eigenvalue-one criterion. Sujadi *et al*. (2019) also reported six PCs with eigenvalues >1.0, which however only explained a total variation of 73.81% among the 47 accessions of oil palm germplasm introduced from Cameroon that were planted in Indonesia. The greatest eigenvalue (8.05) accounted for 38.35% of the total variation contributed by PC1 followed by PC2 (3.54) with 16.86% of the total variation. PC3 with an eigenvalue of 2.41 accounted for 11.47% of the total variation while the eigenvalue of PC4 is 2.30 with 10.96% of the total variation. The subsequent decreasing eigenvalue of PC5 (1.67) and PC6 (1.32) represent 7.97% and 6.29% of total variation among the 31 populations tested, respectively.

The highest variance (PC1) was largely associated with bunch traits including OY (0.313) and TEP (0.303). This PC showed positive effect for all variables studied except for STF (-0.210), FP (-0.190), KTF (-0.155) and KTB (-0.044). PC2 had large positive associations with BI (0.436), BNO (0.412) and KY (0.319) but displayed negative associations with PCS (-0.246), ABWT (-0.225), MNW (-0.199) and RL (-0.199). PC3 is related to the high KTB (0.588) and KTF (0.480). As for PC4, it is characterised by high STF (0.423) with low OTB (-0.398), OTDM (-0.354) and MTF (-0.349). The traits that contribute greatly to PC5 were HI (0.570) and FP (0.434). PC6 has large positive associations with MNW (0.404), FP (0.383) and MFW (0.379) but negative associations with PCS (-0.350) and ABWT (-0.314).

From the score plot between PC1 and PC2, four groups were obtained based on the morphological data of MPOB-Cameroon germplasm (*Figure 3*). Group 1 is the largest group comprising 26 populations positioned at the centre of the plane in the plot, suggesting that they represent the average performance of the variables studied. Populations that are closer to each other have similar values for the respective variables, whereas those far from one another have quite different values (Saleh *et al*., 2018). Group 2, represented by population CMR 03, is distinct and most positive towards PC1 since

TABLE 2. CONTRIBUTIONS OF 21 VARIABLES TO PC1-PC6 IN MPOB-CAMEROON OIL PALM GERMPLASM

Field evaluation	Trait	PC1	PC2	PC3	PC4	PC5	PC6
Bunch yield	FFB	0.272	0.236	-0.060	0.226	0.187	-0.039
	BNO	0.064	0.412	-0.100	0.273	-0.164	0.244
	ABWT	0.218	-0.225	0.055	-0.042	0.375	-0.314
Bunch quality	MFW	0.260	-0.180	0.172	0.047	-0.085	0.379
	MNW	0.217	-0.199	0.218	0.156	-0.045	0.404
	MTF	0.264	-0.034	-0.107	-0.349	-0.128	0.075
	KTF	-0.155	0.197	0.480	-0.064	-0.016	-0.249
	STF	-0.210	-0.068	-0.140	0.423	0.151	0.051
	OTDM	0.134	0.101	-0.256	-0.354	0.300	-0.128
	FTB	0.219	-0.157	0.256	-0.100	-0.182	0.206
	OTB	0.262	0.015	-0.055	-0.398	-0.062	0.069
	KTB	-0.044	0.118	0.588	-0.094	-0.090	-0.183
	OY	0.313	0.205	-0.066	-0.047	0.121	0.081
	KY	0.195	0.319	0.326	0.113	0.120	-0.078
	TEP	0.303	0.247	0.029	-0.009	0.129	0.045
Vegetative measurement	FP	-0.190	-0.020	0.107	-0.141	0.434	0.383
	PCS	0.246	-0.246	-0.017	0.144	-0.016	-0.350
	RL	0.241	-0.199	-0.047	0.301	-0.228	-0.106
	HI	0.069	-0.175	0.165	0.192	0.570	0.111
	LAI	0.279	-0.179	-0.005	0.184	-0.050	-0.237
	BI	0.141	0.436	-0.111	0.151	0.002	-0.039
Eigenvalue		8.05	3.54	2.41	2.30	1.67	1.32
Variance (%)		38.35	16.86	11.47	10.96	7.97	6.29
Cumulative variance (%)		38.35	55.20	66.67	77.63	85.60	91.89

Note: FFB - fresh fruit bunch; BNO - bunch number; ABWT - average bunch weight; MFW - mean fruit weight; MNW - mean nut weight; MTF - mesocarp to fruit ratio; KTF - kernel to fruit; STF - shell to fruit ratio; OTDM - oil to dry mesocarp ratio; FTB - fruit to bunch ratio; OTB - oil to bunch ratio; KTB - kernel to bunch ratio; OY - oil yield; KY - kernel yield; TEP - total economic product; FP - frond production; PCS - petiole cross section; RL - rachis length; HI - height increment; LAI - leaf area index; BI - bunch index.

they performed well in variables which exhibited the highest positive loading in PC1 such as OY (18.48 kg palm^{-1} yr^{-1}), TEP (24.96 kg palm^{-1} yr^{-1}) and FFB (120.71 kg palm^{-1} yr^{-1}). Other traits such as MTF (46.80%), OTDM (75.68%), OTB (15.69%) and KY (10.80 kg palm^{-1} yr^{-1}) were also promising in population CMR 03.

Population CMR 13 in Group 3 showed the most positive along PC2 and the most negative toward PC1. This might be due to the good performance in PCS (12.67 cm^2), RL (4.25 m) and BI (0.45). While having the best performance in some vegetative traits, CMR 13 had the highest KTB (9.31%) and KTF (15.47%), with the lowest LAI (3.27), MTF (36.14%) and ABWT (5.96 kg palm^{-1} yr^{-1}), as well as low FFB (86.83 kg palm^{-1} yr^{-1}) caused CMR 13 to be distinctly placed from other populations. The poor performance of some variables related to PC1 has caused CMR 14 and CMR 31 grouped in Group 4. Both populations have the lowest OY (9.27 kg palm^{-1} yr^{-1} and 9.43 kg palm^{-1} yr^{-1}), TEP (13.71 kg palm^{-1} yr^{-1} and 13.34 kg palm^{-1} yr^{-1}), and among the lowest LAI (3.39 and 3.86) and FFB (83.40 kg palm^{-1} yr^{-1} and 82.60 kg palm^{-1} yr^{-1}). Population CMR 14 was slightly positive towards PC2 because the RL was shorter (4.08 m) than the rest, while the CMR 31 was slightly negative towards PC2 due to the lowest MNW (3.32 g) and MFW (5.50 g).

A PCA biplot was constructed from multidimensional preference analysis to study the inter-relationship between the populations and variables, and to identify the best variables contributing to the population. The variables on the right quadrant such as TEP, OY, LAI, FFB, OTB and MTF were correlated to PC1, however, variables in the left quadrant, *i.e.*, KTB, KTF, FP and STF, were anti-correlated to PC1 (*Figure 4*). Among others, the most important variables that contributed positively to PC2 were BNO, BI, and KY, while PCS, ABWT, MNW and RL negatively contributed to PC2. *Figure 4* clearly shows that PC1 is negatively influenced by KTB, KTF, FP and STF; however, there was a low correlation between KTF and KTB with FP and STF. Variables that are closer to one another indicate positive associations between them. Thus, the increased value of OY is important to entail a high TEP value. CMR 03 and CMR 13 are distinctly located in quadrants 1 and 2 of the plot, respectively, suggesting that CMR 03 could be selected as a potential population for breeding programmes as it has good characters in bunch quality components and vegetative measurements such as OTDM, OTB, OY, TEP, FTB, KY and BI. Population CMR 13 could be further exploited for breeding for non-edible purposes due to the best characteristics in KTB and KTF, which suggests potential for increasing the yield of palm kernel oil.

Highly Diverse Populations Should be Prioritised in Conservation Programme

The average linkage cluster analysis classified the materials depending on the environment or correlation of the individuals as suggested by Granato *et al.* (2018). The result from CA is slightly

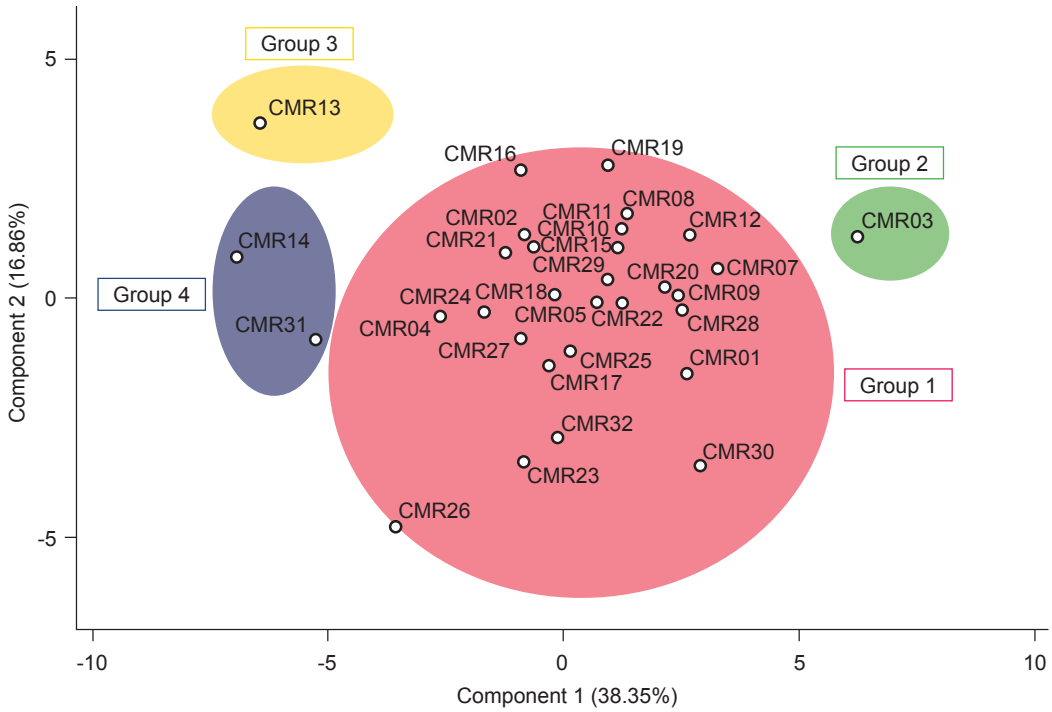

Figure 3. Scores plot of MPOB-Cameroon oil palm germplasm.

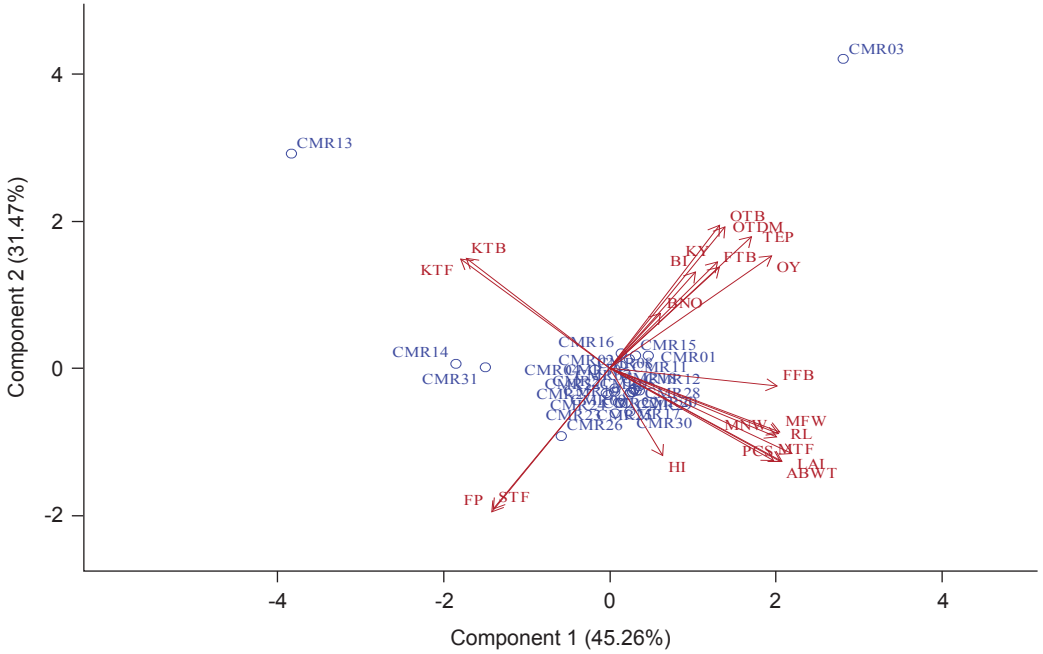

Figure 4. PCA biplot of 21 morphological traits and 31 populations of MPOB-Cameroon oil palm germplasm.

different from PCA as CA groups observations while PCA groups variables rather than observations. Based on the result, it showed that 31 populations of MPOB-Cameroon oil palm germplasm can be grouped into three major clusters with the highest Pseudo F-value of 6.3 (*Figure 5*). All three clusters have two sub-clusters each. Cluster I consist of seven populations with the first sub-cluster containing CMR 30, CMR 23 and CMR 01 joined together with the second sub-cluster which has four populations namely, CMR 18, CMR 26, CMR 32 and CMR 17. Cluster II consists of 11 populations which are CMR 03, CMR 08, CMR 07, CMR 09, CMR 10, CMR 12, CMR 28 and CMR 29 grouped in the first sub-cluster at the distance of 0.81 while CMR 20, CMR 22 and CMR 25 were grouped in second sub-cluster at the distance of 0.65. Cluster III had the largest group, consisting of 13 populations (41.9% of the entire germplasm populations studied). Four populations were grouped in the first sub-cluster at the distance of 0.88 which are CMR 02, CMR 04, CMR 24 and CMR 05, while the remaining populations were clustered together in the second sub-cluster at the distance of 0.96.

Based on *Figure 5*, among the MPOB-Cameroon oil palm germplasm materials, paired populations of CMR 16 and CMR 30 were found extremely diverse, while paired populations of CMR 07 and CMR 09 exhibited the closest relationship. According to Odewale *et al.* (2012), priority should be given to the use of populations with a high genetic distance between them, whilst avoiding those with less genetic distance. This study suggested that the clustering pattern of the MPOB-Cameroon populations did not depend on their geographical locations, as the populations from different locations were randomly distributed into various clusters. This might be due to the high rate of genetic exchange through seed dispersal (Arias *et al.*, 2013). This finding conforms with the results from other studies on the genetic variability of Nigeria and Sierra Leone oil palm germplasm (Li-Hammed *et al.*, 2016; Suzana *et al.*, 2016). On the other hand, a strong relationship between genetic distance and geographical location has been reported during the evaluation of MPOB-oil palm germplasm (Hayati *et al.*, 2004; Zulkifli *et al.*, 2012).

Based on trait-specific clustering (*Table 3*), Cluster II showed the best performance in yield related traits with the highest mean of FFB and ABWT supplemented with high BNO. On the contrary, Cluster I had the lowest FFB contributed by the low BNO, despite their moderate ABWT which placed most of the populations in quadrant 3 and 4 of the score plot (*Figure 3*). The highest BNO of Cluster III would not result in the highest FFB due to the lowest ABWT. In terms of bunch traits, Cluster II was found to have the highest cluster mean of OY owing to its highest MTF, OTDM and OTB, in addition to the lowest STF. On a similar note, Cluster II was also highest in KY and TEP while the lowest cluster mean was found in Cluster 1. For vegetative traits, Cluster I had the highest mean cluster for all vegetative characters except BI. In conjunction with high FP and BI, Cluster III showed better performance with minimum mean clusters for PCS, RL and HI. Meanwhile, Cluster II showed a moderate mean of all vegetative traits except for the highest BI and lowest FP.

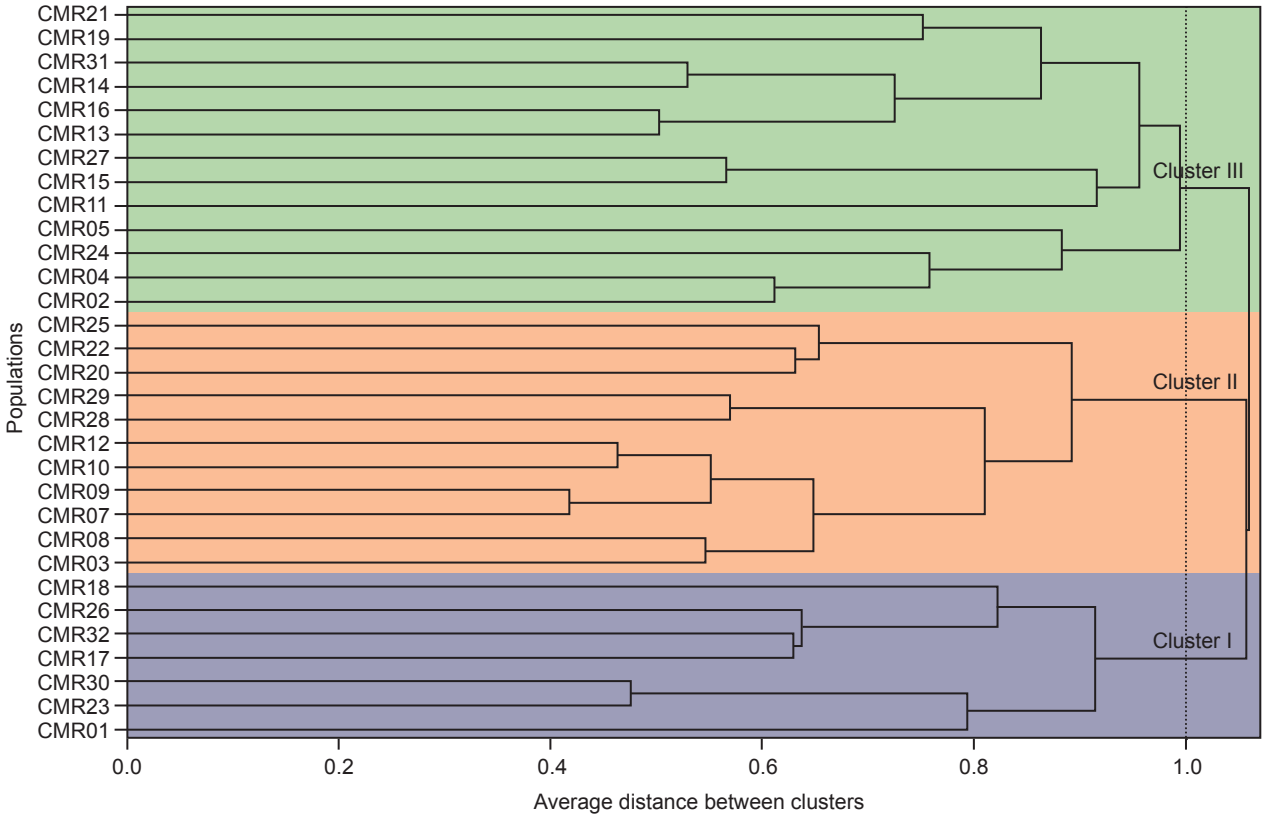

Figure 5. Dendrogram of 31 MPOB-Cameroon germplasm populations based on 21 morphological traits.

High genetic variability was identified in MPOB-Cameroon oil palm germplasm, which was corroborated by Zulkifli *et al*. (2012), who revealed a high level of polymorphism (100%) in the Cameroon germplasm material through molecular markers (EST-SSRs) which could be exploited for oil palm improvement programmes. The germplasm from Cameroon also had the highest heterozygosity, implying that these materials represent a rich source of genes and may possess unique genes associated with traits which may not be found in the current oil palm planting materials. Morphological data in conjunction with molecular data could be very useful for the effective characterisation and utilisation of MPOB-Cameroon oil palm germplasm. Apart from the exploitation for the improvement of planting materials, stratification using multivariate analysis is one of the approaches that can be used to establish a good core collection (van Hintum *et al*., 2000). Creating a core collection is a cost-effective way to improve the conservation strategy, characterisation and utilisation of genetic resources. A core collection can reflect the entire genetic diversity of a large collection with a limited number of accessions as suggested by Brown (1995).

From cluster analysis, the number of palms or families or populations in the same cluster could be reduced as they possess genetic similarities for future regeneration and conservation purposes. Selection and conservation should be taken into account for those traits that contribute to a higher variation in the MPOB-Cameroon oil palm germplasm. Based on this study, the most distant populations, namely CMR 16 and CMR 30 from different clusters are having a higher genetic difference, and populations with unique characteristics, *i.e*., CMR 03 and CMR 13, are recommended for inclusion in the conservation programme for future breeding utilisation.

CONCLUSION

This study compared 21 parameters of yield, bunch quality components and vegetative measurement, and identified high genetic variability in Cameroon oil palm germplasm. It can be concluded from this study that multivariate analysis successfully characterised the MPOB-Cameroon oil palm germplasm populations based on the phenotypic characters. Principal component analysis was able to identify some traits that play an important role in classifying the variation in this germplasm that can be used for oil palm improvement and conservation. The results of the principal component analysis are not in agreement with cluster analysis. Cluster analysis successfully grouped the populations into three major clusters and revealed that there was no relationship between the geographical origin of the

TABLE 3. CLUSTER GROUPS AND QUANTITATIVE TRAITS MEANS

Field evaluation	Trait	Unit	Cluster		
			I	II	III
Bunch yield	FFB	kg palm^{-1} yr^{-1}	98.5	116.32	105.56
	BNO	bunches palm^{-1} yr^{-1}	11.31	13.29	13.63
	ABWT	kg palm^{-1} yr^{-1}	8.99	9.08	8.01
Bunch quality	MFW	g	8.87	8.49	7.22
	MNW	g	5.23	4.87	4.38
	MTF	%	41.11	42.66	39.23
	KTF	%	12.56	12.15	13.38
	STF	%	46.33	45.19	47.39
	OTDM	%	72.74	74.37	73.03
	FTB	%	67.73	66.18	63.73
	OTB	%	12.13	13.1	11.32
	KTB	%	8.19	7.64	8.1
	OY	kg palm^{-1} yr^{-1}	12.39	15.92	12.66
	KY	kg palm^{-1} yr^{-1}	8.37	9.35	9.02
	TEP	kg palm^{-1} yr^{-1}	17.41	21.53	18.07
Vegetative measurement	FP	fronds palm^{-1} yr^{-1}	28.19	27.35	28.03
	PCS	cm^2	20.85	20.33	18.28
	RL	m	4.85	4.77	4.64
	HI	cm yr^{-1}	25.64	24.55	23.96
	LAI	-	4.41	4.39	4.1
	BI	-	0.38	0.44	0.43

Note: FFB - fresh fruit bunch (kg palm^{-1} yr^{-1}); BNO - bunch number (bunches palm^{-1} yr^{-1}); ABWT - average bunch weight (kg palm^{-1} yr^{-1}); MFW - mean fruit weight (g); MNW - mean nut weight (g); MTF - mesocarp to fruit ratio (%); KTF - kernel to fruit (%); STF - shell to fruit ratio (%); OTDM - oil to dry mesocarp ratio (%); FTB - fruit to bunch ratio (%); OTB - oil to bunch ratio (%); KTB - kernel to bunch ratio (%); OY - oil yield (kg palm^{-1} yr^{-1}); KY - kernel yield (kg palm^{-1} yr^{-1}); TEP - total economic product (kg palm^{-1} yr^{-1}); FP - frond production (fronds palm^{-1} yr^{-1}); PCS - petiole cross section (cm^2); RL - rachis length (m); HI - height increment (cm yr^{-1}); LAI - leaf area index; BI - bunch index.

31 populations and their clustering patterns. This finding should be further verified with a molecular-based diversity study to efficiently exploit the collected germplasm materials and improve the conservation strategies to a manageable level towards a sustainable future for the oil palm sector.

ACKNOWLEDGEMENT

The authors wish to express their sincere thanks to the Director-General of MPOB for permission to present this article.

REFERENCES

Aleem, S; Tahir, M; Sharif, I; Aleem, M; Najeebullah, M; Nawaz, A; Batool, A; Khan, M I and Arshad, W (2021). Principal component and cluster analyses as a tool in the assessment of genetic diversity for late season cauliflower genotypes. *Pakistan J. Agri. Res., 34(1)*: 176-183.

Arandas, J K G; da Silva, N M V; Nascimento, R D B; Pimenta Filho, E C; Albuquerque Brasil, L H D and Ribeiro, M N (2017). Multivariate analysis as a tool for phenotypic characterization of an endangered breed. *J. Appl. Anim. Res., 45(1)*: 152-158.

Arias, D; Montoya, C and Romero, H (2013). Molecular characterization of oil palm *Elaeis guineensis* Jacq. materials from Cameroon. *Plant Genet. Resour., 11(2)*: 140-148.

Ahmad, H M; Awan, S I; Aziz, O and Ali, M A (2014). Multivariative analysis of some metric traits in bread wheat (*Triticum aestivum* L.). *European J. Biotechnol. Biosci., 1(4)*: 22-26.

Bakoumé, C; Wickneswari, R; Siju, S; Rajanaidu, N; Kushairi, A and Billotte, N (2015). Genetic diversity of the world's largest oil palm (*Elaeis guineensis* Jacq.) field genebank accessions using microsatellite markers. *Genet. Resour. Crop Evol. 62(3)*: 349-360.

Bhandari, H R; Bhanu, A N; Srivastava, K; Singh, M N and Shreya, H A (2017). Assessment of genetic diversity in crop plants-an overview. *Adv. Plants Agric. Res., 7(3)*: 279-286.

Blaak, G; Sparnaaij, L D and Menendez, T (1963). Breeding and inheritance in oil palm (*Elaeis guineensis* Jacq.). Part II. Methods of bunch quality analysis. *JW Afric. Inst. Oil Palm Res., 4*: 146-155.

Bro, R and Smilde, A K (2014). Principal component analysis. *Anal. Methods, 6(9)*: 2812-2831.

Brown, A H D (1995). The core collection at the crossroads. *Core Collections of Plant Genetic Resources* (Hodgkin, T; Brown, A H; Van Hintum, T J and Morales, E A V eds.). John Wiley and Sons, United Kingdom. p. 3-19.

Castilho, A; Vershinin, A and Heslop-Harrison, J S (2000). Repetitive DNA and the chromosomes in the genome of oil palm (*Elaeis guineensis*). *Ann. Bot., 85(6)*: 837-844.

Corley, R H V and Breure, C J (1981). *Measurements in Oil Palm Experiments*. Internal Report. Unilever Plantations Group, London. 21 pp.

Corley, R H V and Tinker, P B (2016). *The Oil Palm.* 5th edition. Wiley Blackwell, United Kingdom. 639 pp.

Das, S; Das, S S; Chakraborty, I; Roy, N; Nath, M K and Sarma, D (2017). Principal component analysis in plant breeding. *Biomol. Rep., 3*. p. 1-3.

Evgenidis, G; Traka-Mavrona, E and Koutsika-Sotiriou, M (2011). Principal component and cluster analysis as a tool in the assessment of tomato hybrids and cultivars. *Int. J. Agron., 6 (23)*: 334-339.

Fadila, A M; Norziha, A; Mohd, D; Rajanaidu, N and Kushairi, A (2016). Evaluation of bunch index in MPOB oil palm (*Elaeis guineensis* Jacq.) germplasm collection. *J. Oil Palm Res., 28(4)*: 442-451.

Frankel, O H; Arber, W; Llimensee, K; Peacock, W J and Starlinger, P (1984). Genetic perspectives of germplasm conservation. *Genetic Manipulation: Impact on Man and Society* (Arber, W K *et al*., eds.). Cambridge University Press. p. 161-170.

Girgel, U (2021). Principle component analysis (PCA) of bean genotypes (*Phaseolus vulgaris* L.) concerning agronomic, morphological and biochemical characteristics. *Appl. Eco. Environ. Res., 19(3)*: 1999-2011.

Granato, D; Santos, J S; Escher, G B; Ferreira, B L and Maggio, R M (2018). Use of principal 483 component analysis (PCA) and hierarchical cluster analysis (HCA) for multivariate association 484 between bioactive compounds and functional properties in foods: A critical perspective. Trends 485 in *Food Sci. Tech*., 72: 83-90. DOI: 10.1016/j.tifs.2017.12.006.

Hartley, C W S (1988). *The Oil Palm.* 3rd edition. Essex: Longman Scientific and Technical, London. 761 pp.

Hayati, A; Wickneswari, R; Maizura, I and Rajanaidu, N (2004). Genetic diversity of oil palm (*Elaeis guineensis* Jacq.) germplasm collections from Africa: Implications for improvement and conservation of genetic resources. *Theor. Appl. Genetic. 108(7)*: 1274-1284.

Henson, I and Mohd Tayeb, D (2003). Physiological analysis of an oil palm density trial on a peat soil. *J. Oil Palm Res., 15(2)*: 1-27.

Jonah, P M; Abimiku, O E and Adeniji, O T (2014). Multivariate analysis and character association on the growth and yield of bambara groundnut in Mubi, Adanawa state, Nigeria. *Int. J. Manag. Soc. Sci. Res., 3(2)*: 58-65.

Kaiser, H F (1960). The application of electronic computers to factor analysis. *Educ. Psychol. Meas., 20(1)*: 141-151.

Li-Hammed, M A; Kushairi, A; Rajanaidu, N; Mohd Sukri, H; Che Wan Zanariah, C W N and Jalani, B S (2016). Genetic variability for yield, yield components and fatty acid traits in oil palm (*Elaeis guineensis* Jacq.) germplasm using multivariate tools. *Int. J. Agric. For. Plant*., 2: 219-226.

Malaysian Palm Oil Board (2020). *Overview of the Malaysian palm oil industry 2019.* http://bepi.mpob.gov.my/images/overview/Overview_of_Industry_2019.pdf.

Marhalil, M; Rafii, M Y; Afizi, M M A; Arolu, I W; Noh, A; Mohd Din, A; Kushairi, A; Norziha, A; Rajanaidu, N; Latif, M A and Malek, M A (2013). Genetic variability in yield and vegetative traits in elite germplasm of MPOB-Nigerian *dura* x AVROS *pisifera* progenies. *J. Food Agric. Environ., 11(2)*: 515-519.

Mohd Din, A; Rajanaidu, N; Kushairi, A; Marhalil, M and Zaharah, R (2012). MPOB Breeding Information System (MPOB-BIS). *MPOB Information Series No., 512*.

Myint, K A; Amiruddin, M D; Rafii, M Y; Samad, M Y A; Ramlee, S I; Yaakub, Z and Oladosu, Y (2019). Genetic diversity and selection criteria of MPOB-

Senegal oil palm (*Elaeis guineensis* Jacq.) germplasm by quantitative traits. *Ind. Crops Prod. 139(4)*: 111558.

Noh, A; Rafii, M Y; Saleh, G and Kushairi, A (2010). Genetic performance of 40 Deli *dura* x AVROS *pisifera* full-sib families. *J. Oil Palm Res.*, *22*: 781-795.

Noh, A; Rafii, M Y; Saleh, G; Kushairi, A and Latif, M A (2012). Genetic performance and general combining ability of oil palm Deli *dura* x AVROS *pisifera* tested on inland soils. *Sci., World J. 12(1)*: 1-10.

Noor, M R M and Harun, M H (2004). The role of leaf area index (LAI) in oil palm. *Oil Palm Bulletin*. MPOB, Bangi. p. 11-16.

Odewale, J O; Collous, A; Ataga, C D; Aisueni, N O; Ikuenode, C E; Okoye, M N; Odiowaya, G; Edokpayi, A A; Ahanor, M J and Uwadiue, E O (2012). Pattern of genetic diversity and variability in germplasm resources of local and exotic coconut (*Cocos nucifere* L.) cultivars in Nigeria. *J. Agric. Sci. 2(9)*: 202-207.

OECD/Food and Agriculture Organization of the United Nations (2019). 'Oilseeds and oilseed products'. OECD-FAO Agricultural Outlook 2019-2028. OECD Publishing, Paris/Food and Agriculture Organization of the United Nations, Rome. DOI: 10.1787/5f037977-en.

Okwuagwu, C O; Okoye, M N; Okolo, E C; Ataga, C D and Uguru, M I (2008). Genetic variability of fresh fruit bunch yield in Deli/*dura* x *tenera* breeding populations of oil palm (*Elaeis guineensis* Jacq.) in Nigeria. *J. Trop. Agric., 46(1-2)*: 40-45.

Rajanaidu, N (1986). The oil palm (*Elaeis guineensis*) collections in Africa. *Proc. of the International Workshop on Oil Palm Germplasm and Utilisation.* PORIM, Bangi. p. 59-83.

Rajanaidu, N (1994). MPOB oil palm genebank: Collection, evaluation, utilization and conservation of oil palm genetic resources. PORIM, Bangi. 18 pp.

Rajanaidu, N; Ainul, M M; Kushairi, A and Mohd Din, A (2013). Historical review of oil palm breeding for the past 50 years - Malaysian journey. *Proc. of the International Seminar on Oil Palm Breeding - Yesterday, Today and Tomorrow.* Kuala Lumpur, Malaysia. p. 11-28.

Rajanaidu, N; Kushairi, A and Mohd Din, A (2017). *Monograph Oil Palm Genetic Resources*. MPOB, Bangi. 98 pp.

Saleh, H; Li-Hammed, M A; Kushairi, A; Rajanaidu, N; Hassan, M S; Che Wan Ngah, C W Z and Sukaimi, J (2018). Evaluation of oil palm germplasm from Senegal and Gambia using chemometric techniques. *Malays. J. MJoSHT*. *1(1)*: 10-20.

Sapey, E; Adusei-Fosu, K; Darkwah, D O and Agyei-Dwarko, D (2017). Multivariate analysis of bunch yield and vegetative traits of oil palm germplasm conserved at Oil Palm Research Institute (OPRI), Ghana. *Int. J. Plant Breed. Crop. Sci., 4(2)*: 231-236.

Shi, P; Wang, Y; Zhang, D; Htwe, Y M and Ihase, L O (2019). Analysis on fruit oil content and evaluation on germplasm in oil palm. *HortScience, 54(8)*: 1275-1279.

Sohrabi, M; Rafii, M Y; Hanafi, M M; Siti Nor Akmar, A and Latif, M A (2012). Genetic diversity of upland rice germplasm in Malaysia based on quantitative traits. *Sci. World J., 2012*: 1-9. DOI: 10.1100/2012/416291.

Sokal, R R and Michener, C D (1958). A statistical method for evaluating systematic relationships. *Kansas University Science Bulletin*, *38*: 1409-1438.

Sujadi, S; Wandita, T S; Supena, N and Yenni, Y (2019). Genetic distance of 47 accessions of oil palm (*Elaeis guineensis* Jacq.) germplasm from Cameroon based on morphological character. *J. Pen. Kelapa Sawit*, *27(1)*: 25-40.

Suzana, M; Zulkifli,Y; Marhalil, M; Rajanaidu, N and Mohd Din, A (2016). Principal component and cluster analysis as a tool in the assessment of genetic variability of Sierra Leone germplasm populations. *Transactions of Persatuan Genetik Malaysia*, *3*: 213-216.

Suzana, M; Zulkifli, Y; Marhalil, M; Rajanaidu, N and Ong-Abdullah, M (2020). Principal component and cluster analyses on Tanzania oil palm *Elaeis guineensis* Jacq. germplasm. *J. Oil Palm Res., 32(1)*: 24-33.

van Hintum, Th J L; Brown, A H D; Spillane, C and Hodgkin, T (2000). Core collections of plant genetic resources. *IPGRI Technical Bulletin No. 3*. International Plant Genetic Resources Institute. Rome. 48 pp.

Verheye, W (2010). Growth and production of oil palm. *Land Use, Land Cover and Soil Sciences* (Verheye, W ed.). Encyclopedia of Life Support Systems (EOLSS), UNESCO-EOLSS Publishers, Oxford, UK. http://www.eolss.net.

Zeven, A C (1964). On the origin of the oil palm (*Elaeis guineensis* Jacq.). *Grana*, *5(1)*: 121-123.

Zulkifli, Y; Maizura, I and Rajinder, S (2012). Evaluation of MPOB oil palm germplasm (*Elaeis guineensis*) populations using EST-SSR. *J. Oil Palm Res., 24(2)*: 1368-1377.

Journal of Oil Palm Research Vol. 35 (3) September 2023 p. 491-503
DOI: https://doi.org/10.21894/jopr.2022.0049

OIL PALM MSP2 PROMOTER ISOLATION, *IN SILICO* ANALYSIS AND FUNCTIONAL CHARACTERISATION

NURNIWALIS ABDUL WAHAB[1]*; ZUBAIDAH RAMLI[1]; MOHAMAD ARIF ABD MANAF[1] and AHMAD PARVEEZ GHULAM KADIR[1]

ABSTRACT

Arabidopsis *was used as a stable transformation system to characterise the function of the oil palm mesocarp-specific promoter, MSP2. Five MSP2 promoter fragments ranging from 1558 bp to 3044 bp in size were successfully isolated.* In silico *sequence analysis showed various putative plant regulatory elements in the different MSP2 promoter regions. Two vector constructs containing MSP2-GLC and MSP2-GLG promoter fragments were attached to beta-glucuronidase (GUS) reporter gene and transformed into* Arabidopsis thaliana. *Histochemical GUS staining of the transgenic* Arabidopsis *showed that both promoter fragments were expressed in the flower, especially in petal and stigma, silique for MSP2-GLC and in anther and stamen for MSP2-GLG. The QELEMENTZMZM13 motif present only in the MSP2-GLG fragment is likely vital for the anther-specific expression. In MSP2-GLC transgenic* Arabidopsis, *GUS expression was enhanced under cold conditions, unlike MSP2-GLG transgenic* Arabidopsis. *A low-temperature response (LTR) motif present in MSP2-GLC may be important to enhance and drive the expression of a transgene under cold conditions. The deleted region in MSP2-GLG fragment caused the removal of the LTR motif, which most likely indicates that the size of the promoter is not necessarily important to drive gene expression, but the availability of a specific motif is key to determine its strength and specificity.*

Keywords: *Arabidopsis*, *Elaeis guineensis*, heterologous system, mesocarp-specific promoter, model plant.

Received: 13 October 2021; **Accepted:** 22 June 2022; **Published online:** 11 August 2022.

INTRODUCTION

Oil palm biotechnology, especially in genomics and genetic engineering, can be used to expedite crop improvement (Sambanthamurthi *et al.*, 2009). At the Malaysian Palm Oil Board (MPOB), the oil palm genetic engineering programme mainly focuses on producing transgenic palms with higher oleic acid content (Cheah *et al.*, 1995; Parveez *et al.*, 2015). Oleic acid is monounsaturated and can be used for diversification as liquid and salad oils in the food industry. In addition, it can also be an attractive feedstock for further fatty acid modifications in the oleochemical industry in Malaysia (Cheah *et al.*, 1995; Parveez *et al.*, 2015).

To produce transgenic plants with the desired trait, the transgene carrying the trait of interest must be functionally expressed to produce a heterologous protein (Juven-Gershon and Kadonagaa, 2010). The transgene expression is greatly dependent on the promoter. A promoter is responsible for initiating and regulating the transgene's transcription process, allowing gene expression (Porto *et al.*, 2013). There are various types of promoters used in plant genetic engineering. They are grouped as constitutive, tissue-/organ-/cell-specific, inducible, and synthetic; depending on their ability to control gene expression (Mithra *et al.*, 2017). Tissue-specific promoters are normally used to target transgene expression to a target tissue where the promoter activity is high and specific (Zheng and Baum, 2008). Thus, the most important step towards isolating tissue-specific promoters is to isolate their corresponding tissue-specific genes (Nurniwalis *et al.*, 2008; 2015).

In oil palm, to ensure the success of the genetic engineering program, choosing the correct promoter to direct transgene expression is essential. For oil modification and/or production of novel and value-

[1] Malaysian Palm Oil Board,
6 Persiaran Institusi, Bandar Baru Bangi,
43000 Kajang, Selangor, Malaysia.

* *Corresponding author e-mail: nurni@mpob.gov.my*

added products in the mesocarp, the availability of a mesocarp-specific promoter is vital. MSP1 is the first mesocarp-specific promoter isolated from oil palm (Siti Nor Akmar and Zubaidah, 2008). Several transformation vectors containing the MSP1 promoter were constructed to produce the desired traits such as high oleate content in oil palm mesocarp (Masani and Parveez, 2008). These constructs were transformed into oil palm embryogenic cultures where the transformed calli regenerated into plantlets, transformed palms were transferred to soil and grown in the biosafety nursery (Parveez *et al.*, 2015). However, chimeric transgenic palms were also detected, suggesting the need to make further improvements to the developed transformation protocols (Nurfahisza *et al.*, 2014).

It is also notable that different promoters have a varying degree of strength to drive transgene expression (Que *et al.*, 1997). Hence, the need for more oil palm mesocarp-specific promoters is crucial. This is also one of the approaches to avoid epigenetic silencing, resulting in a major drawback in transgenic technologies used for crop improvement (Rajeevkumar *et al.*, 2015). Besides homology between transgene and promoter, the interaction between two homologous promoters can also cause undesirable gene silencing (Matzke *et al.*, 2000). Thus, the dependence on a single promoter to drive transgene expression must be avoided, and the search for the next mesocarp-specific promoter is inevitable. MSP2, the second mesocarp-specific promoter, was isolated, and functional characterisation using mesocarp slices showed mesocarp-specific activity (Nurniwalis *et al.*, 2015).

One of the widely used approaches to analyse promoter activity is via transient gene expression assay using reporter genes. It allows fast expression of the reporter gene and is more cost-effective (Baum *et al.*, 1997; Jelly *et al.*, 2014). This assay requires the promoter to be fused to a reporter gene and then delivered into target tissues via various transformation methods. Different transformation methods have been optimised and developed for transient promoter studies in oil palm (Masani *et al.*, 2013; Parveez, 1998; Shariza Hanim *et al.*, 2018; Zubaidah and Siti Nor Akmar, 2003). The transient gene expression assay was successful in determining the activity of oil palm promoters in a tissue-specific, constitutive and inducible manner (Zubaidah *et al.*, 2018).

Nevertheless, the best way to functionally determine the role of oil palm promoters is to perform *in vivo* oil palm transformation. However, due to the long breeding cycle, the characterisation of the promoter in oil palm would require an extensive amount of time. Another limiting factor would be the low transformation efficiency in oil palm, hence will damper the work for functional analysis of the promoters. As an alternative, *Arabidopsis*, a model plant widely used in plant molecular biology and plant biotechnology research, has many important features to offer. It has a short generation time, compact size that requires less space for growth facilities, efficient, rapid, and high-throughput transformation system, and a complete sequenced genome (The *Arabidopsis* Genome Initiative, 2000). These advantages have enabled researchers to functionally validate the heterologous genes and promoters from valuable oil crops such as oil palm in *Arabidopsis* (Hanin *et al.*, 2016; Parveez *et al.*, 2010; Zubaidah *et al.*, 2017).

The availability of an established *Arabidopsis* laboratory facility in MPOB (Zubaidah, 2005) also paved the way to functionally characterise the MSP2 promoter in *Arabidopsis* as a model system. Thus, this work focuses on the analysis and characterisation of the MSP2 promoter and its regulatory region to provide additional support and/or produce a more accurate promoter expression.

MATERIALS AND METHODS

Plant Material, Growth Conditions and Stress Treatment

Oil palm *Elaeis guineensis* variety *tenera* (*dura* x *pisifera*) spear leaf tissue from MPOB-UKM Research Station, Bangi, Selangor was used for DNA extraction. *Arabidopsis thaliana* ecotype Columbia-0 (Col-0) was used for functional characterisation. Cultivation of *Arabidopsis* plants followed the method of Zubaidah *et al.* (2017). The seeds were sown on Murashige and Skoog media plate, incubated at 4°C for 48 hr and transferred into an environmentally controlled growth chamber with photoperiods of 16 hr light/8 hr dark at 22°C with 70% relative humidity. At the four to six rosette leaf stage, the seedlings were transferred into flowerpots containing a thoroughly wetted soil mixture. Cultivated plants were grown in an environmentally controlled growth chamber with similar conditions as described earlier. The untransformed wild-type *Arabidopsis* plants were used as a negative control, whereas *Arabidopsis* transformed with pBI221 carrying 35S promoter and β-glucuronidase (GUS) as the reporter gene was used as the positive control.

For cold stress treatment, transgenic *Arabidopsis* seeds and two-week-old seedlings carrying the respective MSP2 promoter-fragment constructs were used. The incubation/vernalisation of the seeds at 4°C was performed for an additional one to three days. For seedlings at four to six rosette leaf stage, the seedlings were transferred to a pot and left at 4°C for one to three days. After cold treatments, the seedlings continued to be grown in an environmentally controlled growth chamber

with parameters as described previously. For control plants, the transgenic seeds and two-week-old seedlings carrying the respective MSP2 promoter-fragment constructs were not exposed to cold treatment and grown as described earlier.

PCR Amplification and Purification

Genomic DNA used as a DNA template for PCR amplification was extracted from oil palm spear leaf using DNeasy® Extraction (Qiagen, Germany). The MSP2 promoter and its regulatory region or MSP2 fragments were individually PCR amplified in a 50 µL reaction mixture containing 50 ng oil palm genomic DNA, 1x Advantage 2 PCR buffer (Takara Bio USA, Inc., USA), 0.2 mM dNTP mix (Takara Bio USA, Inc., USA), 0.1 µM each of reverse and forward gene-specific primers and 0.1x Advantage 2 Polymerase Mix (Takara Bio USA, Inc., USA). PCR amplification was performed with denaturation at 94°C for 1 min, amplification at 94°C for 15 s, 58°C for 15 s and 72°C for 3 min for 30 cycles. The final extension was performed at 72°C for 7 min. Some adjustments (± 5°C) were made to the annealing temperatures and time for non-specific amplification. For the MSP2-GLG fragment, a two-step PCR condition was performed with denaturation at 95ºC (1 min); amplification at 95ºC (30 s), 65ºC (3 min) for 30 cycles and a final extension at 65ºC for 5 min.

Cloning using TOPO TA Cloning™ Dual Promoter Kit (Invitrogen, USA) and plasmid isolation using Qiagen Plasmid Mini Kit (Qiagen, Germany) were performed following the protocol as recommended by the manufacturer. Digestion of the plasmid was performed in a 20 µL reaction mixture containing 1 µg plasmid DNA, 1x CutSmart® Buffer and 0.5 U EcoRI-HF® (10 U/µL) (New England Biolabs, UK) at 37°C for 30 min to 2 hr.

Sequence Analyses

Nucleotide sequences were analysed using Bioedit tools (http:// www.mbio.ncsu.edu/BioEdit/bioedit.html). Regulatory motifs in the promoter sequences were identified using PlantCARE (http://bioinformatics.psb.ugent.be/webtools/plantcare/html/), PLACE (www.dna.affrc.go.jp/PLACE/), Softberry (www.softberry.com) and TransFAC (www.genome.jp).

Multiple Promoter-vector Constructions

The Gateway® Technology cloning system (Invitrogen, USA) was used to move the MSP2 promoter fragments of varying sizes into multiple vector systems before *Arabidopsis* transformation. The various MSP2 promoter fragments were initially cloned into an entry vector, pCR®8/GW/TOPO® to generate entry clones. Subsequently, an LR® recombination reaction was carried out to subclone the promoters from the entry clones into destination vector pGWB3 (Nakagawa *et al.*, 2009) to generate the expression constructs. All protocols were carried out as recommended by the manufacturer.

Transformation of *Arabidopsis* Plants

Transformation of the constructed expression vectors into *Agrobacterium tumefaciens* strain C58 was carried out by electroporation (Zubaidah *et al.*, 2017). Subsequently, the expression constructs were transformed into *Arabidopsis* via the floral dip method (Clough and Bent, 1998). Screening of the putative transformants was carried out following Mendel's law to generate T1, T2 and finally T3 homozygous transgenic lines. Three independent T3 homozygous transgenic lines carrying MSP2-GLC (Lines B, F and P) and MSP2-GLG (Lines B, E and J) expression constructs were used in these experiments.

Transformant Verification and Histochemical GUS Assay

Genomic DNA from putative transgenic *Arabidopsis* leaf tissues was extracted using DNeasy® Extraction (Qiagen, Germany). PCR reaction was carried out in a 25 µL reaction mixture containing 2x Advantage 2 PCR Buffer (Clontech), 2x Advantage 2 Polymerase mix (2.5 units mL^{-1}) (Clontech), 0.2 mM dNTP mix (Clontech), 0.2 mM of forward and reverse gene-specific primers and 50 ng DNA template. For the MSP2-GLC promoter, the gene-specific primer pairs used were GLF3 & GUSR1 and GLF4 & GUSR1 for the MSP2-GLG promoter. PCR conditions used are as described earlier. Histochemical GUS assay was carried out as described by Zubaidah *et al.* (2017). Blue spots on the analysed tissues were detected using a stereoscopic microscope (Nikon SMZ800, Japan).

RESULTS AND DISCUSSION

Isolation of Longer MSP2 Promoter and *In Silico* Analysis

Our previous studies have demonstrated that the oil palm mesocarp-specific promoter, MSP2 has mesocarp-specific activity based on transient expression assay using the GUS reporter gene bombarded into oil palm mesocarp slices (Nurniwalis *et al.*, 2015; Nurniwalis, 2017). As the size of the MSP2 promoter was less than 1 kb, we wanted to determine whether the size of the promoter was sufficient to drive gene expression to the target tissue or if a longer promoter is needed to drive a

stronger gene expression. Therefore, in the present study, PCR reaction based on information from the oil palm genome (Singh *et al*., 2013) resulted in the amplification of five fragments that correspond to and are longer than the MSP2 promoter. The five promoter fragments designated as MSP2-GLC, MSP2-GLG, MSP2-GLN, MSP2-GLP and MSP2-GLI contain various sizes ranging from ~1.6–3.0 kb. MSP2-GLC and MSP2-GLI are located at 1558 bp and 3044 bp upstream of the transcription start site (TSS), respectively. MSP2-GLC and MSP2-GLI promoter fragments contain the initial 671 bp MSP2 promoter (Nurniwalis *et al*., 2015) and are located at 887 bp and 2373 bp upstream of the initial MSP2 region. In comparison, MSP2-GLG, MSP2-GLP and MSP2-GLN are located at 1676 bp, 2373 bp and 2662 bp upstream of MSP2 and contain an internal deletion of 323 bp of the initial MSP2 promoter.

In silico analysis of the promoter sequences using the PlantCARE database detected 34 *cis*-acting regulatory elements in the longer MSP2 promoter regions (*Table 1*). Sixteen of the *cis*-acting regulatory elements are present in the initial 671 bp MSP2 promoter (Nurniwalis *et al*., 2015; Nurniwalis, 2017). Eighteen new additional *cis*-acting regulatory elements were detected in the longer MSP2 promoter fragments. They contain mainly *cis*-acting regulatory motifs that are related to stress responses. This includes additional motifs that are involved in light response-associated elements, hormones as well as low-temperature responses. The presence of these additional putative regulatory elements suggests that the longer MSP2 promoter regions may respond to a variety of environmental signals including abiotic stress such as cold and light responses.

One low temperature response element (LTR) was found in the 671 bp MSP2 promoter using PlantCARE and is not detected in the longer promoter regions. In addition, *in silico* analysis using PLACE detected two low temperature response motifs, *i.e*., LTRECOREATCOR15 and LTRE1HVBLT49 in both forward and reverse orientations within the various promoter fragments (*Table 2*). One LTRE1HVBLT49 motif was detected in MSP2-GLC and MSP2-GLI fragments, and the sequence motif is the same as the LTR motif detected by PlantCARE (*Tables 1* and *2*). On the other hand, LTRECOREATCOR15 has a different core sequence motif and was detected in three locations within all five promoter fragments (*Table 1*). Both motifs present in the promoter regions of various plants have been shown to be involved in cold responses either solely or in combination with other responsive elements (Baker *et al*., 1994; Catala *et al*., 2011; Dunn *et al*., 1998).

Another possible *cis* element related to low-temperature stress responses identified in the promoter fragments is as-1 motif (TGACG) (*Table 1*). The motif is present in a single copy and in the reverse orientation in both promoter fragments. In rice seedlings, the as-1 motif is involved with the early responses to chilling stress (Cheng *et al*., 2007). Promoter deletion/mutation analyses also showed that the as-1 motif can repress or induce the cold responsiveness of the promoter (Liu *et al*., 2016).

Generation of the Transformation Promoter: Reporter-vector Constructs

Two recombination reactions were performed to generate the entry and expression clones. The success in generating entry and expression constructs containing the longer MSP2 promoters was confirmed via restriction digest and sequence analyses. Five entry clones were generated and subsequently, four of the expression constructs were transformed into *A. tumefaciens* (C58) by electroporation and the success of the transformation procedure was verified via PCR analysis. The constructs designated as promMSP2-GLCec::GUS, promMSP2-GLGec::GUS, promMSP2-GLPec::GUS and promMSP2-GLIec::GUS carried the longer MSP2 promoter fragments with the expected sizes of ~ 1.6, ~ 2 and ~ 3 kb, respectively.

Screening and Validation of Transformants in Transgenic *Arabidopsis*

To further characterise the promoters in a stable plant transformation system, *A. thaliana* was used as the model plant species. Two fusion vectors containing MSP2-GLC and MSP2-GLG promoter fragments and the GUS gene were transformed into *Arabidopsis*. Both promoters differ in size where MSP2-GLG is 462 bp longer than MSP2-GLC. Six putative transformants were selected on selection media and screening of the transformants was validated via PCR analysis in all including in T1, T2 and T3 homozygous transgenic lines. *Figure 1* represents the verification of the transformants carrying the promMSP2-GLCec::GUS and promMSP2-GLGec::GUS constructs, indicating the presence of the promoters in transgenic *Arabidopsis*.

GUS Gene Expression in Transgenic *Arabidopsis*

GUS histochemical analysis in various transgenic *Arabidopsis* homozygous line tissues showed both MSP2-GLC and MSP2-GLG promoter fragments could regulate GUS gene expression but at different strengths and tissues (*Figure 2*). MSP2-GLC can direct GUS reporter gene expression in the reproductive organs, especially in the flower petals and stigma and in the elongating siliques. No visible GUS expression was observed in the other examined tissues. A close-up view of the flowers (unopen and open) showed that GUS expression was detected in the petals, especially in the unopened flower buds (*Figure 3a*). In addition, GUS expression can also be

TABLE 1. PREDICTION OF THE PUTATIVE *CIS*-REGULATORY ELEMENTS USING PLANT *CIS*-ACTING REGULATORY DNA ELEMENTS (PLANTCARE) DATABASE

Element name	Promoter	Sequence and strand	Function description
AAGAA-motif	GLP, GLI, GLG, GLC	GAAAGAA (-)	
ABRE	GLP, GLI, GLN, GLG	ACGTG (-)	Involved in abscisic acid responsiveness
ACE	GLI, GLC	GCGACGTACC (-)	Involved in light responsiveness
AE-box	GLP, GLI, GLN, GLG, GLC	AGAAACTT (+)	Part of module light response
ARE	GLP, GLI, GLN, GLG	AAACCA (-/+)	Essential for the anaerobic induction
AT1-motif	GLI, GLC	AATTATTTTTTATT (+)	Part of a light responsive module
ATCT-motif	GLP, GLI, GLN	AATCTAATCC (-/+)	Part of a conserved DNA module involved in light responsiveness
As-1	GLP, GLI, GLN, GLG, GLC	TGACG (-)	Involved in shoot-specific expression and light responsiveness
Box4	GLI, GLC	ATTAAT (+)	Part of a conserved DNA module involved in light responsiveness
CAAT box	GLP, GLI, GLN, GLG, GLC	CAAT (+/-)	Common cis-acting element in promoter and enhancer regions
CAT box	GLP, GLI, GLN, GLG, GLC	GCCACT (-)	Cis-acting regulatory element related to meristem expression
CGTCA-motif	GLP, GLI, GLN, GLG, GLC	CGTCA (+)	Involved in the MeJA-responsiveness
chs-CMA1a	GLP, GLI, GLN	TTACTTAA (+)	Part of a light responsive element
chs-CMA2a	GLI, GLC	TCACTTGA (-)	Part of light responsive element
ERE	GLP, GLI, GLN	ATTTTAAA (+ / -)	Ethylene responsive element
G-box	GLP, GLI, GLN, GLG, GLC	CACGTT (+); TCCACATGGCA (+); CACGAC (+)	Involved in light responsiveness
GATA-motif	GLP, GLI, GLN, GLG, GLC	AAGATAAGATT (-); AAGGATAAGG (+); AAGATAAGATT (-)	Part of a light responsive element
GCN4_motif	GLP, GLI, GLN	TGAGTCA (-)	Involved in endosperm expression
GTGANTG10	GLG, GLC	GTGA (+/-)	Involved in pollen-specific expression
I-box	GLP, GLI, GLN, GLG, GLC	CCATATCCAAT (-); GGATAAGGTG (+); CCTTATCCT (-)	Part of a light responsive element
LTRE	GLI, GLC	CCGAAA (-)	Involved in low-temperature responsiveness
MYB	GLP, GLI, GLN	CAACCA (-)	Involved in abiotic stress responses and secondary wall deposition
MYC	GLP, GLI, GLN, GLG, GLC	CATTTG (-/+); CATGTG (+/-); CAATTG	
O2-site	GLP, GLI, GLN, GLG, GLC	GTTGACGTGA	Involved in zein metabolism regulation
P-box	GLP, GLI, GLN	CCTTTTG (-)	Gibberellin-responsive element
POLLEN1LELAT52	GLG, GLC	AGAAA (+/-)	Involved in pollen-specific expression
STRE	GLP, GLI, GLN, GLG	AGGGG (-)	Stress response element
TCA-element	GLP, GLI, GLN, GLG, GLC	CCATCTTTTT (-)	Involved in salicylic acid responsiveness
TCT-motif	GLP, GLI, GLN, GLG, GLC	TCTTAC (+)	Part of a light responsive element
TGACG-motif	GLP, GLI, GLN, GLG, GLC	TGACG (-)	Involved in the MeJA-responsiveness
Unnamed_1	GLP, GLI, GLN, GLG	CGTGG (-)	
Unnamed_4	GLP, GLI, GLN, GLG, GLC	CTCC (+/-)	
W box	GLP, GLI, GLN, GLG	TTGACC (-)	Negative regulators of abiotic stress response/tolerance
WRE3	GLP, GLI, GLN, GLG, GLC	CCACCT (-)	
WUN-motif	GLP, GLI, GLN, GLG, GLC	CAATTACAT (-); AAATTTCTT (-)	Stress response elements

Note: * TATA BOX – A core promoter element around -30 of transcription start is not included in this table.

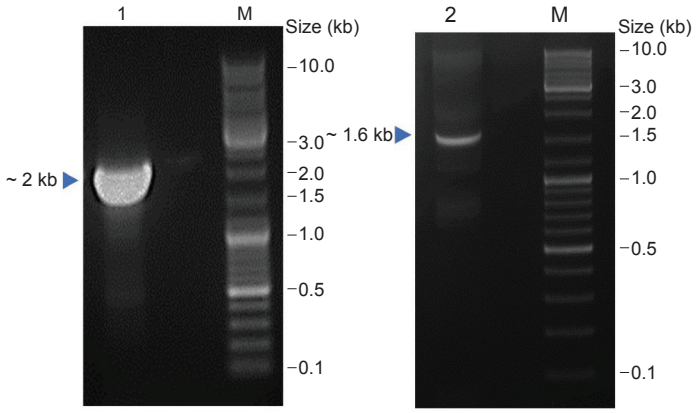

Figure 1. Validation of the promoter-vector expression constructs in transgenic Arabidopsis *via PCR using electrophoresis on 1% (w/v) agarose gel. Lane 1 = promMSP2-GLGec::GUS, Lane 2 = promMSP2-GLCec::GUS, M = Gene Ruler DNA Ladder Mix (Fermentas).*

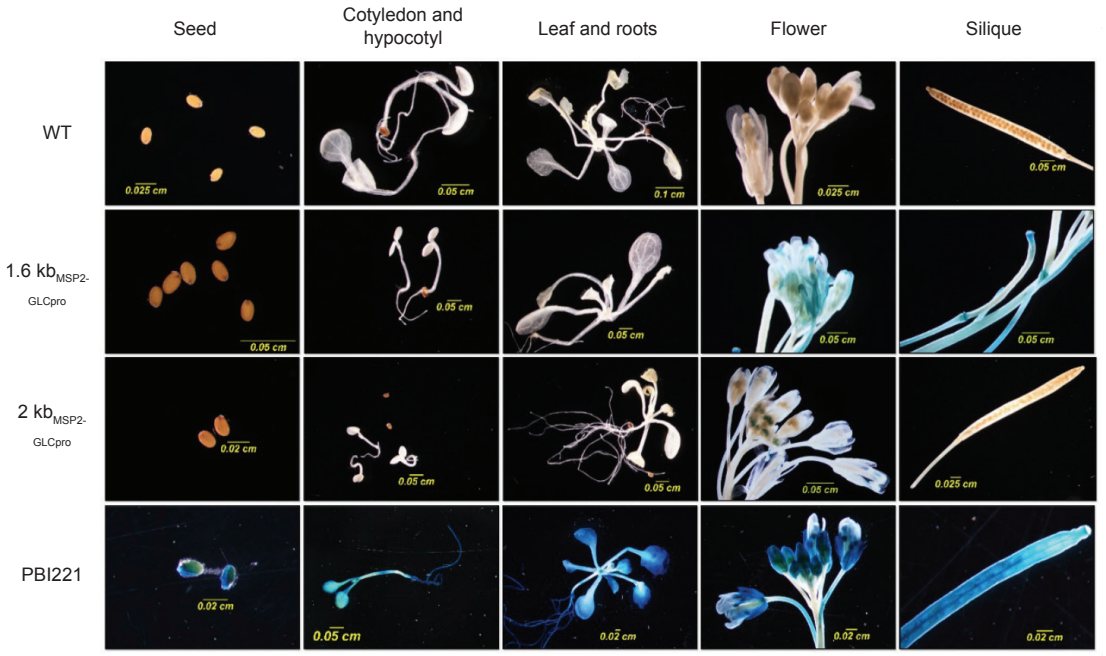

Figure 2. Histochemical GUS assay of the GLC and GLG promoters in various transgenic Arabidopsis *tissues. WT = wild-type* Arabidopsis*, $1.6kb_{MSP2\text{-}GLCpro}$ = transgenic* Arabidopsis *driven by MSP2-GLC promoter, $2kb_{MSP2\text{-}GLGpro}$ = transgenic* Arabidopsis *driven by MSP2-GLG promoter.*

seen in the stigma as the flower matures and the petal starts to open. In the silique, GUS expression was observed in young silique especially in the peduncle and in the silique apex. On the contrary, GUS expression was not detected in the mature silique (*Figure 3a*). These results indicate that the MSP-GLC promoter can drive gene expression in reproductive tissues during different developmental stages and may play a role in modulating floral organ maturity. Similarly, the MSP2-GLG promoter does not drive the GUS gene expression in almost all of the tested tissues except flowers (*Figure 2*). However, the GUS expression of MSP2-GLG promoter in flowers appeared to be much lower based on the strength of the blue-stained colour of the tissues. A close-up view of both young and mature flowers showed that GUS expression was only observed within the anthers of unopen flower buds (*Figure 5a*). GUS gene expression was not detected in the negative control plants but all the tested tissues in the positive control plants (*Figure 2*).

The MSP2 promoter was isolated from an oil palm lipase class 3 gene, *FLL1* (Nurniwalis *et al.*, 2015; Nurniwalis, 2017). In *Arabidopsis*, the most closely related orthologue gene to oil palm *FLL1* is *AtOBL1*, where the transcript is expressed in many tissues, including flower petals and stamen (Klepikova *et al.*, 2016). The enzymatic assay also revealed that *AtOBL1* is localised to lipid droplets, storing TAGs in the pollen tube (Müller and Ischebeck, 2018). Based on the expression of the reporter gene, we presumed that there might be motifs contributing to flower-specific expression in the MSP2 promoter fragments. Sequence analysis using the PLACE database showed an E-box motif (CANNTG) or MYC recognition site (*Table 1*). The *cis*-acting regulatory element was detected in flower-specific promoter in *Arabidopsis* where in combination with

TABLE 2. COMPARISON OF THE PUTATIVE LOW TEMPERATURE RESPONSE MOTIFS IDENTIFIED USING PLANT *CIS*-ACTING REGULATORY DNA ELEMENTS (PLANTCARE) AND A DATABASE OF PLANT *CIS*-ACTING REGULATORY DNA ELEMENTS (PLACE)

Database	Element name	Promoter fragment	Sequence and strand	Function description
PlantCARE	LTR	GLI, GLC	CCGAAA (-)	*Cis*-acting element involved in low-temperature responsiveness
PLACE	LTRE1HVBLT49	GLI, GLC	CCGAAA (-);	*Cis*-acting element involved in low-temperature responsiveness
	LTRECOREATCOR15	GLI, GLC, GLG, GLP, GLN	CCGAC (-/+)	

Source: Lescot *et al.*, (2002) and Higo *et al.* (1999).

MYB elements can drive the expression of the *chs* gene promoter stronger (Hartmann *et al.*, 2005). Both MSP2-GLC and MSP2-GLG promoter fragments also contain several copies of *cis*-acting elements involved in anther/pollen-specific expression (Chen *et al.*, 2010; Geng *et al.*, 2009; Rogers *et al.*, 2001). This includes motifs like 'GTGA' or GTGANTG10 and POLLEN1LELAT52 or 'AGAAA' (*Table 1*). Both motifs are distributed evenly among both promoter fragments. However, using PLACE database, a QELEMENTZMZM13 (AGGTCA) motif was only detected in MSP2-GLG fragment and none in MSP2-GLC. The QELEMENTZMZM13 motif has been reported to enhance pollen-specific activity (Hamilton *et al.*, 1998). Considering the results obtained, the presence of three copies of the putative QELEMENTZMZM13 motif is likely important for anther-specific expression of the MSP2-GLG promoter in transgenic *Arabidopsis*.

Promoter Activity in Response to Cold Treatment

As both MSP2-GLC and MSP2-GLG promoter fragments contained several putative stress-responsive elements, further work was performed to determine if the promoters are affected by low temperature or cold stress conditions. MSP2-GLC contains a predicted LTR or LTRE1HVBLT49 motif (CCGAAA) motif (*Table 2*) absent in the MSP2-GLG promoter. Therefore, we tested the effect of cold treatment on the seeds before seed germination and during seedling growth. For promMSP2-GLC::GUS gene construct, GUS reporter gene in transgenic *Arabidopsis* germinated from seeds given longer cold treatments were expressed in the same tissues as the transgenic control plant (*Figure 3*). GUS gene expression was detected in the flowers and silique and none in the rest of the tested tissues. In the young and mature flowers, GUS gene expression in the petals did not show a noticeable change even after the seeds were exposed up to three days longer to cold treatment (*Figure 3*). GUS gene expression in the stigma of open and mature flowers also remained similar to the control plant. However, GUS signal was also detected in the stamen filament after additional two days of vernalisation treatment (*Figures 3c* and *3d*). In the young developing silique, visual observation of GUS expression in the silique apex and peduncle appears to be slightly stronger in the plants germinated from cold-treated seeds than in the control plant (*Figure 3*). However, the mature silique GUS expression was detected in the silique apex and peduncle after an additional day of vernalisation treatment but at a lower level than the young silique (*Figure 3b*). In addition, GUS expression was also detected in the septum after an additional two-day seed exposure to low temperature (*Figures 3c* and *3d*).

In cold-treated transgenic *Arabidopsis* seedlings carrying promMSP2-GLC::GUS gene construct, the GUS reporter gene was expressed in the same tissue as the transgenic control plant (*Figure 4*). GUS gene expression was detected in the flowers and silique and none in the rest of the tested tissues. In the young and unopen flower buds, GUS expression was detected in the petals. In the open and mature flowers, the GUS expression was detected in the petals and stigmas. However, unlike the untreated control seedling, a one-day cold treatment in transgenic *Arabidopsis* seedlings also resulted in detecting GUS activity in the stamen filament of the mature and open flower (*Figures 4b* and *4c*). After three-days of low-temperature exposure, a GUS signal was also detected in the anther of the cold-treated seedlings (*Figure 4c*). GUS gene expression was also detected in young silique and the expression is stronger at the silique apex and peduncle and appears to be slightly stronger in the cold-treated seedlings than in the control plant (*Figure 4*). In the mature silique, a low level of GUS gene expression was also observed in the silique apex and peduncle in cold-treated seedlings (*Figure 4*). In addition, GUS expression was also observed in the septum region of the mature silique from seedlings exposed longer to low-temperature treatment (*Figure 4*).

In this work, despite whichever plant development stage was tested, observation in both transgenic seeds and seedlings carrying promMSP2-GLC::GUS gene construct exposed to cold temperature showed similar GUS expression

Figure 3. Comparison of GUS histochemical assay of promMSP2-GLC::GUS constructs in transgenic Arabidopsis *tissues under cold treatment prior to seed germination (a – d). a = two days seed vernalisation at 4°C (control), b = three days seed vernalisation treatment, c = four days seed vernalisation treatment and d = five days seed vernalisation treatment.*

Figure 4. Comparison of GUS histochemical assay of promMSP2-GLC::GUS construct in transgenic Arabidopsis *tissues under cold treatment at 4°C during plant growth (a – c). a = control transgenic* Arabidopsis *without cold treatment, b = transgenic* Arabidopsis *plants with one day cold treatment and c = transgenic* Arabidopsis *plant with three days exposure to cold treatment.*

patterns. GUS expression was targeted to the flowers and siliques and increased especially within specific regions in these tissues with prolonged exposure to cold.

For MSP2-GLG promoter, vernalisation treatment before seed germination showed GUS expression in transgenic *Arabidopsis* remained in the flower buds specifically in the anther (*Figure 5*). However, there is a slight change in GUS gene expression compared to the transgenic *Arabidopsis* control tissues (*Figure 5*). Visual observation based on the strength of the blue-stained colour of the anther showed that GUS expression was found to decrease slightly in transgenic *Arabidopsis* germinated from seeds exposed longer to low-temperature treatment. The most prolonged vernalisation treatment (additional three days) showed the lowest GUS expression (*Figure 5d*). In the silique of transgenic *Arabidopsis* germinated from cold-treated seeds, a low GUS expression level was occasionally found in the septum of the mature silique. Still, the observation in the silique was not consistent between all independent homozygous lines studied. The observed variation in GUS gene expression could be attributed to the position effect since the transformants were generated by random *Agrobacterium* transformation.

Figure 5. Comparison of GUS histochemical assay of promMSP2-GLG::GUS construct in transgenic Arabidopsis *tissues under cold treatment prior to seed germination (a – d). a = two days seed vernalisation at 4°C (control), b = three days seed vernalisation treatment, c = four days seed vernalisation treatment and d = five days seed vernalisation treatment.*

Integration of the transgene at different locations of a genome has been shown to affect gene expression levels in many organisms (Betts *et al*., 2019; Chen and Zhang, 2016). Position effects on expression level can also vary with the promoter used (Chen and Zhang, 2016) and/or promoter elements (Wilson, 1990).

For transgenic plants carrying promMSP2-GLG::GUS gene construct, GUS expression in the young flower buds from transgenic *Arabidopsis* seedlings exposed to cold treatment is similar to transgenic *Arabidopsis* germinated from seeds exposed to cold treatment, especially in the flower buds. Visual observation of the blue-stained tissue showed GUS signal was detected only in the anther of young and unopened flowers and the expression decreased as cold treatment was applied (*Figure 6*). The three day cold-treated seedlings showed the weakest GUS expression while the control plant showed the highest expression (*Figure 6*). No GUS expression was observed in the open and mature flowers, young and mature silique as cold treatment was applied to the treated and untreated seedlings. Even with prolonged cold exposure at both seeds and seedling growth development stages, GUS expression in the tested tissues from the two different developmental stages remained similar.

In this work, we found that the transgenic *Arabidopsis* plants react to cold treatment including prolonged cold exposure similarly despite exposure at the different stages of plant development via the GUS reporter gene. Comparison of GUS expression between MSP2-GLC and MSP2-GLG promoter fragments in transgenic *Arabidopsis* showed a differential expression pattern in the tissues tested. In MSP2-GLG transgenic *Arabidopsis* under low-temperature treatments, GUS activity specifically in the anther was not affected or slightly reduced when exposed longer to low temperature during seed incubation as well as seedling growth stages. In contrast, GUS activity in MSP2-GLC transgenic plants specifically in flowers and siliques appeared to be enhanced by low-temperature, especially when exposed longer to cold treatments. The MSP2-GLC promoter fragment contains the LTR motif known to be implicated in cold-regulated gene expression. However, the LTR motif is absent in MSP2-GLG. Deleting 323 bp from the initial MSP2 promoter has resulted in the removal of the LTR motif in MSP2-GLG promoter fragment. In barley, both LTR and LTREs are present in the promoter region of the *blt4.9* gene however, only the LTR motif is required for low-temperature responses (Dunn *et al*., 1998). Therefore, the absence of the LTR motif is likely causing the inability of the MSP2-GLG promoter to drive gene expression under low-temperature influences, despite having a longer promoter size than MSP2-GLC. The LTR element in MSP2-GLC promoter fragment suggests that it may drive the expression of its corresponding gene at a low temperature.

Semi-quantitative RT-PCR demonstrated that the oil palm *FLLI* gene is highly expressed in the mesocarp tissues, especially in the mature and ripening fruits. *FLL1* is also induced under cold treatment (Nurniwalis *et al*., 2015; Nurniwalis, 2017). The result of the MSP2-GLC promoter analysis in transgenic *Arabidopsis* is very much consistent with native *FLL1* the gene expression analysis (Nurniwalis *et al*., 2015; Nurniwalis, 2017) as well as enzymatic assay (Cadena *et al*., 2013; Sambanthamurthi *et al*.,

Figure 6. Comparison of GUS histochemical assay of promMSP2-GLG::GUS construct in transgenic Arabidopsis *tissues under cold treatment at 4°C during plant growth (a – c). a = control plant without cold treatment, b = plants with 1-day cold treatment at 4°C and c = plant with 3 days exposure to cold treatment.*

1991; 1995) where oil palm lipase is activated by cold temperature. The low temperature effect on oil palm fruits can cause tissue damage, allowing the lipases access to their substrates. For oil palm crop that grows in a tropical country, the effect of low temperature on fruit tissue damages is doubtful. However, oil palm is exposed to physiological plant stresses, which include drought (Roslan *et al.*, 2011). Farooq *et al.* (2009) showed that cold and drought stresses are inter-related, where cold stress causes plant osmotic balance destruction, leading to dehydration stress. Characterisation of a dehydration responsive element binding (DREB) transcription factor, *Eg*DREB1, from oil palm also has demonstrated that it plays a role in enhancing tolerance to drought and cold stresses (Azzreena *et al.*, 2017). In addition, a combination of cold and light-responsive elements are also integrated into *Arabidopsis* for adaption to the changes in the environment (Catala *et al*., 2011).

In this work, *Arabidopsis* may not be the most suitable heterologous system for analysing the tissue-specificity of a mesocarp-specific promoter due to the difference in the anatomy structure. Other reasons such as differences in factors that regulate gene expression and differential performance of dicot and monocot plants have also been raised (Hernandez-Garcia and Finer, 2015). However, despite the absence of a fleshy fruit form in *Arabidopsis*, promoter functional characterisation of the oil palm mesocarp-specific promoters has shown a possible role of the promoter. The MSP1 promoter in *Arabidopsis* has mimicked the expression of its corresponding *MT-3* gene in *Brassica napus* (Zubaidah *et al.*, 2017). Similarly, promoter analysis of the oil palm MSP2 promoter fragments in *Arabidopsis* has shown a resemblance to its most closely related orthologue gene, *AtOBL1* (Klepikova *et al*., 2016).

CONCLUSION

We have successfully used *Arabidopsis* to study the function of the MSP2 promoter fragments under low temperature conditions. Deletion of the LTR motif showed that the 1558 bp fragment of MSP2-GLC promoter is required to drive the expression of a transgene under cold-treatment based on the presence of the LTR motif. The size of the promoter is not necessarily important to drive gene expression, but the availability of a specific motif is key to determine its strength and specificity. Information obtained from this study showed that the MSP2 promoter fragments can function in a heterologous system like *Arabidopsis.*

ACKNOWLEDGEMENT

The authors thank the MPOB management for permission to publish this article.

REFERENCES

Azzreena, M A; Siti Nor Akmar, A; Maheran, A A and Edaroyati, P M W (2017). Oil palm drought inducible DREB1 induced expression of DRE/CRT and non-DRE/CRT-containing genes in lowland transgenic tomato under cold and PEG treatments. *Plant Physiol. Biochem., 112*: 129-151.

Baker, S S; Wilhelm, K S and Thomashow, M F (1994). The 5'-region of *Arabidopsis thaliana cor15a* has *cis*-acting elements that confer cold-, drought- and ABA-regulated gene expression. *Plant Mol. Biol., 24*: 701-713.

Baum, K; Groning, B and Meier, I (1997). Improved ballistic transient transformation conditions for tomato fruit allow identification of organ-specific contributions of I-box and G-box to the RBCS2 promoter activity. *Plant J., 12*: 463-469.

Betts, S D; Basu, S; Bolar, J; Booth, R; Chang, S; Cigan, A M; Farrell, J; Gao, H; Harkins, K; Kinney, A; Lenderts, B; Li, Z; Liu, L; McEnany, M; Mutti, J; Peterson, D; Sander, J D; Scelonge, C; Sopko, X; Stucker, D; Wu, E and Chilcoat, N D (2019). Uniform expression and relatively small position effects characterize sister transformants in maize and soybean. *Front Plant Sci., 10*: 1209.

Cadena, T; Prada, F; Perea, A and Romero, H M (2013). Lipase activity, mesocarp oil content, iodine value in oil palm fruits of *Elaeis guineensis*, *Elaeis oleifera*, the interspecific hybrid O×G (*E. oleifera* × *E. guineensis*). *J. Sci. Food Agri., 93(3)*: 674-680.

Catala, R; Medina, J and Salinas, J (2011). Integration of low temperature and light signalling during cold acclimation response in *Arabidopsis. PNAS 108(39)*: 16475-16480.

Cheah, S C; Sambanthamurthi, R; Siti Nor Akmar, A; Abrizah, O; Mohamad Arif, A M; Umi Salamah, R and Parveez, G K A (1995). Towards genetic engineering of oil palm (*Elaeis guineensis* Jacq.). *Plant Lipid Metabolism* (Kader, J C and Mazliakm, P eds.). Kluwer Academic Press, Netherlands. p. 570-572.

Chen, L; Tu, Z; Hussain, J; Cong, L; Yan, Y; Jin, L; Yang, G and He, G (2010). Isolation and heterologous transformation analysis of a pollen-specific promoter from wheat (*Triticum aestivum* L.). *Mol. Biol. Rep., 37*: 737-744.

Chen, X and Zhang, J (2016). The genomic landscape of position effects on protein expression level and noise in yeast. *Cell Systems,* 2: 347-354.

Cheng, C; Yun, K Y; Ressom, H W; Mohanty, B; Bajic, V B; Jia, Y; Yun, S J and de los Reyes, B G (2007). An early response regulatory cluster induced by low temperature and hydrogen peroxide in seedlings of chilling-tolerant japonica rice. *BMC Genom., 8*: 175.

Clough, S J and Bent, A F (1998). Floral dip: A simplified method for *Agrobacterium*-mediated transformation of *Arabidopsis thaliana. Plant J. 16(6)*: 735-743.

Dunn, M A; White, A J; Vural, S and Hughes, M A (1998). Identification of promoter elements in a low-temperature-responsive gene (*blt4.9*) from barley (*Hordeum vulgare* L.). *Plant Mol. Biol. 38*: 551-564.

Farooq, M; Aziz, T; Wahid, A; Lee, D J and Siddique, K H M (2009). Chilling tolerance in maize: Agronomic and physiological approaches. *Crop Pasture Sci., 60*: 501-516.

Geng, A-Q; Zhao, Z-J; Nie, X-L and Xiao, X-G (2009). Expression analysis of four flower-specific promoters of *Brassica* spp. in the heterogeneous host tobacco. *African J. Biotech., 820(20)*: 5193-5200.

Hamilton, D A; Schwarz, Y H and Mascarenhas, J P (1998). A monocot pollen-specific promoter contains separable pollen-specific and quantitative elements. *Plant Mol. Biol., 38*: 663-669.

Hanin, A N; Masani, M Y A and Parveez, G K A (2016). Evaluation of oil palm leaf-specific promoter (*LSP1*) activity for expressing *PHB* genes in *Arabidopsis thaliana. J. Oil Palm Res., 28*: 1-9.

Hartmann, U; Sagasser, M; Mehrtens, F; Stracke, R and Weisshaar, B (2005). Differential combinatorial interactions of *cis*-acting elements recognized by R2R3-MYB, BZIP, and BHLH factors control light responsive and tissue-specific activation of phenylpropanoid biosynthesis genes. *Plant Mol. Biol., 57*: 155-171.

Hernandez-Garcia, C M and Finer, J J (2015). Identification and validation of promoters and *cis*-acting regulatory elements. *Plant Sci., 217-218*: 109-119.

Higo, K; Ugawa, Y; Iwamoto, M and Korenaga, T (1999). Plant *cis*-acting regulatory DNA elements (PLACE) database. *Nucleic Acids Res., 27(1)*: 297-300.

Jelly, N S; Walter, L V B and Maillot, P (2014). Transient expression assays in grapevine: A step towards genetic improvement. *Plant Biotech. J., 12*: 1231-1245.

Juven-Gershon, T and Kadonagaa, J T (2010). Regulation of gene expression via the core promoter and the basal transcriptional machinery. *Dev. Biol., 339(2)*: 225-229.

Klepikova, A V; Kasianov, A S; Gerasimov, E S; Logacheva, M D and Penin, A A (2016). A high resolution map of the *Arabidopsis thaliana* developmental transcriptome based on RNA-seq profiling. *Plant J., 88*: 1058-1070.

Lescot, M; Déhais, P; Thijs, G; Marchal, K; Moreau, Y; de Peer, Y V; Rouzé, P and Rombauts, S (2002). PlantCARE, a database of plant *cis*-acting regulatory

elements and a portal to tools for *in silico* analysis of promoter sequences. *Nucleic Acids Res., 30(1)*: 325-327.

Liu, S; Chen, H; Li, X and Zhang, W (2016). A low-temperature-responsive element involved in the regulation of the *Arabidopsis thaliana At*1g71850/*At*1g71860 divergent gene pair. *Plant Cell Rep., 35*: 1757-1767.

Masani, M Y A; Noll, G; Parveez, G K A; Ravigadevi, S and Prüfer, D (2013). Regeneration of viable oil palm plants from protoplasts by optimizing media components, growth regulators and cultivation procedures. *Plant Sci., 210*: 118-127.

Masani, M Y A and Parveez, G K A (2008). Development of transformation vectors for the production of potentially high oleate transgenic oil palm. *Electronic J. Biotech. 11*: 3.

Matzke, M A; Mette, M F and Matzke, A J (2000). Transgene silencing by the host genome defense: Implications for the evolution of epigenetic control mechanisms in plants and vertebrates. *Plant Mol. Biol., 43*: 401-415.

Mithra, S V A; Kulkarni, K and Srinivasan, R (2017). Chapter 5: Plant promoters: Characterization and applications in transgenic technology. *Plant Biotechnology: Principles and Applications* (Abdin, M Z; Kiran, U and Ali, A eds.). Springer Nature Singapore Pte. Ltd. p. 117-172.

Müller, A O and Ischebeck, T (2018). Characterization of the enzymatic activity and physiological function of the lipid droplet-associated triacylglycerol lipase *AtOBL1*. *New Phytol., 217*: 1062-1076.

Nakagawa, T; Ishiguro, S and Kimura, T (2009). Gateway vectors for plant transformation. *Plant Biotech., 26*: 275-284.

Nurfahisza, A R; Rafiqah, M A; Masani, M Y A; Hanin, A N; Rasid, O A; Parveez, G K A and Ismail, I (2014). Molecular analysis of transgenic oil palm to detect the presence of transgenes. *J. Oil Palm Res., 26*: 73-80.

Nurniwalis, A W (2017). Physiological, biochemical and molecular analyses of fruit development in oil palm (*Elaeis guineensis* Jacq.). PhD thesis. University of Nottingham Malaysia.

Nurniwalis, A W; Zubaidah, R; Siti Nor Akmar, A; Zulkifli, H; Mohamad Arif, A M; Massawe, F J; Chan, K L and Parveez, G K A (2015). Genomic structure and characterization of a lipase class 3 gene and promoter from oil palm. *Biol. Plant., 59(2)*: 227-236.

Nurniwalis, A W; Suhaimi, N; Siti Nor Akmar, A; Aminah, S and Mohamad Arif, M A (2008). Gene discovery via expressed sequence tags from the oil palm (*Elaeis guineensis* Jacq.) mesocarp. *J. Oil Palm Res. Special Issue 2*: 87-96.

Parveez, G K A; Rasid, O A; Masani, M Y A and Sambanthamurthi, R (2015). Biotechnology of oil palm: Strategies towards manipulation of lipid content and composition. *Plant Cell Rep., 34(4)*: 533-543.

Parveez, G K A; Abrizah, O; Nurhafizah, R and Bahariah, B (2010). Functional analysis of oil palm palmitoyl-ACP thioesterase (*Fat B*) via down regulation in model plant: *Arabidopsis thaliana*. *J. Oil Palm Res., 22*: 803-813.

Parveez, G K A (1998). Optimization of parameters involved in the transformation of oil palm using the biolistic method. PhD thesis. Universiti Putra Malaysia, Malaysia.

Porto, M S; Pinheiro, M P; Batista, V G; dos Santos, R C; Filho, Pde A and Lima, L M (2013). Plant promoters: An approach of structure and function. *Mol. Biotech., 56(1)*: 38-49.

Que, Q; Wang, H Y; English, J J and Jorgensen, R A (1997). The frequency and degree of co-suppression by sense chalcone synthase transgenes are dependent on transgene promoter strength and are reduced by premature nonsense codons in the transgene coding sequence. *The Plant Cell., 9*: 1357-1368.

Rajeevkumar, S; Anunanthini, P and Sathishkumar, R (2015). Epigenetic silencing in transgenic plants. *Front. Plant Sci., 6*: 693.

Rogers, H J; Bate, N; Combe, J; Sullivan, J; Sweetman, J; Swan, C; Lonsdale, D M and Twell, D (2001). Functional analysis of *cis*-regulatory elements within the promoter of the tobacco late pollen gene g10. *Plant Mol. Biol., 45*: 577-585.

Roslan, M N M; Mohd Haniff, H and Nur Maisarah, J (2011). Physiological plant stress and responses in oil palm. *Oil Palm Bulletin, 62*: 25-32.

Sambanthamurthi, R; Rajinder, S; Parveez, G K A; Meilina, O A and Kushairi, A (2009). Chapter 11: Opportunities for the oil palm via breeding and biotechnology. *Breeding Plantation Tree Crops: Tropical Species* (Jain, S M and Priyadarshan, P M eds.). Springer Science and Business Media, New York. p. 377-421.

Sambanthamurthi, R; Oo, K C and Siti Hasnah, P (1995). Factors affecting lipase activity in *Elaeis guineensis* mesocarp. *Plant Physiol. Biochem., 33(3)*: 353-359.

Sambanthamurthi, R; Chong, C L; Oo, K C; Yeo, K H and Rajan, P (1991). Chilling-induced lipid hydrolysis in the oil palm (*Elaeis guineensis*) mesocarp. *J. Exp. Bot., 42(9)*: 1199-1205.

Shariza Hanim, Z A; Nurniwalis, A W and Zubaidah, R (2018). Development of agroinfiltration method to study oil palm promoter. *14th International Symposium on Biocatalysis and Agricultural Biotechnology (ISBAB 2018).* Kuala Lumpur. p. 80.

Singh, R; Ong-Abdullah, M; Low, L E T; Manaf, M A; Rosli, R; Nookiah, R; Ooi, L C; Ooi, S E; Chan, K L; Halim, M A; Azizi, N; Nagappan, J; Bacher, B; Lakey, N; Smith, S W; He, D; Hogan, M; Budiman, M A; Lee, E K; De Salle, R; Kudrna, D; Goicoechea, J L; Wing R A, Wilson, R K; Fulton, R S; Ordway, J M; Martienssen, R A and Sambanthamurthi, R (2013). Oil palm genome sequence reveals divergence of interfertile species in old and new worlds. *Nature, 500(7462)*: 335-339.

Siti Nor Akmar, A and Zubaidah, R (2008). Mesocarp-specific metallothionein-like gene promoter for genetic engineering of oil palm. *J. Oil Palm Res., 2*: 1-8.

The *Arabidopsis* Genome Initiative (2000). Analysis of the genome sequence of the flowering plant *Arabidopsis thaliana*. *Nature, 408*: 796-815.

Wilson, C (1990). Position effects on eukaryotic gene expression. *Annu. Rev. Cell Biol., 6*: 679-714.

Zheng, C and Baum, B J (2008). Evaluation of promoters for use in tissue-specific gene delivery. *Methods in Mol. Bio., 434*: 205-219.

Zubaidah, R; Nurniwalis, A W; Chan, P L; Masura, S S; Siti Nor Akmar, A and Parveez, G K A (2018). Tissue-specific promoters: The importance and potential application for genetic engineering in oil palm. *J. Oil Palm Res., 30*: 1-12.

Zubaidah, R; Nurniwalis, A W; Siti Nor Akmar, A and Parveez, G K A (2017). The use of *Arabidopsis thaliana* model system for testing oil palm promoter: Case study on oil palm *MT3-A* promoter. *J. Oil Palm Res., 29(2)*: 189-196.

Zubaidah, R (2005). *Arabidopsis thaliana* laboratory as a research facility in MPOB. *MPOB Information Series 308, MPOB TS No. 9.*

Zubaidah, R and Akmar, A S N (2003). Development of a transient promoter assay system for oil palm. *J. Oil Palm Res., 15(2)*: 62-69.

Journal of Oil Palm Research Vol. 35 (3) September 2023 p. 504-516
DOI: https://doi.org/10.21894/jopr.2022.0057

BUNCH OIL AND FATTY ACID PROFILE IN *Elaeis oleifera* TAISHA-ECUADOR, *E. guineensis* Jacq., INTERSPECIFIC HYBRIDS AND BACKCROSSES

LAURA MENDOZA[1]*; JULIAN BARBA[1] and GUSTAVO LIGARRETO[2]

ABSTRACT

In this study, bunch oil content and fatty acid profile in the Elaeis oleifera *species from Taisha, Morona-Santiago, Ecuador, its interspecific hybrid descendants and backcrosses were determined in contrast to* Elaeis guineensis. *Results showed that* E. oleifera *from Taisha presented an average of 10.74% oil in bunch, being lower than those presented by hybrids of 25.80%, backcrosses of 25.98%, and* E. guineensis *of 29.49%. The most abundant fatty acids in the mesocarp corresponded to C16:0, C18:1n9, and C18:2n6, where* E. oleifera *from Taisha, although it had a lower content of palmitic acid (27.82%) compared to the rest of the genotypes. This did not present statistical differences for C18:1n9 because of the same behaviour as an* E. guineensis, *and therefore did not classify as a high oleic material. However, for C18:2n6, which is in the group of unsaturated fatty acids, it presented higher values than any of the other materials, indicating that its oil synthesis converts C18:1 to C18:2 more easily than other* E. oleifera *of different places in America. The average iodine value was 76.93%, compared to hybrids with 67.14%, backcrosses with 60.20%, and* E. guineensis *with 55.65%.*

Keywords: *Elaeis oleifera*, interspecific hybrids, oleic acid, palmitic acid, Taisha.

Received: 18 July 2021; **Accepted:** 2 August 2022; **Published online:** 13 September 2022.

INTRODUCTION

In 2020, 209.9 million tonnes of vegetable oil were produced, 31.4% of the production corresponded to crude palm oil (CPO) obtained from the mesocarp and palm kernel, which are the two types of oil produced from the oil palm fruit (Oil World, 2020). Approximately 70.0% of world palm oil production is used in the food industry (Lieb *et al*., 2017). The fatty acid composition determines the nutritional suitability of palm oil (Sambanthamurthi *et al*., 2000).

Palm oil is a lipid, composed of glycerol esters and long-chain fatty acids that are insoluble in water, but soluble in various organic solvents such as ether, chloroform, certain alcohols, and benzene (Corley and Tinker, 2009). Fatty acids can be saturated or unsaturated, depending on the number of double bonds in their chain; saturated does not have double bonds and unsaturated do. Its structure is designated by a symbol that indicates the length of the carbon chain and the number of double bonds. Thus, palmitic acid (C16:0) has 16 carbons with no double bonds and oleic acid (C18:1) has 18 carbons and one double bond (Sambanthamurthi *et al*., 2000). The main fatty acids in palm oil are myristic (C14:0), palmitic (C16:0), stearic (C18:0), oleic (C18:1), and linoleic (C18:2). C16:0 is the main saturated fatty acid and is balanced by C18:1 monounsaturated and C18:2 polyunsaturated (Sambanthamurthi *et al*., 2000).

The fatty acids composition of CPO is substantially different within the *Elaeis* genus,

[1] Research and Development Unit,
Palmar del Río, San Sebastián del Coca, Ecuador.

[2] Faculty of Agricultural Sciences,
Department of Agronomy,
Universidad Nacional de Colombia,
Road 30 No. 45-03 Building No. 500,
Sede Bogotá, Colombia.

* *Corresponding author e-mail: ljmendozac@unal.edu.co*

which comprises two species: *Elaeis guineensis* Jacq., originally from Africa, planted commercially worldwide, and *E. oleifera* HBK Cortés from America, which represents an important genetic source in the generation of interspecific hybrids with *E. guineensis*. African palm contains approximately 50% saturated fatty acids, with 44% C16:0, 5% C18:0, and trace amounts of C14:0; unsaturated fatty acids represent approximately 40% of C18:1 and 10% of C18:2 and α-linolenic acid (C18:3) (Montoya *et al*., 2014). Generally, the unsaturated fatty acids content of the American palm varies from 47.0% to 69.0% for C18:1, 2.0% to 19.0% for C18:2, and 0.1% to 1.2% for C18:3 (Montoya *et al*., 2014). *E. oleifera* oil contains more unsaturated fatty acids (C18:1 and C18:2) and a higher iodine value than *E. guineensis*, being quite similar to olive oil in its composition (Corley and Tinker, 2009). Consequently, the iodine value, which is a multiparameter measure of the global degree of unsaturation of fatty acids in vegetable oil, presents values between 70.0% and 87.0% for *E. oleifera*, while the value for *E. guineensis* is between 53.0% and 60.0% (Montoya *et al*., 2014).

The interspecific hybrid resulting from the cross between *E. oleifera* and *E. guineensis* presents an intermediate oil composition between the parents, indicating additive inheritance (Hardon, 1969; Meunier and Boutin, 1975; Sambanthamurthi *et al*., 2000). This oil is called high oleic oil, which comprise 33% saturated fatty acids with around 28% being C16:0, and 66% unsaturated fatty acids with around 54% of C18:1 (Mozzon *et al*., 2013). Backcrosses between hybrids and either parent exhibit intermediate oil between the hybrid and the recurrent parent (Corley and Tinker, 2009; Sambanthamurthi *et al*., 2000), again suggesting additive inheritance.

This study would provide an insight into the variability of oil content and quality within the genus *Elaeis*. The objective was to determine the amount of oil in the bunch and the composition of fatty acids in *E. oleifera* from Taisha, Morona Santiago, Ecuador, its interspecific hybrids and backcrosses, in comparison with *E. guineensis*. This is a new work where the fatty acid profile of *E. oleifera* from the locality of Taisha, Morona Santiago, Ecuador and its hybrids and backcrosses with different *E. guineensis* parents will be shown.

MATERIALS AND METHODS

Study Site

The study was carried out at the Palmar del Río company located in San José de Guayusa, province of Francisco de Orellana, Amazon region of Ecuador. The geographic coordinates of the locations were 0º 19' S and 77º 06' W, at an altitude of 280 m above sea level. The average rainfall was 266 mL/month, solar radiation of 4148 watts/month, minimum temperature of 18.6°C and a maximum of 32.8°C, relative humidity of 78.13% and Inceptisol soils with relatively flat topography (Barba, 2016).

Vegetal Material

The study was focused on *E. oleifera* palms from the town of Taisha, Morona Santiago, Ecuador; interspecific hybrids derived from *E. oleifera* Taisha crossed with *pisifera guineensis* of Yangambi, La Mé, and AVROS origins; backcross from interspecific hybrids of Taisha x AVROS origin crossed with *E. guineensis* AVROS, and *tenera guineensis* palms of AVROS origin. The genotypes and their names are described in *Table 1*.

Oil Content

A bunch of fresh fruit at the point of physiological maturity was harvested from each palm, based on more than five naturally detached fruits, taking into consideration that *E. oleifera* from Taisha do not have loose fruits, unlike some other *oleifera* and interspecific hybrids. The harvested bunch was placed in a bag and labelled with each genotype.

TABLE 1. DESCRIPTION OF THE GENOTYPES OF *Elaeis oleifera* TAISHA, *Elaeis guineensis*, OxG HYBRIDS AND BACKCROSSES PALMS

Genotypes	Treatments	Abbreviation	Age (yr)
E. oleifera Taisha x *E. guineensis* Yangambi	Taisha x Yangambi	H1	13
E. oleifera Taisha x *E. guineensis* La Mé	Taisha x La Mé	H2	13
E. oleifera Taisha x *E. guineensis* AVROS	Taisha x AVROS	H3	14
Backcross: (*E. oleifera* - Taisha x *E. guineensis* - AVROS) x *E. guineensis* AVROS	Backcross	BC	8
E. oleifera - Taisha	Taisha	Taisha	21
E. guineensis AVROS	AVROS	AVROS	9

The bags of fruit bunch were taken to the laboratory for bunch analysis, where the weight of the bunch was recorded and subsequently chopped into peduncle, spikelets, and fruits. The fruits were then separated into fertile, parthenocarpic and abortive fruits, counted and weighed, using the method described by Prada and Romero (2012).

The oil potential in bunch (OB) was estimated using three variables: Fruit in the bunch (FB), mesocarp in fruit (MF), and oil in fresh mesocarp (OFM). In consideration that *oleifera* and hybrids contain two types of oil, the fertile fruits contains the kernels but there are no kernel in the parthenocarpic fruits. A sample of 300 g of each fertile and parthenocarpic fruits were taken from each bunch, manually pulped with pruning shears, separating the mesocarp and kernel from the fertile ones, while the parthenocarpic ones were cut into small pieces. The mesocarp was weighed and dried in an oven at 105°C for 24 hr, then crushed in a blender and dried again in the oven for 12 hr at 60°C. A 5 g sample taken from the crushed mesocarp was put in a thimble, then placed in a soxhlet system with chloroform (98.2% $CHCl_3$) as the oil extraction solvent for approximately 24 hr. Once the oil was extracted, the thimble was dried in the oven at 105°C for 12 hr, then it was weighed and the oil content in wet mesocarp was calculated, according to Equation (1). In bunch analysis, besides measuring the oil content, it also can determine other parameters such as predicting the behavior of other agronomic factors that can be useful in the field and genetic improvement programmes.

$$OB\ (\%) = FB*MF*OFM \quad (1)$$

Determination of the Fatty Acid Profile

A sample of crude oil from the mesocarp was taken from each palm for analysis. The repeatability of measurements for fatty acid composition is high, hence a single measurement is sufficient to describe the fatty acid content of a group (Rajanaidu *et al*., 1983). Three 240 g oil samples were taken from each genotype or treatment, making a total of 18 samples. The chemical analysis of fatty acids content was carried out in the laboratory of the Colombian Oil Palm Research Center, Palmar de la Vizcaina Experimental Field, Barrancabermeja, Colombia. Fatty acid profiles were determined according to the American Oil Chemist's Society method (AOCS, 1994). The fatty acid methyl esters were determined using gas chromatography with flame ionisation detector. Oil samples were saponified with KOH/MeOH. The fatty acids were derivatised to esters using a solution of BF3 in methanol. The esters were extracted and 1 µL was injected into the chromatographic system. The equipment used was a 7890 A gas chromatograph (Agilent Technologies, Wilmington, USA). The column used in the analysis was a DB-23 (J&W Scientific, Cat. No. 1222362) of 60 m x 0.25 mm I.D. x 0.25 µm f.e., and the injection was performed in split mode (50:1). Hydrogen was used as carrier gas at a constant flow rate of 33 cm/s. The reference standard used to determine the retention time was FAME blend of Supelco™ 37 components (Supelco, Bellefonte, PA, Cat. No. 47885U). The fatty acid methyl esters were identified by comparison with the retention times of the standard mixture, analysed under the same chromatographic conditions. The quantification was performed using area normalisation method. Results were expressed as mass to mass percentage (m/m) according to the official method AOCS Ce 1-62 (AOCS, 1997).

The fatty acids used for analysis in this study were myristic acid (C14:0), palmitic acid (C16:0), stearic acid (C18:0), palmitoleic acid (C16:1), oleic acid (C18:1n9c), vaccenic acid (C18:1n7c), linoleic acid (C18:2n6c) and α-linolenic acid (C18:3n3), which are the most representative in CPO.

Determination of the Iodine Value

The method used as described in the AOCS manual, method Cd 1b-87 (AOCS, 1994). This method is used by the laboratory of the Colombian Oil Palm Research Center where the analyses were carried out. The iodine value is defined as the g of iodine that react with 100 g of fat or oil (12 g/100 g oil). This determination is related to the content of unsaturated fat (mono and polyunsaturated fatty acids). In the case of CPO, high iodine values imply higher olein yields during fractionation. This determination can also be used as a criterion for the identity and purity of the product.

Statistical Analysis

A completely randomised design was used with six treatments made up of three experimental units as indicated in *Table 1*. The fatty acid profile and iodine value data were processed through an analysis of variance, after ShapiroWilk checked the normality of the variances and Levene's test for homoscedasticity. To evaluate the interspecific variation between the species, the genetic distance was calculated with the Euclidean distance. The comparison of means was carried out with orthogonal contrast analysis between the groups of *E. oleifera*, OxG hybrids, backcrosses, and *E. guineensis*. To determine the assignment of positive or negative coefficients to each group, the percentage of *E. guineensis* in each palm was considered as a reference, positively favoring the highest percentage of *E. guineensis* in all contrasts, corresponding to each group: *E. oleifera* from Taisha with 0%, OxG hybrids with 50%, backcross with 75% and *E. guineensis* AVROS

with 100%. Additionally, a multivariate principal components analysis was performed to select discriminant variables. For the selection of significant eigenvalues or eigenvalues, the Kaiser criterion was used, which consists of selecting the components whose eigenvalue is > = 1 and a Pearson correlation was performed on the selected variables. Data were processed with Statistical Analysis Systems software (SAS® 9.2).

RESULTS AND DISCUSSION

Bunch Oil Content

The bunch oil content obtained in the laboratory (*Table 2*), statistically shows highly significant differences in the analysis of variance between treatments (*Table 3*). The differences were corroborated with orthogonal contrasts in *Figure 1*. *Elaeis oleifera* from Taisha had an average of 10.74%, the lowest compared to hybrids, backcrosses, and *E. guineensis* AVROS, which together presented 26.58%. Likewise, there was significant differences between hybrids and backcrosses against *E. guineensis* AVROS, and between hybrids and backcrosses; however, there were no significant differences between hybrids. Regarding the low oil content of the Taisha *oleifera*, it was reported that the general yield of *E. oleifera* from different places in Latin America is much lower, with a 5.0% bunch oil ratio, compared to *E. guineensis* type *tenera* with an amount of 25.0% bunch oil (Rajanaidu *et al*., 2000). However, Rey *et al*. (2014), in their study of *oleifera* from the Amazon trapezium reported a range between 4.4% to 13.0% of bunch oil values which are nearer to those found in *E. oleifera* from Taisha. The bunch oil content of OxG hybrids was 18.0% (Ochoa *et al.*, 2013), very similar to the results of Preciado *et al.* (2011) and the hybrids derived from *oleiferas* of Cerete-Colombia was 19.3%. Nevertheless, Torres *et al*. (2014), found variations between 18.0% and 29.0% of oil in the bunch in different progenies of OxG hybrids, while Castro and Amézquita (2007) reported variations from 5.0% up to 25.0%.

In their study of OxG hybrids descending from *E. oleiferas* from Taisha, Barba and Baquero (2013) reported that there are OxG PDR-Taisha hybrids that achieved an average value of 23.39% oil in the bunches with the lowest value at 18.01%, and the average obtained from all the evaluated progenies was 20.89% of oil in bunches. The results of different bunch oil content studies validate

TABLE 2. RESULTS BY GENOTYPE OF BUNCH OIL CONTENT AND FATTY ACID PROFILE

Fatty acid composition	*Elaeis oleífera* Taisha		Hybrids						Backcross		*Elaeis guineensis* AVROS	
			Taisha x La Mé		Taisha x Yangambi		Taisha x AVROS					
C14:0	0.24	±0.1	0.20	±0.1	0.31	±0.1	0.50	±0.2	0.64	±0.2	0.78	±0.3
C16:0	27.82	±3.2	29.59	±1.3	33.60	±6.0	37.41	±2.4	39.2	±0.4	41.25	±1.9
C16:1	3.54	±1.2	0.40	±0.2	0.34	±0.1	0.63	±0.1	0.40	±0.1	0.13	±0.0
C18:0	1.42	±0.1	3.06	±1.0	3.05	±0.0	2.49	±0.3	3.27	±0.1	5.07	±0.3
C18:1n9c	39.37	±5.6	51.64	±2.0	47.95	±5.8	40.63	±4.8	41.7	±0.7	40.41	±0.1
C18:1n7c	4.16	±0.4	1.28	±0.5	1.16	±0.1	1.53	±0.1	1.15	±0.0	0.65	±0.0
C18:2n6c	21.53	±1.4	12.91	±0.9	12.76	±0.3	15.99	±2.4	12.6	±1.3	10.69	±1.9
C18:3n3	1.26	±0.3	0.43	±0.1	0.37	±0.0	0.51	±0.1	0.42	±0.0	0.23	±0.0
Others	0.60	±0.6	0.33	±0.3	0.46	±0.9	0.31	±0.1	0.60	±0.0	0.68	±0.0
SFA	30.15	±3.4	33.27	±1.6	37.34	±6.1	40.71	±2.2	43.65	±0.8	47.75	±2.0
MUFA	47.07	±4.5	53.32	±2.3	49.45	±5.8	42.79	±4.7	43.24	±0.6	41.20	±0.0
PUFA	22.78	±1.7	13.33	±0.9	13.12	±0.3	16.50	±2.5	12.99	±1.3	10.91	±2.0
IV	76.93	±2.7	69.77	±1.0	66.20	±5.6	65.47	±0.3	60.20	±1.8	55.65	±3.7
OB	10.74	±2.7	26.13	±1.6	24.89	±1.1	26.40	±3.0	25.98	±0.7	29.49	±2.2

Note: Others - Including the minor fatty acids 12:0, 15:0, 17:0, 20:0, 20:1n9; SFA - Saturated fatty acids; MUFA - Monounsaturated fatty acids; PUFA - Polyunsaturated fatty acids; IV - Iodine value; OB - Bunch oil.

TABLE 3. ANALYSIS OF VARIANCE FOR BUNCH OIL CONTENT, FATTY ACID PROFILE AND IODINE VALUE

Variable	Oil bunch	Fatty acids								Iodine value
		C14:0	C16:0	C16:1	C18:0	C18:1n9c	C18:1n7c	C18:2n6c	C18:3n3	
Mean squares	132.48	0.17	101.50	5.09	4.35	62.62	4.57	41.40	0.32	164.57
Significance	**	*	*	**	**	*	**	**	*	**
Coefficient of variation (%)	8.57	39.19	8.28	52.94	14.25	8.88	15.04	10.89	32.34	4.66
Mean	23.94	0.44	34.55	0.91	3.05	44.22	1.64	14.33	0.52	65.70

Note: C14:0 - myristic acid; C16:0 - palmitic acid; C16:1 - palmitoleic acid; C18:0 - stearic acid; C18:1n9c - oleic acid; C18:1n7c - vaccenic acid; C18:2n6c - linoleic acid; C18:3n3 - α-linolenic acid; *Significant F-Test (p<0.05); ** Highly significant F-Test (p<0.01).

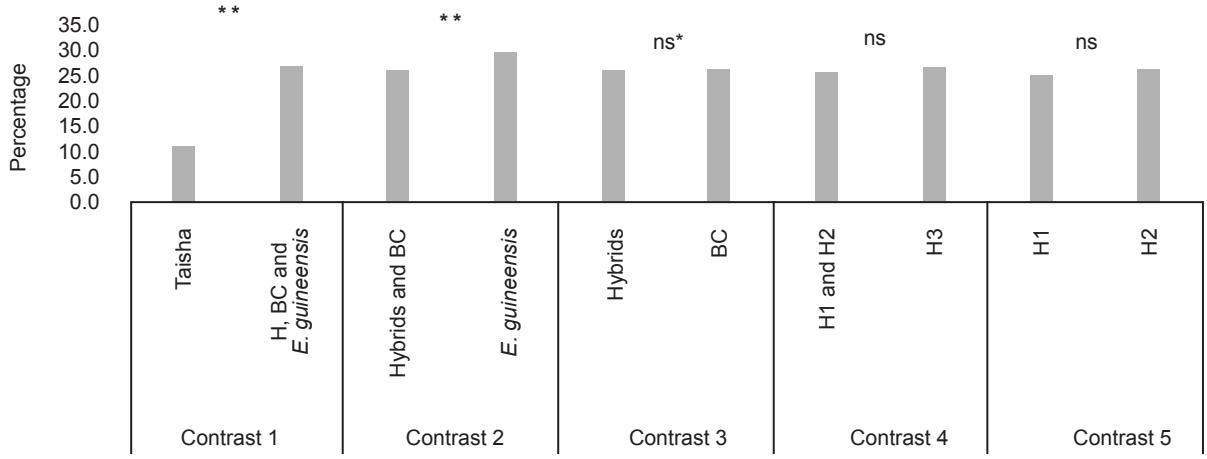

Note: ns - Non-significant F-test; ** - Significant F-Test (p<0.01).

Figure 1. Orthogonal contrasts between treatments of Elaeis oleifera *Taisha, interspecific hybrids (H), backcrosses (BC) and* Elaeis guineensis *Avros for the potential bunch oil variable.*

the results obtained in the analysed OxG hybrids, which did not present significant differences between them. However, it is worth mentioning that the oil content is influenced by the quality in the formation and composition of the bunch, fruits produced in conjunction with pollination. Meanwhile, for backcrosses Bastidas *et al*. (2007), reported 19.60% oil extraction potential in the bunch. When comparing the *E. oleifera* with hybrids, backcrosses, and *E. guineensis*, it can be seen that it has lower amount of oil extracted from the bunch, which is the reason for the difference from the other genotypes.

Fatty Acid Profile and Iodine Value

The profile of fatty acids in the mesocarp of *E. oleifera* palms from Taisha, its hybrids, backcrosses, and *E. guineensis*, made it possible to determine that the main fatty acids found were C14:0, C16:0, C16:1n7, C18:0, C18:1n9, C18:1n7, C18:2n6 and C18:3n3 (*Table 2*). Additionally, trace amount of other minor fatty acids does not exceed 0.60% and these fatty acids are C12:0, C15:0, C17:0, C20:0, and C20:1n9, which were not considered in this study. It should be noted that these fatty acids are part of the normal constitution of crude palm oil, which are predominantly even, while the odd chain saturated fatty acids pentadecanoic (C15:0) and heptadecanoic (C17:0) represent a small part of the total plasma concentration of fatty acids, especially in milk fat, meat, fish and some algae, and can occur endogenously in humans (Jenkins *et al*., 2015). These long, odd-chain fatty acids are oxidised via the same route as the even-numbered fatty acids, by beta-oxidation, starting at the carboxyl end of the chain. However, its penultimate metabolite is an acyl-CoA in which the fatty acid has five carbon atoms. When it undergoes oxidation and breakdown, the products are acetyl-CoA and propionyl CoA. Acetyl-CoA can be oxidised by entering the Krebs cycle, but

propionyl-CoA enters the Krebs cycle as succinyl-CoA for transformation to succinyl-CoA; propionyl-CoA undergoes three enzymatic processes (Nelson and Cox, 2006). For human health, C15:0 and C17:0 acids have been linked to a lower risk of type 2 diabetes and cardiovascular disease (Jenkins *et al*., 2015).

Statistical differences were found between treatments in all the variables as indicated in *Table 3* of the analysis of variance, and the orthogonal contrasts between treatments allowed us to appreciate differences between the means of the different palm genotypes according to the number of fatty acids.

The saturated fatty acids from different palms shows that in the *E. oleifera* of Taisha palmitic acid of 27.82% was different from the group of hybrids with 33.53%, backcrosses with 39.22% and *E. guineensis* with 41.21% (*Figure 2*). This observation shows a differential proportion between materials as reported by Guerin *et al*. (2016), who stated that the level of palmitic acid (16:0) in *E. oleifera* is approximately two times lower than in *E. guineensis*, which is around 25 and 45%, respectively.

For *E. oleifera* from Taisha, 28.2% palmitic acid has been reported (Lieb *et al*., 2017), while for other *E. oleifera* from Brazil, Peru, and Colombia the values were 27.5%, 37.5% and 19.4% respectively (Chaves *et al*., 2018). This indicates that there is a variation of palmitic acid content among *E. oleifera* from different localities. Likewise, palmitic acid content has been reported for OxG hybrids from *E. oleifera* from Taisha, where it was highlighted that the higher or lower palmitic acid content depends on the male parent used. The authors also reported that the hybrids from *E. guineensis* AVROS had an amount of 36.11% while those of La Mé 29.69% (Barba and Baquero, 2013). These results are similar to those obtained in this study for the Taisha x AVROS and Taisha x La Mé hybrids. Likewise, for the backcross, the percentage of C16:0 reported was intermediate with an amount between *E. oleifera* and *E. guineensis*, corroborating results from Guerin *et al*. (2016), who confirmed that for the backcrosses the amount of C16:0 was between 32% to 47%.

These differences between palm materials occur because palmitic acid represents 44.0% of the total fatty acid composition of *E. guineensis* palm oil (Sambanthamurthi *et al*., 2000), while *E. oleifera* ranges from 20.0% to 29.0% (Meunier and Boutin, 1975), with interspecific hybrids and backcrosses recorded intermediate range of their parents (Sambanthamurthi *et al*., 2000). Saturated oils such as palm oil have many advantages for the food industry due to the high oxidative stability and high melting point, which makes them a good alternative to trans fats (hydrogenated oils) (Guerin *et al*., 2016).

Elaeis oleifera from Taisha in comparison to the group of hybrids, backcrosses and *E. guineensis*, did not show statistical differences for the oleic acid, likewise, with regards to hybrids and backcrosses against *E. guineensis* and hybrids against backcrosses, did not differ in the percentage of oleic acid. However, the Taisha x AVROS hybrid with 40.63% oleic acid was statistically different from Taisha x Yangambi and Taisha x La Mé with 49.80%, while there were no significant differences between Taisha x Yangambi and Taisha x La Mé (*Figure 3*).

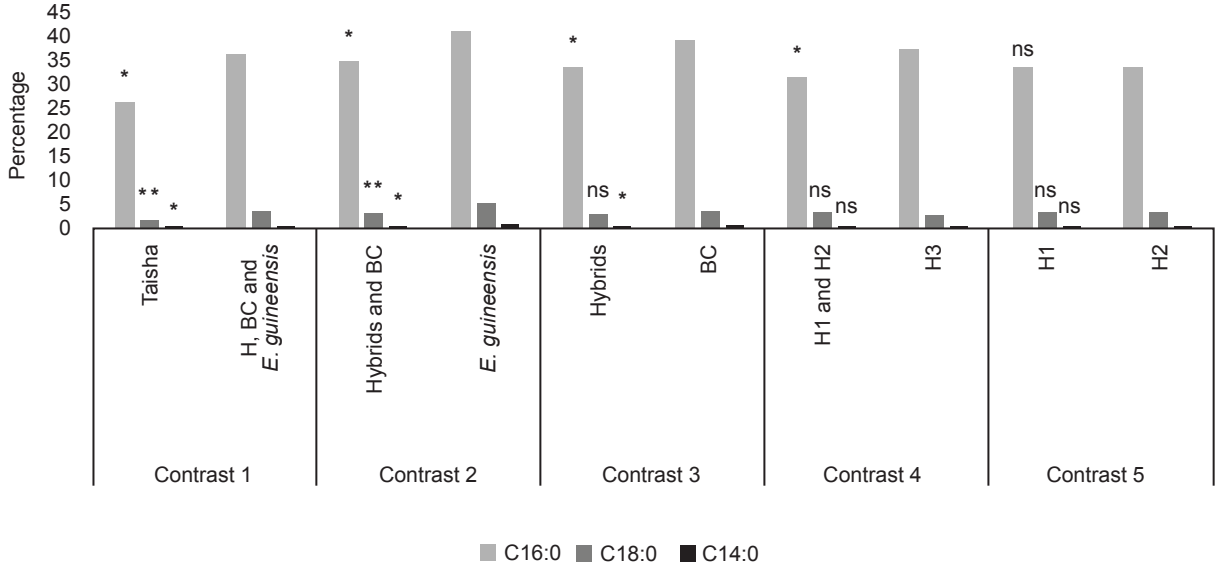

Note: ns - Non-significant F-test; * - Significant F-test (p<0.05); ** - Significant F-Test (p<0.01).

Figure 2. Orthogonal contrasts between groups of Elaeis oleifera *Taisha, hybrids (H), backcrosses (BC) and* Elaeis guineensis *for saturated fatty acids.*

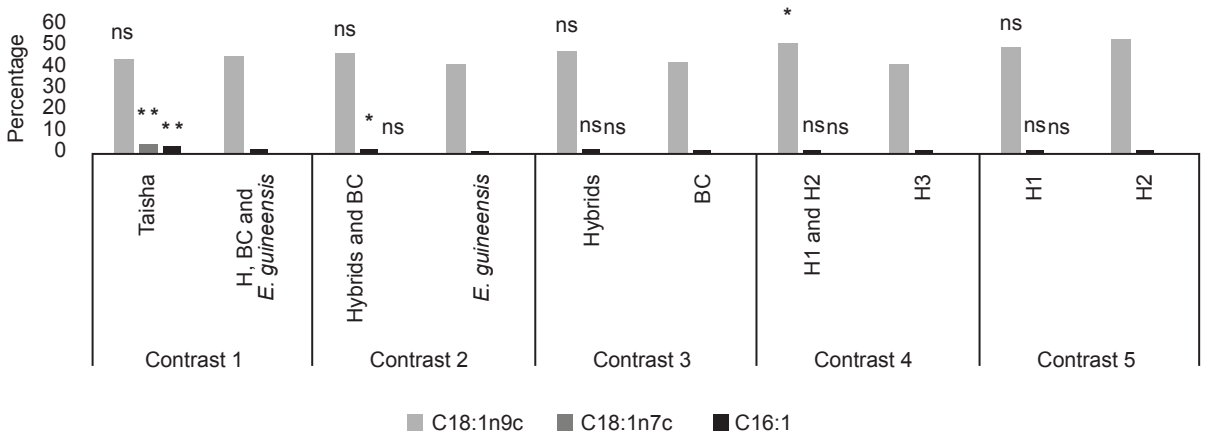

Note: ns - Non-significant F-test; * - Significant F-test (p<0.05); ** - Significant F-Test (p<0.01).

Figure 3. Orthogonal contrasts between groups of Elaeis oleifera *Taisha, hybrids (H), backcrosses (BC) and* Elaeis guineensis *for monounsaturated fatty acids.*

Other studies indicated that *E. oleifera* had oleic acid contents that varied from 47.0% to 69.0% (Montoya *et al*., 2014). Lieb *et al*. (2017), reported oleic acid contents of 36.4%, 61.7% and 46.3%, respectively, for *E. oleifera* from Taisha, Surinam and Manaus. Zapata-Munevar (2010) used the term "high oleic" referring to the high concentration of oleic acid present in the oil of interspecific hybrids OxG-cultivar Coari x La Mé (54.0% to 57.0%, by weight) and this is because of the increase in oleic acid in *oleifera* and their hybrids when compared with the *guineensis*. The oleic acid content is a character transmitted by the *oleifera*, compared to the conventional palm oil *Tenera* DxP (*E. guineensis* x *E. guineensis*), which has a concentration of this fatty acid between 36.0% and 44.0% by weight (Rincón and Martínez, 2009). Since *E. oleifera* from Taisha does not show significant differences from *E. guineensis* in the C18:1 content, hence the oil cannot be categorised as high oleic oil which is an important characteristic of interspecific hybrids.

The additive inheritance of the genes that make up the fatty acids plays an important role in the amount of C18:1 that an OxG interspecific hybrid can inherit, given that the composition of fatty acids is intermediate between the parents, attributing to co-dominant and additive inheritance (Sambanthamurthi *et al*., 2000). In the case of the Taisha x La Mé hybrid, it was the one with the highest C18:1 content compared to AVROS and Yangambi. This was probably due to the La Mé parent and this is supported by Monde *et al*. (2009) who stated that the La Mé origin has a high proportion of C18:1.

Elaeis oleifera from Taisha had the highest values of 3.55% palmitoleic and 4.09% vaccenic acids, in contrast to 0.38% and 1.15% for the group of hybrids, backcrosses, and *E. guineensis* (*Figure 3*). Ngando and Koh (1988) were the first to identify vaccenic acid in palm mesocarp and identified that in *E. oleifera* the proportion reached up to 5.00%, a value that is higher than that found in *E. oleifera* from Taisha, while for hybrids, backcrosses and *E. guineensis* the amount was even lower. *Cis*-vaccenic acid is formed by the elongation of palmitoleic acid, therefore, for these monounsaturated fatty acids such as palmitoleic there is a pharmaceutical demand because of the antithrombotic properties, while for *cis*-vaccenic acid there are industrial applications, hence it may be useful to produce these fatty acids on a large scale in the oil palm industry (Sambanthamurthi *et al*., 2000).

Regarding polyunsaturated fatty acids, the linoleic acid content of *E. oleifera* from Taisha at 21.07% was higher compared to the hybrids, backcrosses, and *E. guineensis* AVROS; although, Taisha x AVROS had a higher content compared to the other hybrids (*Figure 4*). It was reported that the percentage of linoleic acid in *E. guineensis* is 10% (Sambanthamurthi *et al*., 2000), while that of *E. oleifera* varied from 2% to 19%. This amount of linoleic acid is higher than that of *E. oleifera* from Taisha, hence this observation explained the lower amount of oleic acid in comparison with other *E. oleifera* from America. Guerin *et al*. (2016), found that the FAP1 and ACBP6 genes encode the enzyme that converts C18:1 to C18:2, adding as active variables, KASII being the only gene that opposes C16:0, and ACBP6 opposes C18:0, suggesting that cytosolic ACBP converts unsaturated fatty acids into C18:0 fatty acids during rearrangement of triacylglycerol (TAG). However, for hybrids and backcrosses, the values obtained do not differ from those of *E. guineensis*, because linoleic acid has non-additive genetic determinism in the inter and intraspecific genetic material, with *E. guineensis* being predominant over *E. oleifera* (Montoya *et al*., 2014).

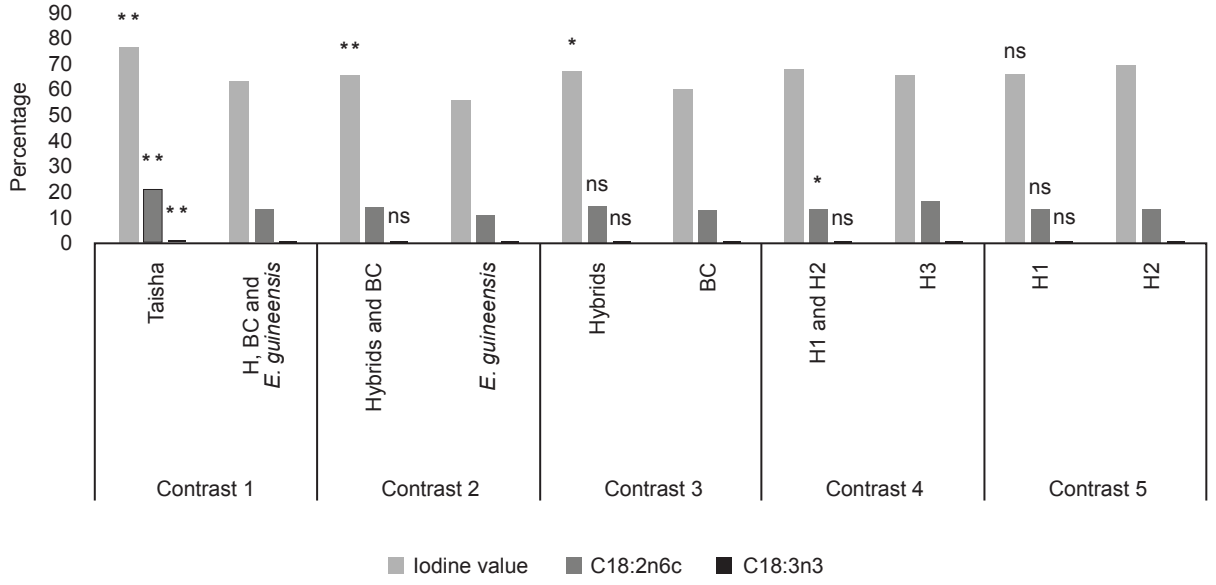

Note: ns - Non-significant F-test; * - Significant F-test (p<0.05); ** - Significant F-Test (p<0.01).

Figure 4. Orthogonal contrasts between groups of Elaeis oleiferas *Taisha, hybrids (H), backcrosses (BC) and* Elaeis guineensis *for polyunsaturated fatty acids and iodine value.*

In the same way as linoleic acid, *E. oleifera* from Taisha had the highest mean value of 1.16% of α-linolenic acid, in contrast to 0.39% for the group of hybrids, backcrosses and *E. guineensis*, and these values are within the range from 0.10% to 1.20% for α-linolenic acid (Montoya *et al*., 2014). In the treatments of *E. oleifera* from Taisha and its OxG hybrids, high proportions of linoleic acid known as omega-6 and traces of α-linolenic acid known as omega-3 were found. Fatty acids such as omega-6 and omega-3 are considered essential fatty acids since they cannot be synthesised by the human body, therefore they must be provided by the diet in an adequate proportion (Turner *et al*., 2011). They fulfill functions within the organism, such as being metabolic regulators in the cardiovascular, pulmonary, immune, secretory and reproductive systems, preserving the functionality of cell membranes and participating in genetic transcription processes (Carrillo *et al*., 2011). Meanwhile, the oleic fatty acid known as omega-9 can be formed in a small proportion by the human body, so it is considered non-essential (León *et al*., 2004). However, the α-linolenic acid found in traces in palm oil differs from a marine oil, which is characterised by its high content of omega-3 polyunsaturated fatty acids, of which the most important are eicosapentaenoic acid (C20:5) and docosahexaenoic acid (C22:6), which are easily ingested by the human body, producing beneficial effects on health and nutrition (Coultate, 2007).

The α-linolenic fatty acid of plant origin, due to its shorter carbon chain length, cannot be directly assimilated by the human body, however, once the body has them, they must act as precursors for the synthesis of C20:5 and C22:6, through a series of elongation and desaturation reactions, so that in this way it produces health benefits (León *et al*., 2004).

With regards to the iodine value, it is higher in *E. oleifera* than in *E. guineensis* because as suggested by Shah and Cha (2000) that there is a unique sesquiterpene synthase gene in the mesocarp of *E. oleifera* during 12 to 20 weeks of age, but absent in *E. guineensis* and in other tissues of both species, hence this requires additional analysis to establish the relationship with quality of American palm oil. Likewise, it has been stated that the differences in the composition of fatty acids must be related to the expression of genes encoding the enzyme KAS II and stearoyl/palmitoyl-ACP D9-desaturase (Mozzon *et al*., 2013). The pathway for fatty acid biosynthesis in which C16:0 is elongated to C18:0 by the enzyme β-ketoacyl-ACP synthase II (KASII), and C18:0 will subsequently be desaturated by atur9-stearoyl-ACP desaturase to form C18:1 (Singh *et al*., 2009). Therefore, in this study, the results reflect an increase in unsaturated fatty acids at the expense of saturated fatty acids.

According to Arias *et al*. (2015), *E. oleifera* from different locations in America, present a specific genetic structure and phenotypic variability with

different characteristics between origins, and the harvest from each country of origin contributed to the increase in total genetic diversity, where the analysis of simple sequence repeat (SSR) markers revealed a high genetic diversity (HT=0.797) and the presence of specific alleles for each country of origin of *E. oleifera*. Additionally, in the same study Arias *et al.* (2015) found that the Taisha *oleifera* are highly monomorphic, presenting a genetic similarity of 92%, compared to the rest of *E. oleifera* that presented 80%, phenotypically the families of *E. oleifera* from Taisha-Ecuador have unique qualitative traits, such as the absence of peduncular bracts, cone-shaped bunches, green immature fruits, and long stems. For this study, a dendrogram was drawn up by calculating the genetic distances between *E. oleifera* from Taisha, its descendants, and *E. guineensis* AVROS (*Figure 5*), considering that *E. oleifera* from Taisha differs from the rest of *E. oleifera* in America, either by its morphoagronomic characteristics or fatty acid profile. It is noted that *E. oleifera* from Taisha distances itself in most of the backcrosses and *E. guineensis*, being the hybrids Taisha x La Mé and Taisha x Yangambi the closest, while the hybrid Taisha x AVROS remains intermediate between *E. oleifera* from Taisha and the *E. guineensis*.

Selection and Association of Variables for Oil Content, Fatty Acid Profile and Iodine Value

In the analysis of principal components (APC) for the selection of the significant eigenvalues, the Kaiser criterion was used, indicating that the first four components are the most important because they present an eigenvalue greater than 1 and, in turn, accumulate 99.67% of the variance total, in their order the first two components accumulate 96.67% of the variance (*Table 4*). Regarding the discrimination of the variables by importance in PC1 with 72.55% of the total variance explained, the iodine value was the variable that contributed most positively to the component, followed by linoleic acid; whereas, bunch oil and palmitic acid were the two variables that contributed most negatively. The iodine value is the measure that determines the number of unsaturations that the triglycerides of the oil have, related to the content of mono and polyunsaturated fatty acids such as linoleic acid (Rincón and Martínez, 2009), which is why the iodine value and linoleic acid are related. In the case of CPO, high iodine value values imply higher olein yields during fractionation. Consequently, the iodine number value will be higher due to the presence of the main oleic acid and linoleic acid.

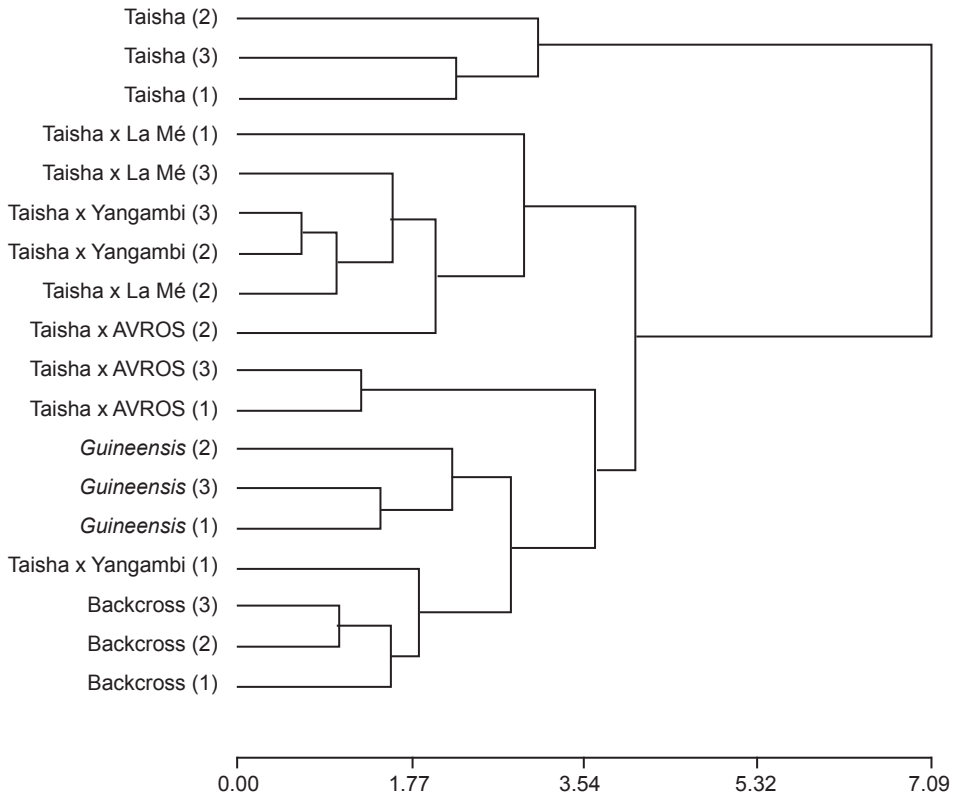

Figure 5. Interspecific variation between genotypes, shown with genetic distances.

TABLE 4. ASSOCIATION BETWEEN BUNCH OIL VARIABLES, FATTY ACID PROFILE AND IODINE VALUE

Pearson correlation coefficients				
Variable	**C18:1n9c**	**C18:2n6c**	**Iodine value**	**Bunch oil**
C16:0	-0.5604 *	-0.4886 *	-0.9316 **	0.5899 *
C18:1n9c	1.0000	-0.4051 ns	0.3656 ns	0.2740 ns
C18:2n6c		1.0000	0.7028 *	-0.9078 **
Iodine value			1.0000	-0.7103 *

Note: Number of observations = 22; ns - Non-significant F-test; * - Significant F-Test (p<0.05); ** - Significant F-Test (p<0.01).

In addition, the first component allows us to interpret that at a higher iodine value and linoleic acid, the genotypes register low bunch oil and palmitic acid values, however, this correlation is likely related to the differences between *E. guineensis* and *E. oleifera*, and the differences in oil in a bunch between materials may be linked to factors unrelated to the characteristics of the oil, such as the percentages of mesocarp, fruit in the bunch, among others. In a different study involving 1182 *E. guineensis* palms from 16 different sibling families, the iodine value was positively correlated (p<0.01) with the percentage of oil in the mesocarp (Billotte *et al*., 2010). In this study a factor to be considered were palms of different origins such as *E. oleifera* from Taisha, its OxG hybrids, backcrosses, and *E. guineensis*, which showed different behaviours in the content of fatty acids, iodine value, and oil content. However, in the olive tree (*Olea europaea* L.), the correlations between the characteristics of the fruit, the components of the oil yield, and the composition of the fatty acids in the progenies of different crosses showed significant positive relationships between the oil content and percentage of oleic acid, which are negatively correlated with palmitic, palmitoleic, and linoleic acid contents (León *et al*., 2004).

For CP2 with 24.12%, the oleic acid variable was the one that contributed positively and importantly to the component to discriminate the genotypes. Oleic acid being the main unsaturated fatty acid for *E. oleifera* from Taisha, hence the mesocarp oil contains higher oleic and linoleic acid, and lower content of palmitic acid and other unsaturated acids. According to Sambanthamurrhi *et al*. (2000), oleic acid is formed by the aerobic desaturation of stearic acid by the action of the enzyme Δ9 stearoyl ACP desaturase. The oleate desaturase is active in the conversion of oleic acid into linoleic acid, which is the reason for the main components to indicate that when a higher percentage of oleic acid was present, linoleic acid was low, but the association was not significant.

It has been reported that β-ketoacyl ACP synthase II (KAS II) is a condensing enzyme exclusively responsible for the conversion of palmitic acid to stearic acid, therefore, there is considerable interest in this enzyme regarding its role in determining the ratio of C16 to C18 fatty acids (Sambanthamurthi *et al*., 2000). In this study, palmitic acid presented a significant negative correlation with oleic and linoleic acids, as argued by Singh *et al*. (2009), and this is due to the enzyme stearoyl ACP desaturase which even though is very specific for the conversion of C18:0 to C18:1, it is also known to sometimes act on C16:0 as a poor substrate for the conversion to C16:1; hence explained the strong negative correlation (r=-0.734) between C18:0 and C16:1.

The variables discriminated in the first two main components were correlated, indicating that palmitic acid presents a significant negative correlation with oleic acid, linoleic acid, and iodine value, while with bunch oil the correlation is positive. Inversely, while bunch oil was positively correlated with palmitic acid, its correlation is negative with oleic and linoleic fatty acids.

The oleic and palmitic fatty acids, which are the most important in the mesocarp oil of the oil palm fruit, presented a significant negative correlation, however, it has been shown that the activities of palmitoyl ACP thioesterase and oleoyl ACP thioesterase are two separate proteins, and therefore, they could be independently susceptible to genetic manipulation (Sambanthamurthi *et al*., 2000). However, Salas and Ohlrogge (2002), report that acyl-ACP thioesterases are divided into two classes, called FATA and FATB, where FATA enzymes preferentially hydrolyse 18:1-ACP while 16:0-ACP is the preferential substrate of the FATB enzymes. Additionally, Guerin *et al*. (2016) state that in plants, KASII is responsible for the elongation of 16:0ACP to 18:0-ACP. Thus, there is competition for the 16:0 substrate between acyl-ACP thioesterases that are capable of hydrolysing 16:0-ACP and KASII. This fact suggested that low transcription of KASII is the main contributing factor in the accumulation of C16:0.

The positive correlation between iodine value and linoleic acid of 0.700, as well as the negative correlation between iodine value and palmitic acid of -0.930 reported in this study, was similar to those reported by Singh *et al*. (2009), where the iodine value showed a correlation of 0.733 and 0.517 for oleic and linoleic acids, respectively, whereas the palmitic acid showed a correlation of -0.879. Moreover, the extracted bunch oil content in terms of percentages showed a positive correlation with palmitic acid and a negative correlation with linoleic acid and iodine value, indicating that a better quality of the oil is linked to the proportion of unsaturated fatty acids, and that it opposes the higher content of oil that is correlated with saturated fatty acids.

CONCLUSION

Improving the quality of palm oil with a higher concentration of oleic acid is not feasible using only *E. oleifera* from Taisha, hence it is necessary to obtain OxG interspecific hybrids, careful selection of the male parent *E. guineensis*, preferably with an outstanding amount of oleic acid such as the material of La Mé origin. Likewise, for the improvement of *E. oleifera* from Taisha, it can be crossed with *E. oleifera* from other American origins that have a high concentration of oleic acid, to preserve the good agronomic characteristics of Taisha such as long peduncle, flower free of spathes, and a high number of fertile fruits in the bunch.

ACKNOWLEDGEMENT

The authors would like to thank the company Palmar del Río for allowing the work to be carried out at its facilities and authorising the publication of the article, especially Engineers Juan Salgado and Fernando Muirragui. Similarly, we thank the entire team of the Research and Development Unit of Palmar del Río. This research was financed by the company Palmar del Río.

REFERENCES

AOCS (1994). Official and recommended methods of the American Oil Chemists' Society. American Oil Chemists' Society. Champaign, IL, USA. 149 p.

AOCS (1997). Official methods and recommended practices of American Oil Chemist' Society method Ce 1-62. *Fatty acid composition by gas chromatography.* AOCS Press. Champaign, ILL, USA. 198 pp.

Arias, D; Gonzalez, M; Prada, F; Ayala-Diaz, I; Montoya, C; Daza, E and Romero, H M (2015). Genetic and phenotypic diversity of natural American oil palm (*Elaeis oleifera* (HBK) Cortés) accessions. *Tree Genetics & Genomes*, *111*: 122. DOI: 10.1007/s11295-015-0946-y.

Barba, J (2016). Introgresión de genes *E. guineensis* en híbridos interespecíficos OxG para recuperar la fertilidad del polen y otras características deseables en palma de aceite. *Revista Palmas, 37 (Especial Tomo I):* 285-293.

Barba, J and Baquero, Y (2013). Hibridos OxG obtenidos a partir de oleíferas Taisha Palmar del Río - Ecuador. Variedad-PDR (Taisha x Avros). *Revista Palmas, 34*, 315-325.

Bastidas, S; Peña, E; Reyes, R; Pérez, J and Tolosa, W (2007). Comportamiento agronómico del cultivar híbrido RC1 de Palma de aceite (*Elaeis oleífera*). *Corpoica. Ciencia y Tecnología Agropecuaria, 8(1)*: 5-11.

Billotte, N; Jourjon, M F; Marseillac, N; Berger, A; Flori, A; Asmady, H; Adon, B; Singh, R; Nouy, B; Potier, F; Cheah, S C; Rohde, W; Ritter, E; Courtois, B; Charrier, A and Mangin, B (2010). QTL detection by multi-parent linkage mapping in oil palm (*Elaeis guineensis* Jacq.). *Theor. Appl. Genet., 120*: 1673-1687. DOI: 10.1007/s00122-010-1284-y.

Carrillo, L; Dalmau, J; Martínez, J; Solà, A and Pérez, SF (2011). Grasas de la dieta y la salud cardiovascular. *Anales de Pediatría. 74*: 192-196.

Castro, J F and Amézquita, M M (2007). Experiencias con los materiales OxG en Unipalma S.A. (CD-ROM). Taller técnico científico sobre avances y resultados en los procesos de investigación y manejo del complejo pudrición del cogollo. Tumaco-Colombia; 24 y 25 octubre de 2007.

Chaves, G; Ligarreto-Moreno, G and Cayon-Salinas, G (2018). Physicochemical characterization of bunches from American oil palm (*Elaeis oleífera* H.B.K. Cortes) and their hybrids with African oil palm (*Elaeis guineensis* Jacq.). *Plant Breed. Plant Genet. Resour. Acta Agron., 67*(1): 170-178. DOI: 10.15446/acag.v67n1.62028.

Corley, R and Tinker, P (2009). La palma de aceite (Vol. 4). Bogotá, Colombia: (B. P. Ltda., Ed., & E. E. (Federación Nacional de Cultivadores de Palma de Aceite, Trad.).

Coultate, T (2007). Manual de Química y bioquímica de los alimentos. Tercera ed, ed. S.A. Acribia. Zaragoza (España). 446 p.

Guerin, C; Thierry, J; Serret, J; Lashermes, P and Vaissayre, V (2016). Gene coexpression network analysis of oil biosynthesis in an interspecific backcross of oil palm. *Plant J., 87*: 423-441. DOI: 10.1111/tpj.13208.

Hardon, J (1969). Interspecific hybrids in the genus *Elaeis*. II. Vegetative growth and yield of hybrids *E. guineensis* x *E. oleífera*. *Euphytica., 18:* 372-379.

Jenkins, B; West, J A and Koulman, A (2015). A review of odd-chain fatty acid metabolism and the role of pentadecanoic acid (C15:0) and heptadecanoic acid (C17:0) in health and disease. *Molecules*, *20*: 2425-2444. DOI: 10.3390/molecules20022425.

León, L; Martín, L M and Rallo, L (2004). Phenotypic correlations among agronomic traits

in olive progenies. *J. Amer. Soc. Hort. Sci., 129*: 271-276.

Lieb, V M; Kerfers, M R; Kronmuller, A; Esquivel, P; Alvarado, A; Jimenez, V M; Schmarr, H G; Carle, R; Schweiggert, R M and Steingass, C B (2017). Characterization of mesocarp and kernel lipids from *Elaeis guineensis* Jacq., *Elaeis oleífera* [Kunth] Cortes, and their interspecific hybrids. *J. Agric. Food Chem., 65(18)*: 3617-3626. DOI: 10.1021/acs.jafc.7b00604.

Meunier, J and Boutin, D (1975). L´Elaeis melanococca et l'hybride *E. melanococca* x *E. guineensis*. *Premieres donnees. Oleagineux*.

Monde, A A; Michel, F; Carbonneau, M A; Tiahou, G; Vernet, M H; Eymard-Duvernay, S; Badiou, S; Adon, B; Konan, E; Sess, D and Cristol, J P (2009). Comparative study of fatty acid composition, vitamin E and carotenoid contents of palm oils from four varieties of oil palm from Coˆte d'Ivoire. *J. Sci. Food Agric. 89*: 2535-2540. DOI: 10.1002/jsfa.3740.

Montoya, C; Cochard, B; Flori, A; Cros, D; Lopes, R; Cuellar, T; Espeout, S; Syaputra, I; Villeneuve, P; Pina, M; Ritter, E; Leroy, T; Billotte, N and Wu, R (2014). Genetic architecture of palm oil fatty acid composition in cultivated oil palm (*Elaeis guineensis* Jacq.) compared to its wild relative *E. oleífera* (H.B.K) Cortes. *PLoS ONE, 9*: 1-13. DOI: 10.1371/journal.pone.0095412.

Mozzon, M; Pacetti, D; Lucci, P; Balzano, M and Frega, N G (2013). Crude palm oil from interspecific hybrid *Elaeis oleífera* × *Elaeis guineensis*: Fatty acid regiodistribution and molecular species of glycerides. *Food Chem., 141*: 245-252. DOI: 10.1016/j.foodchem.2013.03.016.

Nelson, D L and Cox, M M (2006). Lehninger. *Principios de Bioquímica*. 4th edition. Omega, Barcelona. 642 pp.

Ngando, S and Koh, H F (1988). Detection of *cis*-vaccenic acid in palm oil by 13C NMR spectroscopy. *Lipids, 23*: 140-143.

Ochoa, I; Suárez, C and Cayón, G (2013). Desarrollo y maduración de frutos en palma de aceite *Elaeis guineensis* Jacq. e híbridos OxG (*E. oleífera* x *E. guineensis*) de Unipalma S.A. *Revista Palmas, 34(1)*: 326-336.

Prada, F and Romero, H M (2012). Muestreo y análisis de racimos en el cultivo de la palma de aceite. *Tecnologías para la agroindustria de la palma de aceite: Guía para facilitadores.* Bogotá, D.C. (Colombia). 159 pp.

Preciado, C; Bastidas, S; Betancourth, C; Peña, E and Reyes, R (2011). Predicción y control de la cosecha en el híbrido interespecífico *Elaeis oleífera* x *Elaeis guineensis*. *Corpoica Ciencia, Tecnolia, Agropecuaria, 12(1)*: 5-12.

Rajanaidu, N; Rao, V and Tan, B K (1983). Analysis of fatty acids composition (FAC) in *Elaeis guineensis*, *Elaeis oleífera*, their hybrids and its implications in breeding. *PORIM Bulletin, 7*: 9-20.

Rajanaidu, N; Kushairi, A; Rafii, M; Mohd-Din, A; Maizura, I and Jalani, B S (2000). *Oil Palm Breeding and Genetic Resources* (Basiron, Y; Jalani, B S and Chan, K W eds.). MPOB, Bangi. 171 pp.

Rey, L; Gómez, P; Ayala, I; Delgado, W and Rocha, P (2014). Colecciones genéticas de palma de aceite *Elaeis guineensis* (Jacq.) y *Elaeis oleífera* (H.B.K.) de Cenipalma: Características de importancia para el sector palmicultor. *Revista Palmas, 25 No. Especial.*

Rincón, S and Martínez, D (2009). Análisis de las propiedades del aceite de palma en el desarrollo de su industria. *Revista Palmas, 30(2):* 11-24.

Salas, J J and Ohlrogge, J B (2002). Characterization of substrate specificity of plant FatA and FatB acyl-ACP thioesterases. *Arch. Biochem. Biophys., 403*: 25-34.

Sambanthamurthi, R; Sundram, K; and Tan, Y A (2000). Chemistry and biochemistry of palm oil. *Prog. Lipid Res., 39*: 507-558.

Shah, F H and Cha T S A (2000). A mesocarp-and species-specific cDNA clone from oil palm encodes for sesquiterpene synthase. *Plant Sci., 154(2)*: 153-160.

Singh, R; Tan, S G; Panandam, J M; Rahman, A R; Ooi, L C L; Low, E T L; Sharma, M; Jansen, J and Cheah, S C (2009). Mapping quantitative trait loci (QTLs) for fatty acid composition in an interspecific cross of oil palm. *BMC Plant Biol., 9*: 114. DOI: 10.1186/1471-2229-9-114.

Torres, V M; Rey, B L; Gelves, R F and Santacruz, L (2014). Evaluación del comportamiento de los híbridos interespecíficos *Elaeis oleífera* x *Elaeis guineensis* en la plantación Guaicaramo S.A. *Revista Palmas, 25(Número especial, Tomo II)*: 350-357.

Turner, N; Mitchell, T; Else, P and Hulbert, A J (2011). The ω-3 and ω-6 fats in meals: Aproposal for a simple new label. *Nutrition., 27*: 719-726.

Oil World (2020). Oil world anual 2017. http://www.oilworld.biz/app.php, accessed on 15 March 2020.

Zapata-Munévar, L E (2010). *S*ituación y perspectivas del aceite de palma alto oleico OxG en Colombia. *Revista Palmas*, *31(Número especial)*: 349-353.

Journal of Oil Palm Research Vol. 35 (3) September 2023 p. 517-527
DOI: https://doi.org/10.21894/jopr.2022.0068

EXPLORING SENTINEL-2 SATELLITE IMAGERY-BASED VEGETATION INDICES FOR CLASSIFYING HEALTHY AND DISEASED OIL PALM TREES

NARISSARA NUTHAMMACHOT[1]* and DIMITRIS STRATOULIAS[2]

ABSTRACT

*The cultivation of oil palm (*Elaeis guineensis *Jacq.) trees is one of the most important agricultural activities and a major sector of economic development in Thailand. However, oil palm trees are susceptible to diseases that can decrease the profitability of the business. Decreasing productivity sometimes triggers an expansion of the cultivated area, which is often negatively affecting surrounding natural habitats. Remote sensing technology has increasingly been used for investigating, detecting and mapping plant related traits. This study aims to use concurrently acquired Sentinel-2 satellite imagery, Unmanned Aerial Vehicle (UAV) field survey and ground observation data to identify the characteristics of oil palm trees based on three controlled sites (namely healthy, diseased and mixed oil palm tree areas). The GNDVI, NDVI, NDI45, RVI, MSAVI and MTCI vegetation indices (VI) were used as a predictor of plant biomass and indicator of oil palm tree disturbance. A linear regression model was applied to each of the derived VIs to determine the index with the strongest relationship to biomass for each of the three sites. The outcome of this study showed; (1) that the most effective indicators were NDVI for the healthy oil palm area and RVI index for the diseased oil palm area (R^2 = 0.48 and 0.68, respectively), and (2) the MSAVI provided the best R^2 value in patterns correlated to the greenness of vegetation for the mixed oil palm tree areas (R^2 = 0.44). Moreover, the results show that the overall Support Vector Machine (SVM) classification accuracy is 72.97%, with the kappa coefficient is 0.56 for the healthy oil palm area, 64.16% and 0.40 for the diseased oil palm area and 50.00% and 0.37 for the mixed oil palm area. A concurrent UAV survey based on the visible and Visible Atmospherically Resistant Index (VARI) bands and SVM classification provided higher overall accuracy compared to the Sentinel-2 SVM classification.*

Keywords: oil palm diseases, Sentinel-2 Support Vector Machine (SVM) classification, Unmanned Aerial Vehicle (UAV), vegetation indices.

Received: 25 January 2022**; Accepted:** 8 August 2022**; Published online:** 19 October 2022.

INTRODUCTION

Oil palm has been a major Southeast Asian agricultural commodity, with an essential economic contribution especially in the south of Thailand. However, many diseases such as the *Ganoderma boninense* have considerably infected oil palm crops in different regions (Naher *et al.*, 2013). The early identification of diseases is an important first step to controlling and preventing potential outbreaks and decreasing the environmental effect of agrochemicals and economic losses. The traditional methods to halt outbreaks and to detect symptoms inherit have several disadvantages such as the fact that they are time consuming and labour intensive. Therefore, the application of satellite and aerial remote sensing has been widely used to identify automatically oil palms, map the extent and estimate the yield (Cheng

[1] Faculty of Environmental Management, Prince of Songkla University, Hatyai, Songkhla 90110, Thailand.

[2] Asian Disaster Preparedness Center, 24th Floor, SM Tower, 979/69-70 Paholyothin Road, Phyathai, Bangkok 10400, Thailand.

* *Corresponding author e-mail: narissara.n@psu.ac.th*

et al., 2018; 2019; Chong *et al.,* 2017; Yusoff *et al.,* 2017). Remote sensors can detect the energy from the spectral reflection of plants, based on which, the condition of the oil palm leaf can be assessed. Principally the spectral information from the satellite data associates with the biophysical properties of the crops. Several studies have shown that multispectral remote sensing data can discriminate between healthy and diseased oil palm trees. For instance, Malinee *et al.* (2021) detected oil palm disease in Krabi Province, Thailand using a WorldView-2 satellite image with an overall maximum likelihood classification accuracy of 85.98% and kappa coefficient of 0.71.

Santoso *et al.* (2011) selected QuickBird imagery to identify and map basal stem rot disease in oil palms. All the vegetation indices showed different accuracy from diverse palm age fields. The accuracy performance for 15 and 18 years old oil palms was only 35% while in the fields of 10 and 21 years old palms with an accuracy of 62% and 67% respectively were estimated. Santoso *et al.* (2017) mapped Basal Stem Rot (BSR) disease in oil palms using QuickBird imagery. They found that the Random Forest (RF) model performed the best at predicting, classifying, and mapping oil palm trees.

Izzuddin *et al.* (2018) used the airborne hyperspectral image for detecting *Ganoderma* disease in oil palm trees. Five VIs were selected in this study. The VI provided low to moderate percentages (30%-40%) of accuracy classification for oil palm disease. Kamal *et al.* (2018) classified leaf disease symptoms of oil palm trees. A SVM algorithm was applied for *Chimaera* and *Anthracnose* diseases classification. The SVM classification accuracy for *Chimaera* was 97% while the accuracy for *Anthracnose* was 95%. With regard to the classification algorithm, SVM is a non-parametric classifier with increasing popularity and application in remote sensing. SVM has been applied on remotely sensed data in crop related studies and proved useful as they provide high classification accuracy (Chaware *et al.,* 2017; Kamal *et al.,* 2018; Masazhar *et al.,* 2017).

For the above reasons, the SVM classification algorithm was selected for classified healthy and diseased oil palm plants in the current study which deals with the problem of discriminating between diseased and healthy oil palm trees based on the high-resolution multi-spectral image. Therefore, a novel algorithm is suggested. The model of the proposed method is to use the VI with the highest discriminatory power in distinguishing between diseased oil palm and healthy oil palm objects. The proposed method is useful because some VI cannot give good results from certain satellite images and have limited robustness. For example, NDVI indices cannot identify the true phenology of plants because the radiometric information cannot be computed.

The objectives of the current paper are (i) to investigate the correlation of popular VIs by demonstrating the discriminatory power between diseased and healthy oil palm trees, (ii) to detect the plant diseases in oil palms based on Sentinel-2 satellite imagery, (iii) to compare the accuracy of SVM classification when applied on Sentinel-2 satellite and Unmanned Aerial Vehicle (UAV) images, and (iv) to validate two sample data groups Visible Atmospherically Resistant Index (VARI) of UAV and VARI of Sentinel-2 data using regression modelling. The results from this study can be beneficial for developing disease management programmes and infection monitoring systems.

MATERIALS AND METHODS

Study Area

The study area is situated in Chana district, Songkhla province, Thailand which is located around the geographical coordinates 6° 54′ 51″ N and 100° 44′ 26″ E as depicted in *Figure 1*. The climate of southern Thailand is characterised by a rainy season which lasts from May to January of the following year. The average annual temperature is approximately 26.8°C and the average annual rainfall is 1622 mm. These conditions are suitable for the cultivation of oil palm which is the dominant plantation crop in the greater area. The areas sampled were characterised by flat terrain and commercial oil palm plantations with no nutrient deficiencies and pest infestation.

Field Data Collection

Both diseased and healthy oil palm tree samples were selected based on random sampling on the same day (12th June 2020). In study area 1 (healthy oil palm trees), the age of the trees was 5 years and 50 points were selected, in study area 2 (diseased oil palm trees), the age of the trees was 13 years, and 55 points were selected and in study area 3 (mixed diseased and healthy oil palm trees), the age of the trees was 15 years and 100 points were collected. These collected points were described and depicted as point data in *Figure 2.* The distance between oil palm trees was approximately 9 m for all sites. The geopositioned of the tree points were recorded with a Global Navigation Satellite System (GNSS) device and the health status of each oil palm was inspected and evaluated by an experienced farmer. A random selection of 70% of reference points was used as training data for classification and the remaining 30% of samples were used as the validation data for each site. Furthermore, a UAV was used to fly over and acquire images of these areas for validation purposes. DroneDeploy software (14 day trial version) was used to mosaic the images collected and analyse tree health (*Figure 2).* The UAV flew at an altitude of approximately 50 m and covered the entire area.

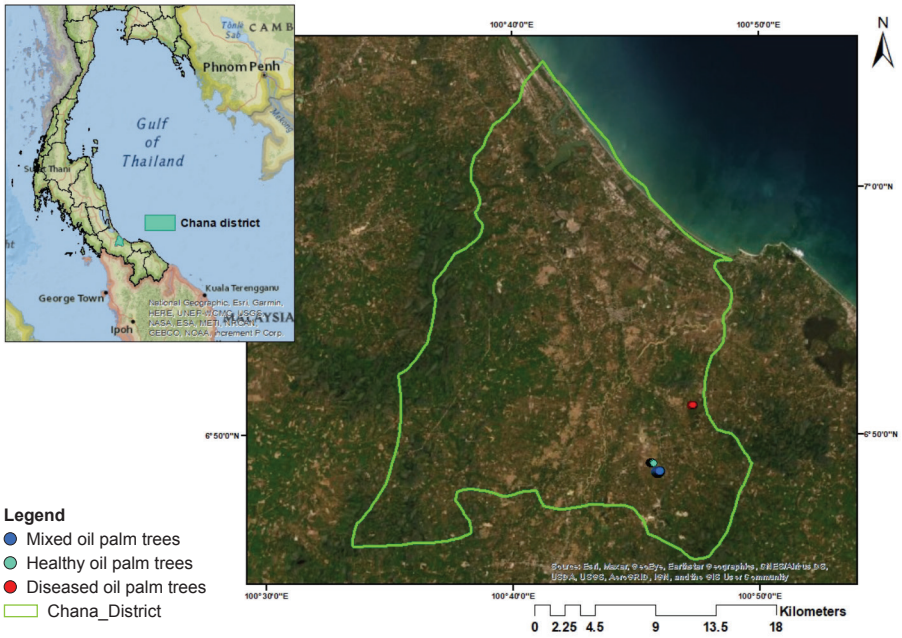

Figure 1. Location of the oil palm planted areas in Chana district, Songkhla province, Thailand.

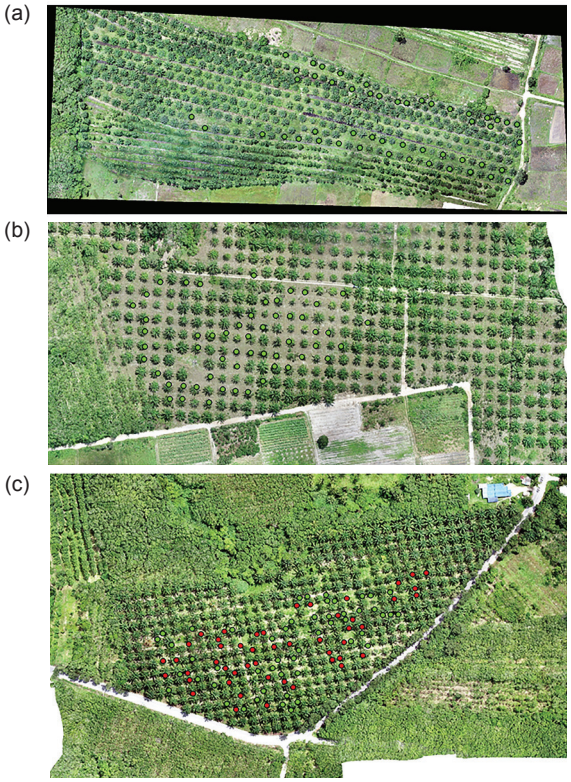

Note: Red point - diseased oil palm; Green point - healthy oil palm.

Figure 2. Sample points of each area and the photos from the UAV (a) healthy oil palm sample points and UAV image, (b) diseased oil palm sample points and UAV image, (c) mixed oil palm sample points and UAV image.

Unmanned Aerial Vehicle (UAV)

A DJI Phantom 4 Pro quadcopter (Da-Jiang Innovations (DJI), China) was used during the survey flights to capture RGB images. The internal RGB device camera uses a Sony 1" complementary metal-oxide-semiconductor (CMOS) sensor with 20M effective pixels. The embedded GNSS and a navigation control system ascribe high positional accuracy and stable flight characteristics to the platform (DJI, 2017).

Data acquisition. Three inspections were carried out over healthy, disease and mix (healthy and diseases) oil palm planted areas. The date, 12th June 2020 was selected, with a clear sky and no rain. For the healthy oil palm tree site, the entire area was covered with 160 images acquired at 48.768 m altitude. Likewise, the diseased oil palm tree and mixed oil palm tree sites covered an area of 0.0627 and 0.2300 km^2 respectively; 154 and 142 images were collected at 51.816 and 51.816 m altitude, respectively. The spatial resolution of the UAV images was approximately 50 mm. Based on visual interpretation of the UAV high spatial resolution images, oil palm trees were recognised by visible symptoms of the disease manifestation. However, the mixed oil palm planted area showed a slightly different in their appearance. More details regarding each site and flight conditions are presented in *Table 1.*

Data processing and analysis. The RGB imagery datasets were processed using the DroneDeploy software. The workflow was implemented with the following major steps: i) plan a mapping flight and fly; ii) upload images; iii) mosaic images; iv) export images. Further processing was carried out in SNAP software version 6.0. The VARI was adjusted to the RGB data as in Equation (1). VARI is used to

TABLE 1. AERIAL PHOTOS CAPTURED BY DJI PHANTOM 4 PRO AT EACH SITE

Site	Date	Images collected	Area (km^2)	Age of oil palm tree (years)	The average height of oil palm trees (m)	UAV flight altitude (m)
Healthy oil palm tree	12th June 2020	160	0.0672	5	4.0	48.768
Diseased oil palm tree	12th June 2020	154	0.0627	13	7.5	51.816
Mixed oil palm tree	12th June 2020	142	0.2300	15	11.0	51.816

evaluate the fraction of vegetation in a scene with low sensitivity to atmospheric effects. It is suitable for monitoring low-altitude drone imagery (ESRI, 2021).

$$VARI = \frac{Green–Red}{Green+Red–Blue} \quad (1)$$

A supervised classification approach was adopted to classify the RGB and VARI bands of the drone imagery in each site using the QGIS software and based on 5 classes namely disease, healthy, forest, road and others.

Sentinel-2 Data Collection and Pre-processing

An image from the Sentinel-2B satellite launched on 7th March 2017 is used in this study. The data are available and can be downloaded from the European Space Agency (ESA) website (https://sentinel.esa.int) (ESA, 2021). The Sentinel-2B satellite carries the high quality Multispectral Instrument (MSI) capable of recording information in 13 spectral bands at 3 nominal spatial resolutions (visible (VIS) – Near Infrared (NIR) bands at 10 m, red-edge, narrow NIR and SWIR bands at 20 m, and three bands (Coastal aerosol, Water Vapor, and Cirrus) at 60 m spatial resolution) (ESA, 2015). The Sentinel-2 mission has 10 day revisit frequency at the equator with one satellite and 5 days with 2 satellites under cloud-free conditions which results in 2-3 days at mid-latitudes. The Sentinel-2B image was acquired on 25 June 2020 and provided a clear image of the study area. It was downloaded at level-1C (Top of Atmosphere) with 13 spectral bands. We selected an image in June (25th June 2020) based on the condition of disease and non-disease oil palm trees. The Sentinel Application Platform (SNAP), free software developed by ESA, was used to pre-process the data and calculate the related spectral indices. Pre-processing of the Sentinel-2 image was spatially re-sampled and subset to the area of interest. The spectral reflectance of bands B3 (Green)-B8A (NIR) was used to predict the vegetation indices estimation. Ten bands (B2-B8A, B11 and B12) were selected to classify the images.

Methodology

Radiometric correction. A clear and cloud-free Sentinel-2 image with 13 spectral bands acquired on 25th Jun 2020 was downloaded at level 1C Top of Atmosphere (TOA) reflectance. L1C data is not atmospherically corrected, therefore the Atmospheric Rayleigh Scattering Correction was selected to convert to Bottom of Atmosphere (BOA) reflectance.

Geometric correction. Level-1C processing includes ortho-rectification and spatial registration on a global reference system with sub-pixel accuracy. The next step of the pre-processing was to do resampling process. This process was done to change spatial resolution images. All images were resampled to 10 m spatial resolution using the nearest neighbour method. The images were subset around the selected three areas of interest to computationally speed up the process.

Vegetation indices. The multispectral bands of visible and NIR were estimated for vegetation indices (Askar *et al.*, 2018). In this study, we used the NIR, Red and Green bands to calculate all indices using the SNAP software version 6.0. The formulas of the vegetation indices selected are presented in *Table 2*. In order to assess the accuracy of the indices, the statistical distributions of the healthy and diseased oil palm tree classes were investigated. The scattering correlation plots between the VARI of UAV and all indices of Sentinel-2 spectral values were calculated. Linear regression was selected to estimate the best parameters from Sentinel-2 satellite data. The coefficient of determination or R^2 indicates that the regression model is in fit performance.

Support Vector Machine (SVM) Classification

Diseased and healthy oil palm trees maps in each area were classified from the Sentinel-2 and UAV images with the SVM classification algorithm. The Sentinel-2 image pattern was classified on 10 bands composite and based on visual interpretation. The Sentinel-2 image from the diseased oil palm planted area was classified into diseased oil palm trees, forest, road and others while the UAV image was classified as diseased oil palm trees, forest, background, road and others. Sentinel-2 image from healthy oil palm trees area was classified into healthy oil palm trees, forest, road and others while

TABLE 2. THE VEGETATION INDICES AND MATHEMATICAL FORMULAS USED IN THIS STUDY

Indices	Formula	References
Green normalised difference vegetation index (GNDVI)	(NIR − GREEN)/(NIR + GREEN)	Gitelson *et al.* (1996)
Normalised difference vegetation index (NDVI)	(NIR − RED)/(NIR + RED)	Tucker (1979)
The normalised difference index (NDI45)	(NIR-RED)/(NIR+RED) Where NIR = B5 and RED = B4	Delegido *et al.* (2011)
The ratio vegetation index (RVI)	RVI = (NIR/RED)	Zhang *et al.* (2021)
The modified soil adjusted vegetation index (MSAVI)	(2 * NIR + 1 – sqrt ((2 * NIR + 1)^2 – 8 * (NIR - R))) / 2	Qi *et al.* (1994)
The meris terrestrial chlorophyll index (MTCI)	(NIR-RED2)/(RED2-RED1) Where NIR = B6, RED2 = B5, RED1 = B4	Pałaś *et al.* (2020)

UAV was classified to healthy oil palm trees, forest, background, road and others. For mixed oil palm planted area, it was classified into five categories namely diseased oil palm trees, healthy oil palm trees, forest, road and others for satellite data while it was classified into diseased oil palm trees, healthy oil palm trees, forest, background, road and others in case of UAV image. The training areas were defined from field survey data and base map from google earth. Each type of data class from field data was calculated in the statistics.

Accuracy Assessment

An accuracy assessment from the supervised classification of the image was based on the reference data with a confusion matrix (Congalton, 1991; Nuthammachot *et al.*, 2019). The field trip data were selected samples of raster or Regions of Interest (ROIs). Then the predicted class from the satellite and UAV images were extracted from the SVM classification method based on the ROIs. Overall accuracy, producer's accuracy, user's accuracy and kappa coefficient of agreement (κ) were performed to determine the accuracy of the diseased and healthy oil palm trees map.

Validation

Validation is generally used to assess the performance of a model (Lu *et al.*, 2011; 2016). The VARI is a vegetation index for estimating vegetation fractions quantitatively with only the visible range of the spectrum (ESRI, 2021). The two sample data groups VARI of UAV and VARI of Sentinel-2 data were selected in each area. The relationship between two variables was estimated to validate the model using linear regression. A scatterplot graph is a powerful tool for defining the strength of the relationship between two variables. The high coefficient of determination R^2 value determines the reliability of the model (Che *et al.*, 2021; Norouzian *et al.*, 2021; Robson *et al.*, 2017; Zhao *et al.*, 2021).

RESULTS

Vegetation indices

Table 3 shows the result of the linear regression analysis between the vegetation indices from Sentinel-2 images values and VARI indices from UAV. It was found that the r-values of vegetation indices ranged from 0.05 to 0.69 and the coefficient of determination (R^2) varied between 0.01 and 0.48 for the healthy oil palm trees area. For the diseased oil palm trees area, the r-values were between 0.07 and 0.82 and R^2 values were between 0.01 and 0.68. Similarly, the r-values of the mixed oil palm trees area were between 0.12 and 0.66 and R^2 values were between 0.02 and 0.44. For the healthy oil palm trees area, NDVI indices gave the best performance (R^2 = 0.48 and r = 0.69). RVI, NDI45, MSAVI, GNDVI and NDVI indices showed a substantial level while the MTCI showed a trivial level of performance. In the case of the diseased oil palm trees area, the RVI was the best performing index (R^2 = 0.68 and r = 0.82) followed by NDVI, MSAVI, NDI45, GNDVI and MTCI. For the mixed oil palm trees area, MSAVI was the best performing index (R^2 = 0.44 and r = 0.66) followed by NDVI, RVI, GNDVI, NDI45 and MTCI.

Support Vector Machine Classification and Accuracy Assessment

The results from the SVM algorithm are presented in *Figure 3*, *4* and *5*. In these figures, the location of the healthy and diseased oil palm trees, which was recorded during the field survey as ground truth data, is indicated by circles at the centre of each oil palm tree. For the accuracy assessment, producer's accuracy, user's accuracy, and kappa coefficient were calculated through an error matrix. The results for disease classification of the Sentinel-2 image indicated an overall accuracy of 64.16% and a kappa coefficient of 0.40 while for UAV image an overall accuracy of 65.61% and a kappa coefficient of 0.55 was calculated. Moreover, the overall accuracy of healthy classification was

TABLE 3. CORRELATION AND LINEAR REGRESSION BETWEEN VEGETATION INDICES FROM SENTINEL-2 DATA AND VARI FROM UAV DATA

Indices	Healthy oil palm trees area		Diseased oil palm trees area		Mixed oil palm trees area	
	R^2	r	R^2	r	R^2	r
RVI	0.47	0.68*	**0.68**	0.82*	0.36	0.60*
NDI45	0.34	0.58*	0.42	0.65*	0.03	0.18*
MSAVI	0.43	0.66*	0.55	0.74*	**0.44**	0.66*
GNDVI	0.29	0.54*	0.29	0.54*	0.17	0.41*
MTCI	0.01	0.05*	0.01	0.07*	0.02	0.12*
NDVI	**0.48**	0.69*	0.67	0.82*	0.36	0.60*

Note: * - Refer to a significant correlation at 0.05 level.

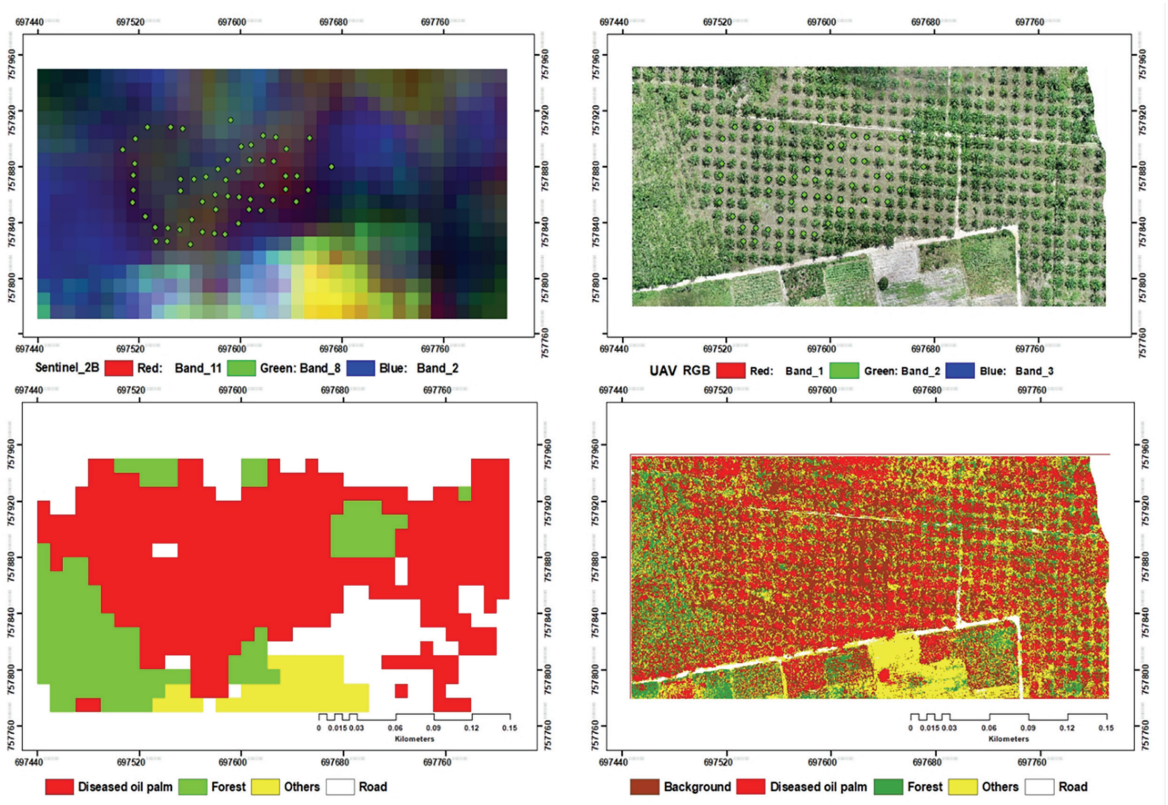

Figure 3. Identification of diseased oil palms planted area by SVM classification.

72.97% and a kappa coefficient of 0.56 was shown in the case of the Sentinel-2 image while for UAV data overall accuracy of 76.77% and a kappa coefficient of 0.68 were estimated. For the mixed oil palm tree area, the overall accuracy was 50.00% and the kappa coefficient was 0.37 while UAV data had an overall accuracy of 67.22% and a kappa coefficient of 0.43 was found.

Validation

Figure 6 presents the results of the correlation between the VARI from Sentinel-2 satellite data and the VARI from UAV imagery. Simple linear regression and R^2 values are used to develop and validate this model. For a healthy oil palm field, the R^2 value is 0.61 so it means that 61.00% of VARI of Sentinel-2 could be explained by VARI of UAV. Moreover, it gave the highest R^2 value than others from diseased and mixed oil palm fields (R^2 = 0.58 and 0.19). It was found that the healthy oil palm tree area is the most reliable model while the mixed oil palm tree area is the least reliable model.

Spectral Response of Healthy and Diseased Oil Palm Trees using Sentinel-2 Satellite Image

The diseased oil palm trees have been observed on a regional scale. The results from this study indicate the potential of Sentinel-2 image for

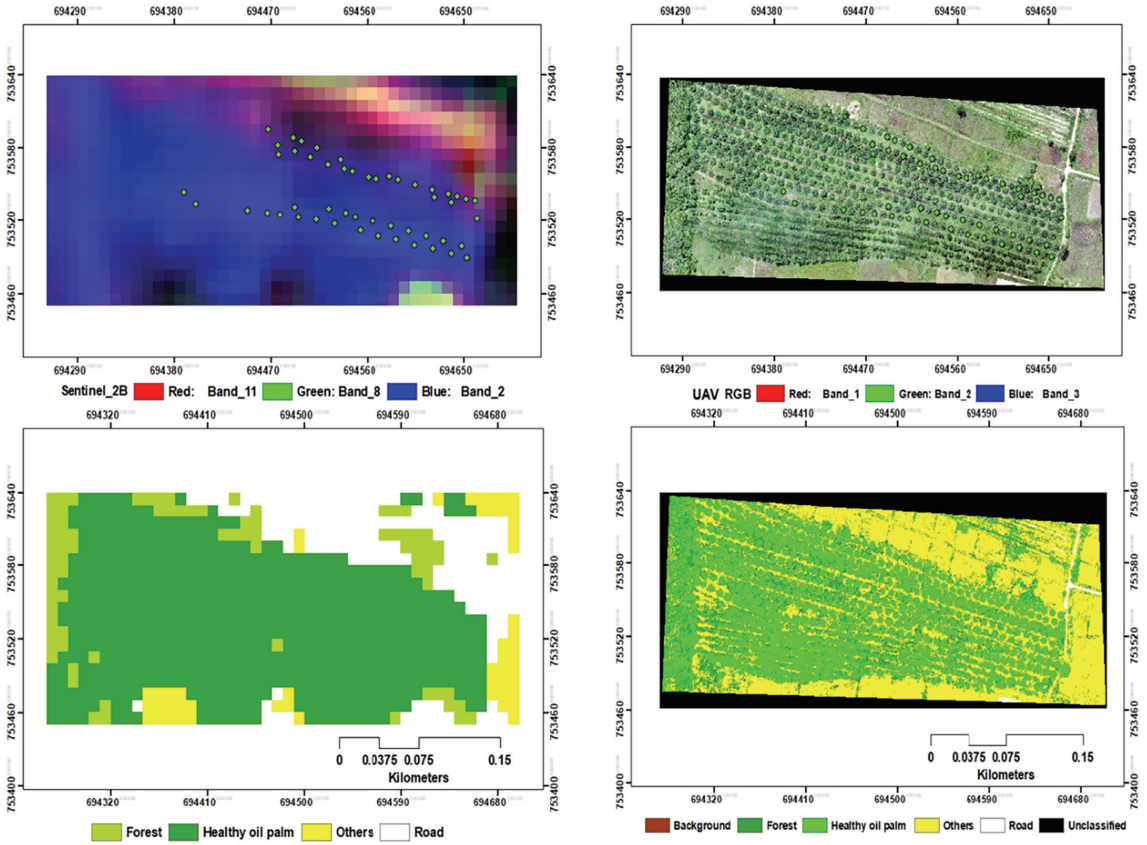

Figure 4. Identification of healthy oil palms planted area by SVM classification.

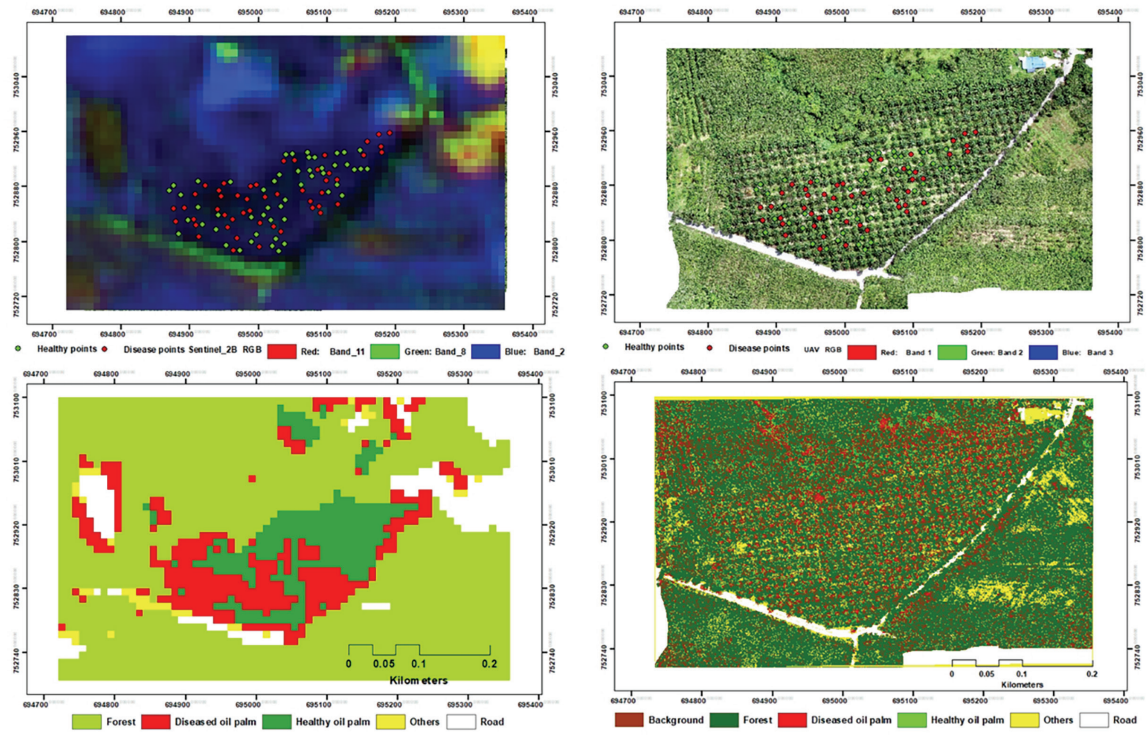

Figure 5. Identification of mixed oil palms planted area by SVM classification.

accurately mapping diseased, healthy and mixed oil palm plantations in Chana district, Songkhla province, Thailand. The vegetation indices NDVI, RVI and MSAVI consistently produced the strongest relationship to the measured diseased, healthy and mixed oil palm parameters. This result indicates that variations in the oil palm canopy are sensitive to measure with the NIR and Red spectral bands,

a finding which is also confirmed by other studies (Malinee *et al.*, 2021; Noor, 2016). Therefore, it follows that the spectral signatures of healthy and diseased oil palm trees can be obtained from Sentinel-2 imagery. Healthy oil palm trees show a higher reflectance in the NIR range of the spectrum (band 6: 740.5 nm, band 7: 782.8 nm, band 8: 832.8 nm and band 8A: 864.7 nm) compared to diseased oil palm trees because the trees were generally greener, with higher chlorophyll content, leading to greater reflection (*Figure 7).*

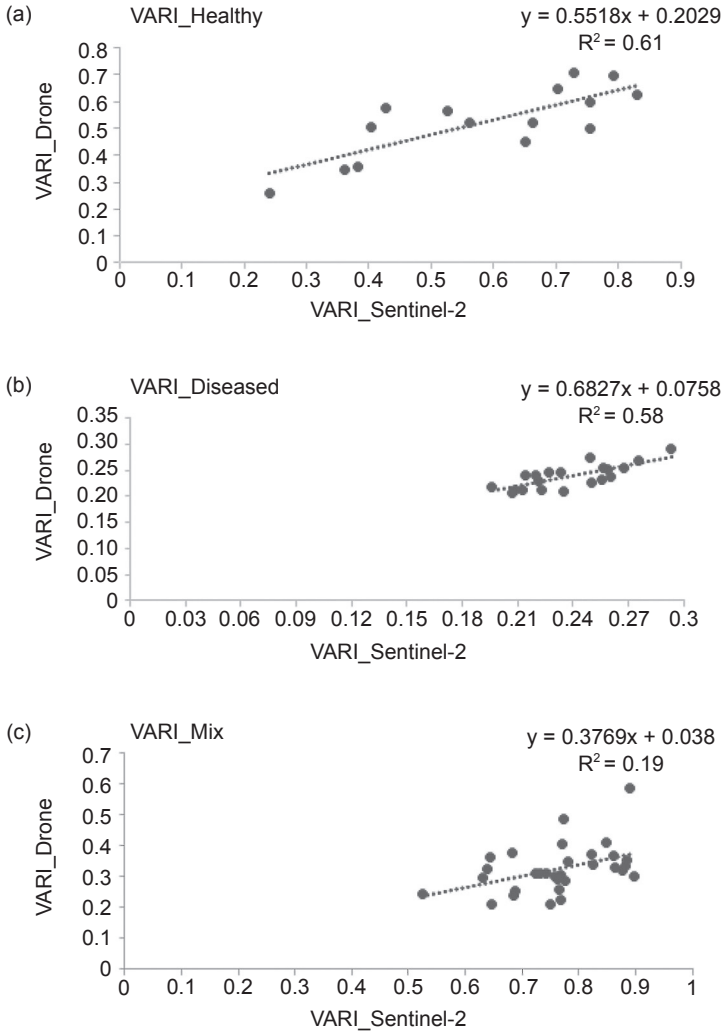

Figure 6. Scatter plot of VARI from Sentinel-2 satellite data and VARI from UAV imagery for the (a) healthy oil palm tree area, (b) diseased oil palm tree area and (c) mixed oil palm tree area.

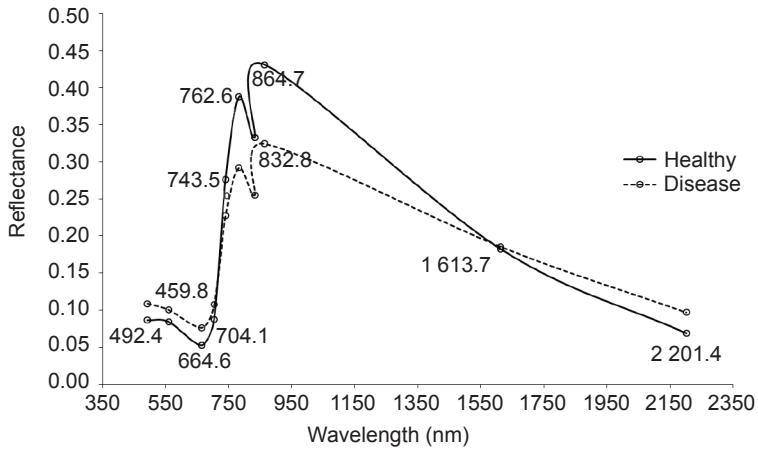

Figure 7. Spectral response of the healthy and diseased oil palm tree samples derived from the Sentinel-2 satellite image.

DISCUSSION

According to the accuracy of Sentinel-2 satellite classification of the two classes of diseased and healthy oil palm trees areas, the error matrix of the SVM classification was estimated. The results of this study show that the overall accuracy is 72.97% and the kappa coefficient is 0.56 (56.00%) in healthy oil palm planted areas and 64.16% and the kappa coefficient is 0.40 (40.00%) in diseased oil palm planted areas while the overall accuracy (50.00%) and the kappa coefficient (0.37) of mixed oil palm planted area are lower than others. The reason is that it is difficult to discriminate between the canopy of healthy and diseased oil palm trees using the medium satellite image. Compared with the results of UAV image, the overall accuracy and kappa coefficient values are higher than the results from Sentinel-2 data in the healthy, diseased oil palm tree and mixed oil palm tree areas. Furthermore, Santoso *et al.* (2017) classified oil palm disease using QuickBird satellite data. The overall accuracy (91.00%) is higher than our result. Also, Malinee *et al.* (2021) classified oil palm disease and provided an overall accuracy of 85.98%, and the kappa coefficient of 0.71 (71.00%) while our result of mixed oil palm trees is lower than their results. It is a fact that the UAV imagery, QuickBird and WorldView-2 satellite images have higher resolution than the Sentinel-2 satellite image.

CONCLUSION

The main finding of this study indicates that the SVM classification yielded satisfactory results for discriminating between plants and other objects in the case of healthy and diseased oil palm planted areas using Sentinel-2 satellite and UAV images. The results showed that the overall accuracy and kappa coefficient of the Sentinel-2 satellite data were 72.97% and 0.56 in the healthy oil palm trees region and 64.16 % and 0.55 in the diseased oil palm trees area. Moreover, UAV data overall accuracy was 76.77% and the kappa coefficient was 0.68 for the healthy oil palm trees area and 65.61% and a kappa coefficient of 0.55 was calculated for the diseased oil palm trees area. However, it is not easy to classify diseased and healthy oil palm trees in the mixed oil palm area (50.00% and 0.37). Future efforts to improve the methodology proposed are suggested to focus on obtaining more precise estimates. First, the satellite image is required to be of a very high radiometric resolution such as a hyperspectral image. Secondly, the UAV should have the NIR or hyperspectral sensor to detect or monitor diseased plants and can calculate narrowband vegetation indices with high accuracy. Finally, other physical parameters, such as nutrition analysis of the oil palm leaf, should be considered as it also contributes to disease infection.

ACKNOWLEDGEMENT

The authors deeply appreciate the support and received funding from Prince of Songkla University (Grant No: ENV6302159S), Research and Development Office, Prince of Songkla University, Thailand.

REFERENCES

Askar; Nuthammachot, N; Phairuang, W; Wicaksono, P and Sayektiningsih, T (2018). Estimating above ground biomass on private forest using Sentinel-2 imagery. *J. Sens., 2018*: 6745629. DOI: 10.1155/2018/6745629.

Chaware, R; Karpe, R; Pakhale, P and Desai, S (2017). Detection and recognition of leaf disease using image processing. *Int. J. Comput. Sci. Eng., 7(5)*: 11964-11967.

Che, X; Zhang, H K and Liu, J (2021). Making Landsat 5, 7 and 8 reflectance consistent using MODIS nadir-BRDF adjusted reflectance as reference. *Remote Sens. Environ., 262*: 112517. DOI: 10.1016/j.rse.2021.112517.

Cheng, Y; Yu, L; Xu, Y; Liu, X; Lu, H; Cracknell, A P; Kanniah, K and Gong, P (2018). Towards global oil palm plantation mapping using remote-sensing data. *Int. J. Remote Sens., 39(18)*: 5891-5906. DOI: 10.1080/01431161.2018.1492182.

Cheng, Y; Yu, L; Xu, Y; Lu, H; Cracknell, A P; Kanniah, K and Gong, P (2019). Mapping oil palm plantation expansion in Malaysia over the past decade (2007-2016) using ALOS-1/2 PALSAR-1/2 data. *Int. J. Remote Sens., 40(19)*: 7389-7408. DOI: 10.1080/01431161.2019.1580824.

Chong, K L; Kanniah, K D; Pohl, C and Tan, K P (2017). A review of remote sensing applications for oil palm studies. *Geo. Spat. Inf. Sci., 20(2)*: 184-200. DOI: 10.1080/10095020.2017.1337317.

Congalton, R G (1991). A review of assessing the accuracy of classifications of remotely sensed data. *Remote Sens. Environ., 37(1):* 35-46. DOI: 10.1016/0034-4257(91)90048-B.

Delegido, J; Verrelst, J; Alonso, L and Moreno, J (2011). Evaluation of sentinel-2 red-edge bands for empirical estimation of green LAI and chlorophyll content. *Sensors., 11(7)*: 7063-7081. DOI: 10.3390/s110707063.

DJI (2017). Phantom 4: User Manual V1, 2016-11. https://dl.djicdn.com/downloads/phantom_4/en/Phantom_4_User_Manual_en_v1.0.pdf, accessed on 7 July 2021.

ESRI (2021). ArcGIS Pro. https://pro.arcgis.com/en/pro-app/latest/arcpy/image-analyst/vari.html, accessed on 17 June 2021.

European Space Agency (ESA) (2021). Sentinel Online. https://sentinel.esa.int, accessed on 17 July 2021.

European Space Agency (ESA) (2015). Sentinel Online (Sentinel-2). https://sentinel.esa.int/web/sentinel/missions/sentinel-2, accessed on 17 July 2021.

Gitelson, A A; Kaufman, Y J and Merzlyak, M N (1996). Use of a green channel in remote sensing of global vegetation from EOS-MODIS. *Remote Sens. Environ., 58(3)*: 289-298. DOI: 10.1016/S0034-4257(96)00072-7.

Izzuddin, M A; Nisfariza, M N; Ezzati, B; Idris, A S; Steven, M D and Boyd, D (2018). Analysis of airborne hyperspectral image using vegetation indices, red edge position and continuum removal for detection of *Ganoderma* disease in oil palm. *J. Oil Palm Res., 30*: 416-428. DOI: 10.21894/jopr.2018.0037.

Kamal, M M; Masazhar, A N I and Rahman, A (2018). Classification of leaf disease from image processing technique. *Indones. J. Electr. Eng., 10(1)*: 191-200. DOI: 10.11591/ijeecs.v10.i1.

Lu, D; Batistella, M; Moran, E; Hetrick, S; Alves, D and Brondizio, E (2011). Fractional forest cover mapping in the Brazilian Amazon with a combination of MODIS and TM images. *Int. J. Remote Sens., 32(22)*: 7131-7149. DOI: 10.1080/01431161.2010.519004.

Lu, D; Chen, Q; Wang, G; Liu, L; Li, G and Moran, E (2016). A survey of remote sensing-based above ground biomass estimation methods in forest ecosystems. *Int. J. Digit. Earth., 9(1)*: 63-105. DOI: 10.1080/17538947.2014.990526.

Malinee, R; Stratoulias, D and Nuthammachot, N (2021). Detection of oil palm disease in plantations in Krabi Province, Thailand with high spatial resolution satellite imagery. *Agric., 11(3)*: 251. DOI: 10.3390/agriculture11030251.

Masazhar, A N I and Kamal, M M (2017). Digital image processing technique for palm oil leaf disease detection using multiclass SVM classifier. *In 2017 IEEE 4th International Conference on Smart Instrumentation, Measurement and Application (ICSIMA)*. p. 1-6.

Naher, L; Yusuf, U K; Ismail, A; Tan, S G and Mondal, M M A (2013). Ecological status of *Ganoderma* and basal stem rot disease of oil palms (*Elaeis guineensis* Jacq.). *Aust. J. Crop Sci., 7(11)*: 1723-1727.

Noor, N M (2016). El uso de sensores remotos para detectar la infección por *Ganoderma*. *Revista Palmas., 37*: 140-150.

Norouzian, M A; Bayatani, H and Alavijeh, M V (2021). Comparison of artificial neural networks and multiple linear regression for prediction of dairy cow locomotion score. *Vet. Res. Forum., 12(1)*: 33-37. DOI: 10.30466/vrf.2019.98275.2346.

Nuthammachot, N and Stratoulias, D (2019). Fusion of Sentinel-1A and Landsat-8 images for improving land use/land cover classification in Songkla province, Thailand. *Appl. Ecol. Environ. Res., 17(2)*: 3123-3135. DOI: 10.15666/aeer/1702_31233135.

Pałaś, K W and Zawadzki, J (2020). Sentinel-2 imagery processing for tree logging observations on the Białowieża forest world heritage site. *Forests., 11(8)*: 857. DOI: 10.3390/f11080857.

Qi, J; Chehbouni, A; Huerte, A R; Kerr, Y H and Sorooshian, S (1994). A modified soil adjusted vegetation index. *Remote Sens. Environ., 48(2)*: 119-126. DOI: 10.1016/0034-4257(94)90134-1.

Robson, A; Rahman, M M and Muir, J (2017). Using worldview satellite imagery to map yield in avocado (*Persea americana*): A case study in Bundaberg, Australia. *Remote Sens., 9(12)*: 1223. DOI: 10.3390/rs9121223.

Santoso, H; Gunawan, T; Jatmiko, R H; Darmosarkoro, W and Minasny, B (2011). Mapping and identifying basal stem rot disease in oil palms in North Sumatra with QuickBird imagery. *Precis. Agric., 12(2)*: 233-248. DOI: 10.1007/s11119-010-9172-7.

Santoso, H; Tani, H and Wang, X (2017). Random forest classification model of basal stem rot disease caused by *Ganoderma boninense* in oil palm plantations. *Int. J. Remote Sens., 38(16)*: 4683-4699. DOI: 10.1080/01431161.2017.1331474.

Tucker, C J (1979). Red and photographic infrared linear combinations for monitoring vegetation. *Remote Sens. Environ., 8(2)*: 127-150. DOI: 10.1016/0034-4257(79)90013-0.

Yusoff, N M; Muharam, F M and Khairunniza-Bejo, S (2017). Towards the use of remote-sensing data for monitoring of abandoned oil palm lands in Malaysia: A semi-automatic approach. *Int. J. Remote Sens., 38(2)*: 432-449. DOI: 10.1080/01431161.2016.1266111.

Zhang, K; Liu, X; Ma, Y; Wang, Y; Cao, Q; Zhu, Y; Cao, W and Tian, Y (2021). A new canopy chlorophyll index-based paddy rice critical nitrogen dilution curve in Eastern China. *Field Crops Res., 266*: 108139. DOI: 10.1016/j.fcr.2021.108139.

Zhao, Y; Liu, X; Wang, Y; Zheng, Z; Zheng, S; Zhao, D and Bai, Y (2021). UAV-based individual shrub above ground biomass estimation alibrated against terrestrial LiDAR in a shrub-encroached grassland. *Int. J. Appl. Earth Obs. Geoinf., 101*: 102358. DOI: 10.1016/j.jag.2021.102358.

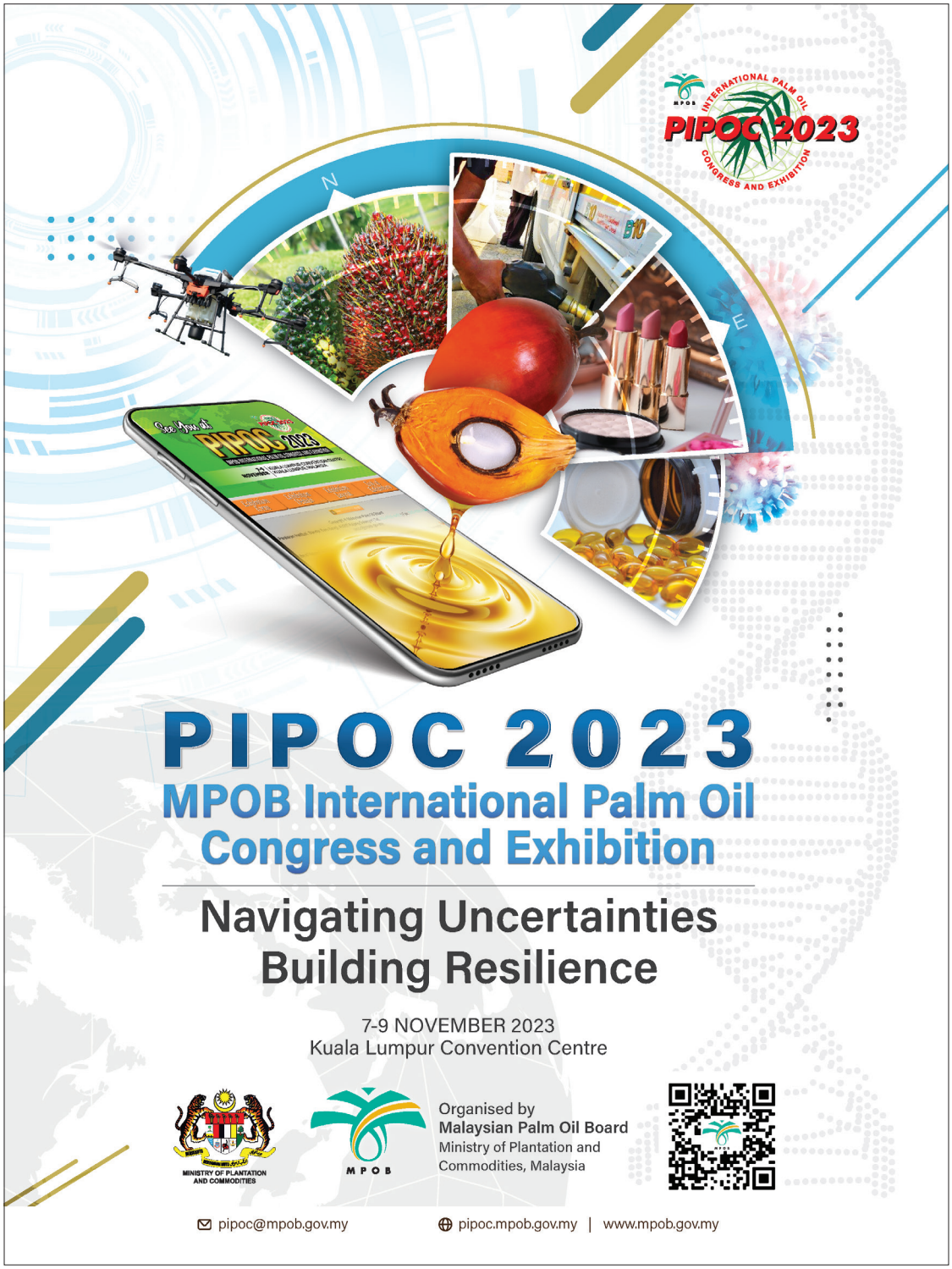

Journal of Oil Palm Research Vol. 35 (3) September 2023 p. 528-537
DOI: https://doi.org/10.21894/jopr.2022.0062

PROTEOMICS OF OIL PALM SOMATIC EMBRYOGENESIS REVEALS THE DIFFERENTIALLY EXPRESSED PROTEINS AS CANDIDATES FOR BIOMARKER DEVELOPMENT

KAMOLWAN KHIANCHAIKHAN[1#]; SUVICHARK AROONLUK[1#]; NARUMON PHAONAKROP[2]; SITTIRUK ROYTRAKUL[2]; MANTIRA SUKSIRT[1]; PAPHAWARIN PINYOKHAM[1]; MYA THUZAR[3] and CHATCHAWAN JANTASURIYARAT[1,4*]

ABSTRACT

Tissue culture through somatic embryogenesis is the best method to produce the true-to-type of an elite oil palm plantlet. However, the mechanism underlying this process in oil palm is still unknown. We aimed to identify differentially expressed proteins during oil palm somatic embryogenesis using embryogenic callus, somatic embryo maturation and plantlet stages. Total proteins were extracted followed by tryptic enzyme digestion. The tryptic digested peptides were examined by nano LC-MS/MS. Identified proteins were classified based on biological process, molecular function and cellular components. Twenty-seven differentially expressed proteins were validated at the transcript level using qRT-PCR. These proteins were involved in plant growth and development, gene regulation, signalling, hormone response and stress response. Moreover, the differentially expressed proteins were categorised and reported as the candidate proteins for the development of biomarkers, which could be used to differentiate the embryo's developmental stages. The information on identified proteins obtained from this study will serve as the foundation for the understanding of the oil palm somatic embryogenesis in the tissue culture process.

Keywords: nano LC-MS/MS, proteome, tissue culture.

Received: 24 April 2022; **Accepted:** 29 August 2022; **Published online:** 28 September 2022.

INTRODUCTION

Oil palm is one of the most efficient oil-bearing crops in the world. With the world's consumption of palm oil increasing, many oil palm-producing countries aim to expand their oil palm plantation area. Oil palm, as a cross-pollinated crop, is propagated through seed production, resulting in segregated yields. Therefore, tissue culture is the best method to produce true-to-type elite oil palm plantlets. The oil palm tissue culture is initiated by embryogenic callus formation and then undergoes somatic embryogenesis. Oil palm somatic embryogenesis usually takes 7-8 months (Thuzar *et al*., 2011). Very little information about somatic embryogenesis in

[1] Department of Genetics, Faculty of Science, Kasetsart University, Bangkok 10900, Thailand.

[2] National Center for Genetic Engineering, and Biotechnology (BIOTEC), National Science and Technology Development Agency (NSTDA), Pathum Thani 12120, Thailand.

[3] Rice Science Center, Kasetsart University, Kamphaeng Saen, Nakorn Pathom 73140, Thailand.

[4] Center for Advanced Studies in Tropical Natural Resources, National Research University-Kasetsart (CASTNAR, NRU-KU), Kasetsart University, Bangkok 10900, Thailand.

[#] Authors contributed equally to this work.

[*] *Corresponding author email: fscicwj@ku.ac.th*

oil palm is reported. Identifying genes and proteins involved in this process will facilitate a better understanding and help to improve this process in oil palm tissue culture.

Somatic embryogenesis is a process used for large-scale plant regeneration, in which somatic cell has the ability to dedifferentiate or re-differentiate and give rise to somatic embryos. Several genes including *Somatic embryogenesis receptor kinase* (*SERK*) (Jiménez-Guillen *et al*., 2019), *Wuschell* (*WUS*) (Bouchabké-Coussa *et al*., 2013), *Leafy cotyledon* (*LEC*) (Guo *et al*., 2013), and *Baby Boom* (*BBM*) (Florez *et al*., 2015) were reported to have important roles in this process.

A biomarker has been defined as a biological molecule such as genes, proteins *etc*. that have the potential to indicate a particular developmental stage, tissue or process. These genes/proteins are specifically exhibited during the process or specific tissues (Aroonluk *et al*., 2018; 2020; Sruthilaxmi and Babu, 2020). Recently, proteomic analysis has been used to identify proteins, which involve in somatic embryogenesis in many plant species including *Musa* spp. (Kumaravel *et al*., 2020), Brazilian pine (Borges Araujo *et al*., 2022), and winter triticale (Krzewska *et al*., 2021). The differentially expressed proteins during the early embryogenic stages including primary callus and pro-embryogenic callus obtained from zygotic embryos were identified and characterised in oil palm (Silva *et al*., 2014). To further identify and characterise proteins during oil palm somatic embryogenesis, we performed proteomic analysis of embryogenic callus, somatic embryo maturation including globular, torpedo and cotyledon stages, and plantlet stage during oil palm somatic embryogenesis to identify differentially expressed proteins and to validate their expression at mRNA level. These identified differentially expressed proteins are the important keys to help reveal the biological mechanism of oil palm somatic embryogenesis and could be used as biomarkers for the different developmental stages during oil palm somatic embryogenesis.

MATERIALS AND METHODS

Plant Materials

Tenera, a common commercial oil palm type, is produced by crossing between a *dura* female and a *pisifera* male. Fifteen-week-old *tenera* zygotic embryo explants from *Golden Tenera* (KB) variety were cultured on an N6 medium supplemented with 2.0 mg/L of 2,4-D to induce embryogenic callus under dark conditions until globular embryos appeared. After three months, embryogenic callus was transferred to an N6 medium supplemented with 0.1 mg/L of 2,4-D, 0.16 g/L of putrescine, 0.5 g/L of casein amino acids, 30 g/L of sucrose, 2 g/L of phytagel, and 2 g/L of activated charcoal under light condition for 16 hr photoperiod until somatic embryo started to come out. After six months, small shoots were then transferred to a modified N6 medium containing 0.5 g/L of activated charcoal and 30 g/L of sucrose under light conditions for 16 hr photoperiod to regenerate new plantlets. The embryogenic callus, globular, torpedo, cotyledon, and plantlet samples were collected for protein extraction (*Figure 1*).

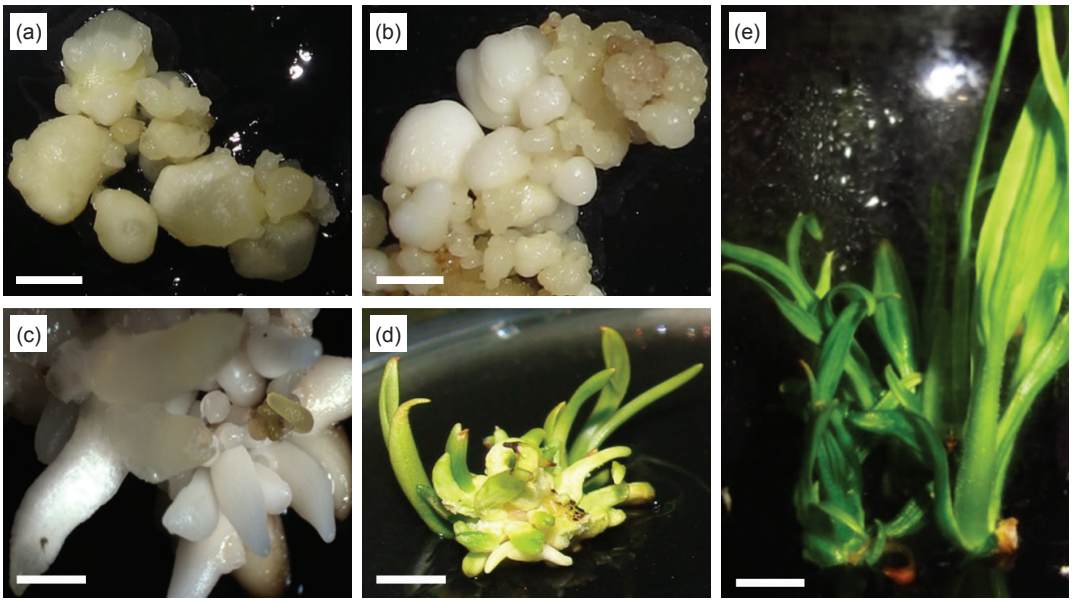

Figure 1. The oil palm tissue samples at 5 stages; (a) embryogenic callus at 3 months on callus induction medium (bar = 5 mm), (b) globular at 1 month on somatic embryo maturation medium (bar = 5 mm), (c) torpedo at 3 months on somatic embryo maturation medium (bar = 3 mm), (d) cotyledon at 5 months on somatic embryo maturation medium (bar = 5 mm), and (e) plantlet at 1 month on plantlet regeneration medium (bar = 8 mm).

Protein Extraction, In-gel Digestion, and Protein Identification Using Nano LC-MS/MS

The protein extracts from oil palm tissue samples were performed according to Kaweewong *et al*. (2013). Samples were ground in liquid nitrogen and dissolved in 0.5% SDS, mixed for 30 min at room temperature and then centrifuged at 13 201 g for 15 min at 4ºC. The supernatant was transferred to a new microcentrifuge tube then added an equal volume of cooled acetone and incubated for 2 hr at -20ºC. To collect the pellet, the samples were centrifuged at 13 201 g for 15 min at 4ºC. Washed the pellet three times with cooled acetone and centrifuged at 13 201 g for 15 min at 4ºC then dissolved in 0.5% SDS and desalted by ZebaTM Desalt spin column (ThermoFisher Scientific, USA) according to the manufacturer's instruction. The Lowry method was used to measure the concentration of soluble protein and stored at -80ºC. Total of 10 µg of protein samples were separated using 15% gel denaturing discontinuous polyacrylamide gel electrophoresis (SDS-PAGE) and stained with Pierce™ Silver Stain Kit (ThermoFisher Scientific, USA).

The protein gel was cut to gel plugs 1 x 1 mm^3, washed and dissolved with 200 µL of 100% acetonitrile and soaked with 50 µL of 10 mM dithiothreitol (DTT) in 10 mM ammonium bicarbonate for 1 hr to breakdown the disulfide bridge and block the reunion of the disulfide bridge with 50 µL of 100 mM iodoacetamide in 10 mM ammonium bicarbonate under the dark light for 1 hr. Protein gels were then dehydrated by 100% acetonitrile and dried at room temperature. Dried protein gels were digested by adding 10 ng of Trypsin in 50% acetonitrile and 10 mM ammonium bicarbonate and kept at room temperature for 20 min before adding 30 µL of 30% acetonitrile solution and incubated overnight. The digested peptide solution was re-extracted with 50% acetonitrile in 0.1% trifluoroacetic acid and 70% acetonitrile in 0.1% trifluoroacetic, respectively. The peptide solution was dried using a Speed Vacuum concentrator and resuspended in 0.1% formic acid (FA) for Nano LC-MS/MS analysis.

The digested peptide samples were subjected to HCT-Ultra PTM Discovery System (Bruker Daltonik, Bremen, Germany) coupled to the Ultimate 3000 LC system (Dionex, USA) using electrospray at the flow rate of 300 nL/min to a nanocolumn (PepSwift monolithic column 100 µm i.d. x 50 mm). Mobile phases of solvent A (0.1% formic acid) and solvent B (80% acetonitrile and 0.1% formic acid) were used to elute peptides with a linear gradient from 10%-70% of solvent A at 0-13 min (the time-point of retention time) following 90% of solvent B at 13-15 min, and final elution of 10% of solvent B at 15-20 min to remove remaining salt. The resolution of the MS step is 0.6 and the accuracy is 0.15 u (m/z). A total of three replicates were performed.

Bioinformatics and Data Analysis

The DeCyder MS 2.0 analysis software (GE Healthcare, USA) was used to measure the quantitative protein intensity based on peptide MS signal intensities of individual LC-MS analysed data. The PepDetect module was used to produce ion peptides at the data set; the mass resolution is 0.6, typical peak width 0.5, TOF resolution 10 000, charge status from 1 to 10 and m/z 22 shift tolerance 0.1 u. The PepMatch module was used to evaluate the signal intensity maps. The highest intensity sample was used as a control presenting the relative abundance of peptides as 2 log intensities with mass tolerance set to 0.5 amu. The criteria of more than a 2-fold change of an average abundance ratio were used to determine the induced protein with a significant standard t-test and one-way ANOVA $p<0.05$. All MS/MS spectra from the Decyder MS analysis were performed by applying the global variable mode of carbamidomethyl (C), peptide charge state (1^+, 2^+ and 3^+), and m/z tolerance 0.1 u and searched against NCBI FTP site of *Elaeis guineensis* genome database to identify matching peptide using Mascot software (Matrix Science, UK). Identified proteins were filtered with a one-way ANOVA $p<0.05$. BSA was used as an internal standard to normalise protein intensities. Bioinformatics and Evolutionary Genomics Tool (http://bioinformatics.psb.ugent.be/webtools/Venn/) was used to determine the similarity and differential protein expression. Gene ontology was used to characterise the function of the identified proteins using appropriate protein annotation that was reported in the UniProt protein database (http://www.uniprot.org/), PANTHER classification system (http://pantherdb.org/) and previously reported proteins. The heat map of differentially expressed proteins from each sample was generated by average linkage clustering using the online Heatmapper (http://www.heatmapper.ca/).

Quantitative Real-Time PCR Verification

Five stages of tissue development including embryogenic callus, globular, torpedo, cotyledon, and plantlet were used for total RNA extraction using Spin Plant RNA (STRATEC Molecular, Germany) according to the manufacturer's protocol with minor modification with DNase I (Vivantis, USA) treatment. The first strand of cDNA was synthesised using a cDNA synthesis kit (Biotechrabbit GmbH, Germany) according to the manufacturer's instructions. The cDNA content of *E. guineensis* elongation factor alpha-1 (NCBI accession number XM_019850296) was used to normalise the expression level of the candidate genes. The qRT-PCR was performed with the

specific primers using KAPA SYBR® FAST qPCR kit Mastermix (2x) Universal (Kapa Biosystems, USA) according to the manufacturer's instruction on Eppendorf Mastercycler ep Realplex (Thermo Fisher Scientific, USA). Three replications were conducted. The expression level was calculated as fold change using the double delta Ct values with the callus expression level as a calibrator.

RESULTS AND DISCUSSION

Somatic embryogenesis is an important process for *in vitro* plant micropropagation. It is described as the differentiation of a somatic cell to form an embryogenic cell. In this study, we identified the differentially expressed proteins during the oil palm somatic embryogenesis. A total of 800 unique proteins were identified, in which 742, 722, 730, 755 and 756 were presented in callus, globular, torpedo, cotyledon and plantlet respectively (*Figure 2*). A total of 584 identified proteins were shared in all stages in which 216 identified proteins were specifically expressed in only certain stages and these proteins could be developed as the oil palm somatic embryogenesis biomarkers. Eight groups of identified proteins were classified based on their expression patterns (*Table 1*). Group 1 is composed of a serine/threonine-protein kinase Nek5, which was specifically expressed in callus and globular stages. Group 2 was composed of 11 identified proteins, which were specifically expressed in callus, globular and torpedo stages including auxin response factor 23-like, rust resistance kinase Lr10-like, importin subunit beta-1-like, vegetative cell wall protein gp1 *etc*. Group 3 is composed of a putative transporter arsB, which was specifically expressed in globular and torpedo stages. Group 4 is composed of a pentatricopeptide repeat-containing protein *At*5g14770, mitochondrial, which was specifically expressed in globular and cotyledon stages. Group 5 is composed of a transmembrane protein 184C-like, which was specifically expressed only in the torpedo stage. Group 6 is composed of three identified proteins, which were specifically expressed in globular, torpedo and cotyledon stages including phospholipase D delta-like isoform X2, solanesyl-diphosphate synthase 3, chloroplastic and LIM domain-containing serine/threonine-protein kinase DDB_G0286997. Group 7 is composed of two identified proteins, which were specifically expressed in globular, torpedo, and plantlet stages including a protein kinase PINOID-like and an uncharacterised protein. Group 8 is composed of seven identified proteins, which were specifically expressed in torpedo, cotyledon and plantlet stages including delta (8)-fatty-acid desaturase-like, RAN GTPase-activating protein, U4/U6 small nuclear ribonucleoprotein Prp3-like, fasciclin-like arabinogalactan protein 2, RING-H2 finger protein ATL13-like, metallothionein-like protein type 2 and one uncharacterised protein.

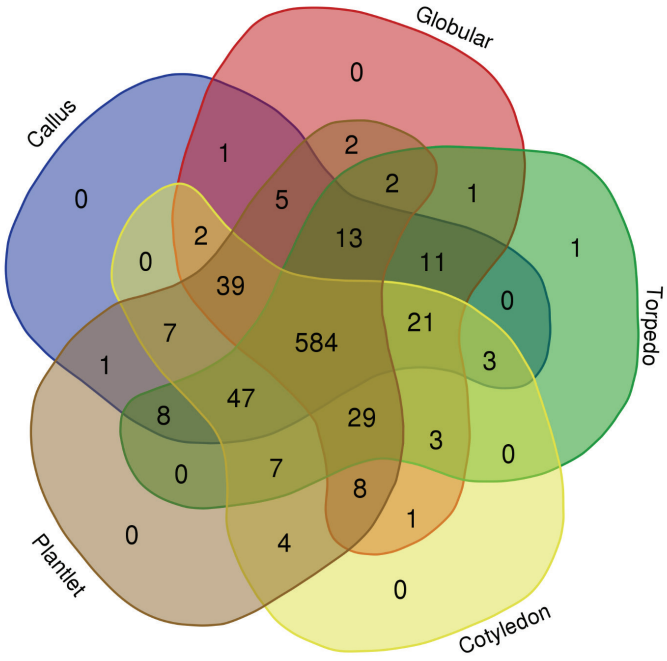

Figure 2. Venn diagram of the differentially expressed proteins during oil palm somatic embryogenesis; callus (blue), globular (red), torpedo (green), cotyledon (yellow) and plantlet (brown). The number indicates the number of identified proteins.

The 27 identified differentially expressed proteins from eight groups were selected for transcriptional expression verification using quantitative Real-Time RT-PCR. These proteins are potential candidates for biomarker development. The result showed that the mRNA expression level was consistence with the level of protein expression (*Table 1*). This result corresponded to a previous study of the genes associated with cDNA-AFLP of oil palm somatic embryogenesis (Pattarapimol *et al*., 2015). However, the correlation between protein and mRNA expression levels partially overlaps but is not identical (Aroonluk *et al*., 2020). This result indicated that many genes/proteins were induced in embryogenic callus to initiate somatic embryogenesis and these genes/proteins were differentially expressed at globular, torpedo, cotyledon and plantlet stages.

Functional Characterisation of Identified Proteins Based on Gene Ontology

Identified proteins were functionally classified based on their gene ontology (GO); (a) biological process, (b) molecular function and (c) cellular component. For the biological process, 10.30% was classified in the metabolic process, 9.84% was classified in the transcription and 6.67% was classified in the transportation process. For the molecular function, 12.53% were classified as the binding proteins, 6.21% were classified as kinases and 5.50% were classified as transcription factors. For the cellular component, 21.55% was classified as nuclear proteins, 14.64% was classified as membrane proteins and 9.72% was classified as cytoplasmic proteins (*Figure 3*). However, the majority of identified proteins had an unknown function.

Differentially Expressed Identified Proteins During Oil Palm Somatic Embryogenesis

Identified proteins were hierarchical clustering based on their expression pattern (*Figure 4*). Five clusters were generated as clusters A to E. Cluster A is composed of 128 identified proteins, which were highly expressed in callus, globular, torpedo and plantlet stages but low expression in the cotyledon stage. Cluster B is composed of 300 identified proteins, which were highly expressed in callus, globular and torpedo stages but low expression in cotyledon and plantlet stages. Cluster C is composed of 108 identified proteins, which can be divided into 2 sub-clusters C1 and C2. Sub-cluster C1 was highly expressed in callus, globular and plantlet stages but low expression in torpedo and cotyledon stages. Sub-cluster C2 was highly expressed in all stages except in the torpedo stage. Cluster D is composed of 186 identified proteins, which can be divided into 2 sub-clusters D1 and D2. Sub-cluster D1 was highly expressed in cotyledon and plantlet stages but low expression in callus, globular and torpedo stages. Sub-cluster D2 was highly expressed in all stages except in the globular stage. Finally, cluster E is composed of 78 identified proteins, which were highly expressed in globular, torpedo, cotyledon, and plantlet stages but with low expression in the callus stage. These differentially expressed proteins could be developed as the biomarkers of the oil palm somatic embryogenesis.

Several proteins, identified in this study, were previously reported to be involved in somatic embryo development. Serine/threonine-protein kinase Nek5 is a member of the NIMA-related kinases (NEKs) family, involved largely in cell cycle control by regulating microtubule organisation during epidermal cell expansion (Motose *et al*., 2011). This protein contributed to controlling cell division for the somatic embryogenesis acquisition process. Receptor protein kinase-like protein ZAR1, a member of the RLK/Pelle kinase family, functions as a membrane integrator for extrinsic cues, Ca^{2+} signal and G protein signalling to regulate the division of zygote and the cell fate of its daughter cells (Yu *et al*., 2016). Putative transporter arsB was specifically expressed in globular and torpedo stages and they could be used as protein biomarkers to determine the somatic embryo stage. This protein is one of the arsenite transporter genes, involved in arsenic and antimony transport pathways using vacuolar transporters of arsenic-phytochelatin complexes in plants (Maciaszczyk-Dziubinska *et al*., 2012). Fasciclin-like arabinogalactan protein 2 is a member of arabinogalactan proteins (AGPs), which have a significant role in the process of competence acquisition and the induction of shoot development (Johnson *et al*., 2003). RAN GTPase-activating protein 1-like is a member of proteins that bind to Ran (Ras-related nuclear small GTP-binding protein). It involves root growth and development and regulation of auxin-induced mitotic progression in root tips (Kim and Roux, 2003). These identified proteins can be used as biomarkers for oil palm somatic embryogenesis.

Moreover, two identified proteins have functions in cell walls to regulate cell shape and the direction of cell differentiation during somatic embryogenesis. First, vegetative cell wall protein gp1 is a constituent chaotropic-soluble glycoprotein in the cell wall and controls mechanisms of cell wall remodelling, signalling pathway from the apoplast to the cell wall, cell wall-sensing process and exchange of cell-cell information (Ringli, 2010; Voigt *et al*., 2009). The other, non-specific lipid-transfer protein is a small protein, involves in plant growth and development (Potocka *et al*., 2012).

Several transcription factors known to be involved in somatic embryogenesis were also identified in this study including the CCCH proteins,

TABLE 1. LIST OF THE SPECIFICALLY EXPRESSED PROTEINS AND mRNA EXPRESSION VALIDATION

Accession No.	Protein name	MOWSE score	Protein abundance					mRNA expression level				
			Callus	Globular	Torpedo	Cotyledon	Plantlet	Callus	Globular	Torpedo	Cotyledon	Plantlet
Group 1												
gi|743858642	PREDICTED: serine/threonine-protein kinase Nek5	5.69	16.07	15.40	0.00	0.00	0.00	1.00	0.63	2.56	1.42	56.49
Group 2												
gi|743858544	PREDICTED: auxin response factor 23-like	4.68	15.81	16.46	15.27	0.00	0.00	1.00	1.68	1.51	1.17	1.84
gi|743768063	PREDICTED: rust resistance kinase Lr10-like	5.24	13.06	14.52	12.99	0.00	0.00	1.00	0.21	4.77	3.45	4.95
gi|743842857	PREDICTED: importin subunit beta-1-like	5.07	14.45	18.89	16.48	0.00	0.00	1.00	2.46	3.01	1.69	4.36
gi|743858365	PREDICTED: vegetative cell wall protein gp1	4.41	16.17	18.17	16.88	0.00	0.00	1.00	1.92	16.49	36.11	48.95
gi|743788936	PREDICTED: probable LRR receptor-like serine/threonine-protein kinase *At*1g06840 isoform X1	3.92	11.23	15.57	17.37	0.00	0.00	1.00	2.14	8.66	7.27	3.08
gi|743835428	PREDICTED: NAC domain-containing protein 78 isoform X1	3.49	17.25	13.73	16.82	0.00	0.00	1.00	1.05	4.89	2.43	4.83
gi|743761936	PREDICTED: peptidyl-prolyl cis-trans isomerase CYP37, chloroplastic	1.54	19.64	17.01	17.64	0.00	0.00	1.00	1.35	2.20	1.44	3.45
gi|743757543	PREDICTED: receptor protein kinase-like protein ZAR1	1.40	17.11	16.19	18.29	0.00	0.00	1.00	10.17	3.29	3.56	7.42
gi|743801725	PREDICTED: dr1-associated corepressor homolog isoform X1	3.67	21.96	20.08	21.35	0.00	0.00	1.00	0.89	2.38	1.78	4.89
gi|743872177	PREDICTED: uncharacterised protein LOC105033396 isoform X3	1.14	18.11	16.95	19.87	0.00	0.00	1.00	9.07	7.43	4.69	7.59
gi|743779448	PREDICTED: uncharacterised protein LOC105044092	3.81	16.17	18.17	16.88	0.00	0.00	1.00	1.64	1.77	1.43	1.65
Group 3												
gi|743776619	PREDICTED: putative transporter arsB	5.06	0.00	13.73	16.03	0.00	0.00	1.00	3.57	52.06	36.31	89.68
Group 4												
gi|743831750	PREDICTED: pentatricopeptide repeat-containing protein *At5*g14770, mitochondrial	4.72	0.00	17.43	0.00	19.14	0.00	1.00	2.11	7.40	4.56	4.40
Group 5												
gi|743761857	transmembrane protein 184C-like	1.52	0.00	0.00	13.94	0.00	0.00	1.00	1.05	6.76	2.93	9.49
Group 6												
gi|743763273	PREDICTED: phospholipase D delta-like isoform X2	9.94	0.00	21.40	19.12	21.40	0.00	1.00	1.05	0.64	0.44	0.00
gi|743758416	PREDICTED: probable solanesyl-diphosphate synthase 3, chloroplastic	9.78	0.00	22.50	22.32	20.51	0.00	1.00	0.81	5.06	1.27	3.28
gi|743756281	PREDICTED: probable LIM domain-containing serine/threonine-protein kinase DDB_G0286997	2.78	0.00	19.80	18.95	20.90	0.00	1.00	1.49	7.13	3.85	7.28
Group 7												
gi|743886489	PREDICTED: protein kinase PINOID-like	6.72	0.00	21.95	20.46	0.00	13.44	1.00	0.61	4.47	2.65	9.98
gi|743765954	PREDICTED: uncharacterised protein LOC105038960	7.37	0.00	21.29	20.98	0.00	18.35	1.00	1.88	3.29	2.30	3.16
Group 8												
gi|743800192	PREDICTED: delta (8)-fatty-acid desaturase-like	3.98	0.00	0.00	17.26	19.19	19.19	1.00	1.87	2.41	1.44	33.69
gi|743839144	PREDICTED: RAN GTPase-activating protein 1-like	2.86	0.00	0.00	18.31	20.11	20.11	1.00	1.61	1.67	1.16	2.31
gi|743759713	PREDICTED: U4/U6 small nuclear ribonucleoprotein Prp3-like	2.21	0.00	0.00	16.33	13.63	13.63	1.00	1.70	4.48	2.28	4.88
gi|743861480	PREDICTED: fasciclin-like arabinogalactan protein 2	7.50	0.00	0.00	21.23	14.26	14.26	1.00	1.40	1.70	1.28	4.32
gi|743811642	PREDICTED: RING-H2 finger protein ATL13-like	2.42	0.00	0.00	20.76	19.18	19.18	1.00	1.25	4.52	2.86	20.74
gi|743841808	PREDICTED: metallothionein-like protein type 2	10.08	0.00	0.00	18.46	18.46	17.58	1.00	1.57	7.62	3.48	27.18
gi|743770889	PREDICTED: uncharacterised protein *At5*g41620-like	13.77	0.00	0.00	17.88	19.11	19.11	1.00	2.43	3.07	1.64	3.07

Note: mRNA expression level of the identified genes is normalised with *E. guineensis elongation factor alpha-1* (NCBI accession number XM_019850296). The callus stage is used as a reference expression level to calculate the fold changes. The blue colour represents the level of gene expression. The higher intensity of the blue colour indicates up-regulated expression and the lower intensity indicates down-regulated expression.

which are zinc finger families containing C3H-type motif proteins (Pi *et al*., 2018). B-box domain family proteins regulate embryo and hypocotyl elongation (Shalmani *et al*., 2019). In addition, a basic leucine zipper transcription factor has been reported to be upregulated in embryo/endosperm in the seed germination stage, and in embryo 25 days after seed development in barley (Pourabed *et al*., 2015).

Somatic embryogenesis can also be regulated by endogenous plant hormones. We identified several hormone-responsive proteins, which were expressed during somatic embryos as plant developmental requirements. For example, an auxin response factor 23-like has a major role in plant growth and developmental processes (Li *et al*., 2016). Moreover, NAC domain-containing protein 78, which plays an important role in the regulation of the transcriptional reprogramming associated with plant stress responses was also identified in this study (Nuruzzaman *et al*., 2013). In addition, two proteins, which were downregulated in the globular stage of somatic embryogenesis (sub-cluster D2), have been revealed to be the repressor proteins. Agamous-like MADs box protein AGL62 plays an important role in endosperm development. Its expression was detected in endosperm but not in the embryos as the result is downregulated during the early stage of somatic embryogenesis (Kang *et al*., 2008). B3 domain-containing protein *Os*07g0563300 is a member of a VAL family, which encodes the repressor of embryogenesis related-gene, *LEC1* (Schneider *et al*., 2016).

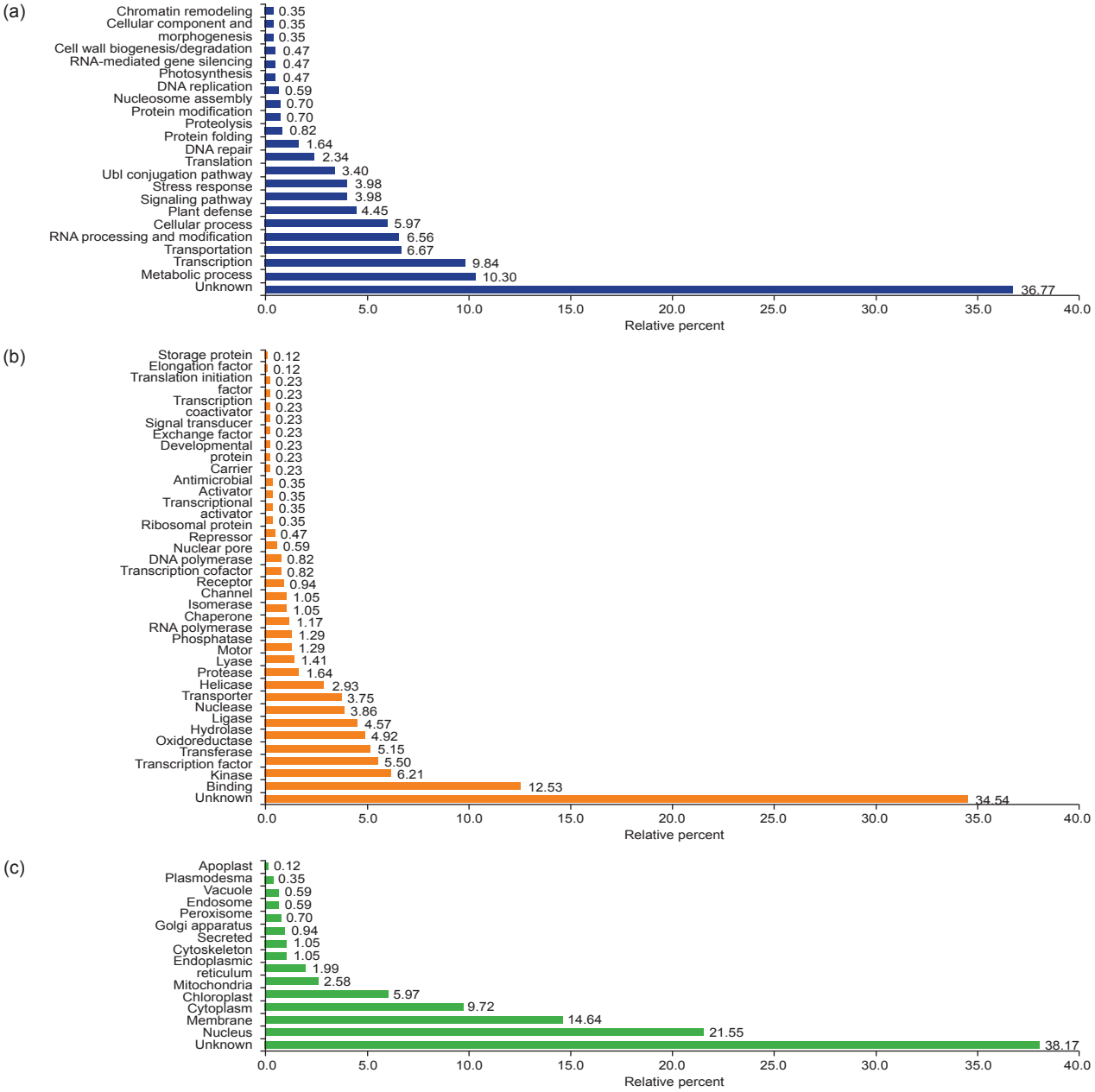

Figure 3. Functional classification of identified proteins based on their gene ontology (GO); (a) biological process, (b) molecular function, and (c) cellular component.

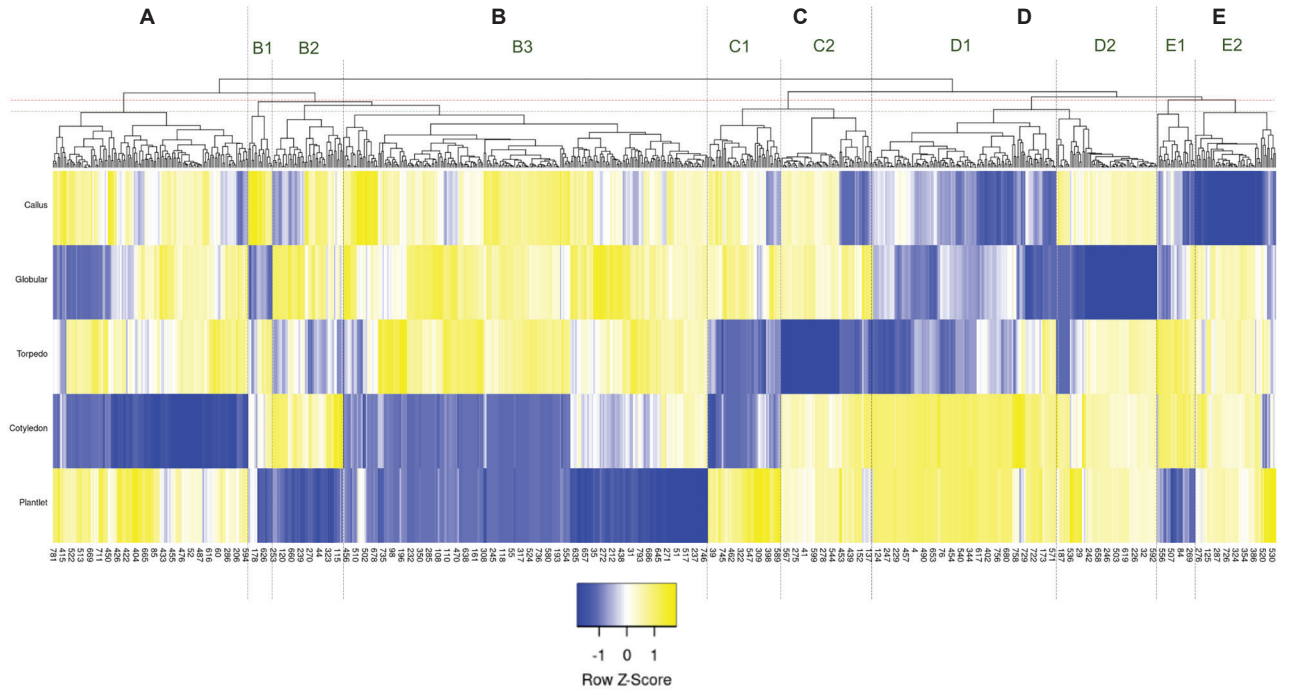

Figure 4. Heat map of the differentially expressed proteins during somatic embryogenesis. Five clusters and sub-clusters were categorised based on the level of average normalised volume of each protein. The blue colour indicates a low level of expression and the yellow colour indicates a high level of expression. The level of expression is proportionate to the colour intensity.

CONCLUSION

In summary, we identified and characterised proteins that are expressed during oil palm somatic embryogenesis. The results revealed that several proteins are involved in plant growth and development, gene regulation, signalling, hormone response, and stress response. The identified proteins could be developed as biomarkers for the oil palm somatic embryogenesis. Furthermore, the information obtained from this study will facilitate the understanding of the regulation mechanism of oil palm somatic embryogenesis.

ACKNOWLEDGEMENT

This research and innovation activity is funded by the National Research Council of Thailand (NRCT) as of the fiscal years 2017 and 2021, the National Research Council of Thailand (NRCT), and the Royal Golden Jubilee (RGJ) Ph.D. Program (Grant No. PHD/0001/2560), through the National Research Council of Thailand (NRCT), and Thailand Research Fund (TRF), Kasetsart University Research and Development Institute (KURDI).

REFERENCES

Aroonluk, S; Roytrakul, S and Jantasuriyarat, C (2020). Identification and characterisation of phosphoproteins in somatic embryogenesis acquisition during oil palm tissue culture. *Plants (Basel)*, *9*: 36.

Aroonluk, S; Roytrakul, S; Yingchutrakul, Y; Kittisenachai, S and Jantasuriyarat, C (2018). Characterisation of glycoproteins during oil palm somatic embryogenesis. *Agric. Nat. Res.*, *52*: 430-438.

Borges Araujo, A J; Cerruti, G V; Zuccarelli, R; Rodriguez Ruiz, M; Freschi, L; Singh, R; Moerschbacher, B M; Floh, E I S and Wendt dos Santos, A L (2022). Proteomic analysis of S-Nitrosation sites during somatic embryogenesis in Brazilian pine, *Araucaria angustifolia* (Bertol.) Kuntze. *Front. Plant Sci.*, *13*: 902068.

Bouchabké-Coussa, O; Obellianne, M; Linderme, D; Montes, E; Maia-Grondard, A; Vilaine, F and Pannetier, C (2013). Wuschel overexpression promotes somatic embryogenesis and induces organogenesis in cotton (*Gossypium hirsutum* L.) tissues cultured *in vitro*. *Plant Cell Rep.*, *32*: 675-686.

Florez, S L; Erwin, R L; Maximova, S N; Guiltinan, M J and Curtis, W R (2015). Enhanced somatic embryogenesis in *Theobroma cacao* using the homologous BABY BOOM transcription factor. *BMC Plant Biol.*, *15*: 121.

Guo, F; Liu, C; Xia, H; Bi, Y; Zhao, C; Zhao, S; Hou, L; Li, F and Wang, X (2013). Induced expression of *AtLEC1* and *AtLEC2* differentially promotes

somatic embryogenesis in transgenic tobacco plants. *PLoS ONE*, *8*: e71714.

Jiménez-Guillen, D; Pérez-Pascual, D; Souza-Perera, R and Zúñiga-Aguilar, J J (2019). Cloning and molecular characterisation of a putative Habanero pepper SERK1 cDNA expressed during somatic and zygotic embryogenesis. *Electron. J. Biotechnol.*, *41*: 48-55.

Johnson, K L; Jones, B J; Bacic, A and Schultz, C J (2003). The fasciclin-like arabinogalactan proteins of *Arabidopsis*. A multigene family of putative cell adhesion molecules. *Plant Physiol.*, *133*: 1911-1925.

Kang, I H; Steffen, J G; Portereiko, M F; Lloyd, A and Drews, G N (2008). The AGL62 MADS domain protein regulates cellularization during endosperm development in *Arabidopsis*. *Plant Cell*, *20*: 635-647.

Kaweewong, K; Garnjanagoonchorn, W; Jirapakkul, W and Roytrakul, S (2013). Solubilization and identification of hen eggshell membrane proteins during different times of chicken embryo development using the proteomic approach. *Protein J.*, *32*: 297-308.

Kim, S H and Roux, S J (2003). An *Arabidopsis* ran-binding protein, *AtRanBP1c*, is a co-activator of ran GTPase-activating protein and requires the C-terminus for its cytoplasmic localization. *Planta*, *216*: 1047-1052.

Krzewska, M; Dubas, E; Gołębiowska, G; Nowicka, A; Janas, A; Zieliński, K; Surówka, E; Kopeć, P; Mielczarek, P and Żur, I (2021). Comparative proteomic analysis provides new insights into regulation of microspore embryogenesis induction in winter triticale (× *Triticosecale* Wittm.) after 5-azacytidine treatment. *Sci. Rep.*, *11*: 22215.

Kumaravel, M; Uma, S; Backiyarani, S and Saraswathi, M S (2020). Proteomic analysis of somatic embryo development in *Musa* spp. cv. Grand Naine (AAA). *Sci. Rep.*, *10*: 4501.

Li, S B; Xie, Z Z; Hu, C G and Zhang, J Z (2016). A review of auxin response factors (ARFs) in plants. *Front. Plant Sci.*, *7*: 47.

Nuruzzaman, M; Sharoni, A M and Kikuchi, S (2013). Roles of NAC transcription factors in the regulation of biotic and abiotic stress responses in plants. *Front. Microbiol.*, *4*: 248.

Maciaszczyk-Dziubinska, E; Wawrzycka, D and Wysocki, R (2012). Arsenic and antimony transporters in eukaryotes. *Int. J. Mol. Sci.*, *13*: 3527-3548.

Motose, H; Hamada, T; Yoshimoto, K; Murata, T; Hasebe, M; Watanabe, Y; Hashimoto, T; Sakai, T and Takahashi, T (2011). NIMA-related kinases 6, 4, and 5 interact with each other to regulate microtubule organisation during epidermal cell expansion in *Arabidopsis thaliana*. *Plant J.*, *67*: 993-1005.

Pattarapimol, T; Thuzar, M; Vanavichit, A; Tragoonrung, S; Roytrakul, S and Jantasuriyarat, C (2015). Identification of genes involved in somatic embryogenesis development in oil palm (*Elaeis guineensis* Jacq.) using cDNA AFLP. *J. Oil Palm Res.*, *27*: 1-11.

Pi, B; He, X; Ruan, Y; Jang, J C and Huang, Y (2018). Genome-wide analysis and stress-responsive expression of CCCH zinc finger family genes in *Brassica rapa*. *BMC Plant Biol.*, *18*: 373.

Potocka, I; Baldwin, T C and Kurczynska, E U (2012). Distribution of lipid transfer protein 1 (LTP1) epitopes associated with morphogenic events during somatic embryogenesis of *Arabidopsis thaliana*. *Plant Cell Rep.*, *31*: 2031-2045.

Pourabed, E; Ghane Golmohamadi, F; Soleymani Monfared, P; Razavi, S M and Shobbar, Z S (2015). Basic leucine zipper family in barley: Genome-wide Characterisation of members and expression analysis. *Mol. Biotechnol.*, *57*: 12-26.

Ringli, C (2010). Monitoring the outside: Cell wall-sensing mechanisms. *Plant Physiol.*, *53*: 1445-1452.

Schneider, A; Aghamirzaie, D; Elmarakeby, H; Poudel, A N; Koo, A J; Heath, L S; Grene, R and Collakova, E (2016). Potential targets of *VIVIPAROUS1/ABI3-LIKE1* (*VAL1*) repression in developing *Arabidopsis thaliana* embryos. *Plant J.*, *85*: 305-319.

Shalmani, A; Jing, X Q; Shi, Y; Muhammad, I; Zhou, M R; Wei, X Y; Chen, Q Q; Li, W Q; Liu, W T and Chen, K M (2019). Characterisation of B-BOX gene family and their expression profiles under hormonal, abiotic and metal stresses in Poaceae plants. *BMC Genom.*, *20*: 27.

Silva, R D C; Carmo, L S T; Luis, Z G; Silva, L P; Scherwinski-Pereira, J E and Mehta, A (2014). Proteomic identification of differentially expressed proteins during the acquisition of somatic embryogenesis in oil palm (*Elaeis guineensis* Jacq.). *J. Proteom.*, *104*: 112-127.

Sruthilaxmi, C B and Babu, S (2020). Proteome responses to individual pathogens and abiotic conditions in rice seedlings. *Phytopathology, 110*: 1326-1341.

Thuzar, M; Vanavichit, A; Tragoonrung, S and Jantasuriyarat, C (2011). Efficient and rapid plant regeneration of oil palm zygotic embryos cv. *tenera* through somatic embryogenesis. *Acta Physiol. Plantarum*, *33*: 123-128.

Voigt, J; Frank, R and Wöstemeyer, J (2009). The chaotrope-soluble glycoprotein GP1 is a constituent of the insoluble glycoprotein framework of the *Chlamydomonas* cell wall. *FEMS Microbiol. Lett.*, *291*: 209-215.

Yu, T Y; Shi, D Q; Jia, P F; Tang, J and Li, H J (2016). The Arabidopsis receptor kinase ZAR1 is required for zygote asymmetric division and its daughter cell fate. *PLoS Genet.*, *12*: e1005933.

SHORT COMMUNICATION

Journal of Oil Palm Research Vol. 35 (3) September 2023 p. 538-542
DOI: https://doi.org/10.21894/jopr.2022.0067

CARBON DIOXIDE EMISSIONS FROM FROND DECOMPOSITION IN OIL PALM PLANTATIONS ON TROPICAL PEAT

NUR WAKHID[1]* and TAKASHI HIRANO[2]

ABSTRACT

Up to now, many studies have been trying to reveal the impact of oil palm plantations on tropical peat on the global carbon (C) balance. Although there are some publications on soil respiration in oil palm plantations on peat soil, information on carbon dioxide (CO_2) emissions from palm litter (pruned fronds) decomposition is limited. Therefore, we quantified the CO_2 emissions through frond decomposition in two different mature oil palm plantations established on peat, an industrial plantation in Riau and a smallholder plantation in Jambi, Indonesia. Frond decomposition was measured using a litter bag method and the decomposition rate constant was determined using a negative exponential equation. Annual CO_2 emissions from frond decomposition were estimated at 1.48 and 1.12 Mg C ha^{-1} yr^{-1}, respectively, in industrial and smallholder plantations. As a result, CO_2 emissions from frond decomposition accounted for 10%-14% of heterotrophic respiration from mature oil palm plantations on tropical peat.

Keywords: industrial plantation, mature plantation, palm litter, smallholder plantation.

Received: 17 April 2022**; Accepted:** 21 September 2022**; Published online:** 19 October 2022.

INTRODUCTION

Tropical peatland has become one of the most efficient carbon sinks on the earth and plays an important role in the global carbon (C) cycle. This ecosystem mostly concentrated in Southeast Asia (SEA), the upper Amazon and in Congo Basin, covers only 16% of global peatland areas but is stored up to 105 Pg of C (Dargie *et al.,* 2017; Page *et al.,* 2011). However, this huge C deposit is now becoming vulnerable to being changed as a massive C source due to the land conversion that promotes peat decomposition and peat fires (Hooijer *et al.,* 2012; Miettinen *et al.,* 2017).

[1] Research Center for Ecology and Ethnobiology, National Research and Innovation Agency, 16911, Cibinong, Bogor, Indonesia.

[2] Research Faculty of Agriculture,Hokkaido University, 060-8589, Sapporo, Japan.

* *Corresponding author e-mail: n_wakhid@yahoo.com*

Driven by population growth and economic development, during the last two decades, many areas of tropical peat swamp forest in SEA have been converted to agricultural plantations, mostly for oil palm and acacia trees (Miettinen *et al.,* 2012). The total area of peat swamp forest in Peninsular Malaysia, Sumatra and Borneo has been estimated to decrease from 64 x 105 ha in 2007 to 46 x 105 ha, while oil palm plantations on peatland had extended up to 31 x 105 ha in 2015 (Miettinen *et al.,* 2016). The global demand for palm oil in the world is expected to double by 2030 compared to 2000 (Yan, 2017). Thus, the impact of this plantation on the global C balance could be large.

To date, there are several publications on oxidative peat decomposition or heterotrophic respiration in oil palm plantations on peat (*e.g.* Dariah *et al.,* 2014; Hergoualc'h *et al.,* 2017; Ishikura *et al.,* 2018; Manning *et al.,* 2019; Melling *et al.,* 2013 and Wakhid and Hirano, 2021a). Unfortunately, none of these have studied carbon dioxide (CO_2)

emissions through palm litter (pruned fronds) decomposition, except Wakhid and Hirano (2021a), which conducted the study on a young oil palm plantation (7 years old). More field experiments are necessary, particularly in mature oil palm plantations to understand the contribution of CO_2 emissions through frond decomposition to the C balance of oil palm plantations on peat. The objective of this study was to quantify how much CO_2 is emitted from the decomposition of pruned fronds left on the ground in mature oil palm plantations on peat soil.

MATERIALS AND METHODS

The study was conducted over one year from February 2018 to March 2019, in mature oil palm (*Elaeis guineensis* Jacq.) plantations in Sumatra, Indonesia. One site was an industrial plantation in Riau (0° 42′ 16″ N, 101° 42′ 52.8″ E), and another site was a smallholder plantation in Jambi (1° 14′ 20″ S, 103° 35′ 23″ E). The oil palm cultivar in Riau was Marihat and in Jambi was mixed between the Marihat and Socfin with a ratio of 4:1. Thus, weighting factors of 0.8 and 0.2 were applied to the data for Marihat and Socfin, respectively, for the calculation of the CO_2 emissions in Jambi. Further information about the study sites was described in Wakhid *et al.* (2022).

To estimate the decomposition, fresh fronds were cut down, separated into two parts (tip and base), and put into litter bags. The litter bags were 40 × 80 cm, with a mesh size of 2 mm. Before being inserted into the litter bags, the fresh weight of each frond was recorded. Each bag contained about 800 g of frond. Also, the initial values of dry weight and C content of fronds were measured (n = 3). In Riau, the litter bags were set on the top of frond heaps in February 2018 with a total of 100 bags for each tip and base. The bags were retrieved in September 2018, January 2019 and June 2019, but only 99 bags were in total because most of them were missing. In Jambi, 36 bags of tips and bases for each of Marihat and Socfin were set equally on the top of and under frond heaps, in February 2018. In total, six bags of each tip and base from the two positions were retrieved in September 2018, February 2019 and July 2019. Each litter bag was cleaned after being retrieved, and the dry weight and C content were measured.

The dry weight was measured by oven drying for 48 hr at 70°C. The C content was estimated by the loss of ignition method, using a conversion factor from organic matter to organic C of 0.58 (Agus *et al.*, 2011). The decomposition rate constant (k) was estimated using a negative exponential equation from the plot of the residual ratio of C amount (Y) against elapsed time (t) following Moradi *et al.* (2014) as shown in Equation (1).

$$Y = Y_0 \exp(-kt) \quad (1)$$

where C loss through frond decomposition was estimated using the k and initial C amount (Y_0). Then, the annual CO_2 emission was calculated using pruned frond production × monthly amount of CO_2 emissions. The annual C input was estimated from annual pruned fronds × tree density × dry weight × C content. Statistical analysis (ANOVA, Tukey HSD test, and exponential graph) were conducted using Excel and R software (R Development Core Team 2019, version 3.5.3). Further detail about CO_2 emissions calculation was described in Wakhid and Hirano (2021a; 2021b).

RESULTS AND DISCUSSION

The C content of pruned fronds in Riau and Jambi was in the range of 53%-57% (*Table 1*). C and Nitrogen (N) contents of leaf were significantly different with rachis (*Table 1*). However, the C and N contents of the tip and base parts were not significantly different. CN ratio was significantly higher in rachis than in leaf. Socfin in Jambi has the lowest CN ratio than that of Marihat in Riau and Jambi, respectively (*Table 1*).

In Riau, the amount of litter bags in the second and third retrieving was smaller than that of the first retrieving (n = 45, 27 and 27 litter bags, respectively, for the first, second and third retrieving) because several bags were lost during the study. Thus, the k value was calculated using all retrieved samples without tip and base parts separation to be 1.86 yr^{-1} (*Figure 1*). The annual C input was 2.54 Mg C ha^{-1} yr^{-1}, and CO_2 emissions from frond decomposition were estimated at 1.48 Mg C ha^{-1} yr^{-1} *(Table 2).*

In Jambi, although, the k values among tip and base parts and between two cultivars were not significantly different, CO_2 emissions through frond decomposition should be different among the cultivars because the size of Socfin was 1.4 times larger than that of Marihat (*Table 1*). Thus, the k values were calculated using all data for each cultivar (n = 12), to be 1.57 and 1.81 yr^{-1}, respectively, for Marihat and Socfin (*Figure 1*). The annual C input and CO_2 emissions from pruned fronds were estimated at 2.07 and 1.12 Mg C ha^{-1} yr^{-1}, respectively *(Table 2).*

CO_2 emissions from frond decomposition in this study were higher than in a young oil palm plantation in Banjarbaru (Wakhid and Hirano (2021a): 0.38 Mg C ha^{-1} yr^{-1}). This discrepancy was most likely caused by the production of frond that was larger in mature than in young plantations. The CO_2 emissions (1.48 and 1.12 Mg C ha^{-1} yr^{-1}, in Riau and Jambi, respectively) accounted for 14% and 11% of heterotrophic respiration from mature oil palm

TABLE 1. INITIAL AMOUNT OF CARBON (C), NITROGEN (N), CN RATIO, AND WATER CONTENT (WC) OF FROND (MEAN ± 1 SD, n = 3).

Samples	C (%)	N (%)	CN ratio	WC (%)
Marihat (*M*) in Riau (dry weight = 2578 ± 509 g frond^{-1}, n = 5)				
Leaf (tip)	54.60 ± 0.54a	1.23 ± 0.58a	50.30 ± 19.10a	59.30 ± 0.30
Rachis (tip)	56.70 ± 0.28b	0.38 ± 0.13b	160.90 ± 58.90b	60.20 ± 8.30
Leaf (base)	55.00 ± 0.29a	1.62 ± 0.44a	35.40 ± 8.40a	59.10 ± 1.60
Rachis (base)	55.60 ± 0.35b	0.39 ± 0.06b	143.70 ± 20.00b	37.80 ± 6.60
Marihat (*M*) in Jambi (dry weight = 2254 ± 188 g frond^{-1}, n = 5)				
Leaf (tip)	54.00 ± 0.33a	1.90 ± 0.33a	29.20 ± 5.70a	54.90 ± 2.70
Rachis (tip)	57.10 ± 0.07b	0.66± 0.08b	87.20 ± 11.40b	65.90 ± 4.20
Leaf (base)	54.40 ± 0.40a	2.00 ± 0.19a	27.40 ± 2.30a	58.50 ± 2.30
Rachis (base)	56.90 ± 0.25b	0.60 ± 0.10b	96.20 ± 15.40b	71.10 ± 7.50
Socfin (*S*) in Jambi (dry weight = 3387 ± 567 g frond^{-1}, n = 5)				
Leaf (tip)	53.10 ± 0.89a	2.27 ± 0.16a	23.50 ± 1.50a	50.10 ± 11.40
Rachis (tip)	56.80 ± 0.09b	0.75 ± 0.13b	77.00 ± 13.30b	69.80 ± 3.70
Leaf (base)	53.60 ± 1.32a	2.15 ± 0.51a	25.90 ± 6.00a	56.50 ± 2.60
Rachis (base)	56.40 ± 0.11b	0.79 ± 0.20b	74.90 ± 20.60b	71.10 ± 4.80
ANOVA (*p*- value)				
Component (leaf *vs*. rachis)	<0.001	<0.001	<0.001	0.210
Position (tip *vs*. base)	0.76	0.64	0.68	0.50
Site (*M* in Riau *vs*. *M* in Jambi)	0.74	0.18	0.08	0.13
Cultivar (*M vs*. *S* in Jambi)	0.42	0.06	<0.05	0.16
Interaction (component-position)	<0.05	0.62	0.98	0.06

Note: Data of C (%) of Marihat and Socfin in Jambi was adapted from Wakhid and Hirano (2021b).
Different letters denote significant differences between leaf and rachis.

TABLE 2. CARBON (C) INPUT AND CARBON DIOXIDE (CO_2) EMISSIONS FROM FROND DECOMPOSITION IN RIAU AND JAMBI

Site and cultivar	Tree density (trees ha^{-1})	Frond production (dry weight, Mg ha^{-1} yr^{-1})	C input (Mg C ha^{-1} yr^{-1})	CO_2 emissions (Mg C ha^{-1} yr^{-1})
Industrial in Riau *(Marihat)*	148	4.58	2.54	1.48
Smallholder in Jambi	125	3.72	2.07	1.12
Marihat	100	2.71	1.51	0.80
Socfin	25	1.02	0.56	0.32

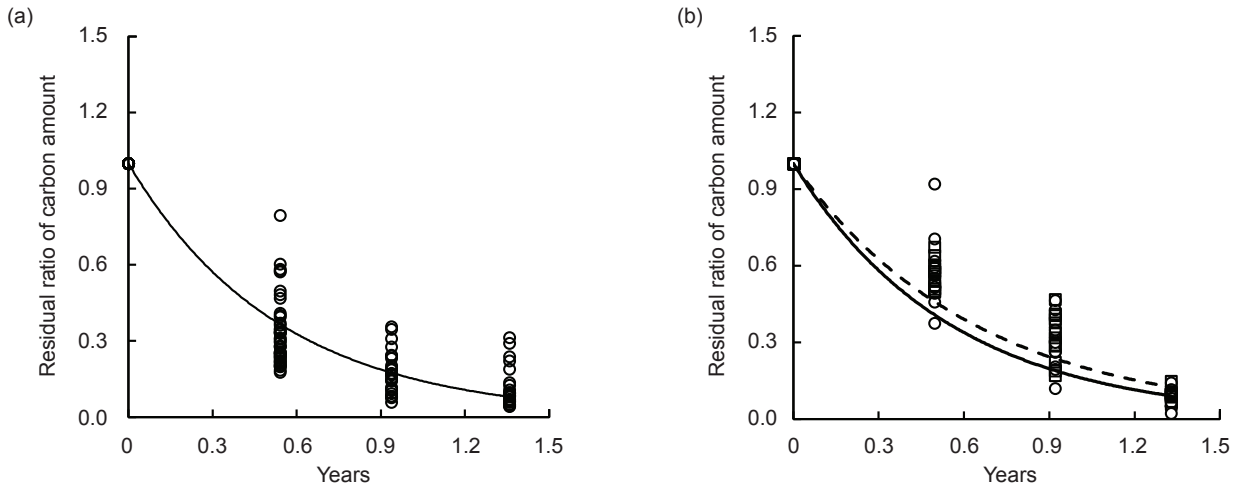

Figure 1. C loss pattern of a) Marihat in Riau and b) Marihat (squares, dash line) and Socfin (circles, solid line) in Jambi. An exponential curve is fitted for each retrievement time. Riau: $Y = e^{-1.86x}$ ($r^2 = 0.83$), and Jambi: $Ym = e^{-1.57x}$ ($r^2 = 0.90$), $Ys = e^{-1.81x}$ ($r^2 = 0.84$). Ym and Ys represent the equations for Marihat and Socfin cultivars, respectively.

plantations on tropical peat (Dariah *et al.* (2014): 15 years old, 10.4 Mg C ha^{-1} yr^{-1}). Also, accounted for 13% and 10 %, in Riau and Jambi, respectively, to a default CO_2 emission factor Tier 1 methodology of oil palm plantation on peat soil (11 Mg C ha^{-1} yr^{-1}) from the Intergovernmental Panel on Climate Change (IPCC, 2014). Following the amount of CO_2 emissions, the contribution in mature was larger than in young oil palm plantations (Wakhid and Hirano (2021a): Accounting for 2.4% of heterotrophic respiration).

Some data in Jambi from February 2018 to February 2019 was presented at International Conference on Sustainable Tropical Land Management (Wakhid and Hirano, 2021b). Unexpectedly, CO_2 emission in Jambi from February 2018 to February 2019 (Wakhid and Hirano (2021b): 1.09 Mg C ha^{-1} yr^{-1}) was similar to February 2018 to September 2019 (this study: 1.12 Mg C ha^{-1} yr^{-1}). Frond decomposition could likely be estimated in a short study as long as the disturbance and environmental changes are minimal. To our knowledge, previous studies on CO_2 emissions from frond decomposition were limited, thus more studies for comparison were not found.

The annual C input from pruned fronds and *k* values from this study were compared with some previous studies. Annual C input in this study (2.54 and 2.07 Mg C ha^{-1} yr^{-1}, respectively, in Riau and Jambi) was lower than the C input of pruned fronds from oil palm on mineral soil in Jambi (Kotowska *et al.* (2016): 2.89 Mg C ha^{-1} yr^{-1}). However, our result was higher than that of 1.33-1.79 Mg C ha^{-1} yr^{-1} of C input from pruned fronds in an oil palm plantation on mineral soil in North Sumatra (Lamade and Bouillet, 2005). *k* values of Marihat in Riau and Socfin in Jambi (*Figure 1*) were similar to the *k* value of pruned fronds from oil palms on mineral soil in Malaysia (1.80 yr^{-1}; Moradi *et al.*, 2014), but higher than that of another study also in Malaysia (0.73 yr^{-1}; Khalid *et al.*, 2000).

CONCLUSION

CO_2 emissions from frond decomposition were investigated in mature oil palm plantations on tropical peat, industrial and smallholder plantations, in Riau and Jambi. Using decomposition rate constant (*k*), initial carbon (C) amount, and pruned frond production, CO_2 emissions from frond decomposition were estimated to be 1.48 and 1.12 Mg C ha^{-1} yr^{-1}, respectively, in Riau and Jambi. These CO_2 emissions accounted for 10%-14% of heterotrophic respiration in oil palm plantations on peat. The contribution of frond decomposition is not large but should be considered in peat soil respiration calculation.

ACKNOWLEDGEMENT

We thank Fahmuddin Agus and Ai Dariah for permitting us to use their field research for the study. This study was supported by Indonesian Agency for Agricultural Research and Development and JSPS KAKENHI (No.17H01477, 18H02238, and 19H05666).

REFERENCES

Agus, F; Hairiah, K and Mulyani, A (2011). *Measuring Carbon Stock in Peat Soils: Practical Guidelines*. World Agroforestry Centre (ICRAF) Southeast Asia Regional Program, Indonesian Centre for Agricultural Land Resources Research and Development. Bogor, Indonesia. 78 pp.

Dargie, G C; Lewis, S L; Lawson, I T; Mitchard, E T A; Page, S E; Bocko, Y E and Ifo, S A (2017). Age, extent and carbon storage of the central Congo Basin peatland complex. *Nature, 542*: 86-90. DOI: 10.1038/nature21048.

Dariah, A; Marwanto, S and Agus, F (2014). Root- and peat-based CO_2 emissions from oil palm plantations. *Mitig. Adapt. Strateg. Glob. Chang., 19*: 831-843. DOI: 10.1007/s11027-013-9515-6.

Hergoualc'h, K; Hendry, D T; Murdiyarso, D and Verchot, L V; (2017). Total and heterotrophic soil respiration in a swamp forest and oil palm plantations on peat in Central Kalimantan, Indonesia. *Biogeochemistry, 135*: 203-220. DOI: 10.1007/s10533-017-0363-4.

Hooijer, A; Page, S; Jauhiainen, J; Lee, W A; Lu, X X; Idris, A and Anshari, G (2012). Subsidence and carbon loss in drained tropical peatlands. *Biogeosciences, 9(3)*: 1053-1071. DOI: 10.5194/bg-9-1053-2012.

IPCC (2014). *2013 Supplement to the 2006 IPCC Guidelines for National Greenhouse Gas Inventories*. IPCC, Wetlands, Switzerland. 354 pp.

Ishikura, K; Hirano, T; Okimoto, Y; Hirata, R; Kiew, F; Melling, L; Aeries, E B; Lo, K S; Musin, K K; Waili, J W; Wong, G X and Ishii, Y (2018). Soil carbon dioxide emissions due to oxidative peat decomposition in an oil palm plantation on tropical peat. *Agric. Ecosyst. Environ., 254*: 202-212. DOI: 10.1016/ j.agee.2017.11.025.

Khalid, H; Zin, Z Z and Anderson, J M (2000). Decomposition processes and nutrient release patterns of oil palm residues. *J. Oil Palm Res., 12(1)*: 46-63.

Kotowska, M M; Leuschner, C; Triadiati, T and Hertel, D (2016). Conversion of tropical lowland forest reduces nutrient return through litterfall and alters nutrient use efficiency and seasonality of net primary production. *Oecologia, 180*: 601-618. DOI: 10.1007/s00442-015-3481-5.

Lamade, E and Bouillet, J P (2005). Carbon storage and global change: The role of oil palm. *Oléagineux Corps Gras Lipides (OCL)*, *12*: 154-160. DOI: 10.1051/ocl.2005.0154.

Manning, F C; Kho, L K; Hill, T C; Cornulier, T and Teh, Y A (2019). Carbon emissions from oil palm plantations on peat soil. *Front. For. Glob. Change*, *2*: 37, 21. DOI: 10.3389/ffgc. 2019.00037.

Melling, L; Yun Tan, C S; Goh, K J and Hatano, R (2013). Soil microbial and root respirations from three ecosystems in tropical peatland of Sarawak, Malaysia. *J. Oil Palm Res., 25*: 44-57.

Miettinen, J; Hooijer, A; Shi, C; Tollenaar, D; Vernimmen, R; Liew, S C; Malins, C and Page, S E (2012). Extent of industrial plantations on Southeast Asian peatlands in 2010 with analysis of historical expansion and future projections. *Glob. Change Biol. Bioenergy, 4*: 908-918. DOI: 10.1111/j.1757-1707.2012.01172.x.

Miettinen, J; Shi, C and Liew, S C (2016). Land cover distribution in the peatlands of Peninsular Malaysia, Sumatra and Borneo in 2015 with changes since 1990. *Glob. Ecol. Conserv., 6*: 67-78. DOI: 10.1016/j.gecco.2016.02.004.

Miettinen, J; Hooijer, A; Vernimmen, R; Liew, S C and Page, S E (2017). From carbon sink to carbon source: Extensive peat oxidation in insular Southeast Asia since 1990. *Environ. Res. Lett., 12*: 024014.

Moradi, A; Teh, C B S; Goh, K J; Husni, M H A and Ishak, C F (2014). Decomposition and nutrient release temporal pattern of oil palm residues. *Ann. Appl. Biol., 164(2)*: 208-219. DOI: 10.1111/aab.12094.

Page, S E; Rieley, J O and Banks, C J (2011). Global and regional importance of the tropical peatland carbon pool. *Glob. Change Biol., 17*: 798-818. DOI: 10.1111/j.1365-2486.2010.02279.x.

Wakhid, N and Hirano, T (2021a). Soil CO_2 emissions and net primary production of an oil palm plantation established on tropical peat. *Mires Peat, 27*: 11. DOI: 10.19189/MaP.2021.OMB.StA.2159.

Wakhid, N and Hirano, T (2021b). Contribution of CO_2 emission from litter decomposition in an oil palm plantation on tropical peatland. *1st International Conference on Sustainable Tropical Land Management. IOP Conf. Series: Earth and Environmental Science. 648*: 012133. DOI: 10.1088/1755-1315/648/1/012133.

Wakhid, N; Hirano, T; Dariah, A and Fahmuddin, A (2022). Net primary production of oil palm plantations on tropical peat. *Mires and Peat, 28*: 02-12. DOI: 10.19189/MaP.2021.SNPG. StA.2288.

Yan, W (2017). A makeover for the world's most hated crop. *Nature, 543(16)*: 306-308.

JOURNAL OF OIL PALM RESEARCH

GUIDE FOR AUTHORS

(for more details, kindly surf http://jopr.mpob.gov.my)

Type of Articles

1. **Regular Article**
   Full-length original empirical investigations, consisting of introduction, materials and methods, results and discussion, conclusions. Original work must provide references and an explanation on research findings that contain new and significant findings. Conclusion should be brief and focus on the research output, should not be in point form. These papers should not exceed 6000 words of text (including tables, figures and references) and generally not more than a total of 10 figures and tables. After peer-review, the article word count limit can be extended to a maximum of 8000 words to better address the reviewers' and editors' comments. Any additional figures or tables can be included in the supplementary data. Please note that papers submitted to JOPR will be sent back to authors because of poor figure resolution or exceeding the number of figures permitted.

2. **Short Communication**
   Significant new information to readers of the Journal in a short but complete form. Preferably not exceeding 3000 words (including tables, figures and references), and is intended for rapid publication. They are not intended for publishing preliminary results or to be a reduced version of regular article.

3. **Review Article**
   Critical evaluation of materials about current research that have already been published by organising, integrating, and evaluating previously published materials. Re-analyses as meta-analysis and systemic reviews are encouraged. Review articles provide systemic overview, evaluation and interpretation of research in a given field. They should not exceed 12 000 words (excluding references only) and should contain no more than a total of 20 figures and tables. Any additional figures or tables can be included in the supplementary data. Please note that papers submitted to JOPR will be sent back to authors because of poor figure resolution or exceeding the number of figures permitted. The same information should not be repeated in a figure and a table.

Language

Please write your text in good English (only British English is accepted). We do not accept American English or a mixture of these.

JOPR's Template

JOPR's template, which is a standard format that facilitates the manuscript writing and copyediting process. This template is created to provide a detail and clear house style of JOPR. The template is drafted according to JOPR's house style, but in standard word version format. When writing a paper, authors need to format their papers to fit into the journal's house style. To make this easier, Word templates are available for many of other established journals, ready for them to download and apply to their research paper format. It is crucial for author to write a research paper while considering formatting. Each journal has its own guidelines for formatting; hence, the template defines how an article will look when it is published online or in print.

JOPR's Aims & Scope

This is established to provide a detail and clear aims and scope for author reference. Authors should declare in the cover letter how the research fits the aims and scope of JOPR.

JOPR's House Style

A detail listing of JOPR's house style for authors and a checklist to facilitate the copyediting process and standardise the copyediting process. The JOPR's house style remains the same and is drafted into a detail version for author's reference.

Manuscript Submission

- Manuscripts should be submitted via: https://mc04.manuscriptcentral.com/jopres
- JOPR does not permit dual submission, publication and/or any archive platform (preprint) in violation of journal ethical practices.

For more details and to download the JOPR's House Style and Template, kindly surf http://jopr.mpob.gov.my

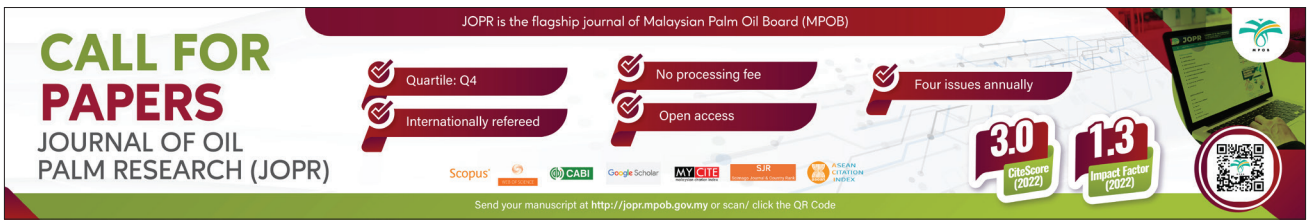

Contents of the Coming Issue
Journal of Oil Palm Research
Vol. 35 (4) December 2023*

Note: * Subject to change.